Generation of a model for human prostate development using patient derived induced pluripotent stem cells

Emma Louise Curry

A Thesis submitted for the degree Doctor of Philosophy

September 2017

Northern Institute for Cancer Research

Faculty of Medical Sciences

Newcastle University

Abstract

Research into highly prevalent prostate diseases is limited by lack of a relevant human model for prostate development and disease. The finding that stem cells can be generated from somatic cells, termed induced pluripotent stem cells (iPSCs), has revolutionised the field of human developmental and disease modelling. However, iPSCs retain an epigenetic signature from their parental tissue of origin which can result in a skewed differentiation potential. In this study, we have generated integration-free iPSCs from patient derived prostatic fibroblasts. These ProiPSCs show typical pluripotent stem cell characteristics including ESC-like morphology, expression of pluripotency markers and the ability to differentiate to cells from the three embryonic germ layers both *in vitro*, by formation of embryoid bodies, and *in vivo*, by teratoma formation.

Using inductive rodent urogenital sinus mesenchyme (UGM), we have successfully generated prostatic tissue from the ProiPSCs using a tissue recombination approach. The generated tissue shows a normal spatial organisation with a basal and luminal layer characterised by expression of p63 and cytokeratins (CK) 8 and 18 respectively. Furthermore, the epithelial glands generated express the prostate markers androgen receptor (AR) and prostate specific antigen (PSA), confirming full functional differentiation. By harnessing the inductive nature of UGM, we subsequently developed a novel 3D co-culture system which allowed formation of prostatic organoids from both ProiPSCs and urinary tract derived iPSCs (UTiPSCs). The organoids were multi-layered with a basal layer expressing p63 and 34βe12 and a luminal layer which expressed CK8/18. Prostatic differentiation was confirmed by positive staining for AR and PSA. In conclusion, we have demonstrated successful reprogramming of human prostate fibroblasts into iPSCs and subsequent differentiation of these cells to prostate epithelial cells *in vitro* and *in vivo*. This model provides a novel opportunity for studying prostate development as well as a potential system for disease modelling and drug testing.

Acknowledgements

I would like to thank my supervisor's Dr Rakesh Heer and Professor Craig Robson for their support, guidance and the knowledge they have shared during this PhD. I would also like to gratefully acknowledge the Medical Research Council for their financial support in this project. I thank my progression panel, Dr Lyle Armstrong and Dr Che Connon, for their guidance and astute comments.

I also gratefully acknowledge the Urology Stem Cell team for their help in the lab and for answering my many questions without complaint. In particular, my thanks go to Laura Wilson, Dr Mohammad Moad and Dr Anastasia Hepburn, for teaching me everything they know and for providing support and encouragement throughout my time at the NICR. I also thank the members of the Solid Tumour Target Discovery Group for making me feel welcome and for their friendship and laughs during my PhD, especially to Amy and Alice for the emergency cake trips when things haven't gone to plan! Thanks also go to Dr Helen Blair, for performing the *in vivo* teratoma grafts and to the Northern Molecular Genetics Service for performing the DNA fingerprinting and karyotyping.

I would like to extend my deepest thanks to the Hayward laboratory at the NorthShore Research Institute, Evanston, Illinois, for hosting me for a 3 month visit and sharing their unique knowledge and skills. I would like to thank Dr Omar Franco, Dr Takeshi Sasaki, Yana Filipovich, Rodrigo Javier and LaTayia Aaron for giving up their time to assist with the intricate dissections required for this project as well as performing the *in vivo* grafting. I will be forever grateful to Dr Simon Hayward and his wife Dr Joanne Hayward for not only making this visit and work possible, but for welcoming me into their family during my stay.

Above all, I would like to thank my family and friends for their unwavering support over the past 4 years. In particular, I would like to thank my Mum, Margaret, for her endless encouragement and belief in me as well as the many hours spent proof-reading this thesis. I could not have completed this without her support.

List of abbreviations

2D- Two-dimensional

3D- Three-dimensional

αSMA- α-smooth muscle actin

ADT- Androgen deprivation therapy

AFP- α-fetoprotein

AP- Alkaline phosphatase

AR- Androgen receptor

BMP- Bone morphogenetic protein

BPE- Benign prostatic enlargement

BPH- Benign prostatic hyperplasia

Brdu- 5'-bromo-2'-deoxyuridine

BSA- Bovine serum albumin

CARNs- Castration-resistant Nxk3.1 expressing cells

cDNA- Complementary DNA

CK- Cytokeratins

CM- Conditioned medium

CRPC- Castrate resistant prostate cancer

DAB- 3, 3 –diaminobenzidine

DAPI- 4', 6-diamidino-2-phenylindole

DE- Definitive endoderm

DEPC: Diethyl pyrocarbonate

DHT- 5α-dihydrotestosterone

DLK1- Delta-like homolog 1

DMEM- Dulbeccos' modified Eagle medium

DNA- Deoxyribonucleic acid

DNMT3B- DNA Methyltransferase 3 Beta

DPBS- Dulbeccos phosphate buffered saline

E8- Essential 8

E18- Embryonic day 18

EB- Embryoid body

ECM- Extracellular matrix

EDTA- Ethylenediaminetetraacetic acid

EGF- Epidermal growth factor

Epcam- Epithelial cell adhesion molecule

ESC- Embryonic stem cell

FCS- Foetal calf serum

FFPE- Formalin fixed paraffin embedded

FGF- Fibroblast growth factors

FOXA1- Forkhead box A1

FOXA2- Forkhead box A2

GABA- γ-aminobutyric acid

GABRB3- Gamma-Aminobutyric Acid Type A Receptor Beta3

GDF3- Growth Differentiation Factor 3

GFP- Green fluorescent protein

GM-CSF- Granulocyte-macrophage colony-stimulating factor

GSTpi- Glutathione S-transferase pi

HDF- Human dermal fibroblasts

hESC- Human embryonic stem cells

HoLEP- Holmium laser enucleation of the prostate

HOX- Homeobox

HSC- Haematopoietic stem cells

ICM- Inner cell mass

iPSCs- Induced pluripotent stem cells

ISCBI- International stem cell banking initiative

ITS- Insulin, transferrin, selenium

IVF- In vitro fertilisation

KLF4- Kruppel-like factor 4

KO DMEM- KnockOut DMEM

KOSR- KnockOut serum replacement

KSFM- Keratinocyte Serum-Free Medium

LIF- Leukaemia inhibitory factor

LUTS- Lower urinary tract symptoms

MEFs- Mouse embryonic fibroblasts

MET- Mesenchymal-epithelial transition

MMLV- Moloney murine leukaemia virus

MOI- Multiplicity of infection

mRNA- Messenger RNA

MSC- Mesenchymal stem cell

mTOR- Mechanistic target of rapamycin

$NaHCO_3$- Sodium bicarbonate

NE- Neuroendocrine

Nkx3.1- NK3 homeobox 1

NSG- NOD scid gamma

ntESC- Nuclear transfer ESC

OCT4- Octamer-binding transcription factor 4

OSKM- Oct4, Sox2, Klf4 and c-Myc

PAP- Prostatic acid phosphatase

PBS- Phosphate buffered saline

PI3K- Phosphoinositide 3-kinase

PrEGM- Prostate epithelial growth medium

ProiPSCs- Prostate induced pluripotent stem cells

PSA- Prostate specific antigen

PSC- Pluripotent stem cell

PSMA- Prostate specific membrane antigen

PTEN- Phosphatase and tensin homologue

REX1- Reduced Expression Protein 1

RNA- Ribonucleic acid

ROCK- Rho associated kinase

RPMI- Roswell Park Memorial Institute medium

RT-PCR- Real time polymerase chain reaction

SeV- Sendai virus

SCBM- Stromal cell basal medium

SCID- Severe combined immunodeficient

SCNT- Somatic cell nuclear transfer

shRNA- Short hairpin RNA

Shh- Sonic hedgehog

SOX2- SRY (Sex determining region)-related HMG-box gene 2

SSEA- Stage-specific embryonic antigen

STR- Short tandem repeat

SV40- Simian virus 40

SV40LT- Simian virus 40 large T gene

SVM- Seminal vesicle mesenchyme

TA- Transit amplifying

TDGF1- Teratocarcinoma-Derived Growth Factor 1

TGFβ- Transforming growth factor beta

TURP- Transurethral resection of the prostate

UGE- Urogenital sinus epithelium

UGM- Urogenital sinus mesenchyme

UGS- Urogenital sinus

UTiPSCs- Urinary tract induced pluripotent stem cells

Table of Contents

List of Figures and Tables

Chapter 1. Introduction

1.1 Prostate anatomy

The prostate is a walnut-shaped accessory gland of the male reproductive system situated directly below the urinary bladder, surrounding the urethra and anterior to the rectum in the subperitoneal compartment (Bhavsar and Verma, 2014). Together with the seminal vesicle, the prostate is responsible for secretion of proteins and ions which form part of the seminal fluid (Hayward and Cunha, 2000; Timms, 2008). The most well-known prostatic secretion is prostate specific antigen (PSA), a serine protease belonging to the kallikrein family which is involved in proteolysis of seminal fluid proteins such as semenogelin 1, resulting in liquefaction of the seminal coagulum formed after ejaculation (Lilja, 1985). Prostatic luminal cells also express prostatic acid phosphatase (PAP), a glycoprotein which is also secreted from the prostate into the seminal fluid (Lilja and Abrahamsson, 1988).

The adult human prostate is a compact structure weighing approximately 20g and measuring 4x2.5cm (Marker *et al.*, 2003). It consists of three distinct zones; the central, transition and peripheral zones (Figure 1-1)(McNeal, 1978). The largest of the three zones is the peripheral zone which covers the posterior and lateral prostate gland, accounting for 70% of the prostate gland. The central zone forms 20-25% of the glandular tissue of the prostate and surrounds the ejaculatory ducts, whilst the transitional zone comprises 5-10% of the prostate gland and is separated from the other glands by fibromuscular stroma (Verze *et al.*, 2016).

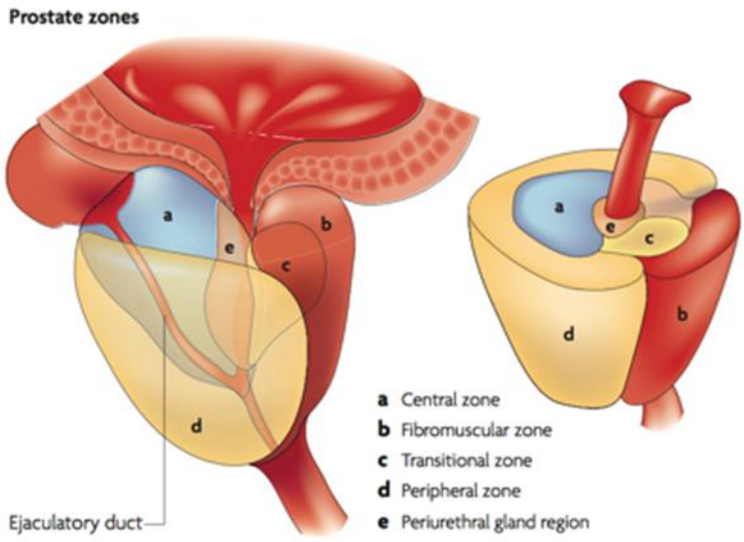

Figure 1-1. Schematic representation of the prostatic zones (De Marzo et al., 2007)

At a cellular level the organ comprises tubuloalveolar glandular tissue surrounded by fibromuscular stroma in a ratio of approximately 2:1 (Prajapati *et al.*, 2013), forming a highly branched structure. In the adult prostate, the complex network of ducts consist of luminal and basal epithelial cells along with rare neuroendocrine (NE) cells (Figure 1-2) (Wang *et al.*, 2001). Luminal cells are the major cell type in normal prostate epithelium (Lang *et al.*, 2009). They express CK8/18 (Wang *et al.*, 2001) Nkx3.1 (Bhatia-Gaur *et al.*, 1999) and high levels of androgen receptor (AR) (Sar *et al.*, 1990), a steroid dependent transcription factor which binds to androgen response elements resulting in enhanced gene expression (Brinkmann *et al.*, 1999). These luminal cells are also responsible for secretion of PSA and prostatic acid phosphatase (PAP) (Lang *et al.*, 2009). Basal cells form a layer between the luminal cells and the basement membrane (Marker *et al.*, 2003). In contrast to luminal cells, basal cells express low or no AR (Shen and Abate-Shen, 2010) and possess no secretory activity. These cells are characterised by expression of CK5/14 (Wang *et al.*, 2001) and the classical basal epithelial cell marker p63 (Signoretti *et al.*, 2000). Recent evidence has also suggested that a subset of basal prostate cells express Nkx3.1 (Chen *et al.*, 2005). The third type of cell present in the prostatic ducts are the NE cells, which are AR negative but express endocrine markers including chromogranin A and synaptophysin (Shen and Abate-Shen, 2010).

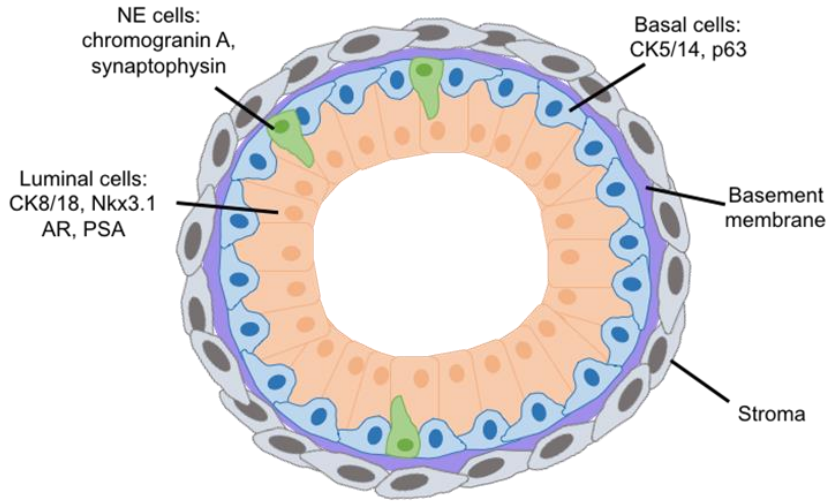

Figure 1-2 Schematic cross-section of a human prostate acinus illustrating the presence of several cell types; luminal, basal, neuroendocrine (NE) and stromal cells. Adapted from (Marker et al., 2003).

1.2 Embryogenesis of the prostate

Following fertilisation, the human embryo undergoes cell division and by about the 4th day following fertilisation has formed a blastocyst consisting of an inner cell mass (ICM) surrounded by an epithelial layer known as the trophoblast. The ICM goes on to form the embryo whilst the trophoblast forms the extraembryonic structures including part of the placenta. Prior to implantation, the ICM divides into two layers of cells known as the epiblast and hypoblast. The epiblast undergoes gastrulation during the 3rd week of embryogenesis to form the three embryonic germ layers; the ectoderm, which arises from embryonic ectoderm, and the endoderm and mesoderm which arise from the mesoblastic cells of the primitive streak (Carlson, 2009).

The prostate epithelium is formed from the endodermal germ layer during embryogenesis, whilst the prostate stroma is derived from the mesodermal layer. Following gastrulation, the endoderm undergoes embryonic folding to generate the primitive gut. During weeks 4-5 of embryogenesis, this primitive gut develops into the foregut, midgut and hindgut which form the gastrointestinal tract, along with the cloaca which develops at around the 6th week to form the urogenital sinus and anorectal canal. The urogenital sinus (UGS) further develops to form the urinary bladder at week 10 and in the male, the urethra, prostate gland and bulbourethral glands during weeks 9-12 (DeCherney, 2013).

The UGS sits just below the developing bladder and consists of an epithelial layer, the urogenital sinus epithelium (UGE) surrounded by the mesodermal urogenital sinus mesenchyme (UGM) (Marker *et al.*, 2003). Mesenchymal-epithelial interactions are critical during organogenesis, whereby specialised mesenchyme acts to induce epithelial differentiation of several tissues including the prostate, lung and mammary glands (Vanpoucke *et al.*, 2007). During prostate development, the urogenital sinus mesenchyme specifies prostate differentiation, induces formation of prostate buds and drives branching morphogenesis to form the branched structure of the prostate (Vanpoucke *et al.*, 2007).

The prostate gland is induced to form from the UGE at around the 10th week of gestation in response to the production of 5α-dihydrotestosterone (DHT) by the foetal testis, which begins at gestational week 8 (Timms, 2008). DHT binds to the AR in the UGM resulting in establishment of a prostatic epithelial identity. This prostatic identity is characterised by expression of the earliest prostate marker Nkx3.1, which is

identified in the UGE prior to the onset of budding (Marker *et al.*, 2003). The androgenic action results in formation of prostatic buds from the UGE which grow into the surrounding UGM (Hamilton, 1959; Shannon and Cunha, 1983). These buds are initially solid epithelial cords which co-express CK5, 8, 14, 18, p63 (Xue *et al.*, 2001). Prior to and during budding, AR can be identified only in the stromal compartment and is not present within the prostatic epithelium, providing further evidence for the critical role of UGM in prostate development (Takeda *et al.*, 1985). Androgen signalling is essential for prostate development, as evidenced by lack of prostate formation in *tfm* mutant mice who lack functional AR (Cunha and Lung, 1978).

The solid buds subsequently elongate and undergo branching morphogenesis to generate distinct lumina and clear basal and luminal cells with individual expression profiles. Luminal cells express CK8 and CK18 whilst the basal cells express CK5, CK14 and p63. CK19 and glutathione S-transferase pi (GSTpi) are expressed in both the luminal and basal layers; in the basal layer expression is global whilst only a proportion of luminal cells express CK19 and GSTpi. This subset of luminal cells is thought to be a population of immature luminal cells which have not yet fully differentiated. Canalization occurs starting at the proximal ducts closest to the urethra and continuing into the branches of the prostatic ducts(Wang *et al.*, 2001).

By the 15th week of gestation, the prostate epithelial cells are functional as determined by their ability to secrete PSA (Wang *et al.*, 2001). The final cell type identified within prostate glands, NE cells, can be identified by week 12 and are seen in 100% of prostates by week 20 (Xue *et al.*, 2001). These cells are rare and can be characterised due to expression of chromogranin A and absence of AR and PSA (Wang *et al.*, 2001). The precise origin of these cells is controversial. One model suggests that NE cells are a result of differentiation of basal prostate stem cells due to the expression of basal cell markers in NE cells (Bonkhoff and Remberger, 1996). An alternative explanation is that the NE cells have migrated from the neural crest. A recent publication using three-dimensional (3D) reconstruction of serial sections of human foetal prostates stained for chromogranin found a pattern of positive cells which suggest migration of cells from the neural crest to the prostatic epithelium (Szczyrba *et al.*, 2017).

The UGM concurrently differentiates under influence of the developing prostate epithelium to form the layer of fibromuscular stroma which surrounds the epithelial ducts (Hayward and Cunha, 2000). This reciprocal interaction is evidenced by tissue recombination experiments whereby UGM grafted alone forms small amounts of smooth muscle, whilst UGM grafted in combination with UGE generates prostatic ducts surrounded by smooth muscle sheaths (Cunha *et al.*, 1983).

Proliferation in the developing human prostate is highest during the first half of gestation, particularly in the budding tips where the proliferative rate is at least twice that of cells in the acini and collecting ducts. Initially both basal and luminal cells proliferate, but over time proliferation decreases in luminal cells. Stromal cells are also highly proliferative during this time. Postnatally, the prostate gland is quiescent until puberty when an increase in testosterone level stimulates proliferation of the prostatic epithelial cells and formation of the complex adult prostate gland (Wang *et al.*, 2001).

1.3 Factors important for prostate development

Although the precise mechanisms of human prostate development are not known, several growth factors, proteins and receptors have been implicated in prostate morphogenesis. Whilst these may control prostate development in part, they do not explain the interactions required for prostatic development. In particular, the complete spectrum of mesenchymal factors which act to drive differentiation of prostatic epithelium via androgenic action remain unknown (Marker *et al.*, 2003).

1.3.1 Nkx3.1

Nk3 homebox 1 (Nkx3.1) is critical for prostate development and is one of the earliest prostate markers, expressed in areas where prostatic buds will emerge and subsequently throughout the prostatic epithelium. *Nkx3.1* mutant mice can form prostate glands however these have a significant reduction in the number of ducts and secretory proteins (Bhatia-Gaur *et al.*, 1999). Further evidence for the importance of Nkx3.1 comes from a recent study which found that viral expression of Nkx3.1 in seminal vesicle epithelium results in formation of prostatic tissue when combined with wild type UGM *in vivo*. In contrast, normal seminal vesicle epithelium in combination with UGM forms seminal vesicle. In further support for the role of Nkx3.1 in prostate specification, the RWPE1 cell line, which has a basal phenotype and low levels of prostate markers, could form prostate-like tissue in a tissue

recombination assay when Nkx3.1 was overexpressed, whilst control RWPE1 cells failed to grow. Nkx3.1 was shown to interact with the histone methyltransferase G9a, and depletion of G9a with a short hairpin ribonucleic acid (RNA) (shRNA) impaired Nkx3.1 induced prostate differentiation. Depletion of the Nkx3.1 target gene UTY also impaired prostate differentiation, suggesting that Nkx3.1 is regulated by both G9a and UTY, and that this interaction is required for prostate differentiation (Dutta *et al.*, 2016). A separate study has also implicated Nkx3.1 as a master regulator of prostate differentiation. Reprogramming omouse embryonic fibroblasts (MEFs) to pluripotency using the Yamanaka factors octamer-binding transcription factor 4 (OCT4), SRY (Sex determining region)-related HMG-box gene 2 (SOX2), kruppel-like factor 4 (KLF4) and c-MYC was followed by lentiviral expression of NKX3.1, AR and FOXA1. These "induced epithelial cells" were then recombined with UGM and engrafted under the renal capsule of mice. The generated tissue contained CK8/18 positive luminal cells and p63/CK5 positive basal cells, and showed expression of AR, Nkx3.1 and the mouse prostate secretory protein probasin (Talos *et al.*, 2017).

1.3.2 FOXA1 and FOXA2

Forkhead box A1 (FOXA1) is a regulator of AR-mediated transcriptional activity (Gao *et al.*, 2003). It is present in all cells of the mouse UGE from embryonic day 18 (E18) and this expression persists in the adult prostate epithelium. Prostate rudiments from *Foxa1*$^{-/-}$ mice are identical to wild type rudiments, confirming that FOXA1 is not required for prostate formation. However, when grafted under the renal capsule of male mice, *Foxa1-/-* tissues showed altered luminal differentiation with co-expression of the luminal marker CK8 and the basal marker p63. Rather than formation of clear lumens, these cells formed solid epithelial cords. In comparison with wild type prostate there was an expansion in both basal and smooth muscle cells. Overall this suggests that FOXA1 is important for normal prostate ductal morphogenesis and differentiation (Gao *et al.*, 2005).

In contrast, Forkhead box A2 (Foxa2) expression is restricted to early prostatic development where it localizes to areas of epithelial budding (Mirosevich *et al.*, 2005). In *Foxa1*$^{-/-}$ prostate epithelium, Foxa2 expression persists although it is unable to rescue prostatic morphogenesis, suggesting that the two proteins have important but different roles in prostate development (Gao *et al.*, 2005).

1.3.3 Homeobox containing transcription factors

The homeobox (HOX) containing transcription factors HOXA13 and HOXD13 both play a role in prostate morphogenesis (Marker *et al.*, 2003). Mutation or deletion of either factor in mice results in reduced prostatic size and branching morphogenesis (Podlasek *et al.*, 1997; Podlasek *et al.*, 1999a). In the rodent, a specific *Hox* "code" seems to characterise each accessory gland. Whilst all prostate glands showed high expression of all *Hox*13 genes, they could each be distinguished by specific *Hox* expression (Huang *et al.*, 2007). In addition, *Hoxa*-10 knockout mice show reduced size and branching of the anterior prostate (Podlasek *et al.*, 1999b).

1.3.4 Fibroblast growth factors

Fibroblast growth factors (FGF) have key roles in the developmental of several organs (Meeks and Schaeffer, 2011). FGF7 is expressed in the rat ventral prostate mesenchyme whilst its receptor FGFR2b is localised to the ventral prostate epithelium, suggesting secretion of FGF7 from the mesenchyme acts in a paracrine manner on the prostate epithelium. Whilst branching morphogenesis of the neonatal rat ventral prostate is dependent on testosterone, in the absence of testosterone, FGF7 can stimulate ventral prostate growth and branching morphogenesis at a similar level to that of testosterone. Blocking of FGF7 with a monoclonal anti-FGF7 antibody or through use of peptide 412 which binds FGF7 and competes with FGFR2b results in an overall inhibition of ventral prostate growth and branching morphogenesis (Sugimura *et al.*, 1996). These observations indicate that FGF7 has a critical role in the normal development of the prostate, at least in rodents.

Another FGF family member, FGF10, is a known regulator of lung and limb development (Min *et al.*, 1998). It is expressed in both the prostate and seminal vesicle mesenchyme, with its highest expression occurring during early organogenesis and neonatal growth. In the absence of testosterone, FGF10 can stimulate development of both prostate and seminal vesicle in organ culture experiments, and these effects are not altered by the presence of anti-androgens, suggesting that FGF10 is not regulated by androgens (Thomson and Cunha, 1999). *In vivo*, absence of *Fgf*10 results in lack of prostatic budding from the UGS in mice which is partially reversed by supplementation with FGF10 and testosterone (Donjacour *et al.*, 2003).

1.3.5 Conserved developmental signalling pathways

Sonic hedgehog (Shh) is part of the hedgehog signalling pathway which results in upregulation of *Shh* genes via Gli transcription factors. Shh is expressed in the UGE whilst its receptor patched and the downstream transcription factors Gli1 and Gli2 are expressed in the UGM surrounding areas of prostatic buds (Lamm *et al.*, 2002). Whilst *Shh* mutant embryos are unable to generate prostates, they can form prostatic tissue positive for Nkx3.1 when combined with wild-type UGM in tissue recombination experiments. Furthermore, supplementation with androgens in both pregnant mice and organ culture experiments rescued the prostatic defect, suggesting that Shh plays a role in prostatic patterning but not initial organ development (Berman *et al.*, 2004).

Another conserved signalling pathway which has been implicated in prostate development is the Wnt pathway. Wnt5a is expressed in the UGM prior to and during bud formation, and is specifically localised around areas of emerging buds. In addition, *Wnt5a* null foetuses either do not form a UGS or have prostatic budding defects. However, testosterone in *Wnt5a* null foetuses was also greatly reduced, and when wild-type UGS were grown in organ culture with DHT and a WNT5A inhibitory antibody, budding was not affected, confirming that it is testosterone and not WNT5A which is required for prostate bud formation. Addition of WNT5A to wild-type UGS organ cultures resulted in a decrease in prostatic budding and was shown to impair ventral prostate development in *in vivo* grafts. Overall, this suggests that Wnt5a is secreted from the UGM and acts as a negative regulator of the UGE (Allgeier *et al.*, 2008).

1.3.6 Bone morphogenetic proteins

The UGS mesenchyme also expresses the bone morphogenetic proteins (BMP) BMP4 and BMP7. BMP4 is highly expressed in mouse UGS from E14 until birth. When UGS in organ culture were supplemented with BMP4, prostate epithelial growth was significantly reduced whilst mesenchymal growth did not change, suggesting that BMP4 specifically inhibits epithelial cell proliferation. Quantification of prostatic buds in organ culture of mouse prostate rudiments showed that BMP4 inhibits budding in a dose dependent manner (Lamm *et al.*, 2001). Interestingly, the BMP inhibitor Noggin is also expressed in the mouse UGM and is required for ventral prostate development and budding by opposing BMP4 inhibition of epithelial cell proliferation (Cook *et al.*, 2007).

BMP7 is also expressed in the UGM before bud formation, and then appears in the UGE around the budding tips. As with BMP4, BMP7 inhibits prostate morphogenesis in organ culture experiments, and in BMP7 null mouse prostates, branching is increased. BMP7 was shown to interfere with Notch signalling in the prostate epithelium, which is usually concentrated around areas of bud formation. However, addition of FGF10 could neutralise BMP7 mediated inhibition of Notch signalling, suggesting that FGF10 and BMP7 act to regulate Notch signalling in prostatic development (Grishina *et al.*, 2005). Removal of Notch1 expressing cells in mice inhibits branching morphogenesis, growth and differentiation in organ culture of postnatal prostates (Wang *et al.*, 2004).

1.4 Diseases of the prostate

1.4.1 Benign prostatic hyperplasia

The prostate is associated with several conditions resulting in morbidity and mortality. The most highly prevalent prostatic disease is benign prostatic hyperplasia (BPH), defined as a non-malignant growth of the prostate (Roehrborn, 2005) which occurs as a result of epithelial and stromal cell proliferation in the transitional and periurethral zones of the prostate (Untergasser *et al.*, 2005). BPH is strongly correlated with advancing age, with autopsy studies showing histological evidence of the condition in only 10% of men in their 30's, rising sharply to 80-90% of men aged 70-80 (Roehrborn, 2002). BPH itself may not be problematic, but it can be associated with lower urinary tract symptoms (LUTS), particularly in elderly men where up to 50% develop LUTS due to BPH or benign prostatic enlargement (BPE) (Untergasser *et al.*, 2005). LUTS may be divided into two categories; obstructive and irritative symptoms. Obstructive symptoms include straining, urinary retention, hesitancy and weak flow. Irritative symptoms are often more troublesome to the patient and consist of increased frequency and urgency, nocturia and pain. BPH is also associated with bladder outlet obstruction, defined as a pressure gradient at the bladder neck or prostatic urethra (Roehrborn, 2005). BPH represents a serious medical issue due to its association with serious complications including urinary tract infections, haematuria and urinary retention. In particular urinary retention is painful and when chronic can result in renal failure (Thorpe and Neal, 2003).

The precise cause of BPH is debated, with several potential contributors. One of the earliest suggested causes was the theory of "embryonic reawakening" proposed by McNeal, whereby the inductive ability of the prostatic stroma results in renewed

growth of the epithelium (McNeal, 1978). This is supported by studies showing the ability of embryonic UGM to induce formation of prostate epithelial glands from adult rodent urothelium (Cunha *et al.*, 1983). An alternative explanation has also been proposed by Lin et al., who found that stromal cells in BPH patients express mesenchymal stem cell markers and are able to differentiate into a number of cell lineages, suggesting a role of stem cells in the development of BPH (Lin *et al.*, 2007).

Treatment for BPH generally consists of drug treatment with α antagonists and/or 5α-reductase inhibitors or surgical intervention which can range from minimally invasive options such as thermotherapy to transurethral resection of the prostate (TURP) (Wilt and N'Dow, 2008). TURP is the standard method of surgical BPH management however it is associated with several risks including urinary tract infection (3.6% of patients) and severe blood loss requiring transfusion (2.9% of patients) (Reich *et al.*, 2008).

1.4.2 Prostate cancer

Prostate cancer is the second most common malignancy in the UK accounting for 46,700 new cases in 2014 alone. In males, prostate cancer is the most common cancer and rates of incidence have increased 6% in the last decade. Prostate cancer is strongly age-associated, with 54% of prostate cancer cases identified in men aged 70 or over, and is predicted to rise in incidence by 12% between 2014 and 2035 (Cancer Research UK).

Currently, treatment for localised tumours consists of surgery, radiotherapy or active surveillance. In advanced or metastatic disease, androgen deprivation therapy (ADT) is the mainstay and may be carried out using either surgical or chemical castration to reduce androgen synthesis and circulating androgens (Harris *et al.*, 2009). This is based on the dependence of the prostate gland on androgenic signalling. Androgens are critical for both normal prostate development and prostate cancer, and elicit their action through activation of the nuclear transcription factor AR. Testosterone, produced by the Leydig cells of the testes and adrenal glands is present in the circulation whilst in the prostatic tissue itself, the major androgen is DHT. Generation of DHT is mostly due to conversion of testosterone by 5α-reductase enzymes within tissues including the prostate and skin, although 25% of circulating DHT is secreted by the testes (Imamoto *et al.*, 2008).

Despite the initial success of ADT, many patients go on to develop androgen-independent disease, termed castrate resistant prostate cancer (CRPC) within 12-18 months (Marques *et al.*, 2010). CRPC is associated with a poor prognosis particularly due to the presence of metastases in over 84% of patients at the time of diagnosis with CRPC (Kirby *et al.*, 2011). At this stage, treatment is predominantly palliative (Berruti *et al.*, 2005), and median survival is 9-13 months (Kirby *et al.*, 2011). As a result, further research into the development of prostate cancer is necessary to facilitate new treatment strategies for this disease. However, current models available for research limit this progress.

Interestingly, embryogenesis has been implicated in both BPH and cancer. In BPH, the embryonic reawakening theory of McNeal suggests that the stromal epithelial interactions which occur during normal prostate development are reactivated later in life with the prostatic stroma inducing new epithelial growth (McNeal, 1978). In several cancers, embryonic stem cell-like gene expression signatures are associated with poorly differentiated tumours (Ben-Porath *et al.*, 2008). Gene expression analysis of mouse UGS from day E16-17 found that androgen exposure during this time results in expression of genes which have been implicated in prostate carcinogenesis including Wnt and FGFs as well as components of the phosphatase and tensin homologue (PTEN)/phosphoinositide 3-kinase (PI3K)/mechanistic target of rapamycin (mTOR) signalling pathway. Cancer hallmarks including angiogenesis and migration were also upregulated in response to androgen exposure. Furthermore, invasive cancers showed increased expression of developmental genes, providing further evidence for a role of developmental processes in prostate carcinogenesis (Schaeffer *et al.*, 2008). An embryonic stem cell (ESC) gene predictor signature could also estimate survival in a cohort of prostate cancer patients (Peng *et al.*, 2014). In further support of the role of developmental genes in prostate carcinogenesis, overexpression of the ESC marker NANOG results in tumour regeneration and castration-resistant tumour formation in the DU145 and LNCaP prostate cancer cell lines respectively (Jeter *et al.*, 2011).

1.5 Current models for prostate development and disease

1.5.1 Cell lines

Essentially there is a lack of relevant human prostate models to study development and disease. Historically, two-dimensional (2D) *in vitro* cell line cultures have been widely used to study prostate cancer. Despite the high prevalence of prostate cancer, a very limited number of cell lines are available in public repositories, primarily due to the difficulty in growing prostate cancer cells *in vitro* (Gao *et al.*, 2014). Such cell lines are derived from individual cases of prostate cancer, which is known to be highly heterogeneous, and therefore the major commonly used lines (DU145, PC3 and LNCaP) are not representative of the complex heterogeneity of the disease as a whole (van Bokhoven *et al.*, 2003). Prostate cancer cell lines also show a wide range of characteristics and androgen responsiveness. For example, the LNCaP cell line is androgen-dependent, luminal-like and expresses mutant AR whilst PC3 does not express AR, is androgen-independent and has a basal/intermediate cell phenotype (van Bokhoven *et al.*, 2003). In each cell line, AR has a different role, and this can also depend on the specific cell culture method used, therefore use of single cell lines for AR research is disadvantageous (Yu *et al.*, 2009b). Furthermore, analysis of commonly used human prostate cancer cell lines identified heterogeneity within cell lines resulting from genetic and phenotypic drift (van Bokhoven *et al.*, 2003). A significant number of AR binding sites identified in CRPC are not present in prostate cancer cell lines, further demonstrating their lack of suitability for studies of this disease (Sharma *et al.*, 2013). Finally, cell line cultures lack both the complex environment and surrounding cells which are important in tumour biology (Kamb, 2005).

In addition to prostate cancer cell lines, benign prostate epithelial cell lines are also available. The majority of these were generated from primary prostate cells which were immortalised using simian virus 40 (SV40). Such cell lines are easy to grow and can be maintained for many passages. However, immortalisation of cells using methods such as SV40 results in interference with normal cellular processes (May *et al.*, 2004). In addition, several of these cell lines do not show expression of AR or PSA, and do not respond to androgen (summarised in Table 1-1).

Cell line	Characteristics	Reference
PNT1A	AR+ PSA- after passage 10 No response to DHT	(Cussenot *et al.*, 1991)
BPH-1	CK8/18/19+ AR/PSA- No response to DHT	(Hayward *et al.*, 1995)
PWR-1E	AR/PSA+ (after synthetic androgen stimulation) DHT responsive	(Webber *et al.*, 1996)
PNT2-C2	CK8+ (strong), weakly CK1/5/10/14 PSA/PSMA+	(Cussenot *et al.*, 1991; Berthon *et al.*, 1995; Lang *et al.*, 2001a)
RWPE-1	CK8/18+, weakly CK5/14+ AR, PSA+ (after synthetic androgen stimulation) Growth stimulation in response to androgen	(Bello *et al.*, 1997)

Table 1-1. Benign prostate cell lines and their characteristics. PSMA= prostate specific membrane antigen.

1.5.2 Primary culture

The limitations of cell lines for studying prostatic development and disease can be circumvented with the use of primary prostate cells collected from patients, typically from those undergoing bladder or prostate surgery. Primary cultures of epithelial and stromal cells from normal and malignant tissue as well as from BPH have been established (Lee and Peehl, 2004). In contrast with cell lines, primary culture more accurately represents the in vivo tissue, making them an attractive option for *in vitro* research (Rhim *et al.*, 2011).

However, cultured human cells *in vitro* have a limited capacity for division (Shay and Wright, 2000). As with cell lines, when cultured *in vitro* primary cells are deprived of their normal microenvironment and interactions with other cell types which may influence their growth and behaviour. Despite the importance of AR signalling in the prostate, most normal prostate epithelial cultures show no or low expression of AR and PSA although AR messenger RNA (mRNA) is expressed. This is consistent with the notion that the majority of primary prostate epithelial cells in culture display a basal phenotype with expression of CK5/14 and proliferative ability (Peehl, 2005). As

the luminal cells represent the major epithelial cell in the prostate, attempts have been made to grow primary luminal prostate epithelial cells in culture. Whilst some improvements have been made, for example addition of retinoic acid to culture medium which can increase the expression of luminal cytokeratins (Peehl *et al.*, 1994), growth of these cells in primary culture remains difficult, particularly due to the low replicative rate in luminal cells, as the vast majority (70%) of proliferating cells within normal and hyperplastic prostate acini are of a basal phenotype (Bonkhoff *et al.*, 1994). Furthermore, acquisition of primary human cells is complex and their expansion is difficult.

1.5.3 Animal models

The use of animal experiments provides an *in vivo* setting to study prostate development and disease. In prostate biology, rodents are commonly used. However, there are several inherent differences between rodent and human prostate anatomy, including the presence of distinct lobes in rodent prostate which are lacking in the adult human prostate as well as the difference in cellular composition, as the human prostate epithelium consists of two defined cell layers whilst the mouse prostate epithelium consists of a single mixed layer of cells (Packer and Maitland, 2016). In addition the thick fibromuscular stroma present in the human prostate is absent in rodents (Shappell *et al.*, 2004). This is critical as the stroma is known to be important in both normal development and carcinogenesis of the prostate (Cunha *et al.*, 2002). Furthermore, rodents have an extremely low incidence of both neoplastic and non-neoplastic disorders in the prostate, putting their suitability as a model for such diseases under scrutiny (Shappell *et al.*, 2004). The high telomerase activity within the mouse is also problematic when attempting to model human cancers. Telomerase activity results in immortalization of cells and so malignant transformation occurs with less genetic changes than would be required in the human. Furthermore, the presence of high telomerase activity means that genetic instability cannot be studied (Cheon and Orsulic, 2011).

An alternative is the use of xenograft models such as that performed by Saffarini et al using human foetal prostate tissue implanted beneath the renal capsule of immunodeficient mice. By day 7 proximal to distal growth was evident with the appearance of secondary buds and the differentiation of initial buds to secretory acinar epithelium formed from basal and luminal cells surrounded by connective tissue. By day 200, the xenografts showed a 16-fold increase in weight along with

further vascularisation and the formation of canalized acini and ducts from solid buds. Ki67, a marker of proliferation was highly expressed at days 7 and 30 but decreased by day 200 in both epithelia and stroma, consistent with the enhanced growth rate of the prostate during early foetal growth (Saffarini *et al.*, 2013). Whilst this model provided knowledge of human foetal prostate development, studies using foetal human tissue are ethically controversial and not readily accessible.

1.5.4 Spheroid and organoid based models

Several studies have used primary prostate epithelial cells to generate 3D spheroids which more closely mimic the *in vivo* environment through the use of extracellular matrices (ECM). Human prostate epithelial cell lines grown in Matrigel, a commercial ECM, along with the presence of serum, testosterone, oestrogen and stromal cells generated spheroids with evidence of both functional and morphological differentiation specific to prostate. Whilst prostate epithelial cells grown in serum free media in Matrigel form solid spheres, the addition of serum, testosterone, oestrogen and stromal cells resulted in lumen formation, epithelial cell polarisation and expression of AR (Lang *et al.*, 2001b).

Recent advances in cell culture have led to the development of organoid based culture methods. Organoids are defined as 3D structures containing multiple cell types which are representative of the organ of origin in terms of both structure and function (Wang *et al.*, 2017). The first major organoid paper was based upon the culture model developed by Sato et al., which allowed generation of mouse intestinal organoids from single Lgr5-positive intestinal stem cells using defined media containing the factors R-spondin 1, Noggin and epidermal growth factor (EGF). The organoids resembled intestinal crypts and contained stem cells, Paneth cells, transit amplifying (TA) cells, enterocytes, goblet cells and enteroendocrine cells. Furthermore, the organoids could be passaged for more than 8 months, allowing expansion of the original cells (Sato *et al.*, 2009).

This protocol was modified to allow growth of human colonic organoids by addition of several factors to the murine organoid medium including nicotinamide, A83-01 (an Alk inhibitor) and SB202190 (a p38 inhibitor) (Sato *et al.*, 2011). Subsequently, this method has been used to generate human organoids from adult cells of several tissues including, liver (Huch *et al.*, 2015), pancreas (Boj *et al.*, 2015) and prostate (Karthaus *et al.*, 2014). Human organoids from pluripotent stem cells have also been

generated for a number of organs including lung (Chen *et al.*, 2017), intestine (Spence *et al.*, 2011) and kidney (Takasato *et al.*, 2015).

Several groups have further investigated the use of organoid culture for propagation of primary prostate cells. Single human primary prostate epithelial cells seeded into Matrigel in the organoid medium described above with the addition of FGF2, FGF10, prostaglandin E2, A83-01, nicotinamide, the p38 inhibitor SB202190 and DHT formed solid multi-layered spheres which further differentiated to form organoids with a visible lumen consisting of mostly CK8 positive luminal cells with some basal cells as evidenced by p63 and CK5 expression. However, no NE cells were identified. These organoids expressed Nkx3.1 and AR and were hormonally responsive as evidenced by PSA secretion in response to stimulation by DHT. The organoids could be successfully passaged for over 12 months (Karthaus *et al.*, 2014). This method was also used to generate organoids from patients with metastatic prostate cancer. The organoids are representative of the histology of the original patient sample and retained these histological features following in vivo engraftment. However, the efficiency of organoid generation was only 15-20%, due to overtaking of the tumour samples by normal prostate epithelium or tumour-associated spindle cells (Gao *et al.*, 2014). Additionally, attempts to recreate such organoid formation from non-metastatic prostate cancer has been unsuccessful (Karthaus *et al.*, 2014).

Similarly, a method for organoid formation from a luminal epithelial progenitor population of castration-resistant NKX3.1 expressing cells (CARNs) using growth of cells in 3D Matrigel culture with hepatocyte medium and EGF was also used for primary prostate epithelial cells. Epithelial cells from radical prostatectomy samples could generate spheroids with an outer layer of double positive intermediate cells expressing the basal and luminal markers p63 and CK8, and an inner layer of luminal cells expressing CK8 alone. The organoids showed evidence of cystic morphology but no lumen formation was seen (Chua *et al.*, 2014).

1.6 Stem cells for developmental and disease modelling

Stem cells are undifferentiated cells defined by their ability for self-renewal and differentiation into both progenitor and terminally differentiated cells (Wagers and Weissman, 2004). Stem cells are classified based on their developmental potential: totipotent cells, found in the zygote and early blastomeres are able to generate both embryonic and extra-embryonic cell types; pluripotent cells can develop into all cell

lineages of the embryo; multipotent cells can generate a range of cell types within a specific lineage; and unipotent cells can generate a single cell type (Wagers and Weissman, 2004; Jaenisch and Young, 2008). There are three major categories of human stem cells; human embryonic stem cells (hESCs), adult stem cells and induced pluripotent stem cells (iPSCs).

1.6.1 Human embryonic stem cells

hESCs were first isolated in the Thomson laboratory from donated human embryos which were cultured to the blastocyst stage. The derived cell lines showed typical stem cell characteristics including a large nucleus, high telomerase activity and grew in colonies. The cells expressed stage-specific embryonic antigen (SSEA)-3, SSEA-4, TRA-1-60, TRA-1-81 and alkaline phosphatase, which are characteristic of undifferentiated nonhuman primate ESCs and embryonal carcinoma cells. The hESCs could from teratomas consisting of the three embryonic germ layers; mesoderm, endoderm and ectoderm, upon injection into severe combined immunodeficient (SCID) mice, confirming their identity as pluripotent stem cells (Thomson *et al.*, 1998). Although the generation of these cells provided a new human model for human development and disease, they are associated with significant ethical issues due to their isolation from human embryos, primarily from those which are surplus to *in vitro* fertilisation (IVF) requirements. As a result, stringent restrictions are in place for use of hESCs.

1.6.2 Adult stem cells

In somatic tissue, adult stem cells exist to replace and regenerate mature cell types. Adult stem cells are known to exist in several tissues including intestine, skin, blood, and muscle. However, markers defining these populations are largely unknown, making isolation of stem cells difficult (Wagers and Weissman, 2004).

Traditionally, adult stem cells were believed to differentiate only to cells from their tissue of origin; however recent studies have shown that some adult stem cells can transdifferentiate to other lineages (Wagers and Weissman, 2004). For example, haematopoietic stem cells (HSCs), which usually differentiate to a range of haematopoietic cell lineages (Kondo *et al.*, 2003), have been shown to contribute at low frequencies to a range of other tissues. Following irradiation and bone marrow replacement with male bone marrow cells in female recipients, Y chromosome

positive cells could be identified in the bronchus, oesophagus, stomach and hair follicles, confirming the plasticity of HSCs (Krause *et al.*, 2001).

1.6.3 Stem cells in the prostate

Upon castration, the prostate regresses, but if supplied with testosterone it can regenerate, providing evidence for the presence of stem cells within the prostate (Isaacs, 1985). In the mouse prostate, 5′-bromo-2′-deoxyuridine (BrdU) incorporation experiments identified a population of epithelial cells within the proximal prostatic ducts which were slow cycling and showed an enhanced proliferative potential *in vitro*. These proximal cells could also generate glandular structures consisting of basal and luminal cells, and which were capable of prostatic secretions when seeded into collagen gels (Tsujimura *et al.*, 2002). This is in accordance with the notion of prostate stem cells being localised to the proximal ducts. To isolate and study adult stem cells, markers of these cells must be identified. In the prostate, several stem and progenitor cell markers have been described.

$\alpha 2\beta 1$

As stem cells are known to associate with the basement membrane, study of specific integrins can be used to identify stem cells in a range of tissues (Jones *et al.*, 1995; Li *et al.*, 1998; Shinohara *et al.*, 1999). Using this strategy, Collins et al., found a rare subpopulation of human prostatic basal cells (1% of all basal cells) with increased $\alpha 2$ integrin expression (termed $\alpha_2\beta_1^{hi}$ cells). These cells could be directly selected by rapid adhesion to collagen I and showed evidence of stem cell characteristics including a fourfold greater colony forming ability compared to the total basal cell population *in vitro*. Furthermore, unlike slow adherent cells, the rapidly adherent population could form differentiated prostate epithelium when engrafted into nude mice with human stroma (Collins *et al.*, 2001).

CD133

CD133, a known cell surface marker of human HSCs (Yin *et al.*, 1997), has also been identified as a marker of human prostate stem cells. Approximately 1% of basal cells in the human prostate express CD133, and these cells are limited to the $\alpha_2\beta_1^{hi}$ population previously described by Collins et al. Ki67 staining indicated that this $CD133^+$ population represents a group of quiescent basal cells. $CD133^+$ selection of the $\alpha_2\beta_1^{hi}$ population found that this subpopulation has the highest proliferative

capacity, generating over twice the number of cells as the $CD133^-$ population. As for the $\alpha_2\beta_1^{hi}$ cells, $CD133^+$ cells were capable of forming fully differentiated prostate epithelium *in vivo* (Richardson *et al.*, 2004). However, a subsequent study investigating CD133 expression in the human prostate found that its expression is not specific to stem cells in the basal compartment, but is also present in a subpopulation of luminal cells (Missol-Kolka, 2011). Therefore, the murine model of CD133 as a prostate stem cell marker does not fully mirror the human prostate.

p63

p63, a homologue of the tumour suppressor protein p53, is a marker of basal prostate epithelial cells and has also been implicated in prostate development, with no ductal or epithelial budding structures identified in newborn *p63-/-* male mice (Signoretti *et al.*, 2000). More recently, using lineage tracing of knock-in mice expressing Cre recombinase under the control of the *ΔNp63* promoter, Pignon et al., were able to show that ΔNp63-positive cells generated all epithelial lineages of the prostate, implicating p63 as a marker of prostate epithelial stem cells (Pignon *et al.*, 2013).

CARNs

Despite considerable evidence for the presence of basal stem cells in the prostate, it has been shown that UGS from p63 null mice are able to form prostatic tissue when grafted into male adult mice, suggesting the presence of a luminal prostate stem cell, although the generated tissue lacked basal cells (Kurita *et al.*, 2004). However, other studies have shown that p63 null mice do not develop prostates (Signoretti *et al.*, 2000). Nkx3.1, which is critical in prostate development, is lost after castration and subsequently restored after addition of androgens. However, a rare population of cells (corresponding to 0.7% of the anterior prostate in androgen-deprived male mice) retain expression of Nkx3.1 after castration. These cells are termed castration-resistant Nkx3.1-expressing cells (CARNs). CARNs express CK18 and AR but lack basal markers, and are growth quiescent as determined by lack of Ki67 expression. Interestingly, CARNs can generate both luminal and basal epithelial cells, and can self-renew *in vivo*. Furthermore, single CARNs can generate prostatic ducts which express basal, luminal and NE markers and are secretory in function (Wang *et al.*, 2009). Overall, this suggests CARNs represent a rare luminal stem cell population in the prostate.

DLK1

Delta-like homolog 1(Dlk-1), a member of the epidermal growth factor-like family was initially implicated as putative prostate stem cell marker due to its expression in candidate prostate epithelial stem cells and its suppression following culture of primary cells (Ceder *et al.*, 2008). Subsequently, Moad et al., used *in situ* lineage tracing and 3D reconstruction of adult human prostates and identified discrete stem cell niches located at the junction between the proximal ducts and the urethra (Moad *et al.*, 2017). Using laser capture microdissection of these areas and mRNA sequencing, DLK1 was identified as being highly upregulated in the niche area. This finding was validated by immunofluorescence, which showed that DLK1 is co-localised with the basal cell marker α6-integrin. By sorting primary prostate basal cells into $DLK1^{+ve}$ and $DLK1^{-ve}$ populations and subsequent 3D spheroid culture, clear differences could be identified. Whilst $DLK1^{-ve}$ cells could form spheroids, these could not be serially passaged and became exhausted by 6-8 weeks of culture. In addition, the spheroids expressed only luminal markers CK8, AR and PSA. In contrast, $DLK1^{+ve}$ cells could be successfully serially passaged beyond 8 weeks and formed acinar and ductal structures consisting of both basal and luminal cells. These findings suggested that DLK1 enriches for basal prostate stem cells.

Although a number of putative prostate stem cell markers have been suggested, lack of a definitive marker profile (Takao and Tsujimura, 2008) and the limited ability for long term culture limits the application of such cells for research.

1.7 Pluripotent stem cell culture

Human pluripotent stem cells have a characteristic morphology, growing in flat colonies with distinct borders consisting of compact, round cells with a high nuclear to cytoplasmic ratio and prominent nucleoli. Changes from this typical morphology usually represent differentiation of the cells, which typically occurs around the edges of the colonies (Amit, 2012).

Early hESC culture was dependent on the use of feeder cells, predominantly mitotically inactivated MEFs, for maintenance of the pluripotent state. MEFs provide both an ECM and secrete growth factors which play a role in stem cell proliferation and maintenance (Celiz *et al.*, 2014). Traditionally, this feeder-dependent culture system was used in combination with Dulbeccos' modified Eagle medium (DMEM) containing 20% foetal calf serum (FCS) (Thomson *et al.*, 1998; Reubinoff *et al.*,

2000). As technology has progressed, a move away from undefined and animal-based components has occurred. This is particularly important for therapeutic use of pluripotent stem cell, as animal-derived products can contain pathogens (Celiz *et al.*, 2014).

To address part of this issue, a serum free media specifically developed for culture of mESCs; KnockOut DMEM (KO DMEM) with 20% KnockOut Serum Replacement (KOSR), was used in combination with 4ng/ml bFGF to culture hESC lines (Amit *et al.*, 2000). The same group went on to show that use of human foreskin fibroblasts in combination with KO DMEM, KOSR and bFGF could maintain the growth and characteristics of hESCs after prolonged culturing (Amit *et al.*, 2003).

The first feeder-free hESC culture system tested MEF conditioned medium with a range of ECM and found that MEF conditioned medium (CM) used with Matrigel or laminin allowed successful culture of hESCs (Xu *et al.*, 2001). Matrigel is an extracellular matrix isolated from Engelbreth-Holm-Swarm murine sarcoma tumour, consisting of several components including laminin, collagen and heparin sulphate proteoglycan which is now widely used for stem cell culture (Kleinman *et al.*, 1986; Mallon *et al.*, 2006).

A major improvement in pluripotent stem cell culture was the development of a completely defined stem cell culture medium, TeSR1 which contains bFGF, transforming growth factor beta (TGFβ), pipecolic acid, γ-aminobutyric acid (GABA), lithium chloride and human serum albumin (Ludwig *et al.*, 2006). mTeSR1, a modified version of TeSR1 which contains bovine serum albumin and bFGF was later developed to reduce costs where a xeno-free medium is not required (Celiz *et al.*, 2014). Further optimisation resulted in development of Essential 8 (E8) medium, which contains only 8 components; insulin, selenium, transferrin, L-absorbic acid, bFGF, TGFβ and sodium bicarbonate ($NaHCO_{3)}$ in a DMEM/F12 base medium. In combination with vitronectin, this provided a completely xeno-free culture system for hESCs and iPSCs (Chen *et al.*, 2011).

Inclusion of a Rho-associated kinase (ROCK) inhibitor Y-27632 into pluripotent stem cell culture systems reduces apoptosis in hESCs following dissociation resulting in improved survival and increased cloning efficiency, even in serum-free media (Watanabe *et al.*, 2007). This finding was critical for improving viability of single cell hESCs and iPSCs and thus their downstream applications.

1.8 Characterisation of pluripotent stem cells

To confirm cells as true pluripotent stem cells, several tests are required as recommended by the International Stem Cell Banking Initiative (ISCBI). This includes analysis of ESC markers, pluripotency testing to confirm differentiation capacity both *in vitro* and *in vivo*, karyotype analysis to confirm genetic stability, deoxyribonucleic acid (DNA) fingerprinting to confirm identity of the cells and microbiological testing (International Stem Cell Banking Initiative, 2009).

1.8.1 ESC expression markers

Pluripotent stem cells express several markers which are used for characterisation. The first test which is generally performed on pluripotent stem cells is detection of alkaline phosphatase (AP), a membrane enzyme (Marti *et al.*, 2013). AP expression is a simple assay which can quantify undifferentiated stem cells colonies (O'Connor *et al.*, 2008) and allows for rapid indication of successful reprogramming (Singh *et al.*, 2012).

Following confirmation of AP positivity, complete immunostaining of pluripotent stem cells is required to confirm their pluripotency. A panel of markers including Oct4, Sox2, Nanog, Tra-1-60, Tra-1-81, stage specific embryonic antigen (SSEA) 3 and SSEA4 are used in human pluripotent stem cells (Marti *et al.*, 2013). Several other pluripotency markers are established for undifferentiated pluripotent stem cells including DNA Methyltransferase 3 Beta (DNMT3B), Growth Differentiation Factor 3 (GDF3), Teratocarcinoma-Derived Growth Factor 1 (TDGF1), Aminobutyric Acid Type A Receptor Beta3 (GABRB3) and Reduced Expression Protein 1 (REX1). In an analysis of 59 hESC lines, DNMT3B, GDF3, TDGF1 and GABRB3 showed strong correlation with NANOG expression (International Stem Cell Initiative *et al.*, 2007). REX1, a zinc-finger protein, is a known marker of pluripotency which is expressed in ESCs (Rogers *et al.*, 1991).

1.8.2 In vitro differentiation

To confirm their pluripotency, putative stem cells must also demonstrate the ability to form cells from the three embryonic germ layers; endoderm, mesoderm and ectoderm. *In vitro*, ESCs aggregate in suspension culture to form structures known as embryoid bodies (EBs) which express a range of germ layer-specific genes (Itskovitz-Eldor *et al.*, 2000). There are several techniques to generate EBs, although the most commonly used is to culture the ESCs in an environment which lacks the

factors required for maintenance of the undifferentiated state, such as removal of feeder cells or leukaemia inhibitory factor (LIF), and use of petri dishes rather than standard tissue culture ware to prevent adherence to the surface. As a result, ESCs will clump together to form EBs. Other methods for EB formation include hanging drop culture, where ESCs are cultured in small drops of media to encourage aggregation, or growth of the ESCs on stromal cells which promote differentiation. Following EB formation, EBs may be analysed for germ layer markers or subjected to further adhesion culture to allow outgrowth of adhesive cells (Keller, 1995). EBs can generate a wide range of differentiated cell types including hepatocytes, muscle, neuronal, endothelial and haematopoietic cells (Drab *et al.*, 1997; Itskovitz-Eldor *et al.*, 2000; Hamazaki *et al.*, 2001; Levenberg *et al.*, 2002).

1.8.3 In vivo differentiation

The most stringent test for pluripotency is the ability of cells to form a chimera, defined as an organism whose cells are derived from more than one fertilised egg (McLaren, 1976). Whilst this method may be used for characterisation of non-human stem cells such as mouse ESCs and iPSCs (Nagy *et al.*, 1993; Okita *et al.*, 2007), use of chimera formation assays or other methods involving creation of living organisms with human ECSs or iPSCs is not ethical (Smith *et al.*, 2009).

After chimeric contribution, teratoma formation is the most rigorous assay for pluripotency. This involves injection of the pluripotent cells into immunocompromised mice by subcuntaneous, intramuscular, intratesticular or kidney capsule injection. True pluripotent cells will form teratomas containing of benign cells of endodermal, ectodermal and mesodermal origin (Smith *et al.*, 2009). As a result, the ISCBI recommends that every banked pluripotent stem cells must be tested for teratoma formation in immunocompromised mice (International Stem Cell Banking Initiative, 2009).

1.9 Methods for cellular reprogramming

Due to the ethical and practical considerations of embryonic and adult stem cells for use in modelling development and disease, alternative models are required. One potential solution is the use of pluripotent stem cells (PSCs) generated by reprogramming somatic cells. As well as providing a limitless supply of cells for research, reprogramming somatic cells would allow generation of patient and disease specific models.

1.9.1 Somatic cell nuclear transfer

Reprogramming of somatic cells has been studied for decades with a variety of methods. The first method for reprogramming somatic cells was somatic cell nuclear transfer (SCNT), based on the original nuclear transplantation experiments established by Briggs and King (1952). In 1962, John Gurdon demonstrated that transplantation of adult frog intestinal epithelial cell nuclei into enucleated donor eggs generated normal feeding tadpoles, which subsequently matured into adult frogs (Gurdon, 1962; Gurdon and Uehlinger, 1966). This was the first evidence for the ability of somatic cells to be reprogrammed.

The ability of mammalian cells to replicate Gurdon's findings was investigated using adult mammary epithelium induced into quiescence and transplanted into a donor egg. This generated the first mammal cloned from an adult cell: Dolly the sheep (Wilmut *et al.*, 1997). This study confirmed that differentiated mammalian cells could also be reverted to an embryonic state, opening up a new avenue for developmental research and the potential for patient-specific transplantation (Jaenisch and Young, 2008). However, cloning via SCNT is very inefficient, ranging from 0-10% live births, and is associated with developmental defects, miscarriage and neonatal death (Tian *et al.*, 2003). It is also possible to generate ESCs from blastocysts produced by SCNT (Wakayama *et al.*, 2001). Termed nuclear transfer ESCs (ntESCs), these cells are generated with a much higher efficiency of ~20% (Yamanaka and Blau, 2010).

1.9.2 Cell fusion

A second method for reprogramming cells is by cell fusion of a somatic cell with an embryonic cell. Male mouse ESCs fused with female mouse thymocytes harbouring an Oct4 promoter driven green fluorescent protein (GFP) reporter generated hybrid cells which showed activation of the previously inactivated X chromosome as well as the Oct4 gene, and were confirmed as pluripotent cells by their ability to contribute to all 3 germ layers in chimeric embryos (Tada *et al.*, 2001). Similarly, hESCs can be fused with human fibroblasts to form hybrids with characteristics typical of hESCs including enhanced growth rate and marker expression. The hybrid cells were also capable of differentiation into the 3 embryonic germ layers both *in vitro* and *in vivo* (Cowan *et al.*, 2005). However, the cell fusion method for cellular reprogramming has several limitations. Despite the higher efficiency of reprogramming using this method (~95%), use of this technique is limited due to the tetraploidy of the resultant cell hybrids. As the cells still contain antigens from the ESCs, their use for cellular

therapies is problematic due to the risk of rejection (Kim *et al.*, 2011). Furthermore, this method still requires the use of ESCs and therefore is associated with ethical issues.

1.9.3 Induced pluripotent stem cells

In a seminal paper, Takahashi and Yamanaka reported the derivation of pluripotent stem cells from mouse embryonic and adult fibroblast cells. A screen of 24 candidate genes was performed by introduction of each gene into mouse embryonic fibroblasts (MEFs) and selection of cells with activation of the Oct4 target gene *Fbx15*. Whilst no single factor in isolation was capable of generating colonies, all 24 factors together could generate pluripotent cell colonies similar to ESCs in both morphology, phenotype and expression analysis. By removing individual factors, it was revealed that iPSCs could be generated using four key factors; Oct3/4, Klf4, Sox2 and c-Myc, termed the 'Yamanaka factors'. The iPSCs were similar to ESCs morphologically and were capable of forming teratomas consisting of all three embryonic germ layers when injected into nude mice. The Yamanaka factors could also reprogram adult mouse tail-tip fibroblasts to iPSCs, showing that somatic cells could gain pluripotency (Takahashi and Yamanaka, 2006).

However, these iPSCs were unable to contribute to chimera formation and did not express endogenous Oct4 and Nanog, suggesting a partially reprogrammed cell type. By selecting colonies based on Oct4 or Nanog expression, a later study showed that iPSCs could also form chimeras and contribute to the germline- the gold standard in stem cell characterisation (Okita *et al.*, 2007).

Subsequently, retroviral transduction of the same four factors was used to generate iPSCs from adult human dermal fibroblasts. The iPSCs displayed typical hESC morphology and expressed the hESC markers SSEA-3, SSEA-4, TRA-1-60, TRA-1-81 and NANOG. At transcript level, iPSCs expressed hESC markers including OCT3/4, SOX2, NANOG, GDF3 and REX1 at equivalent or higher levels than H9 hESCs. As expected for stem cells, the iPSCs possessed high levels of telomerase and underwent rapid proliferation. The pluripotency of the cells was confirmed by formation of EBs *in vitro* and formation of teratomas *in vivo* upon subcutaneous injection into SCID mice (Takahashi *et al.*, 2007). The landmark finding that iPSCs could be generated from adult human somatic cells has revolutionised the fields of developmental biology, disease modelling and drug screening. Since Takahashi and

Yamanaka's seminal papers, iPSCs have been generated from several other somatic cell types including blood cells, keratinocytes and renal cells obtained from urine (Loh *et al.*, 2009; Aasen and Izpisua Belmonte, 2010; Zhou *et al.*, 2011).

1.10 Methods for reprogramming using defined factors

Since the first reports of iPSC generation using defined factors, a range of reprogramming methods have been developed which vary in efficiency, intensity of labour and quality of the generated cells.

1.10.1 Integrative methods

Retroviral based reprogramming vectors

Traditionally, moloney murine leukaemia virus (MMLV)-derived retroviral reprogramming vectors were used for iPSC generation. The vector containing the cloned reprogramming factor complementary DNA (cDNA) is transfected into a packaging cell line to generate replication deficient viruses. MMLV-derived vectors have a high infection efficiency with up to 90% of cells infected, and a reprogramming efficiency of ~0.1% for MEFS and 0.01% for human fibroblasts when each reprogramming gene is expressed separately. These vectors do however integrate into the host genome resulting in multiple random integration sites (Takahashi and Yamanaka, 2006) and a risk of neoplasia, gene inactivation and dysregulation. Some studies have shown that the viral transgenes are highly methylated in immature cells so their expression is supressed (Jahner *et al.*, 1982; Stewart *et al.*, 1982). However, re-activation of the retroviral transgenes has also been shown, resulting in tumour formation in 20% of mice derived from the iPSC line tested (Okita *et al.*, 2007).

Lentiviral vectors

Following from the use of retroviral vectors, several studies used lentiviral delivery vectors. Lentiviral vectors have several advantages over retroviral vectors, including a higher infection efficiency and their ability to infect non-dividing and proliferative cells. Several modifications to traditional lentiviral vectors have improved their properties further, for example development of single cassette vectors which avoid multiple integration sites and a variation in the number of factors infecting each cell (Carey *et al.*, 2009; Chang *et al.*, 2009; Sommer *et al.*, 2009). However, the viral transgenes do still integrate into the host genome and are not as well supressed as retroviral genes. This issue can be partially circumvented with the use of loxP sites

created in the vector to allow excision by Cre-recombinase overexpression (Chang *et al.*, 2009; Sommer *et al.*, 2010) or use of inducible vector constructs which allow controlled expression of the viral transgenes (Brambrink *et al.*, 2008).

piggyBac

An alternative non-viral method for iPSC generation is the use of transposons, naturally occurring mobile genetic elements. The piggyBac transposon consists of the PiggyBac transposase and transposon containing the sequence of interest within 5'- and 3'- repeats (Cary *et al.*, 1989). Whilst this original piggyBac system consisted of a single element, it may also be divided into two vectors; one containing the transposase and the other containing the transposon: the sequence of interest flanked by the inverted repeat elements (Wilson *et al.*, 2007). The piggyBac system is also advantageous as it can carry multiple genes, allowing for packaging of all desired reprogramming factors into a single vector (Ding *et al.*, 2005). Unlike other transposons, the piggyBac system does not usually leave a footprint following excision (Wilson *et al.*, 2007).

The inserted transgenes can also be removed by re-expressing the transposase. In this way, a polycistronic vector containing the reprogramming factors Oct4, Sox2, klf4, cMyc and Lin28 was used to generate integration free iPSCs from MEFs with the same reprogramming efficiency as retrovirus (~1%) (Yusa *et al.*, 2009). Subsequently, the piggyBac system was used to deliver doxycycline-inducible transcription factors, generating iPSCs from human embryonic fibroblasts (Woltjen *et al.*, 2009). However, reprogramming efficiency in other human cell types is significantly lower. In human mesenchymal stem cells (MSCs), the rate of reprogramming is 50-fold less than retroviral based methods (Mali *et al.*, 2010).

1.10.2 Non-integrative methods

Episomal plasmids

Another footprint free method for iPSC generation is the use of episomal plasmids to transiently express reprogramming factors. In human foreskin fibroblasts, oriP/EBNA1 based plasmids expressing a combination of factors including OCT4, SOX2, NANOG, LIN28, c-Myc, KLF4 and the SV40 large T gene (SV40LT) could produce iPSC colonies. However, the efficiency of generation was low at 0.0003-0.0006%, and only one third of the iPSC subclones were cleared of episomal vectors

(Yu *et al.*, 2009a). The same episomal plasmids were also used to generate iPSCs from bone marrow mononuclear cells. In this cell type, the efficiency was greatly increased at 100 times that of fibroblasts (~0.035%), and all clones were cleared of plasmids by passage 15 (Hu *et al.*, 2011).

Subsequently an EBNA1/OriP plasmid expressing 5 reprogramming factors; OCT4, SOX2, KLF4, c-MYC and LIN28 was used to reprogram cord blood mononuclear cells generating up to 1000 iPSCs per $2x10^6$ cord blood cells (~0.05%) after 14 days of culture. Reprogramming of adult peripheral blood mononuclear cells was less efficient but with addition of a pEB-Tg vector expressing the SV40LT could be increased to generate 14 iPSCs per $2x10^6$ mononuclear cells (~0.0007%) (Chou *et al.*, 2011). Episomal plasmid based reprogramming may represent a viable choice in blood cells. The improved efficiency in haematopoietic cells versus fibroblast may be due to endogenous expression of genes such as KLF4 and c-MYC, which are much more highly expressed in cultured bone marrow CD34+ cells compared to mesenchymal stem cells (Chou *et al.*, 2011). A recent study has used oriB episomal plasmids in combination with EBNA mRNA and defined culture in E8 medium to generate iPSCs from several fibroblast cell lines with efficiencies between 0.0004-0.02% depending on the cell line used. This method could also reprogram fibroblasts obtained from skin biopsies with an efficiency of 0.006-0.1% (Chen *et al.*, 2011).

mRNA

mRNA containing the gene of interest flanked by a 5’ UTR containing transition initiation signal and a 3’UTR with polyA tail modified to include modified ribonucleoside bases. Using a 4-factor cocktail of the reprogramming factors KLF4, c-MYC, OCT4 and SOX2, iPSCs could be generated from dH1f fibroblasts using modified RNA with an efficiency of 1.4%. dH1f fibroblasts transduced in parallel with the same four factors using a retroviral approach generated iPSCs with an efficiency of 0.04% (Warren *et al.*, 2010). Unfortunately, the use of mRNA based reprogramming is limited by the requirement for daily additions of mRNA, making the process significantly more labour intensive than other reprogramming methods.

Sendai virus

Sendai virus (SeV) is a negative single-stranded RNA virus from the Paramyxoviridae family. The SeV consists of six genes; the nucleoprotein (NP),

phosphoprotein (P) and large protein (L) which form a ribonucleoprotein complex; a matrix protein (M) which allows assembly of the viral particles; and haemagglutinin-neuraminidase (HN) and fusion (F) proteins which mediate viral attachment and fusion. The virus replicates solely in the host cell cytoplasm and does not have a DNA phase, so cannot integrate into the host genome (Lamb, 1996). An F-deficient SeV vector which contains the F protein but not the F gene (SeV/ΔF) is able to infect cells, including non-dividing cells, with high efficiency but is unable to transmit viral particles (Li *et al.*, 2000). Further modification of SeV/ΔF introduced amino acid substitutions found in temperature-sensitive SeV mutants into the M and HN proteins (M: G69E, T116A, A183S, HN: A262T, G264R, K461G) to from a temperature-sensitive SeV (SeV/TSΔF) (Inoue *et al.*, 2003).

Using a GFP tagged SeV/TSΔF vector, Fusaki et al. could demonstrate efficient infection of human neonatal foreskin (BJ) and dermal fibroblasts (HDFs), with the majority of cells GFP positive at an MOI of 3. To investigate the ability of the modified virus to reprogram fibroblasts, cDNAs for Oct3/4, Sox2, Klf4 and c-Myc were cloned into SeV/TSΔF vectors. $1x10^6$ BJ or HDSs were seeded out and infected with SeV vectors containing Oct3/4, Sox2, Klf4 and c-Myc at an MOI of 3. After 1 week, cells were harvested and re-seeded onto MEF feeder cells, and the following day media was changed to primate ESC medium supplemented with bFGF. ESC like colonies emerged and were confirmed as iPSCs by hESC marker expression, EB generation and teratoma formation. Interestingly, RT-PCR using SeV-specific primers found that the SeV vector and transgenes decrease with each cell division resulting in gradual clearance from the iPSCs. Furthermore, persistent SeV positive cells could be removed using an antibody against the HN protein. This provided the first evidence that transgene-free iPSCs could be generated from human fibroblasts at a high efficiency (up to 1%) using SeV vectors (Fusaki *et al.*, 2009).

Further improvement to the SeV reprogramming vectors was obtained by use of new TS vectors. The TS15 (HNL/TS15 c-MYC) vector (carrying mutations in P (D433A, R434A, and K437A) and L (L1361C, and L1558I)) showed high temperature sensitivity and was negative by RT-PCR in 80% of transduced cells at passage 4. Any residual SeV could be removed using a temperature shift to 38°C for 3-5 days (Ban *et al.*, 2011). Subsequently, another SeV vector, TS12KOS, was developed which contains KLF4, OCT3/4 and SOX2 as well as the 3 P gene mutations (D433A,

R343A, K437A) present in the TS15 vector. Using a combination of the TS12KOS and HNL/TS15 c-MYC vectors generated iPSCs from skin fibroblasts and peripheral blood cells with an efficiency of ~4% and ~2% respectively. Temperature shifting of TS12KOS infected cells confirmed loss of the viral genome in 84% of cells at passage 1 (Fujie *et al.*, 2014).

Overall, SeV vectors have a higher efficiency in reprogramming human fibroblasts than lentiviral, adenoviral, piggyBac and plasmid based methods (Malik and Rao, 2013). Additionally SeV is non-pathogenic to humans, representing an important safety feature, particularly for therapeutic use of iPSCs (Nakanishi and Otsu, 2012). The features of SeV described here make SeV vector based reprogramming an attractive method for iPSC generation, and as such it has been used to generate iPSCs from several cell types.

Protein based reprogramming

The direct delivery of reprogramming proteins is an appealing option for cell reprogramming as it abolishes the need for a viral delivery system and its associated safety concerns. This method has been used to generate iPSCs from both MEFs (Zhou *et al.*, 2009) and human newborn fibroblasts (Kim *et al.*, 2009). Whilst the ability of proteins to cross the cell membrane is limited, fusion of protein transduction domains can allow delivery of proteins into host cells (Tammam *et al.*, 2016). In particular, peptides composed of 6 or more L- or D-arginine amino acids have been shown to give more efficient cellular uptake than other homopolymers (Mitchell *et al.*, 2000).

Kim et al. generate stable HEK293 cell lines expressing a 9 arginine (9R) peptide fused to each of the reprogramming proteins Oct4, Sox2, Klf4 and c-Myc. Following incubation of HNFs with cell extracts from these HEK293 cell lines, efficient translocation of all 4 reprogramming proteins was confirmed. Originally the extracts were used for a 16-hour treatment of HNFs followed by 6 days of culturing in an ESC media, at which point the cells were transferred onto MEFs and cultured for a further 4 weeks. However, this did not result in formation of any iPSC colonies, and the protocol was modified with the addition of several protein treatment cycles. Repeating the 16-hour protein treatment and subsequent ESC media culture at least 6 times was required for generation of iPSC colonies. Due to this, generation of iPSCs took 8 weeks and was very inefficient with only 0.001% of cells generating

iPSCs (Kim *et al.*, 2009). This is a significantly longer protocol and a 10-fold reduction in efficiency compared to viral based reprogramming methods.

A later paper showed generation of iPSCs from human foreskin fibroblasts using a cationic bolaamphiphile complexed to each of the reprogramming factors Sox2, Nanog, Klf4 and NR5A2 (an upstream regulator of OCT3/4) in combination with valproic acid, a histone deacetylase inhibitor. Following a 3-hour incubation with the protein-bolaamphiphile complexes cells were cultured in MEF conditioned medium. Colonies were identified at 14 days of culture and were transferred to MEF feeder cells. Reprogramming efficiency was higher using this method at 0.05% (Khan *et al.*, 2013), however use of chemicals such as valproic acid could result in chemically induced mutations in the iPSCs (Yamanaka, 2009). Protein based reprogramming is an attractive choice for iPSC generation, but its use is currently limited by low efficiency in the absence of chemicals. Further optimisation of protein based systems may allow generation of footprint-free iPSCs with acceptable efficiency in the future.

1.11 Stages of reprogramming

Reprogramming of somatic cells can be divided into 3 distinct phases; initiation, maturation and stabilisation (Samavarchi-Tehrani *et al.*, 2010) (Figure 1-3). The initiation phase is the earliest phase in reprogramming, covering the first 5 days. During this stage, there is an induction of epithelial genes including E-cadherin and Epithelial cell adhesion molecule (Epcam) and a repression of mesenchymal regulators such as Snail, Slug, Zeb1 and Zeb2. This is represented in culture by morphological change from fibroblasts to epithelial-like colonies, termed mesenchymal-epithelial transition (MET). MET occurs before the upregulation of any pluripotency markers, making it the first indication of reprogramming. This phase is promoted by BMP signalling which stimulates expression of *Sall4*, *Nanog* and *Oct4*. During the initiation phase cell fate is elastic, and removal of Oct4, Sox2, Klf4 and c-Myc (OSKM) can result in a reversion of cells to a differentiated state (Samavarchi-Tehrani *et al.*, 2010).

At around day 8 the maturation phase begins with expression of Nanog, Sall4, Esrrb, Rex1, Tcl1, Cripto and Nodal. A later study sorted cells on the basis of Tra-1-60 positivity, a known ESC marker. At day 7, expression of some ESC marker genes including NANOG and endogenous OCT3/4 is increased in the Tra-1-60 positive cells whilst other markers such as LIN28 and SOX2 do not show any change.

However, only a small percentage of these Tra-1-60 positive cells formed iPSC colonies, with the majority reverting back to a Tra-1-60 negative phenotype and showing a change in gene expression (Tanabe *et al.*, 2013). This demonstrated that whilst the initiation stage occurs in most cells, the reprogramming process subsequently stalls in the majority resulting in a “bottleneck” between initiation and maturation (David and Polo, 2014).

Following maturation, a transition to the stabilisation phase is achieved with expression of the full panel of pluripotency genes including *Gdf3* and *Sox2*. *Gdf3* is present in reprogrammed and partially reprogrammed cells, whilst *Sox2* expression is restricted to fully reprogrammed cells and thus acts as a late phase marker of reprogramming. This activation of endogenous *Sox2* is thought to represent the first step in a sequence which allows the cell to become pluripotent (Buganim *et al.*, 2012; Golipour *et al.*, 2012).

The stabilisation phase represents the changes occurring after iPSCs have acquired pluripotency. Transition to this phase depends on the silencing of OSKM transgenes which otherwise suppress the genes associated with stabilisation. These genes, including *Lin28*, *Pecam*, endogenous *Sox2* and *Utf1* are expressed in the maturation phase but fail to be activated until transgenes are removed (Golipour *et al.*, 2012).

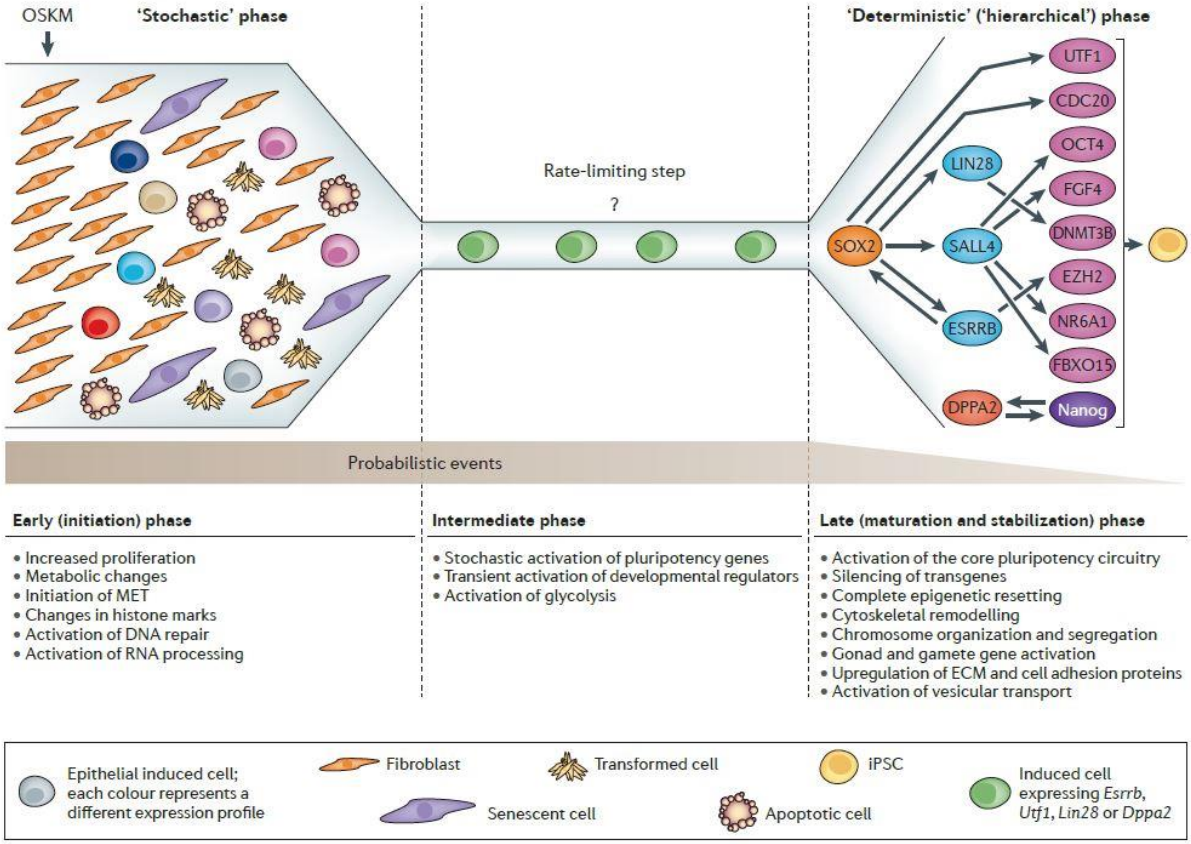

Figure 1-3. Schematic showing the phases of reprogramming and their associated hallmarks (Buganim et al., 2013).

1.12 Limitations of iPSCs

A potential issue associated with iPSCs is how closely they resemble hESCs. Whilst gene expression in iPSCs and ESCs is similar, some studies have shown that several embryonic, pluripotency and tissue specific genes are differentially expressed in iPSCs and hESCS (Chin *et al.*, 2009; Marchetto *et al.*, 2009). However, other factors including reprogramming method, genetic background of the cells and even the laboratory the iPSCs were generated in can also affect gene expression (Newman and Cooper, 2010; Liu *et al.*, 2012; Rouhani *et al.*, 2014). A more recent study which compared genetically matched iPSCs and ESCs found that they are molecularly and functionally equivalent (Choi *et al.*, 2015).

iPSCs are also associated with safety concerns due to the integrative nature of reprogramming vectors including retroviruses and lentiviruses. Integration of viral DNA into the host genome can result in disruption of genes (Seki and Fukuda, 2015). To address this issue, research into non-integrative methods for iPSC generation has been greatly expanded and several safer alternatives are now available.

The reprogramming factors used for iPSC generation also raise concerns as they are associated with tumour development (Ben-Porath *et al.*, 2008). 20% of offspring from iPSC derived chimaeric mice due to reactivation of the c-Myc transgene. More recently, long-term follow up of iPSC-derived neurospheres engrafted into a mouse model of spinal cord injury found tumour formation as a result of reactivation of the Oct4 transgene (Nori *et al.*, 2015). iPSCs can be generated from somatic cells without the use of c-Myc and/or Klf4, but the efficiency of this is very low (Nakagawa *et al.*, 2008; Mukherjee and Thrasher, 2011). The exception to this is cells with high endogenous expression of one or more of the Yamanka factors such as CD133+ cord blood stem cells which express high levels of KLF4 and c-MYC and therefore can be successfully reprogrammed with only OCT4 and SOX2 (Giorgetti *et al.*, 2009). Whilst these limitations have hindered the ability of iPSCs for therapeutic use, in the short term they can be successfully used for *in vitro* studies including drug testing and modelling development and disease.

1.13 Epigenetic memory in iPSCs

Hierarchical gene expression analysis of iPSCs from several tissue sources along with hESCs found that iPSCs cluster more closely to their donor cell of origin (Ghosh *et al.*, 2010). This has been shown to influence the differentiation capacity of iPSCs, as blood-derived iPSCs are able to differentiate into haematopoietic cells more readily than fibroblast-derived cells, whilst in turn fibroblast-derived iPSCs show osteogenic differentiation more readily than blood-derived iPSCs. Further analysis found that residual methylation retains an epigenetic memory of the tissue of origin in iPSCs (Kim *et al.*, 2010a).

This evidence suggests that derivation of iPSCs from the specific tissue of interest is important. In support of this hypothesis, generation of iPSCs from prostate and bladder tissue showed an enhanced ability of prostate-derived iPSCs (Pro-iPSCs) and urinary tract iPSCs (UT-iPSCs) to differentiate to prostate and bladder cells in comparison to skin derived iPSCs. This study used conditioned medium from prostate stromal cells to differentiate ProiPSCs into cells expressing the prostate markers AR and PSA at levels comparable to primary prostate epithelial cells (Moad *et al.*, 2013). Of note, skin iPSCs were unable to differentiate to prostate specific cells when cultured under the same conditions, suggesting further evidence for the importance of cell type of origin during iPSC generation. However, the efficiency of

this approach both in terms of reprogramming prostatic cells and differentiation of the derived ProiPSCs to prostate epithelial cells was very low.

1.14 Methods for differentiation of pluripotent stem cells

1.14.1 Embryoid bodies

Use of iPSCs for disease modelling, drug testing or clinical use requires differentiation to the cell type of interest. There are several approaches which vary in complexity, efficiency and timing. Early attempts at iPSC differentiation used the intrinsic ability of iPSCs to form EBs in culture. As EBs contain the three embryonic germ layers, similar to the developing embryo, they may be used to form specific tissues. Culturing EBs in medium containing specific factors can also direct their differentiation. For example, neurons have been differentiated from iPSCs using EB formation followed by culture with the FGF/ERK inhibitor PD0325901, TGFβ/SMAD2 inhibitor SB431542 and the BMP/SMAD1 inhibitor dorsomorphin, which induce neuroectoderm formation (Greber *et al.*, 2011). After seeding out the hPSCs as single cells, a density of 8000 cells was found to give the best neuronal differentiation with an efficiency of approximately 70% (Zhang *et al.*, 2013). However, endodermal tissues are formed as a minority in embryoid bodies, with the majority of differentiated cells from mesoderm and ectoderm (Kim *et al.*, 2010b). In addition, the spontaneous nature of EB differentiation makes gaining a specific cell type difficult.

1.14.2 Co-culture

Differentiation of pluripotent stem cells can also be induced using co-culture with other cell types. Co-culture of hESCs with mouse visceral-endoderm like cells resulted in formation of cardiomyocytes (Mummery *et al.*, 2003), providing the first evidence of specific induction signals for cardiomyocyte formation. Co-culture with hepatocytes can generate definitive endoderm-like cells which differentiate to endocrine cells after inhibition of Shh and addition of retionoids. Further co-culture of these endocrine cells with endothelial cells resulted in differentiation to insulin secreting cells at a high efficiency of 60% (Banerjee *et al.*, 2011).

1.14.3 Defined differentiation

The ideal method for PSC differentiation is the use of defined factors which specifically drive differentiation to the lineage of interest, in a manner which recapitulates embryonic development. Protocols for differentiation of hESCs and iPSCs to a specific germ layer are often used as the first step in such protocols. To

generate endodermal-derived tissues, definitive endoderm (DE) specification using Activin A and increasing concentrations of foetal calf serum generates cultures with around 80% of cells expressing SOX17/FOXA2 (D'Amour *et al.*, 2005). The DE cells can be further differentiated to more mature cell types by monolayer differentiation. Spence et al., cultured DE cells with Wnt3a and FGF4 to direct hindgut formation (Spence *et al.*, 2011) followed by an intestinal organoid system (Sato *et al.*, 2009). Using this method, the authors were able to generate intestinal organoids containing enterocytes, goblet, Paneth and enteroendocrine cells (Spence *et al.*, 2011). The limitation of this method is that the precise factors which govern differentiation into the cell of interest must be known.

1.14.4 In vivo differentiation

Alternatively, PSC differentiation can also be achieved *in vivo.* For PSCs which have already been partially differentiated to an immature tissue type, implantation *in vivo* can allow further differentiation and maturation of the cells. Takebe et al., used hepatic specification of iPSCs and co-culture with human mesenchymal stem cells and umbilical vein endothelial cells to generate liver buds *in vitro*. These buds were subsequently engrafted into immunocompromised mice where they formed functional liver tissue (Takebe *et al.*, 2013).

1.15 Prostate specific differentiation from pluripotent stem cells

To use iPSCs for modelling of prostate development and disease, a reproducible means of prostate differentiation is required. Despite the well-known role of the UGM in prostate differentiation, the breadth of precise factors which are secreted and act upon the UGE remain unknown. Development of a normal human model for prostate development would allow interrogation of these factors and enhance our knowledge which to date is based mainly upon animal studies.

1.15.1 Prostate from hESCs

The first report of prostate tissue generation using pluripotent stem cells used hESC lines in an *in vivo* tissue recombination model. Taylor et al., generated tissue recombinants consisting of approximately $1x10^3$ hESCs with either $5x10^4$ UGM cells or $1x10^5$ seminal vesicle mesenchyme (SVM) cells. After 24 hours of growth, the recombinants were grafted under the kidney capsule of adult male SCID mice who were supplemented with subcutaneous testosterone pellets. Grafts were grown for 2, 4, 8 or 12 weeks. By weeks 2-4, immature prostatic glands could be identified by

expression of CK8/18, p63, Nkx3.1 and AR. These were confirmed as human derived by positivity for anti-human laminin B1, and were surrounded by α-actin positive smooth muscle. In the grafts harvested between 8-12 weeks, more mature prostatic tissue was evident with 12% of hESC+UGM and 82% of hESC+SVM glandular tissue expressing PSA. These glands also showed a more mature organisation with a clear basal layer expressing p63 and high molecular weight cytokeratin. NE cells expressing chromogranin A were also seen. Grafts consisting of hESCs alone formed teratomas which showed no PSA positivity, confirming the role of the UGM and SVM in driving prostatic differentiation of the hESCs, whilst UGM/SVM alone did not form any glandular tissue (Taylor *et al.*, 2006). This study provided a new model for the study of prostate development from pluripotent stem cells.

A second study on prostate differentiation from hESCs used previously described conditions for intestinal organoid formation (Spence *et al.*, 2011) modified to direct prostate differentiation *in vitro*. As the prostate epithelium is an endodermal derivative, hESCs were first specified to form endoderm using an established protocol (D'Amour *et al.*, 2005). Endoderm cells were then cultured in media containing human WNT10B and FGF10 for 4 days to drive prostate specification. During this specification phase, 3D structures formed and at day 4 these were transferred to Matrigel culture in prostate medium containing both organoid- and prostate-specific factors including R-Spondin 1, Noggin, EGF and testosterone. By day 8, areas of budding could be seen and epithelial-like ducts were visible by day 28. Immunostaining showed expression of AR, CK8/18, NKX3.1, PSA and TMPRSS2 in the organoids and presence of surrounding vimentin positive stromal cells (Calderon-Gierszal and Prins, 2015). However, the organisation of the organoids was not mature with CK8/18 positivity seen throughout the structure rather than restricted to the luminal layer. A clear lumen was not identifiable in all immunostained structures shown. Furthermore, AR and NKX3.1 staining was very faint.

1.15.2 Differentiating iPSCs to prostate

Differentiation of iPSCs to prostate has also been attempted. Zhao et al., used lentiviral vectors in an attempt to generate iPSCs from prostate epithelial cells. The resultant cells were not fully reprogrammed as shown by incomplete demethylation of the Oct4 and Nanog promoters, and failure to form teratomas, and were termed E-PZ-iPS-like cells. Growth of these cells as spheres in PFMR-4A medium resulted in

expression of p63, CK18 and low level AR in the presence of androgens. By co-culturing the cells with rat UGS, some spheres also expressed PSA. *In vivo* growth of E-PZ-iPS-like cells in combination with rat UGM formed tissue containing cell structures with an outer p63 positive layer and some nuclear AR expression (Zhao *et al.*, 2013). However, the panel of markers is not convincing for complete prostate differentiation due to lack of PSA positivity. Furthermore, as the cells were not completely reprogrammed, differentiation back to prostate is likely easier in comparison to differentiation of true iPSCs to prostate.

Our group has previously generated iPSCs from human prostate fibroblasts using a lentiviral vector expressing OCT4, SOX2, KLF4 and c-MYC. Culture of these Pro-iPSCs in prostate stromal cell conditioned medium for 3 weeks resulted in expression of the epithelial marker CD24 as well as focal AR and PSA (Moad *et al.*, 2013). Unfortunately, the efficiency of this process was very low with only a subset of cells expressing prostate markers, histology was not confirmed with this method and *in vivo* differentiation was not shown.

Based on the current literature, no successful methods for prostate specific differentiation of iPSCs have been identified either *in vitro* or *in vivo*. As iPSCs are known to retain epigenetic memory from their parental cell of origin, and this has been shown to result in skewed differentiation towards that lineage, we aimed to derive iPSCs from human prostate tissue and then re-differentiate these cells to form prostatic tissue both *in vitro* and *in vivo*. To generate integration-free iPSCs, the Cytotune 2.0 vectors expressing KOS, Klf4 and c-Myc were used to reprogram patient prostate fibroblasts, generating a total of 49 iPSC clones. The generated iPSCs are free of transgenes, express pluripotency markers at the transcript and protein level and can differentiate to cells of the 3 embryonic germ layers both *in vitro* and *in vivo*. Subsequently, using rat UGM we have generated prostate organoids which show correct organisation with a p63 positive basal cell layer and a CK8/18 luminal layer, and express AR and PSA. Furthermore, *in vivo* engraftment of the iPSCs with UGM generated human prostatic tissue in a parallel manner.

1.16 Project aims

The aims of this PhD project were to:

1. Generate iPSCs from human primary prostate cells
2. To investigate the ability of the iPSCs to generate prostatic tissue *in vitro* and *in vivo*

Chapter 2. Materials and Methods

2.1 Cell culture

2.1.1 Primary culture

Human primary prostate samples were obtained from the Freeman Hospital, Newcastle upon Tyne. All samples were collected according to ethical and legal regulations, with informed patient consent under HTA licence 12534. To obtain fibroblasts and epithelial cells, prostate tissue was first washed with PBS and chopped finely with scissors before incubation at 37°C with gentle agitation in Roswell Park Memorial Institute medium (RPMI) 1640 (Gibco) containing 6mg/ml Type 1 collagenase (Worthington Biochemical Corporation) for at least 20 hours. The digested tissue was sequentially pipetted and subjected to centrifugation at 1500rpm for 5 minutes. The supernatant was aspirated and the pellet resuspended in phosphate buffered saline (PBS) and centrifuged at 1500rpm for 5 minutes. The pellet was resuspended in 10ml RPMI and centrifuged for 1 minute at 800rpm, allowing epithelial cells to deposit at the bottom of the tube whilst fibroblasts remained in the supernatant.

The supernatant containing fibroblasts was centrifuged at 2000rpm for 15 minutes, and the pellet resuspended in 10ml RPMI with HEPES modification supplemented with 10% FCS (Sigma), 2mM L-Glutamine (Sigma), 100U/ml penicillin (Sigma) and 100µg/ml streptomycin (Sigma), transferred to a T75 flask (Corning) and incubated at 37°C. After 5 days, the cells were washed with PBS and new RPMI medium added. Following this, medium was changed every 2-3 days. The epithelial fraction was collected with a pipette, resuspended in 1x trypsin and incubated at 37°C for 30 minutes. Trypsin was neutralised by the addition of RPMI, and cells were then centrifuged at 1500rpm for 5 minutes and serum removed. A PBS wash was performed to ensure removal of all serum before cells were resuspended in 5ml of Keratinocyte Serum Free Media (KSFM) (Gibco) and added to a BioCoat collagen coated 25cm^2 flask (Corning) with approximately 33,000 irradiated STO feeder cells which are established from mouse SIM embryonic fibroblasts (Murakami *et al.*, 2013). Medium was changed every 2-3 days and fresh STO cells added as appropriate.

Primary fibroblasts were maintained in RPMI medium with HEPES modification supplemented with 10% FCS (Sigma), 2mM L-Glutamine (Sigma), 100U/ml penicillin

(Sigma) and 100µg/ml streptomycin (Sigma). Primary epithelial cells were maintained on irradiated STO feeder cells in flasks coated with Collagen I in keratinocyte serum free medium (KSFM) consisting of keratinocyte growth medium (Invitrogen) supplied with Epidermal Growth Factor (EGF) and Bovine Pituitary Extract (BPE), 2mM L-Glutamine (Sigma), 0.2ng/ml Leukaemia Inhibitory Factor (LIF) (Sigma), 0.1ng/ml Granulocyte-macrophage colony-stimulating factor (GM-CSF) (Sigma), 0.2 ng/ml stem cell factor (SCF) (Sigma), 100ng/ml Cholera Toxin (Sigma), 100U/ml penicillin (Sigma) and 100µg/ml streptomycin (Sigma). All cells were grown at 37°C with 5% CO_2.

2.1.2 iPSC culture

Newly generated iPSCs were originally grown in Essential 8 Medium (Gibco) on Vitronectin (Gibco) coated plates. Once established, iPSCs were cultured on hESC-qualified Matrigel (Corning) coated plates in mTESR1 medium (Stem Cell Technologies). Cells were grown at 37°C with 5% CO_2 and medium was changed every 48 hours. Essential 8 Medium was prepared by thawing the Essential 8 supplement overnight at 4°C. 10ml of basal medium was removed from the bottle and the entire volume of Essential 8 supplement added. The medium was mixed by swirling and stored at 4°C for up to 2 weeks or aliquoted and stored at -20°C. mTESR1 medium was prepared by thawing of the mTESR1 5X supplement at room temperature or at 4°C overnight and addition of the whole bottle (100ml) to 400ml of mTESR1 basal medium. The complete medium was swirled to mix, aliquoted and stored at -20°C. Thawed aliquots were stored at 4°C and used within 2 weeks.

Vitronectin plates

Stock vitronectin was thawed and divided into 60µl aliquots before storage at -80°C. Plates were coated with vitronectin at a concentration of 0.5µg/cm^2. To coat 1 6-well plate, 1 aliquot of vitronectin was thawed and added to a 15ml tube containing 6ml of Dulbecco's phosphate buffered saline (DPBS) without Calcium and Magnesium (Gibco) and gently pipetted to mix. 1ml of diluted vitronectin was added to each well and plates incubated at room temperature for 1 hour. Plates could then be used immediately or sealed with Parafilm and stored at 4°C for up to 1 week. Before use, stored plates were pre-warmed for 1 hour at room temperature, and vitronectin solution aspirated immediately before addition of iPSCs.

Passaging iPSCs from vitronectin-coated plates

To passage cells from vitronectin-coated plates, medium was aspirated and cells rinsed twice with 2ml DPBS without Calcium or Magnesium. 1ml of 0.5mM Ethylenediaminetetraacetic acid (EDTA) (Gibco) was added per well and swirled to cover the surface. Plates were incubated at 37°C for 5 minutes until the edges of colonies began to round up and holes were visible. EDTA was then removed and 2ml warm Essential 8 Medium added per well. Cells were removed by gently pipetting the medium over the surface of the well, and colonies collected in a 15ml conical tube. Fresh Essential 8 medium was added to the tube and the cell suspension added to the appropriate number of wells giving a total of 2ml medium per well. The plate was then incubated at 37°C and media was changed every 48 hours.

Making Matrigel plates

hESC-qualified Matrigel (Corning) was thawed on ice overnight at 4°C and aliquoted into working volumes (2x6 well plates per aliquot) dependant on the dilution factor for each individual lot. Aliquots were prepared using chilled pipette tips and Eppendorf's to prevent solidification of Matrigel and were stored at -80°C. To make Matrigel coated plates, one aliquot of hESC-qualified Matrigel was thawed on ice and added to 13ml of cold DMEM/F12 (Sigma). 1ml of the diluted Matrigel was added to each well of a 6 well plate and plates were left to set for 1 hour at room temperature. Plates could then be used immediately or sealed with parafilm and stored at 4°C for up to 1 week. Stored plates were pre-warmed to room temperature for 30 minutes before use. Prior to addition of iPSCs, Matrigel was removed and mTESR1 medium added.

Passaging iPSCs from Matrigel coated plates

iPSCs were passaged once they reached approximately 80% confluency. To passage cells, media was removed and the cells washed with 2ml DPBS before the addition of 1mg/ml dispase (Stem Cell Technologies). Cells were incubated at 37°C for 5 minutes until the edges of the colonies began to lift off the plate. Dispase was then gently removed and the wells washed with 2ml of DMEM/F12 to remove any residual dispase. 2ml of mTESR1 was added before manual selection of colonies under a dissection microscope (Nikon SMZ1000) using a 200μl pipette. Colonies were transferred directly to new Matrigel plates with 2ml mTESR1 per well and

incubated at 37°C for 24 hours to allow the colonies to settle. Cultures were carefully monitored and media changed every 48 hours.

Freezing and thawing of iPSCs

iPSCs were frozen using StemCell Banker (AMSBIO). Cells were harvested once they reached an appropriate confluency of 80% and harvested in the same way as passaging. Colonies were transferred to a 15ml falcon tube and centrifuged at 200g for 4 minutes to pellet the cells. The supernatant was removed and 1ml of StemCell Banker was added to resuspend the pellet. The cell suspension was transferred to a labelled cryovial and frozen using a Mr. Frosty freezing container (Nalgene) in a -80°C freezer to allow a gradual, controlled rate of freezing. After 24 hours, cryovials were removed from the Mr Frosty and stored at -80°C.

To thaw iPSCs, cryovials were placed in a 37°C water bath to rapidly thaw the cells. The thawed cells were added to 9ml of DMEM/F12 and subjected to centrifugation at 200g for 4 minutes. The supernatant was removed and the pellet gently resuspended in mTESR1 medium containing 1μg/ml ROCK inhibitor Y-27632 (STEMCELL Technologies) and plated onto Matrigel coated plates. Cultures were carefully monitored and media changed to fresh mTESR1 every 48 hours. ROCK inhibitor was used for up to 1 week post-thaw. Use of the Mr Frosty when cryopreserving the iPSCs allowed us to greatly enhance recovery of the iPSC following freezing.

Generating a single cell suspension of iPSCs

To generate a single cell suspension of iPSCs, media was aspirated and the cells washed with 2ml/well DPBS. 1ml of Gentle Cell Dissociation Reagent (StemCell Technologies) was added to each well and the plates incubated for 8-10 minutes at 37°C. After incubation, the solution was gently pipetted over the surface of the well 2-3 times to dislodge the iPSCs, and transferred to a tube containing an equal volume of DMEM/F12. Wells were washed twice with 1ml DMEM/F12 and the complete volume centrifuged for 5 minutes at 300g. Cells were resuspended in 250μl to 1ml of media dependent on the size of the cell pellet. Cells were counted on a haemocytometer using trypan blue to exclude dead cells.

2.2 Optimising viral transduction efficiency

For optimisation of transduction parameters, primary prostate fibroblasts were seeded at a density of 30,000 cells per well in 12 well plates. Cells were transduced using the Cytotune-EmGFP Sendai reporter (Life Technologies) at a range of MOI (multiplicity of infection) in their respective media for 48 hours at 37°C. Images of the cells were taken at 24 and 48 hours post transduction. Cells were harvested after 48 hours by trypsinisation and analysed by flow cytometry to determine the percentage of GFP positive cells. The MOI, defined as the number of infectious particles per cell, was calculated using the following equation.

$$\mathrm{MOI} = \frac{Number\ of\ transducing\ units/well}{Number\ of\ target\ cells\ in\ a\ well}$$

2.3 Reprogramming primary prostate cells to iPSCs

2.3.1 Fibroblasts

To generate iPSCs, primary patient fibroblasts were seeded in fibroblast medium (high glucose DMEM (Gibco), 10% ESC-qualified FBS (Gibco), 1% MEM non-essential amino acids (Gibco), 100µl 55mM β-mercaptoethanol (Sigma), 100U/ml penicillin (Sigma) and 100µg/ml streptomycin (Sigma)) at a density of 100,000 cells per well in 12 well plates. After 24 hours, cells were transduced with the Cytotune 2.0 Sendai Virus reprogramming vectors (KOS, Klf4 and c-Myc, Life Technologies) at an MOI of 5-5-3 (KOS MOI=5, hc-Myc MOI=5, hKlf4 MOI=3) as recommended by the manufacturer's instructions. After 24 hours of incubation with the viral vectors, the medium was replaced with fresh fibroblast medium, and was subsequently changed every 48 hours. At day 7 cells were transferred to vitronectin-coated plates at a concentration of $1.5x10^4$ cells per well of 12 well plate. To do this, medium was removed from the wells and the cells washed once with PBS. 0.5ml of 0.05% trypsin-EDTA (Gibco) was added to the wells and left for 1-3 minutes at room temperature until the cells began to round up. 2ml of fibroblast medium was added and the cell suspension was transferred to a 15ml conical tube and centrifuged for 4 minutes at 200g. Supernatant was removed and the cell pellet gently resuspended in 2ml of fresh fibroblast medium. Cells were counted using a haemocytometer and trypan blue to exclude dead cells. Cells were then seeded out at $1.5x10^4$ cells per well of a 6 well plate and incubated at 37°C. After 24 hours on vitronectin (day 8 of the

experiment) the medium was changed to Essential 8 medium (Gibco) and media changes occurred every other day. Plates were carefully monitored for the emergence of colonies. From day 21 onwards colonies had reached a suitable size and were manually picked using a p200 pipette and transferred to individual vitronectin-coated wells for clonal expansion. Once a suitable confluency of around 70% was reached, colonies were transferred to Matrigel coated plates for characterisation and expansion.

2.3.2 Epithelial cells

Two methods were used for transducing prostate epithelial cells using Cytotune 2.0 viral vectors; transducing within the original flask or after seeding the epithelial cells onto gelatin-coated plates.

Transducing in the original flask

Before transducing the epithelial cells, media was aspirated and the cells washed with PBS. Cytotune 2.0 vectors were added at the determined MOI in KSFM and incubated for 24 hours at 37°C. Media containing the virus was removed after 24 hours and replaced with fresh epithelial cell medium. Cultures were monitored daily and the media changed every 48 hours. For the first transduction, cells were transferred on day 7 to a hESC environment consisting of a MEF feeder layer and hESC medium. Cells were monitored daily by microscopy (Olympus CK40 microscope). For the second transduction, the protocol was modified and cells were transferred to vitronectin coated plates in E8 medium or MEFs in hESC medium on day 15 after colonies were visible. Again, cultures were monitored by phase contrast microscopy and harvested at day 28 for RNA extraction.

Seeding cells onto gelatin

The second method used for epithelial reprogramming was to seed the epithelial cells into 3 individual wells on gelatin coated plates. Cells were transduced with the Cytotune 2.0 vectors in epithelial cell medium at the designated MOI and incubated at 37°C for 24 hours. The media containing the virus was then removed and fresh medium added. Cells were monitored by microscopy and the media changed every 48 hours. At day 7, the medium was changed to E8 medium and on day 8 and 11 one well of each sample was transferred to vitronectin coated plates whilst the remaining well was kept on gelatin for further culture. As in the previous method, the

media was changed every 48 hours, cells were closely monitored by microscopy and all wells were harvested at day 28 for RNA extraction.

2.4 Alkaline phosphatase detection

Alkaline phosphatase staining was carried out using the ESC characterisation kit (Millipore). Media was aspirated from iPSCs before fixation with 4% paraformaldehyde in PBS for 2 minutes. Fixative was aspirated and cells washed with 1X rinse buffer. 0.5ml stain solution (Fast Red Violet solution and Napthol AS-BI phosphate solution diluted with water in a ratio of 2:1:1 (Fast Red Violet:Napthol:water)) was added to cells and incubated in the dark for 15 minutes at room temperature. The solution was aspirated and cells rinsed with 1X rinse buffer. Cells were covered with PBS and imaged using an Olympus CK40 microscope and Visicam 5.0 software.

2.5 Embryoid body formation

For formation of embryoid bodies (EBs), iPSCs were harvested by manually picking colony pieces with a p200 pipette and transferred to a 15ml conical tube. Colonies were left for 5 minutes at room temperature to settle to the bottom of the tube. Medium was removed and fresh medium added at a ratio of 1:1 mTESR1 and EB medium (80% Knock-out DMEM, 20% FCS, 1% Glutamax, 1% MEM and 1% penicillin-streptomycin). Colonies were then transferred into low-adhesion dishes and incubated at 37°C for 48 hours. At this point, media was changed to EB medium alone and cultures monitored by microscopy. Medium was changed every 48 hours until EBs of a suitable size were formed. EBs were then seeded onto gelatin coated 6 well plates for explant culture for a further 2 weeks. Cells were analysed by immunofluorescence or harvested for RNA extraction.

2.6 Teratoma formation assay

To determine the pluripotency of the generated cells *in vivo*, a teratoma formation assay was performed. iPSCs were dissociated using gentle cell dissociation reagent to generate a single cell suspension, counted with trypan blue to exclude dead cells, and aliquoted into tubes at a density of $1x10^6$ live cells per tube. The cells were mixed 1:1 with Matrigel and injected subcutaneously into NOD *scid* gamma (NSG) mice. NSG mice were chosen as they are the most immunodeficient strain of mice due to deficiencies in T, B, and NKC cells and macrophages (Ito *et al.*, 2012), and therefore should not be able to reject the transplanted cells. Mice were weighed and

checked for general health and emergence of palpable tumours at least once weekly. Once tumour formation was apparent, tumour size was regularly monitored using callipers. The mice were culled by cervical dislocation if tumours reached the maximum size allowable under the license or alternatively at 90 days which constituted the end of the experiment.

Tumours were isolated by making an incision into the skin of the mouse and opening this to reveal the tumour. Tumours were cut away from the mouse skin, weighed, measured and photographed. Each tumour was cut in half. One half was fixed in Bouins solution for 24 hours at room temperature, processed using the conditions outlined below, and embedded in paraffin wax. The second half was frozen in isopentane and stored at -80°C. Paraffin blocks were sectioned at 4μm (Anna Long, Pathology, RVI) and sections stained with haematoxylin and eosin. Multiple sections from each tumour were kindly analysed by Amira El Sharif (Pathologist, RVI).

2.7 DNA fingerprinting

DNA fingerprinting was performed to confirm the iPSCs were generated from the parental stroma and were not a result of contamination from another pluripotent cell source. Cells were harvested to a single cell suspension and pelleted by centrifugation at 200g for 4 minutes. The pellets for iPSCs and parental fibroblasts were sent to the Northern Molecular Genetics Service (Centre for Life, Newcastle Upon Tyne) for DNA extraction and detection of microsatellite markers. Using the PowerPlex 16 HS System, 16 loci were amplified from each sample; D18S51, D21S11, TH01, D3S1358, Penta E (labelled with fluorescein); FGA, TPOX, D8S1179, vWA, Amelogenin (labelled with carboxy-tetramethylrhodamine); CSF1PO, D16S539, D7S820, D13S317, D5S818 and Penta D (labelled with 6-carboxy-4´,5´-dichloro-2´,7´- dimethoxy- fluorescsein). Analysis was performed using an ABI 377 sequence detector (Applied Biosystems).

2.8 Karyotyping

iPSCs were subjected to G-banding to allow identification, pairing and analysis of chromosomes and to confirm a normal male karyotype. This was performed by the Northern Genetics Service (Centre for Life, Newcastle upon Tyne).

2.9 Flow cytometry

For analysis of GFP positivity by flow cytometry cells were trypsinized at 37°C for 5 minutes, resuspended in RPMI medium and subjected to centrifugation at 1500rpm for 5 minutes. The supernatant was removed and pellets resuspended in 10ml MACS buffer (PBS with 2mM EDTA and 0.5% FCS) and centrifuged again. Cell pellets were resuspended in 0.5ml MACS buffer and transferred to FACS tubes (BD) before analysis of up to 10,000 cells per sample by FACSCalibur™ (BD Biosciences). The cell population was gated according to forward and side scatter. Further gates were applied based on GFP expression to determine the percentage of transduced cells. Data was tested for statistical significance using a two-way ANOVA.

2.10 RNA extraction, reverse transcription and RT-PCR

2.10.1 RNA extraction using Qiagen® RNeasy Micro kit

For samples containing $\leq 5 \times 10^5$ cells, RNA was extracted using the Qiagen RNeasy Micro kit according to manufacturers' instructions. Cells were resuspended in 350μl buffer RLT and mixed by pipetting. 350μl of 70% ethanol was added and mixed well before transferring the sample to an RNeasy MinElute spin column in a 2ml collection tube and centrifuging for 15 seconds at 10,000rpm. After discarding the flow-through, 350μl of Buffer RW1 was added and the samples were centrifuged for 15 seconds at 10,000rpm. The flow-through was discarded and DNase I incubation mix (10μl DNase I stock solution + 70μl Buffer RDD) was added to the column for 15 minutes at room temperature. The column was washed with 350μl Buffer RW1 and centrifuged for 15 seconds at 10,000rpm. The flow-through and collection tube were discarded and the column placed into a new collection tube. 500μl Buffer RPE was added and the sample centrifuged for 15 seconds at 10,000rpm. The flow-through was discarded and 500μl of 80% ethanol added to the column before centrifugation for 2 minutes at 10,000rpm. The flow-through and tube were discarded and the column placed into a new collection tube and centrifuged for 5 minutes at full speed. Finally, the column was placed into a 1.5ml collection tube and 14μl of RNase-free water added to the centre of the column membrane. RNA was eluted by centrifugation for 1 minute at full speed and stored at -80°C.

2.10.2 Quantification of RNA

RNA was quantified using the NanoDrop 1000 spectrophotometer (Thermo Scientific). Before use, RNase free water (Qiagen) was added to the sample

retention platform and wiped with a clean tissue. A water sample was then added to initialise the spectrometer. 2μl of RNase free water was used to blank the spectrophotometer. To quantify samples, 1.2μl of RNA was pipetted onto the lower measurement pedestal and the sampling arm lowered. This allows the sample to be drawn between the upper and lower pedestals for a measurement to be made. The RNA concentration in ng/μl was noted and the 260/280 and 260/230 ratios checked to ensure purity of the RNA. A 260/280 value of ~2 is expected for pure RNA, whilst the 260/230 ratio should be 1.8-2.2. Between each sample, the pedestals were wiped using a laboratory tissue to prevent carryover. RNA was kept on ice during the process.

2.10.3 cDNA generation

cDNA was generated from RNA using SuperScript™ III Reverse Transcriptase (Invitrogen). Up to 5μg of RNA was combined with 1μl of random primers and 1μl of 10mM dNTP mix in an Eppendorf tube and made up to 13μl with Diethyl pyrocarbonate (DEPC) water. Tubes were incubated at 65°C for 5 minutes and then placed on ice for at least 1 minute. cDNA synthesis mix containing; 4μl 5X First-Strand Buffer, 1μl 0.1M DTT, 1μl RNaseOUT Recombinant RNase Inhibitor and 1μl SuperScript III RT was added to each tube and mixed gently. Tubes were centrifuged before incubation for 10 minutes at 25°C followed by 50 minutes at 50°C. The reaction was stopped by incubation at 85°C for 5 minutes and tubes were chilled on ice before storage at -20°C.

2.10.4 Real-time PCR

To analyse transcript levels of genes, real-time PCR (RT-PCR) was performed in 384 well plates using the primers described in Table 2-1. Each well contained 9μl of mastermix (containing 5μl of SYBR Green, 0.4μl forward primer, 0.4μl reverse primer and 3.2μl of sterile distilled water). Plates were run on an Applied Biosystems 7900HT using SYBR green (Invitrogen) detection. SYBR green is a double-stranded DNA binding dye which detects double-stranded DNA produced during PCR, producing a fluorescent signal proportional to the amount of PCR product. This signal is normalised to the ROX passive reference dye included in the SYBR Green mastermix to control for fluctuations in fluorescence.

Plates were run at 50°C for 2 minutes, 95°C for 2 minutes and then for 40 cycles of 95°C for 15 seconds followed by 60°C for 1 minute. Analysis was performed using Applied Biosystems SDS 2.3. The amount of cDNA in the samples was quantified by interpolating values from a standard curve of known expression and expression of each gene was normalised to the housekeeping genes glyceraldehyde-3-phosphate dehydrogenase (GAPDH) or hypoxanthine phospho ribosyl transferase (HPRT1). Each sample was run in triplicate and water only wells containing no cDNA were used as a control in all experiments. Dissociation curves were checked for all samples to ensure they contained only a single specific peak.

Gene	Forward primer	Reverse primer
GAPDH	CGACCACTTTGTCAAGCTCA	GGGTCTTACTCCTTGGAGGC
HPRT1	TTGCTTTCCTTGGTCAGGCA	AGCTTGCGACCTTGACCATCT
OCT4	GCAAGCCCTCATTTCACCAGGCC	AGGATCAACCCAGCCCGGCT
SOX2	TCACATGTCCCAGCACTACC	CCCATTTCCCTCGTTTTTCT
NANOG	CCAAATTCTCCTGCCAGTGAC	CACGTGGTTTCCAAACAAGAAA
DNMT3B	TGCTGCTCACAGGGCCCGATACTTC	TCCTTTCGAGCTCAGTGCACCACAAAAC
REX1	CGTACGCAAATTAAAGTCCAGA	CAGCATCCTAAACAGCTCGCAGAAT
SeV	GGATCACTAGGTGATATCGAGC	ACCAGACAAGAGTTTAAGAGATATGTATC
SeV-KOS	ATGCACCGCTACGACGTGAGCGC	ACCTTGACAATCCTGATGTGG
SeV-Klf4	TTCCTGCATGCCAGAGGAGCCC	AATGTATCGAAGGTGCTCAA
SeV-c-Myc	TAACTGACTAGCAGGCTTGTCG	TCCACATACAGTCCTGGATGATGATG
CD24	TGAAGAACATGTGAGAGGTTTG	GAAAACTGAATCTCCATTCCAC
CD45	GAAATTGTTCCTCGTCTGAT	CTTTGCCCTGTCACAAATAC
a-SMA	CTCACGGAGGCACCCCT	GAAAGTCTCAAACATAATTTG
CD90	CACACATACCGCTCCCGAACC	GCTGATGCCCTCACACTTGAC
AFP	AGCTTGGTGGTGGATGAAA	TCTGCAATGACAGCCTCAAG
PAX6	TGTCCAACGGATGTGTGAGT	TTTCCCAAGCAAAGATGGAC
FOXA2	TCCGACTGGAGCAGCTACTATG	CCACGTACGACGACATGTTC
NKX3.1	AGCCAGAAAGGCACTTGGG	GGCGCCTGAAGTGTTTTCA
AR	GCAAAGCCTAAAGCCAGAT	GAGTTCATGGGTGGCAAAG
PSA	TCGGCACAGCCTGTTTCAT	TGGCTGACCTGAAATACCTGG

Table 2-1. Primer sequences used for RT-PCR.

2.11 Haematoxylin and Eosin (H&E) staining

Formalin fixed paraffin embedded (FFPE) sections were placed into xylene for 5 minutes to allow deparaffinisation before rehydration of the sections through decreasing concentrations of alcohol at 100%, 95%, 70% and 50%. Slides were washed in running water before addition of Gills II Haematoxylin (Fisher) for 5 minutes to stain the nuclei of cells. Slides were washed in running water and dipped twice into acid alcohol (1.4L absolute ethanol (Fisher), 580ml distilled water, 20ml concentrated hydrochloric acid (Fisher). to remove excess haematoxylin before blueing of the haematoxylin stain by incubation in Scott's water (2L of distilled water, 7g sodium hydrogen carbonate (VWR), 40mg magnesium sulphate (Fisher) and thymol (VWR)) for 30 seconds. Slides were rinsed in water and placed into Eosin (500ml Eosin (Fisher), 250ml absolute ethanol (Fisher), 250ml distilled water)) for 2 minutes. Slides were rinsed to remove excess eosin and dehydrated through ethanol from 50%-100%. Alcohol was cleared from the sections by 3 incubations in xylene, and slides were coverslipped using DPX Mountant (Sigma).

2.12 Immunofluorescence

2.12.1 Standard immunofluorescence for cells

Specific markers were detected using immunofluorescence. Medium was removed and the cells washed twice with PBS. Cells were fixed with 4% paraformaldehyde for 15 minutes at room temperature before washing twice with 1X rinse buffer (TBST: 20mM Tris-HCl, pH 7.4, 0.15 NaCl, 0.05% Tween-20) for 5 minutes each. 0.1% Triton X-100 was added for 10 minutes at room temperature to permeabilise the cells before 2 further washes with rinse buffer. Cells were blocked in 4% goat serum (Dako) or bovine serum albumin (BSA) (depending on the species of the secondary antibody) for 30 minutes at room temperature to prevent non-specific binding. Primary antibodies were diluted in 4% goat serum or BSA at concentrations specified in Table 2. Cells were incubated with the primary antibody overnight at 4°C before washing 3 times with rinse buffer. Secondary antibodies were diluted 1:400 in PBS and added to cells for 1 hour at room temperature in the dark. Cells were washed three times with PBS and VECTASHIELD® hard set mounting medium with 4', 6-diamidino-2-phenylindole (DAPI) (Vector Laboratories) was spotted onto each well. Plates were left to dry before the addition of PBS whilst slides were coverslipped. Immunofluorescent staining was visualised by fluorescent microscopy (Leica DMR).

2.12.2 Immunofluorescence on FFPE tissue

For immunofluorescence with FFPE tissue, slides were first placed into xylene for 5 minutes to deparaffinise before rehydration through an ethanol gradient of 100-50%. Slides were rinsed in running water and antigen retrieval was performed using citrate buffer pH6 in a decloaking chamber (A. Menarini Diagnostics). Following retrieval, slides were rinsed with water and blocked with 3% hydrogen peroxide to remove endogenous peroxidase activity. After rinsing, slides were placed briefly into TBST and sections lined using a PAP pen (Dako). Non-specific binding was blocked by incubation in 4% serum or BSA for 1 hour at room temperature before addition of the primary antibody/ antibodies (listed in Table 2-2) for 1 hour at room temperature. Slides were washed twice with PBS for 5 minutes and the appropriate fluorescent secondary antibody (diluted 1:400) applied for 30 minutes at room temperature in the dark. Slides were then washed a further 2 times for 5 minutes with PBS before VECTASHIELD® hard set mounting medium with DAPI (Vector Laboratories) was spotted onto each slide and coverslips added. Immunofluorescence was visualised using confocal microscopy (Zeiss).

Antibody	Company	Species	Concentration
SSEA1 MC-480	EMD Millipore	Mouse	1:100
SSEA4 MC-813-70	EMD Millipore	Mouse	1:100
Tra-1-60 TRA-1-60	EMD Millipore	Mouse	1:100
Tra-1-81 TRA-1-81	EMD Millipore	Mouse	1:100
Oct4 MAB4401A4	EMD Millipore	Mouse	1:200
α-fetoprotein (AFP) A8452, clone C3	Sigma	Mouse	1:100
βIII tubulin MMS-435P	Covance	Mouse	1:100
Vimentin Ab8978 [RV202]	Abcam	Mouse	1:100
FOXA2 AF2400	R&D	Rabbit	1:10
SOX17 AF1924	R&D	Goat	1:20
CK8/18 Ab17139 [5D3]	Abcam	Mouse	1:50
34BE12 M0630	Dako	Mouse	1:100
P63 NCL-L-p63	Leica Biosystems	Mouse	1:50
Nkx3.1 0314	AthenaES	Rabbit	1:50
AR (N20) Sc-816	Santa Cruz	Rabbit	1:50
AR (441) Sc-7305	Santa Cruz	Mouse	1:50
PSA A0562	DAKO A	Rabbit	1:100
PSA BIOG.AR014-10RE	Biogenex	Rabbit	1:50

Table 2-2. Antibodies used for immunofluorescence

2.13 Immunohistochemistry

Cells or organoids were collected and fixed in 10% normal buffered formalin overnight at room temperature before processing and embedding in paraffin blocks. For IHC, slides were dewaxed by placing in xylene for 5 minutes followed by subsequent dips into fresh xylene. Slides were hydrated by passing through an ethanol gradient from 100% to 50% ethanol and then rinsed in water. A decloaking chamber was used for antigen retrieval using citrate buffer pH 6 (trypsin retrieval used for PSA antibody). Following antigen retrieval, slides were washed and endogenous peroxidase activity was blocked using 3% hydrogen peroxide solution for 10 minutes. Nonspecific binding of the primary antibody was blocked for 20 minutes using 2.5% horse serum for mouse and rabbit antibodies, or BSA for all other species. Primary antibodies (listed in Table 2-3) were made up in 4% BSA and incubated for 1 hour at room temperature. Slides were then rinsed with TBST and incubated with anti-rabbit or anti-mouse IgG for 30 minutes, or the appropriate secondary antibody for 1 hour. 3, 3 -diaminobenzidine (DAB) solution (Vector Laboratories) was added to the sections and incubated for 5 minutes followed by washing in water and counterstaining with haematoxylin. Slides were dehydrated using a reverse ethanol gradient from 50% to 100% ethanol and then placed into xylene. Slides were mounted onto coverslips using DPX Mountant (Sigma). Images were obtained using the Aperio system (Leica).

Antibody	Company	Species	Dilution
Anti-human mitochondria Ab92824 [113-1]	Abcam	Mouse	1:200 (xenografts) 1:500 (growth factor differentiation)
Pan CK Ab7753 [C-11]	Abcam	Mouse	1:500
CK8/18 Ab17139 [5D3]	Abcam	Mouse	1:50
34BE12 M0630	Dako	Mouse	1:500
P63 NCL-L-p63	Leica Biosystems	Mouse	1:50
AR 554225 Clone G122-434	BD Pharmigen	Mouse	1:50
PSA BIOG.AR014-10RE	Biogenex	Rabbit	1:25
Vimentin Ab8978 [RV202]	Abcam	Mouse	1:1000
βIII tubulin MMS-435P	Covance	Mouse	5000

Table 2-3. Antibodies used in immunohistochemistry.

2.14 Colony counts:

To determine the number of cells per mm^2, colonies were photographed using the EVOS system and colony area measured using ImageJ software. Colonies were individually picked, digested to a single cell suspension using gentle cell dissociation reagent (StemCell Technologies), diluted 1:1 with trypan blue and counted using the BioRad TC20 automated cell counted.

2.15 Urogenital sinus mesenchyme dissection and xenografting

Urogenital sinus mesenchyme dissection was carried out in collaboration with and under the supervision of the Hayward laboratory, North Shore University HealthSystem Research Institute, Evanston, Chicago. Xenografting was kindly performed by Dr Takeshi Sasaki and Dr Omar Franco. UGM was dissected from Sprague-Dawley E18 pregnant female rats. After culling, foetuses were removed and complete urogenital systems were dissected. To remove the urogenital system, an incision was made in the foetal abdomen to expose the intestinal and urogenital

systems (Figure 2-1). To remove the urogenital system, forceps were used to pull gently on the bladder and the urethra was cut. The bladder, urethra, Wolffian and Müllerian ducts and testes or ovaries were removed leaving the UGS (Figure 2-2). UGS were incubated in 10mg/ml trypsin at 4°C for 90 minutes. Trypsin was neutralised by serial washes with RPMI containing FCS. DNase was added to prevent stickiness of the UGS during dissection. To separate the UGM from the UGE, the UGS was gently opened to reveal the epithelial tubes. Using needles, these were removed along with any fat surrounding the UGM (Figure 2-3). To generate tissue recombinants, UGM was combined with pieces of iPSC colony and resuspended in collagen isolated from rat tails. This was incubated at 37°C for 30 minutes to solidify before addition of RPMI containing 10% FCS. Tissue recombinants were further incubated overnight.

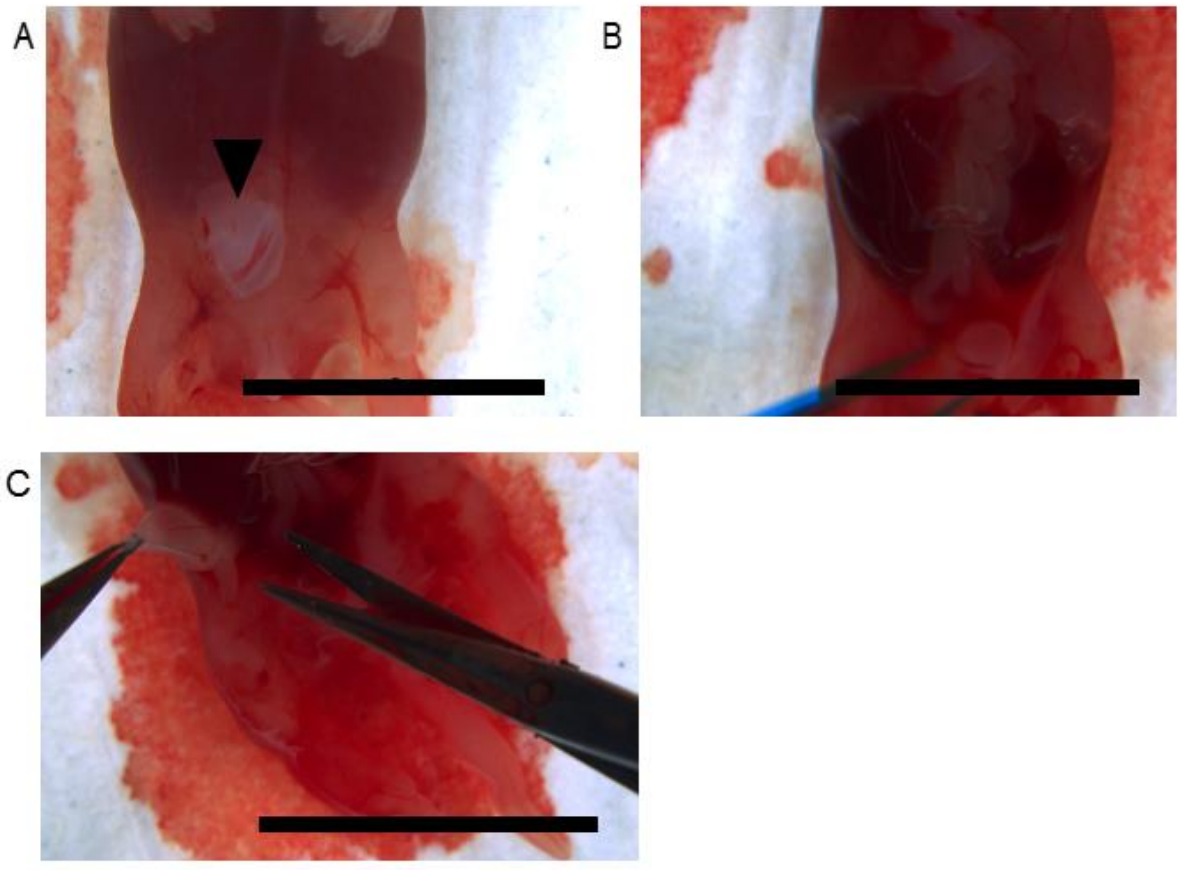

Figure 2-1. Locating and removing the urogenital system from E18 rats. A) Photograph showing the umbilical cord (arrowhead). B) After opening the abdomen, the liver and intestinal system can be clearly identified. C) The urogenital system is removed by pulling gently up on the bladder and making a cut at the base of the urethra. Scale bar 10mm.

Figure 2-2. A) Complete male urogenital system from E18 rat. The testes, bladder and urethra are visible along with the urogenital sinus (UGS). B) The urethra, bladder, Müllerian and Wolffian ducts and testes or ovaries are removed leaving behind the UGS. Scale bar 5mm.

Nude mice (Hsd:Athymic Nude-Foxn1nu) were used for the sub renal capsule xenografts as these have been identified as generating better prostate glandular structures and are also immune deficient as they lack mature T cells. Mice were sedated with isofluorane and castrated by surgical removal of the testis. To expose the kidney, a small incision was made in the skin of the mouse followed by a small incision in the peritoneum. The kidney could then be exposed and a small incision made in the outer layer of the kidney capsule. One graft was inserted into each side of the kidney and stitched before repeating on the other kidney. A testosterone pellet was inserted into the scruff of the neck before the wound was stapled. Mice were carefully monitored until they were culled and the grafts harvested for further analysis. Upon harvesting, grafts were imaged and measured before formalin fixation, processing and embedding in paraffin.

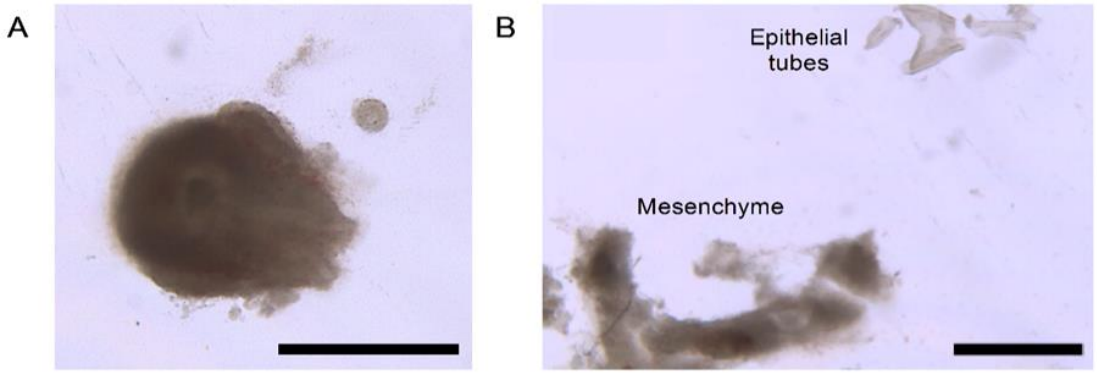

Figure 2-3. A) High magnification image of the UGS. The dense area is the mesenchyme which surrounds the epithelial tubes. B) The mesenchyme (UGM) is removed from the epithelial tubes (UGE). Scale bar 1mm.

2.16 Definitive endoderm generation from iPSCs

To generate definitive endoderm (DE) from iPSCs, cells were harvested to a single cell suspension and seeded out at a density of $2x10^6$ cells per well of a Matrigel coated 6 well plate in mTESR1 medium containing 1μg/ml ROCK inhibitor Y-27632. Cells were incubated at 37°C for 24 hours before removal of medium and washing with PBS. DMEM/F12 medium containing 100ng/ml Activin A (R&D) was added and cells incubated for a further 24 hours. Media was replaced after 24 hours with fresh DMEM/F12 containing 100ng/ml Activin A and 0.02% FCS and cells incubated for a further 24 hours. Finally, media was again replaced after 24 hours with DMEM/F12 containing 100ng/ml Activin A and 0.2% FCS. Following a final 24-hour incubation, cells were fixed and stained for the definitive endoderm markers SOX17 and FOXA2 by immunofluorescence, or harvested using gentle cell dissociation reagent for RNA extraction.

2.17 3D co-culture of iPSC-derived endoderm and rat urogenital sinus mesenchyme cells

For co-culture of UGM and DE cells, chamber slides were coated with 40μl of neat GFR-Matrigel (Corning) and left to set at 37°C for 20 minutes. UGM and DE cells were counted using trypan blue to exclude any dead cells. Cells were resuspended at the desired concentration in GFP Matrigel diluted 1:1 with DMEM/F12 Ham and pipetted into the chamber slide wells. This layer was left to set at 37°C for 30 minutes as above before addition of DMEM/F12 Ham containing 2% ITS (insulin, transferrin, selenium) (Gibco) and 10nm DHT (Sigma). Cultures were monitored and photographed daily. After 7 days of culture, media was changed to UGM conditioned media which was collected from whole pieces of UGM incubated in DMEM/F12 Ham containing 2% ITS and 10nm DHT. From this point media was changed 3 times per week. For the first experiment, wells were harvested after 3 weeks of 3D culture by removal of the entire Matrigel plug, fixed in 10% neutral buffered formalin (Sigma) overnight and processed before embedding into paraffin.

For the second UGM co-culture, cells were set up as described above. Again, UGM CM was used from day 7 onwards. After 6 weeks of 3D culture, the media was changed to prostate organoid medium (Karthaus *et al.*, 2014). Wells were harvested after 6 or 8 weeks for histology or RNA extraction. Wells for histology were removed as a Matrigel plug, fixed in 10% formalin overnight and processed before embedding

into paraffin. For RNA extraction, the Matrigel was digested by incubation with dispase at 37°C until the gel was completely dissolved. The mixture was pipetted up and down to further break up the Matrigel, and transferred to an Eppendorf for centrifugation at 2000rpm for 5 minutes. The supernatant was removed and the pellet snap frozen in isopentane and stored at -80°C.

2.18 Growth factor differentiation

For directed differentiation using growth factors, a published protocol was used (Calderon-Gierszal and Prins, 2015). Definitive endoderm was primed to prostatic differentiation using RPMI 1640 containing 2mM L-Glutamine, 100U/ml penicillin-100μl streptomycin and 2% FCS with 500ng/ml FGF10 (R&D systems) and 500ng/ml human WNT10B (R&D systems). This media was changed daily for a total of 4 days at which point any 3D structures which had formed were transferred to 3D culture. To do this, structures were harvested under a sterile dissecting scope using a p1000 pipette, transferred to a 15ml conical tube and centrifuged at 400g for 3 minutes. Media was aspirated and 25μl of medium added. The 25μl of cell suspension was mixed with 50μl GFR Matrigel (Corning) containing 1X B27 supplement (Invitrogen), 100ng/ml Noggin (R&D systems) and 100ng/ml EGF (R&D systems). Each cell/Matrigel mixture was pipetted into one well of a 24 well plate and incubated at 37°C for 20 minutes to set. Medium was then added which consisted of 1:2 prostate epithelial growth medium (PrEGM) (Lonza) and stromal cell basal medium (SCBM) (Lonza) containing 2mM L-glutamine, penicillin-streptomycin, 15mM HEPES (Gibco), 500ng/ml R-Spondin1 (R&D systems), 100ng/ml Noggin 100ng/ml EGF, 1X B27 supplement, 10nM ATRA and 1.7μM DHT.

Growth was monitored daily by microscopy and media changes occurred every 48 hours. After 28 days, the 3D structures were harvested for either histology or RNA extraction. For histology, spheroids were extracted using a P1000 pipette with the end of the tip cut off. Structures were fixed for 1 hour in 10% neutral buffered formalin then placed into low melt agarose to form a small plug. This was subsequently processed and embedded into paraffin for sectioning. To obtain cells for RNA extraction, the Matrigel was dissolved by addition of dispase for 15 minutes at 37°C. The mixture was pipetted up and down to further break up the Matrigel, and transferred to an Eppendorf for centrifugation at 2000rpm for 5 minutes. The

supernatant was removed and the pellet resuspended in buffer RLT before beginning RNA extraction.

Chapter 3. Generation and characterisation of integration-free iPSCs from human prostate fibroblasts using Sendai virus vectors

3.1 Introduction

This chapter will describe the methods for reprogramming human primary prostate cells to iPSCs and subsequent characterisation of the generated cells. Reprogramming somatic cells using overexpression of the Yamanaka factors Oct4, Sox2, Klf4 and c-Myc has most commonly been achieved using lentiviral expression vectors, however these are associated with low reprogramming efficiency and viral integration into the host genome.

In this study, three Sendai virus vectors (Cytotune 2.0 kit) were used to introduce the Yamanaka reprogramming factors Oct4, Sox2, Klf4 and c-Myc into patient cells. Sendai virus replication is restricted to the cell cytoplasm therefore abrogating the potential for genomic integration (Fusaki *et al.*, 2009), and following reprogramming the virus is gradually cleared from the transduced cells during subsequent cell divisions. Furthermore the Cytotune 2.0 Sendai viral vectors have a higher iPSC generation efficiency from human fibroblasts in comparison to both traditional lentiviral based reprogramming as well as other non-integrative methods including adenovirus, PiggyBac and plasmid-based methods (Malik and Rao, 2013). The vectors used in this study were F-deficient Sendai virus vectors containing temperature sensitive mutations in viral genes (Figure 3-1)(Inoue *et al.*, 2003) to enhance safety and ensure clearance of any persistent virus could be achieved by temperature shifting.

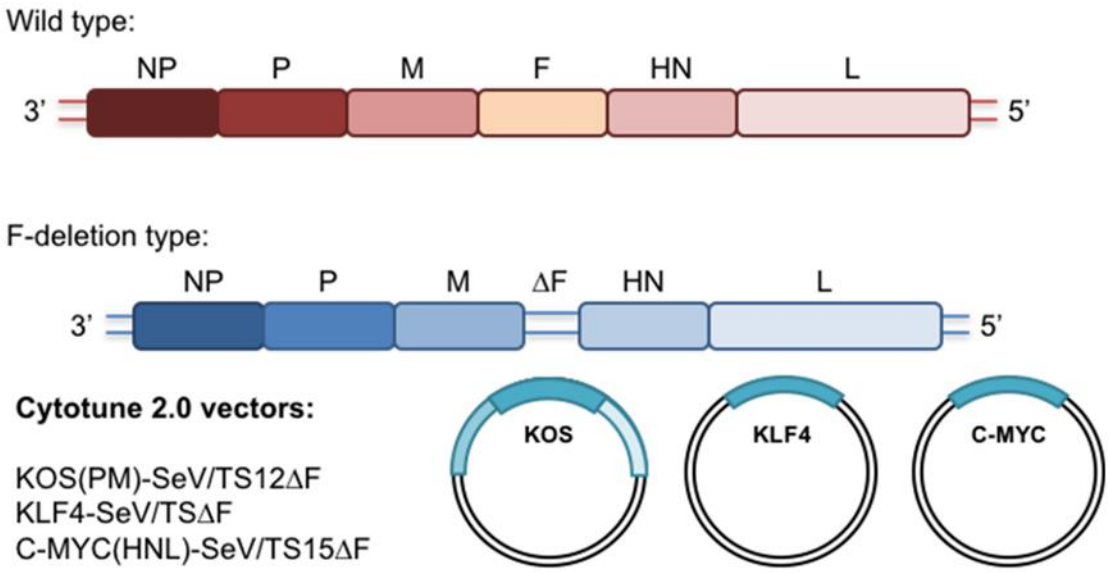

Figure 3-1. Schematic representation of the Cytotune 2.0 viral vectors. The kit consists of 3 vectors; Klf4-Oct4-Sox2, Klf4 alone and c-Myc alone. The wild-type SeV genome consists of nucleoprotein (NP), phosphoprotein (P), large protein (L), matrix (M), fusion (F) and hemagglutinin-neuraminidase (HN) proteins (Bernal, 2013). The Cytotune 2.0 vectors have deletion of the F gene to prevent budding from the infected target cells.

3.2 Aims

- To culture primary prostate stromal and epithelial cells
- To generate integration-free iPSCs from primary human prostate tissue
- To undertake full characterisation of the generated iPSCs

3.3 Results

3.3.1 Primary culture of prostate specimens

Primary prostate fibroblasts and epithelial cells were isolated from patient biopsies from Transurethral Resection of the Prostate (TURP) or Holmium Laser Enucleation of the Prostate (HoLEP) with appropriate consent and ethics review. Stromal fractions were grown in 75cm^2 flasks in RPMI medium with a success rate of approximately 90%. From day 7 of culture, areas of spindle-shaped cells could be observed (Figure 3-2) which expanded to form a monolayer typical of stromal cells (Figure 3-3). Cells could be easily passaged using trypsin and expanded up to at least passage 8 without any evident alterations in cell morphology or growth.

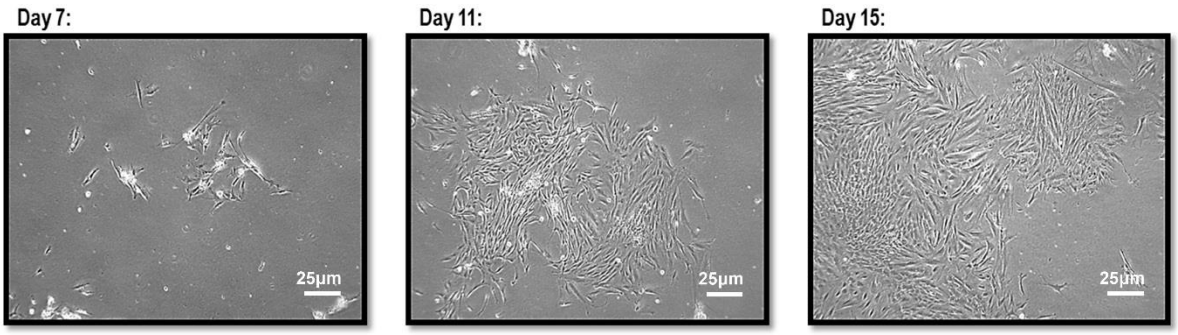

Figure 3-2. Phase contrast micrographs showing growth of prostate fibroblasts after 7, 11 and 15 days in culture. Small clusters of cells expand over time to form cell monolayers. Scale bars 25µm.

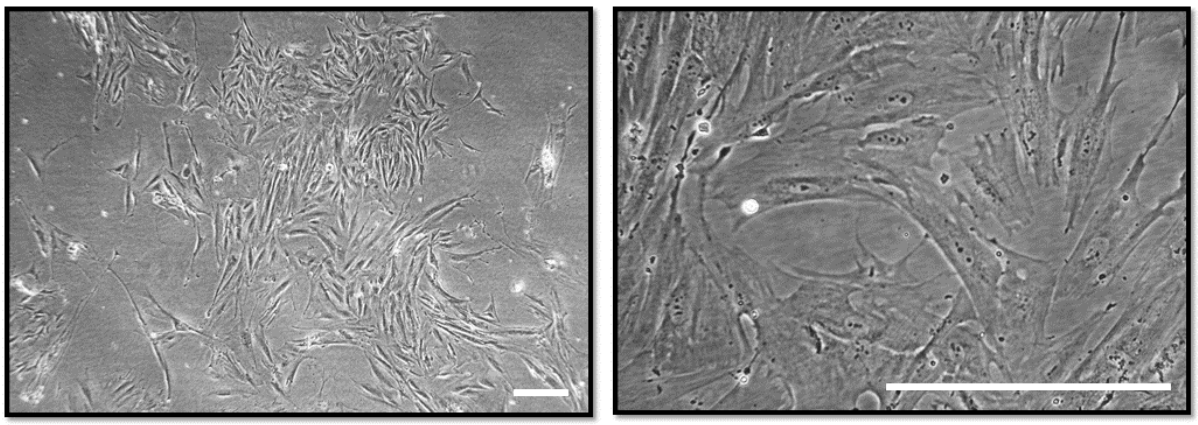

Figure 3-3. Phase contrast micrographs demonstrating morphology of typical prostate fibroblast cultures. Cells are elongated and spindle shaped. Scale bar 25µm.

Culture of primary prostate epithelial cells was significantly more challenging in comparison to fibroblasts. Epithelial fractions were plated out on collagen coated 25cm^2 flasks in KSFM medium with the addition of STO feeder cells (inactivated by irradiation) at a confluency of approximately 65%. The STO feeder cells provide stromal support for the epithelial cells without promoting the epithelial differentiation which occurs when prostate epithelial cells are cultured with prostate stroma (Niranjan *et al.*, 2013). Unfortunately, initial cultures did not grow well despite the monitoring of STO cells and addition of fresh STOs when appropriate. An alternative method was trialled by adding the epithelial fraction to the flasks alone and leaving these cells to settle for 1 hour at 37°C. At this time, the cells which had not adhered were removed and fresh medium added along with 33,000 STO cells per 25cm^2 flask. This method had more success with generating primary prostate epithelial cell cultures. By day 4, emerging colonies could be identified which proliferated to form tightly packed colonies with a typical epithelial cobblestone morphology (Figure 3-4). STO cells were added until the colonies began to proliferate and increase in confluency, at which point the surrounding epithelia were able to support themselves. Passage of primary prostate epithelial cell cultures was also challenging. Cells could be successfully passaged using trypsin-EDTA but did not grow well following passage. This protocol therefore requires further optimisation to allow stable passaging of prostate epithelial cell cultures.

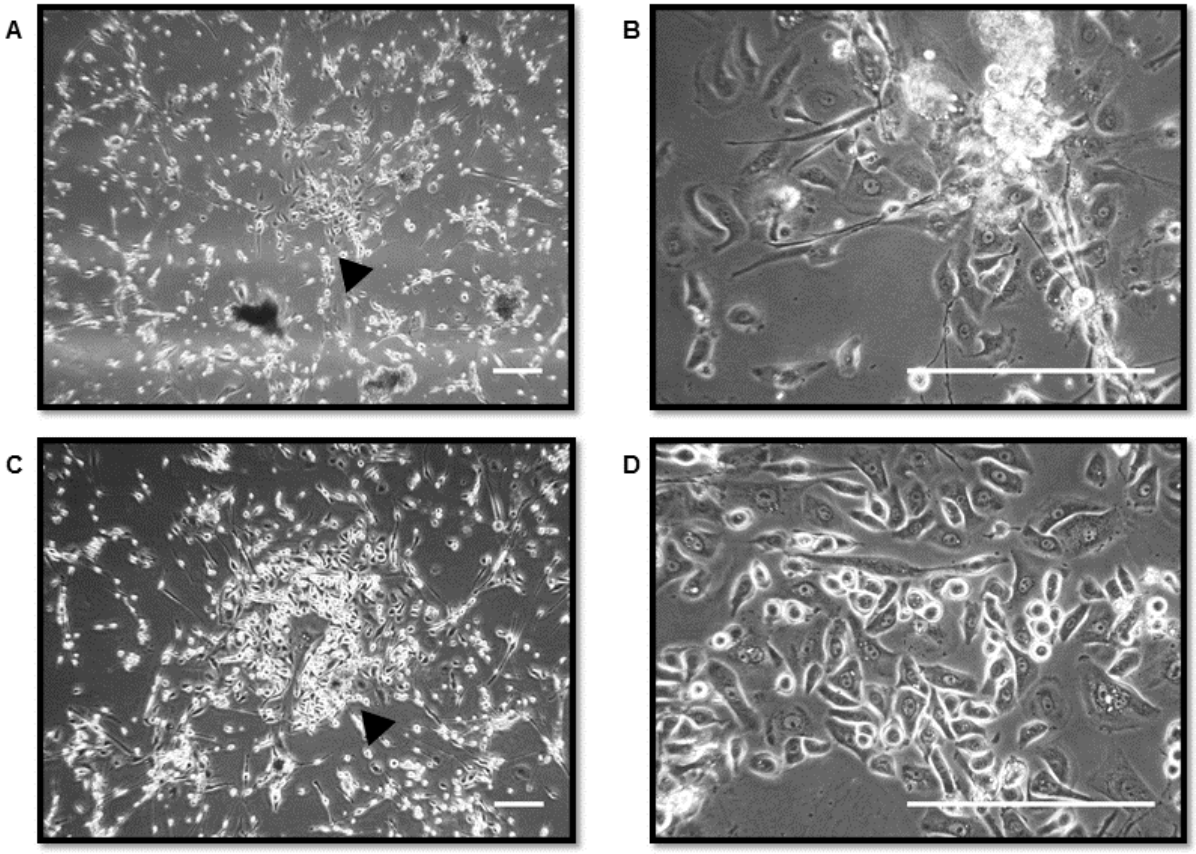

Figure 3-4. Phase contrast micrographs showing morphology of primary prostate epithelial cells following culture with STO feeder layer for 4 (A, B) and 6 (C, D) days. Small cell clusters (A, arrowhead) can be identified by day 4 of culture. These expand to form tightly packed colonies with a cobblestone appearance typical of epithelial cultures by day 6 (C, arrowhead). Scale bar 25µm.

3.3.2 Confirming purity of stromal culture

Before using the Cytotune 2.0 reprogramming vectors it was necessary to check the purity of the stromal cultures. This was performed using RT-PCR for primers against epithelial (CD24), haematopoietic (CD45) and fibroblastic (α-SMA, CD90) cells. Standard curves and obtained ct values for each gene confirmed the suitability of each primer set. The results (Figure 3-5) confirm the expression of fibroblast markers and absence of other cell lineage markers in a patient sample at passage 3. Previous work in the group has also confirmed the purity of stromal cultures by passage 2 (Pal, 2014).

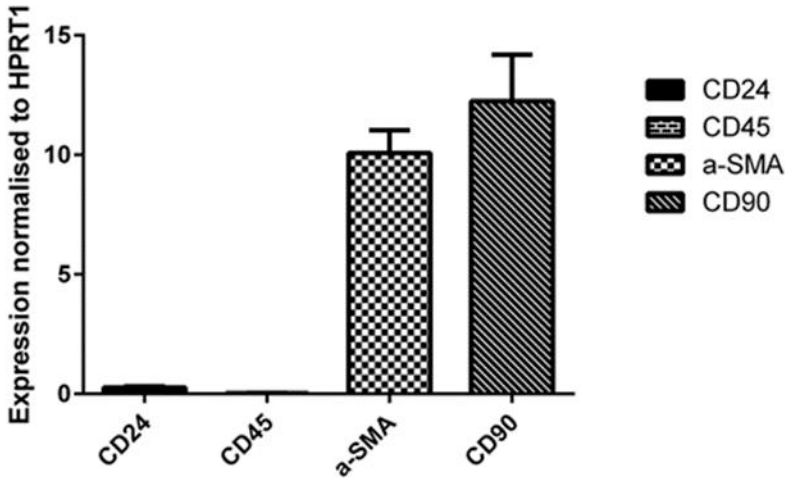

Figure 3-5. RT-PCR analysis showing expression of CD24 (epithelial cell marker), CD45 (haematopoietic marker), and a-SMA and CD90 (stromal markers) in a primary prostate fibroblast culture at passage 3.

3.3.3 Efficiency of Sendai viral vector entry to prostate fibroblasts

Before transducing cells with the Cytotune 2.0 Sendai reprogramming vectors, it was necessary to investigate the efficiency of Sendai virus entry to the target cells. To do this, 30,000 prostate fibroblasts, urinary tract fibroblasts or human dermal fibroblasts (as a known control) were seeded into each well of a 12 well plate and allowed to settle for 24 hours. At this point, the Cytotune Sendai EmGFP control virus was added to wells at multiplicity of infection (MOI) of 0, 1, 5, 10, and 20. After 24 hours of incubation with the virus, the medium containing the EmGFP vector was removed and standard medium was added. Cells were checked and imaged using a fluorescent microscope to check for the presence of GFP positive cells. At 48 hours post transduction, cells were imaged again and then analysed using flow cytometry to quantify the percentage of GFP positive cells.

As expected, there was an increase in the percentage of GFP positive cells in all three cell types as the MOI increased from 0 to 20 (Figure 3-7,Figure 3-6) In primary prostate fibroblasts (n=3) there was a significant increase in the percentage of GFP positive cells between MOI 0 and 1 ($p \leq 0.01$), and MOI 1 and 5 ($p \leq 0.0001$). At higher MOI, the percentage of GFP positive cells did not increase significantly. As a result, we decided to continue with the suggested MOI of 5-5-3 (KOS MOI=5, hc-Myc MOI=5, hKlf4 MOI=3) for the Cyotune 2.0 reprogramming vectors.

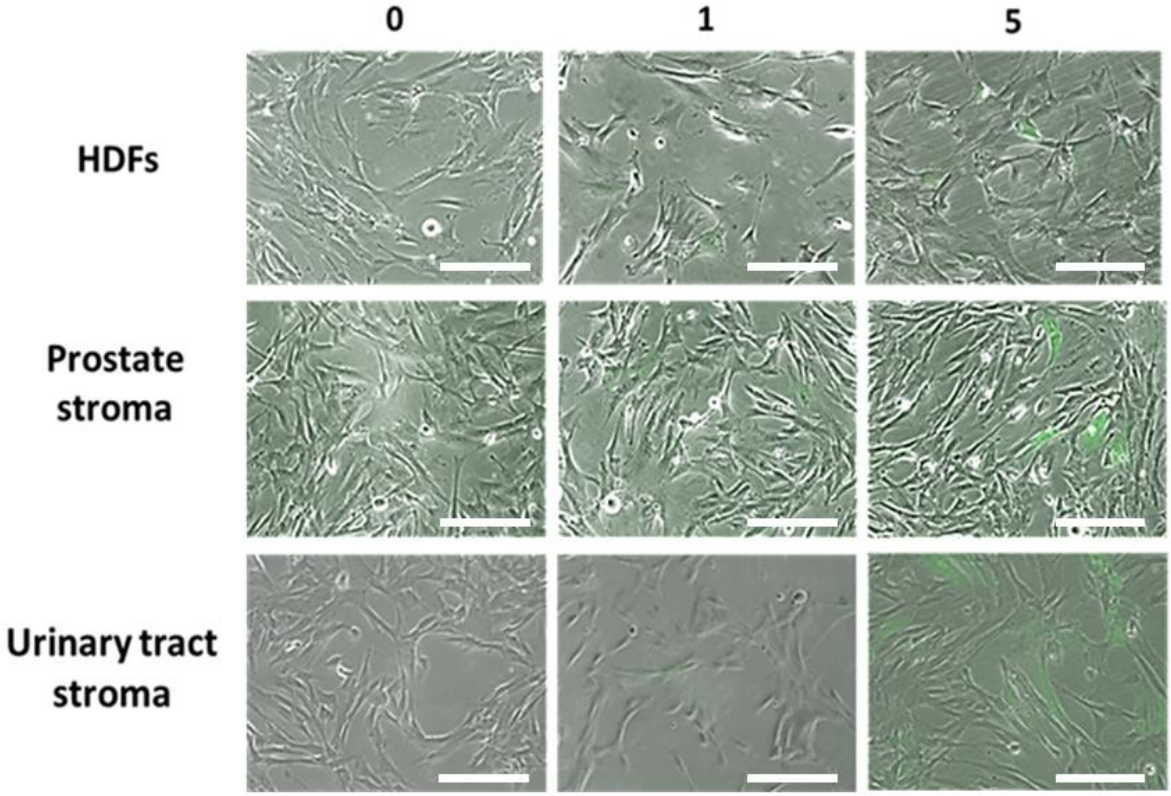

Figure 3-6. Merged phase contrast and fluorescent micrographs showing increase in GFP positive cells at higher MOI after 24 hours of transduction. Scale bar 5µm.

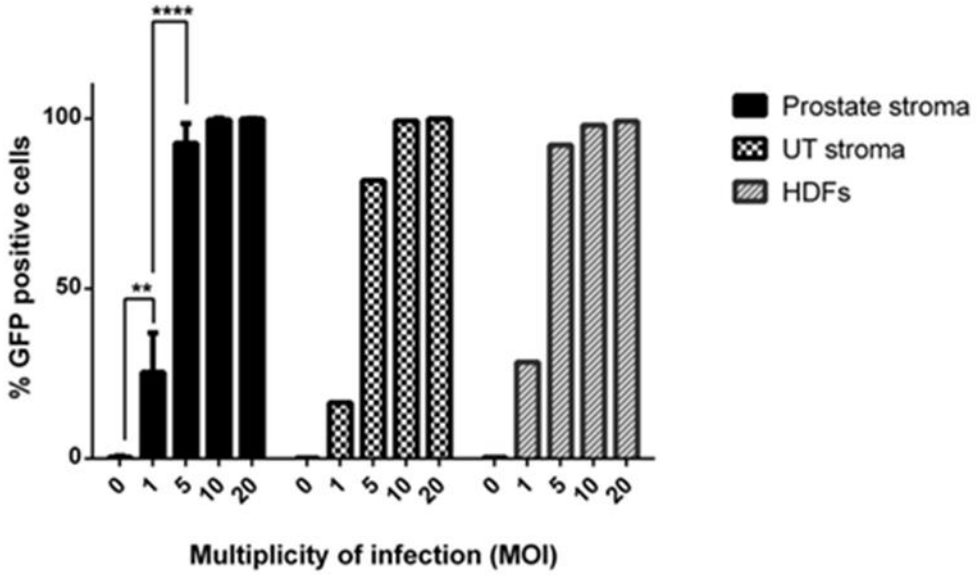

Figure 3-7. FACS analysis showing the percentage of GFP positive prostate stroma, UT stroma or HDFs following a 48 hour transduction with EmGFP Sendai control virus at a range of MOI.

3.3.4 Reprogramming primary human prostate fibroblasts into iPSCs using Sendai virus vectors

To generate iPSCs, benign primary prostate fibroblasts from an 82 year old patient were seeded out in fibroblast medium at a density of 1 x10^5 cells per well in two 12 well plates. After 24 hours (designated as day 0), cells in the experimental plate were transduced with Cytotune 2.0 Sendai virus vectors containing the reprograming factors Klf4, Oct4, Sox2 and c-Myc at an MOI of 5-5-3 (KOS-Myc-Klf4), whilst the control plate received fresh medium without the addition of viral vectors. At 24 hours post-transduction the reprogramming medium was removed and fresh fibroblast medium added. Media was then changed every 48 hours and the cultures closely monitored by phase contrast microscopy to identify any changes in morphology and potential colony formation. By day 5, small areas of MET could be seen which were not apparent in the control plate, which retained a purely stromal phenotype (Figure 3-8). MET involves a shift from the typical fibroblast phenotype of elongated, spindle-shaped cells to tightly packed, small, cuboidal cells with evident intercellular junctions. This morphological change is accompanied by an increase in epithelial markers and down regulation of mesenchymal markers, and marks the initiation of cellular reprogramming (Li *et al.*, 2010b).

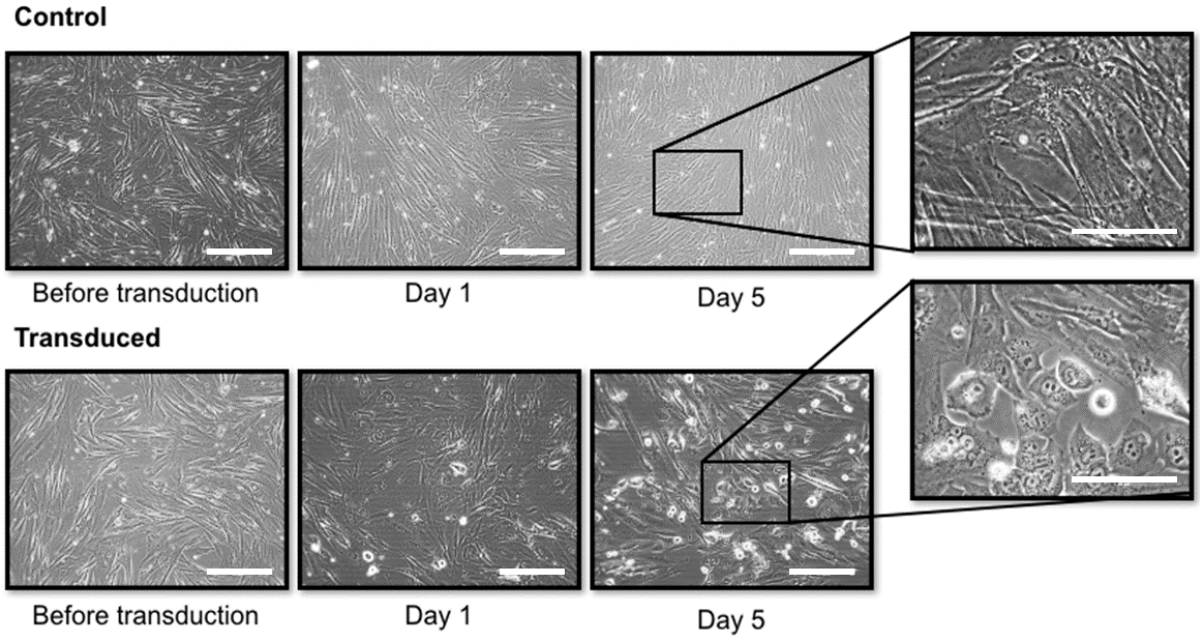

Figure 3-8. Phase contrast micrographs showing a clear change in morphology following transduction of cells with Cytotune 2.0 viral vectors. Cell death could be seen from 24 hours post transduction. At day 5, areas of MET could be identified. Scale bars 25μm. Inset shows high magnification of this area. Scale bar 10μm.

On day 7, cells were transferred to vitronectin coated 6 well plates at a density of $1.5x10^4$ cells per well. Vitronectin is a defined ECM protein which can be used for growth of stem cells, which bind to the matrix through the αVβ5 integrin (Braam *et al.*, 2008). After 24 hours on vitronectin, the medium was changed to Essential 8 medium, a defined, serum-free DMEM/F12 based medium developed by James Thompson's laboratory (Chen *et al.*, 2011). From this point the medium was changed every 48 hours and cells were carefully monitored for the presence of emerging colonies (Figure 3-9). Between week 2 and 3 colonies which resembled ESCs began to emerge. These colonies proliferated rapidly and contained small, tightly-packed cells with a high nuclear to cytoplasmic ratio. Two types of colony were identifiable; the first had typical ESC morphology and very well defined borders, whilst the second showed less defined borders (Figure 3-10). Colonies were picked manually under a dissecting microscope within a sterile laminar flow hood and transferred to individual wells for clonal expansion. An average of 49 colonies were identified per $1.5x10^4$ cells plated giving a reprogramming efficiency of 0.33%.

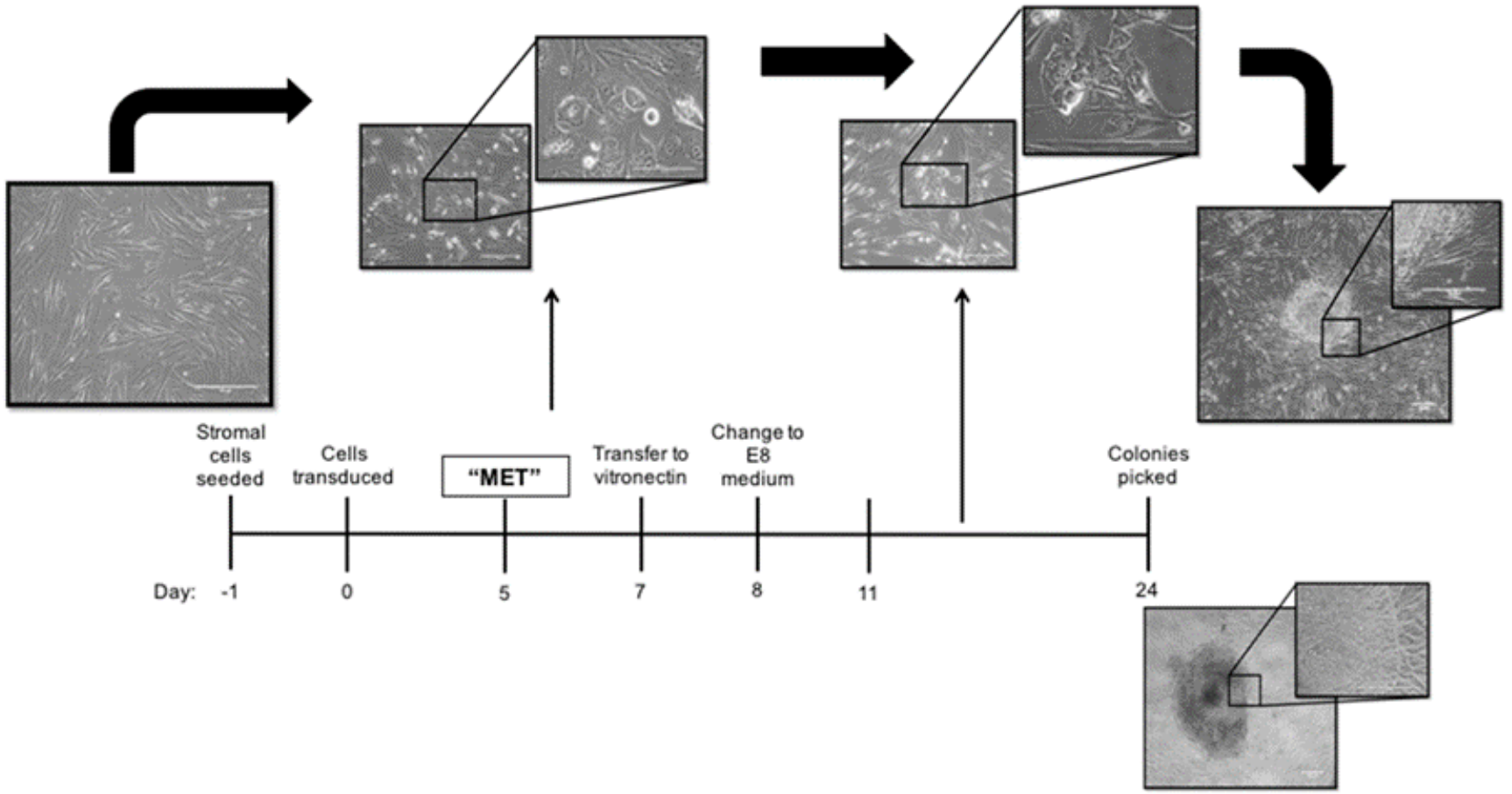

Figure 3-9. Schematic showing the timescale for reprogramming primary prostate fibroblasts to iPSCs using Cytotune 2.0 Sendai viral vectors. Micrographs show the change in cell morphology over this period from MET to appearance of ESC-like colonies.

To determine the optimum conditions for subsequent culture, the growth of colonies was compared in the major feeder-free stem cell culture environments; mTESR1 or E8 medium on Matrigel or vitronectin plates. mTESR1 is a DMEM/F12 based medium supplemented with a range of growth factors, vitamins, minerals and lipids including bFGF, TRGF beta 1, insulin, transferrin and human serum albumin, which was specifically developed as a defined medium for hESCs (Ludwig *et al.*, 2006). Matrigel is an extracellular matrix isolated from Engelbreth-Holm-Swarm murine sarcoma tumour, consisting of a number of components including laminin, collagen and heparin sulphate proteoglycan which is widely used for stem cell culture (Kleinman *et al.*, 1986; Mallon *et al.*, 2006). When cultured in E8 or mTESR1 medium on vitronectin-coated plates, colony morphology was that of a typical iPSC colony, but spontaneous differentiation occurred at a significant rate and passaging of cells proved challenging. In contrast, colonies grown on Matrigel in mTESR1 medium showed characteristic iPSC morphology and growth, and passaging with dispase was simpler and produced less differentiation (Figure 3-11) . Therefore, once colonies were established they were transferred to Matrigel culture in mTESR1 medium and clonally expanded before characterisation. This culture method is the most widely used within the stem cell field and has previously been used for successful feeder-free iPSC culture in our lab. The morphological appearance of the clones was very similar to that of hESCs; the colonies showed defined borders and cells were tightly packed together (Figure 3-12). Cells had obvious, large nucleoli and were roughly oval in shape. During culture, spontaneous differentiation was observed in the cultures, with numerous cell types identified. The differentiation occurred either at the centre of colonies or arising from the periphery of the colony (Figure 3-13). This is a known phenomenon in hESCs (Sathananthan and Trounson, 2005) and demonstrated evidence of the pluripotency of the generated cells. During iPSC culture, these areas of spontaneous differentiation were manually removed with a pipette under a dissecting microscope to maintain clean cultures.

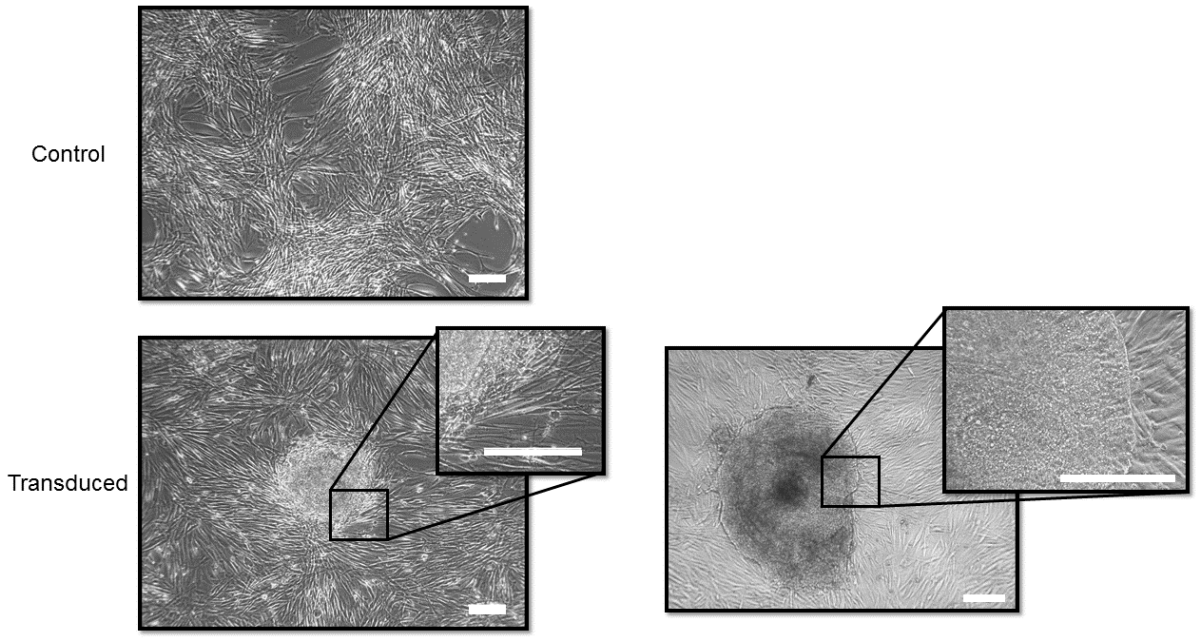

Figure 3-10. Phase contrast micrographs showing morphology of colonies generated from reprogramming of primary prostate fibroblasts. Cells within the control plate remain spindle-shaped whilst compact colonies with defined borders and small cells are evident within the transduced cells. Scale bar 25µm.

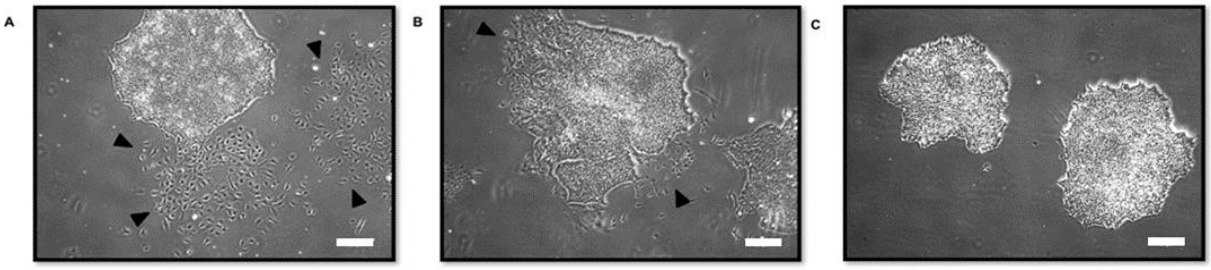

Figure 3-11. Phase contrast micrographs showing iPSCs cultured on vitronectin with E8 medium (A), on Matrigel with E8 medium (B) or on Matrigel in mTESR1 medium (C). Culturing the iPSCs on Matrigel in mTESR1 medium reduced levels of spontaneous differentiation (marked by arrowheads) occurring after passage. Scale bar 25μm.

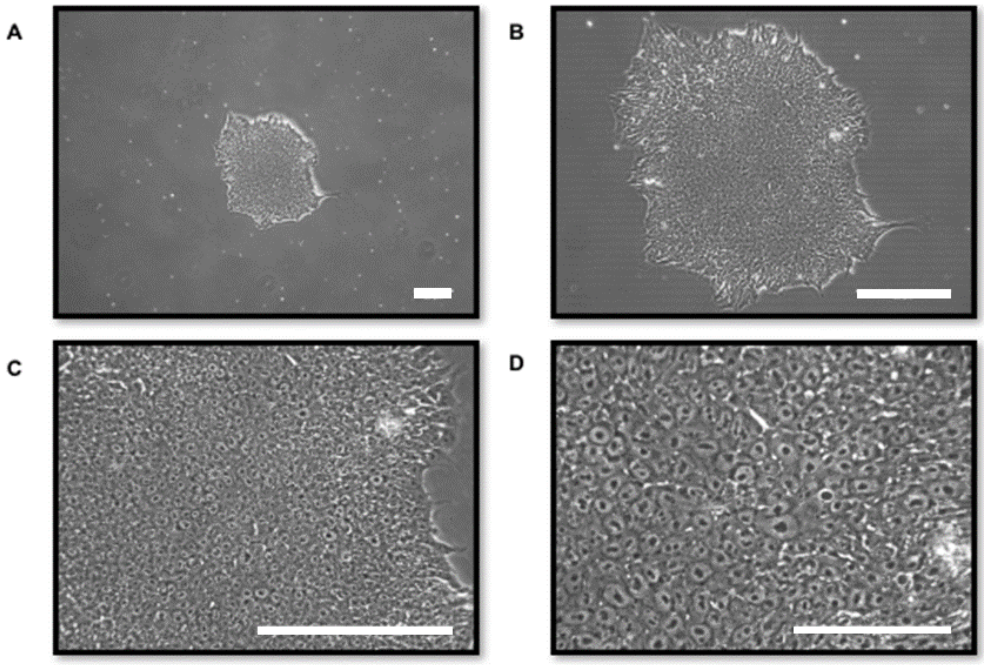

Figure 3-12. Phase contrast micrographs showing typical morphology of iPSCs following picking of individual clones and transfer to Matrigel. Cells grew as round, tightly-packed colonies with defined borders. Cells were compact with a large nucleus. Magnification shown A) 40x, B) 100x, C) 200x, D) 400x. Scale bar A-C 25μm, D 10μm.

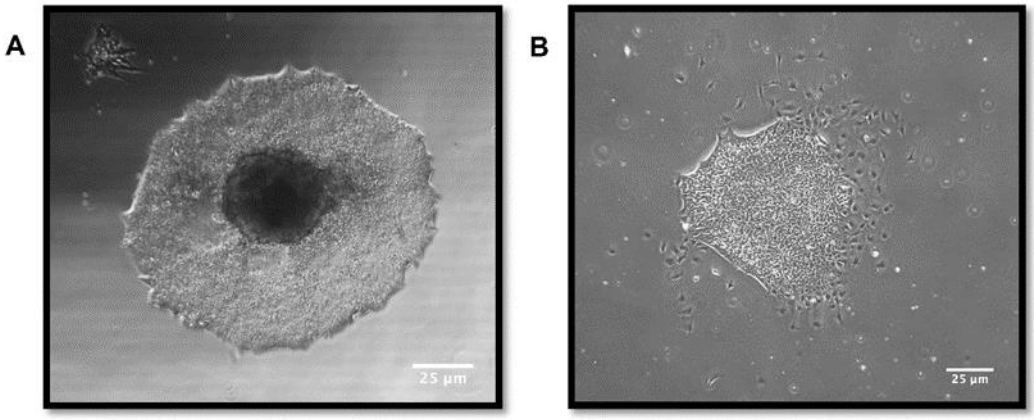

Figure 3-13. Spontaneous differentiation arising from the centre (A) or periphery (B) of colonies. Scale bar 25μm.

3.3.5 Characterisation of iPSCs

To confirm the identity of the generated cells as iPSCs a range of characterisation steps are required as set out by the International Stem Cell Banking Initiative including antigen and gene expression analysis, confirmation of pluripotency both *in vitro* and *in vivo*, karyotype analysis, cell identity and microbiological testing (International Stem Cell Banking Initiative, 2009).

One of the initial tests for iPSC characterisation is alkaline phosphatase expression, which is a known marker of undifferentiated hESCs (O'Connor *et al.*, 2008). All colonies tested stained positive for alkaline phosphatase expression with no staining found in the parental fibroblasts which were used as a negative control (Figure 3-14). Areas of differentiation at the centre of colonies were also negative for alkaline phosphatase acting as an internal negative control.

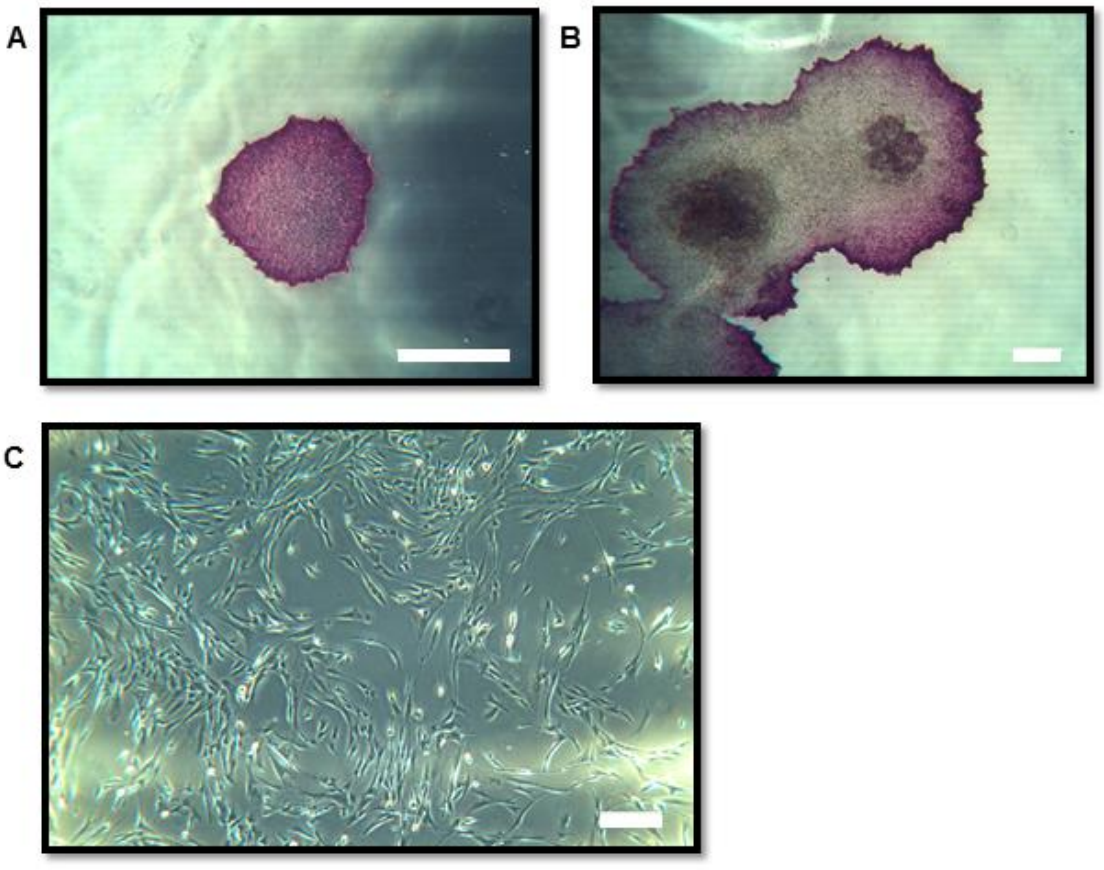

Figure 3-14. Alkaline phosphatase staining of iPSC colony (A) shows strong expression. Areas of differentiation within colonies are negative for alkaline phosphatase (B) acting as an internal negative control. Parental fibroblasts are negative for alkaline phosphatase expression (C). Scale bar 25μm.

Sendai virus is cleared from cells after approximately 10 passages by a dilution effect during cell division (Malik and Rao, 2013). The Cytotune 2.0 vectors also contain temperature sensitive mutations in key viral genes which allow for clearance of vectors by incubation at the non-permissive temperatures of 38-39°C for 5 days if necessary (Ban *et al.*, 2011). To check for clearance of the viral vector genes from the generated cells, RT-PCR was performed using primers specific to the Sendai virus genome and each of the three viral vectors. The results confirmed no detectable expression of viral genome or vectors in iPSC clones after 35 PCR cycles (Figure 3-15). Parental stroma was used as a negative control whilst transduced cells at day 7 were used as a positive control.

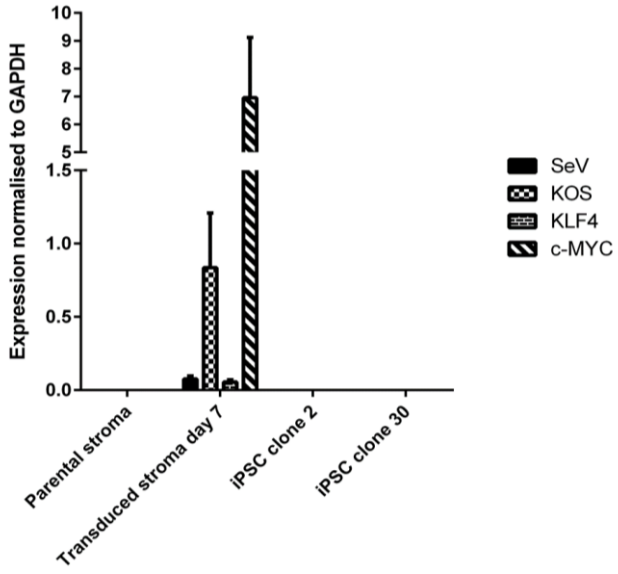

Figure 3-15. Expression of Sendai viral vectors in parental stroma, transduced stroma and iPSC clones. iPSC clones show no expression of the viral backbone or vectors confirming viral clearance. Error bars show SD, *n*=3.

A number of markers specific to hESCs were measured in the generated cells at both protein and mRNA level using immunofluorescence and RT-PCR respectively. hESCs express Oct4, Sox2, Nanog, Tra-1-60, Tra-1-81 and SSEA4, which are all crucial for maintenance of the pluripotent state (Marti *et al.*, 2013). SSEA1 is present in murine ESCs but absent in hESCs and was used as a negative control. Parental stroma was also tested alongside the iSPC as a control. The generated cells showed expression of all markers tested with the exception of SSEA1 which was expected as the negative control (Figure 3-16). Furthermore, no expression of hESC markers was evident in the parental fibroblast control. All markers showed correct localisation with SSEA4, Tra-1-60 and Tra-1-81 present on the cell surface and Oct4 co-localised with DAPI in the cell nucleus.

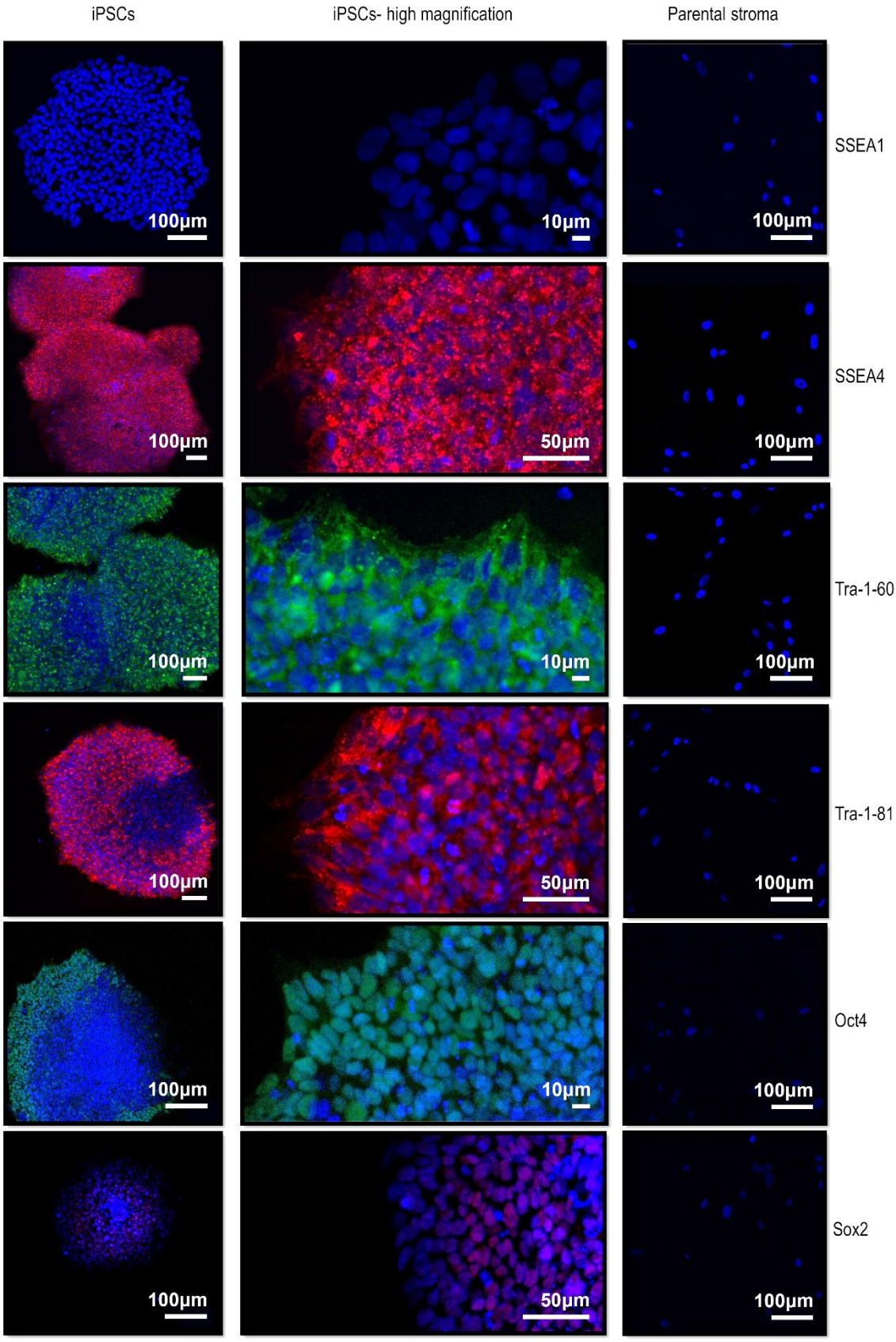

Figure 3-16. Immunofluorescence showing expression of the stem cell markers SSEA1, SSEA4, Tra-1-60, Tra-1-81 and Oct4 in the iPSCs. Central panel shows high magnification images for each stem cell marker. Parental stroma is used as a negative control. Scale bars; left and right hand columns 100µm. Middle column; 10µm (SSEA1, Tra-1-60, Oct4), 50µm SSEA4, Tra-1-81, Sox2.

Additional analysis of the stem cell markers OCT4, SOX2, NANOG, DNMT3B and REX1 was carried out by RT-PCR using the primers detailed in Table 1. Figure 3-17 shows that the iPSCs (*n*=3) showed expression of these markers at levels comparable to the hESC line H9 which was used as a positive control. The parental fibroblast cells were again included as a negative control.

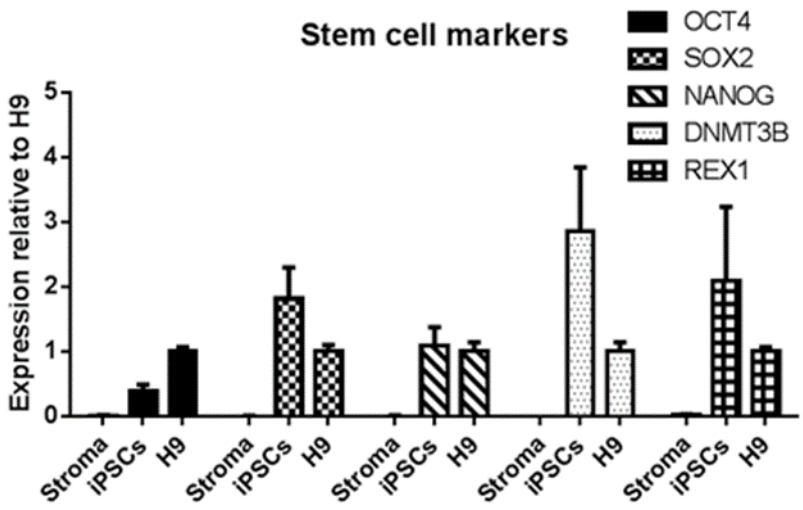

Figure 3-17. Expression of the stem cell markers OCT4, SOX2, NANOG, DNMT3B and REX1 in parental stroma, iPSCs and the H9 hESC line. Error bars represent SD, *n*=3

To confirm that the iPSCs were generated from the parental fibroblasts which were reprogrammed rather than resulting from contamination from another cell source, DNA fingerprinting was performed. To do this, 16 short tandem repeat (STR) sequences including the sex locus Amelogenin were analysed in both the iPSCs and parental fibroblasts. STRs are sequences 2-7 nucleotides long which are highly polymorphic between individuals and can therefore be used to determine identity of samples (Thompson et al., 2012). Analysis revealed identical expression of all 16 markers confirming that the iPSCs originated from the parental fibroblasts (Table 3-1).

Marker	iPSCs	Fibroblasts
Amelogenin	X-Y	X-Y
D3S1358	16-16	16-16
THO1	6-9.3	6-9.3
D21S11	30-30	30-30
D18S51	12-13	12-13
PentaE	13-14	13-14
D5S818	11-13	11-13
D13S317	10-12	10-12
D7S820	11-12	11-12
D16S539	10-13	10-13
CSF1PO	10-10	10-10
PentaD	9-10	9-10
vWA	16-17	16-17
D8S1179	14-16	14-16
TPOX	8-8	8-8
FGA	23-25	23-25

Table 3-1. DNA fingerprinting results showing identical STR sequences in the iPSCs and fibroblasts.

Genomic alterations can occur in pluripotent stem cells as a result of the reprogramming process or after prolonged *in vitro* culture, and may impact on the developmental potential of such cells (Lund *et al.*, 2012). To confirm the genetic stability of the generated cells, the iPSC karyotype was analysed at passage 24 using G-band karyotyping (Centre for Life, Newcastle upon Tyne). Analysis of 30 metaphases showed a normal 46 XY karyotype (Figure 3-18).

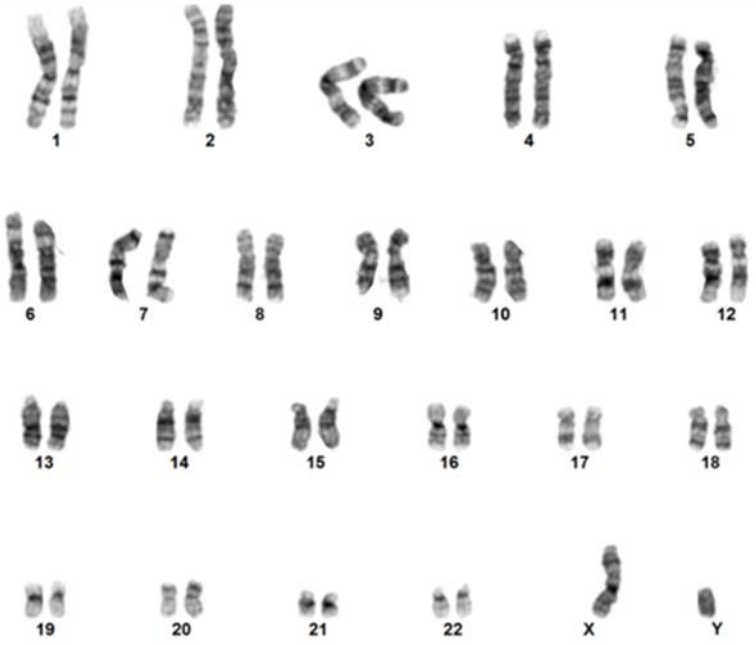

Figure 3-18. G-banding of the iPSCs shows a normal 46 XY karyotype.

3.3.6 In vitro pluripotency testing by formation of embryoid bodies

Suspension culture of embryonic stem cells generates three-dimensional aggregates termed embryoid bodies, which contain cells derived from all three embryonic germ layers (Itskovitz-Eldor *et al.*, 2000). To determine the pluripotency of the putative iPSCs *in vitro*, colony pieces were suspended into differentiation medium in low adherence dishes. Cell aggregates formed which increased in size over a period of 2 weeks (Figure 3-19). The embryoid bodies were then seeded onto gelatin coated plates or chamber slides to allow for explant culture. Cells grew out from the embryoid bodies and were monitored by microscopy. A variety of cellular morphologies were visible including neuronal-like, epithelioid-like and stromal-like cells. Cells in the chamber slides were fixed in 4% paraformaldehyde and stained

using antibodies against markers of the embryonic germ layers. Cells within plates were harvested for RNA extraction and RT-PCR analysis.

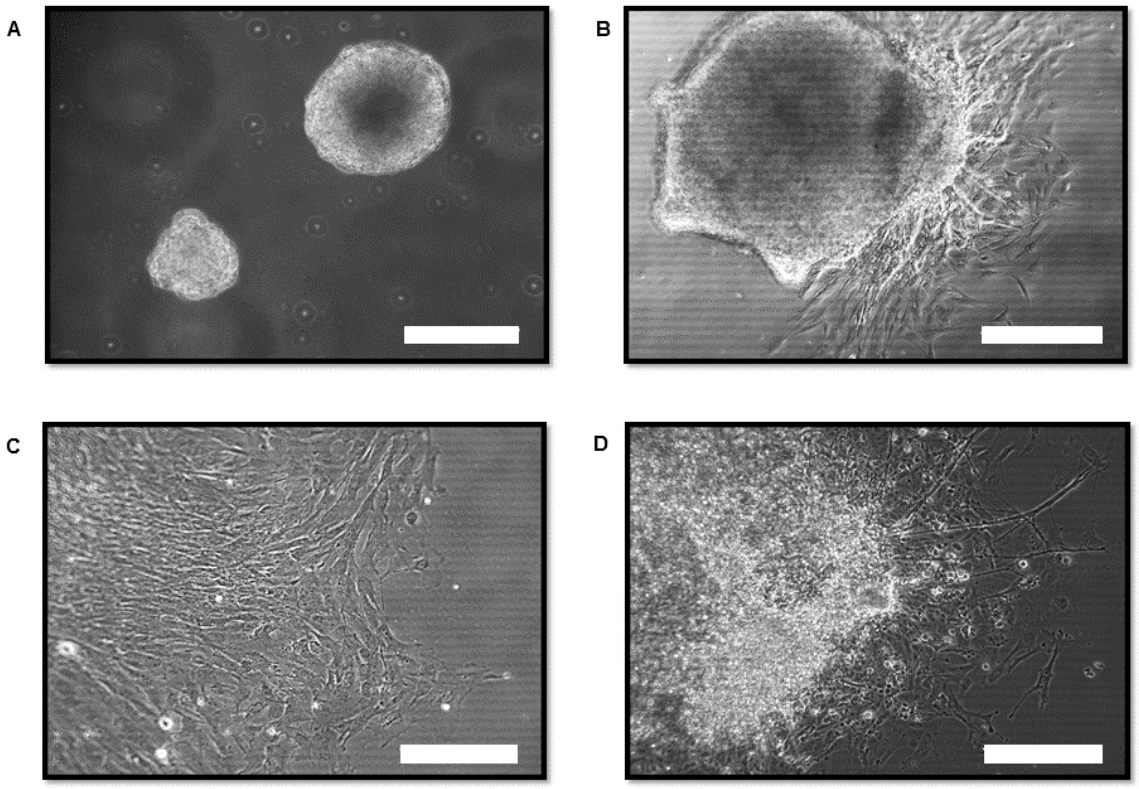

Figure 3-19. Phase contrast micrographs showing formation of embryoid bodies from iPSCs (A). A range of cell morphologies can be seen when the embryoid bodies are explanted (B-D) including stromal-like (B), endothelial-like (C), and neuronal-like (D) cells. Scale bar 25µm.

Immunofluorescence showed the embryoid bodies had generated cells which expressed the mesodermal marker vimentin, the endodermal marker α-fetoprotein

(AFP) and the ectodermal marker βIII tubulin at protein level (

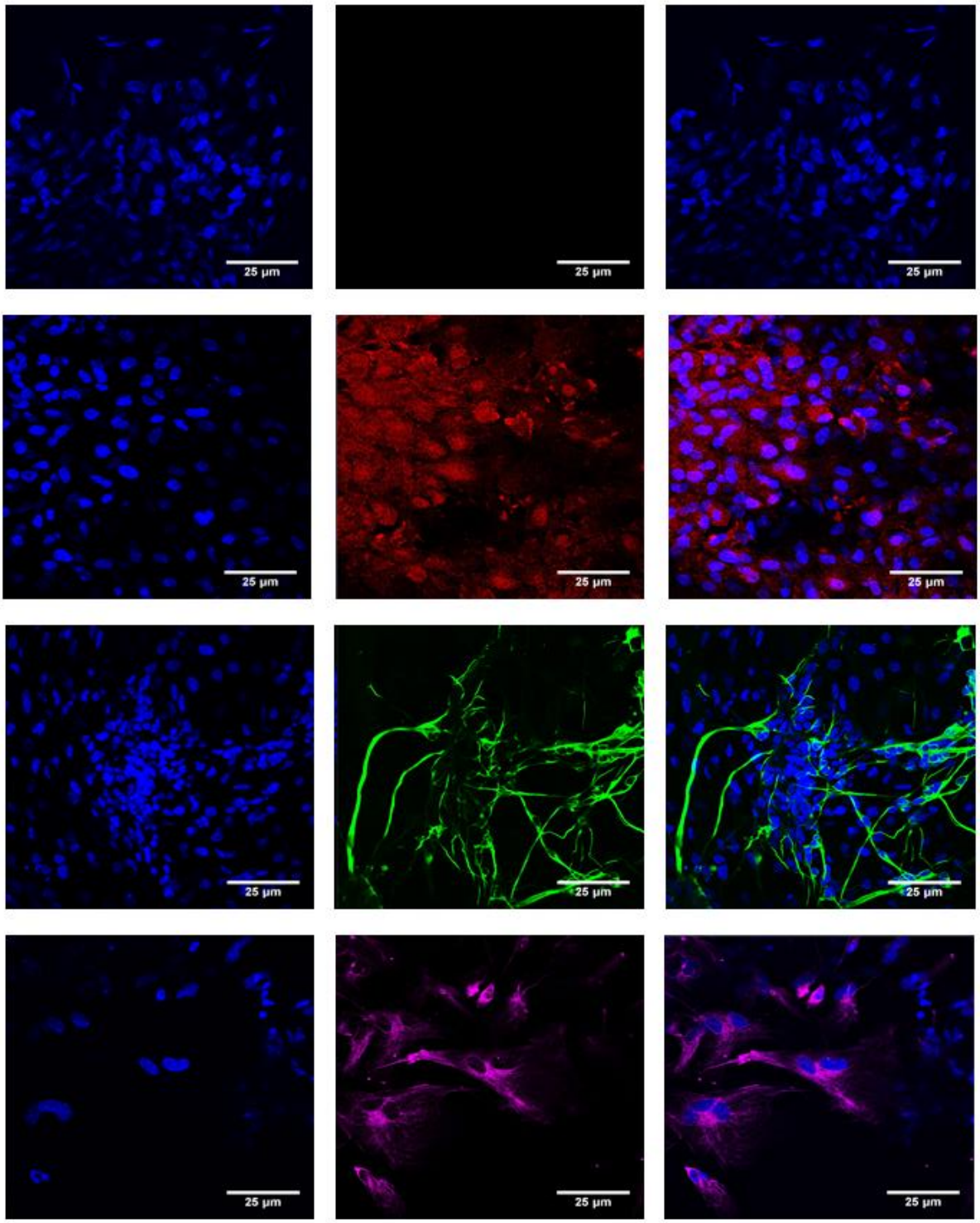

Figure 3-20). RT-PCR analysis was also conducted, showing an increase in transcript level expression of the mesodermal marker α-smooth muscle actin (αSMA), the endodermal marker AFP and the ectodermal marker PAX6 in comparison to undifferentiated iPSCs, along with a concurrent decrease in the stem

cell markers OCT4, SOX2 and NANOG (Figure 3-21, Figure 3-22). Together these results confirm the pluripotency of the putative iPSCs *in vitro*.

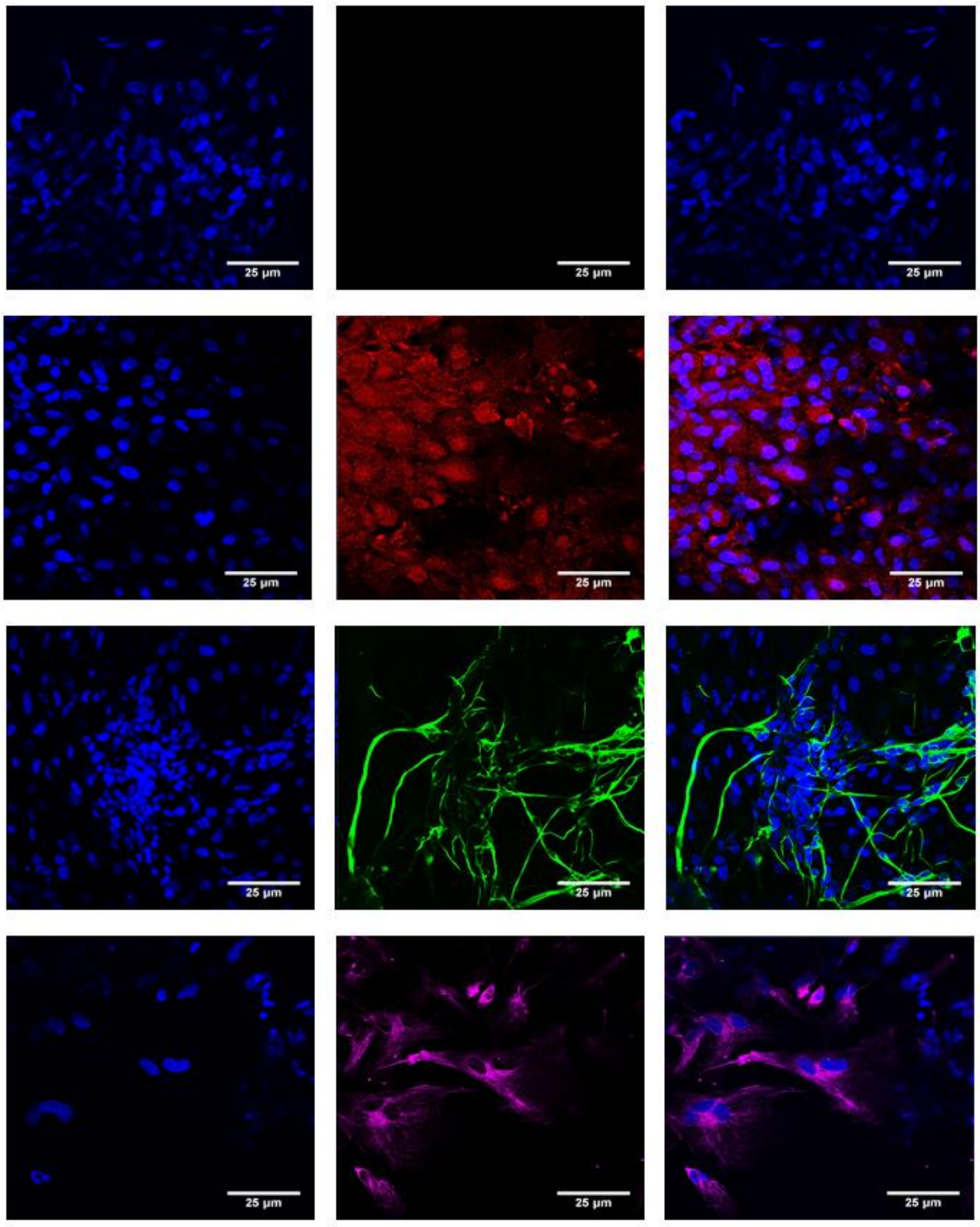

Figure 3-20. Immunofluorescence showing cells of all three embryonic germ layer origins formed by embryoid body explants. AFP; endoderm; BIII tubulin; ectoderm; Vimentin, Mesoderm. Scale bar 25µm.

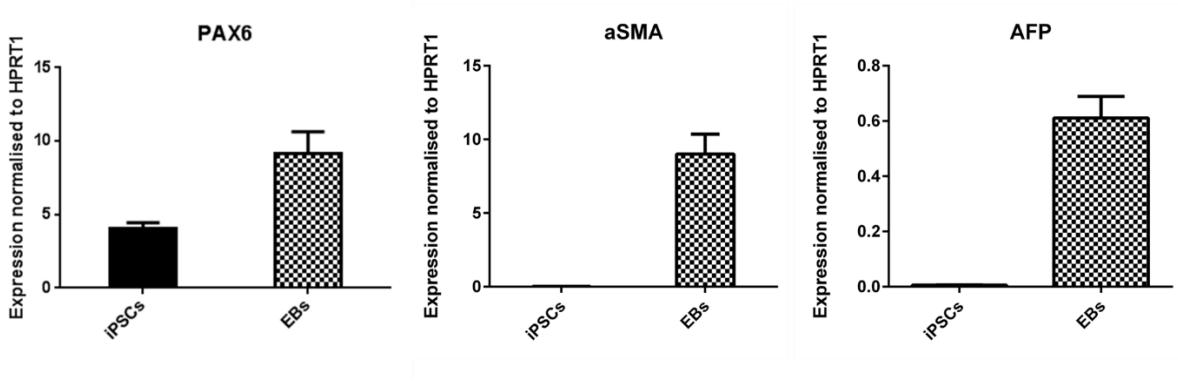

Figure 3-21. Expression of PAX6 (ectoderm), aSMA (mesooderm) and AFP (endoderm) in iPSCs and embryoid bodies. All 3 markers are upregulated in the embryoid bodies. Error bars represent SD, results show average of *n*=3 experiments.

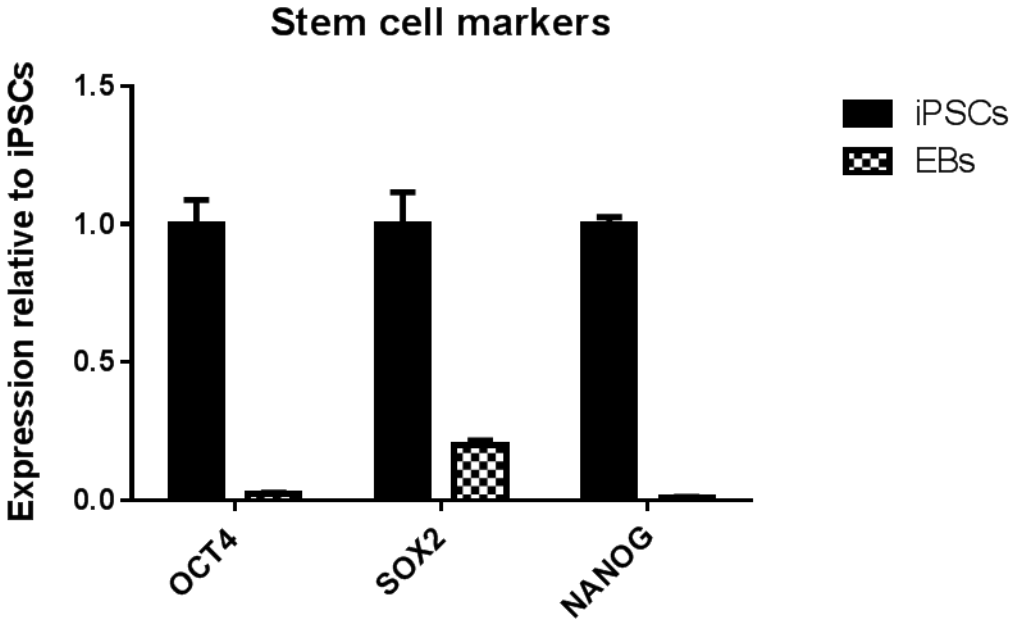

Figure 3-22. RT-PCR analysis of the stem cell markers OCT4, SOX2 and NANOG in EBs compared to iPSCs. EBs show decreased expression of all three stem cell markers. Error bars represent SD, *n*=3.

3.3.7 In vivo pluripotency testing using teratoma assays

Despite the ability to differentiate to cells from the three embryonic germ layers *in vitro*, the *in vivo* differentiation capacity of the putative iPSCs also needed to be tested. The current gold standard for measuring pluripotency of human cells is teratoma formation upon injection of cells into immune compromised mice (International Stem Cell Banking Initiative, 2009) . A teratoma is a benign tumour containing a mixture of tissues from the three embryonic germ layers including hair, teeth, organs and cartilage, showing true pluripotential ability (Zhang *et al.*, 2008). The teratoma assay was therefore performed to test the *in vivo* pluripotency of the generated cells.

1 x 10^6 iPSCs were mixed 1:1 with Matrigel and injected subcutaneously into NSG mice (*n*=3 per clone). Measurable tumour formation occurred from day 32 onwards with a rapid increase in size (Figure 3-23). Teratomas were harvested and divided into two parts, with one part fixed in Bouin's solution and paraffin embedded for histology and the second part snap frozen in isopentane. The tissue sections were analysed histologically to check for presence of cells from the three embryonic germ layers. Teratoma formation, defined as the presence of tissue from all three germ layers, was seen in 5 out of 6 mice tested (*n*=3 per clone). The teratomas formed varied widely in gross appearance and contained mesodermal, ectodermal and endodermal tissue. Representative low and high magnification images of a teratoma formed in this experiment are shown, containing fat, cartilage, ciliated respiratory epithelium, squamous epithelium and hair follicle (Figure 3-24, Figure 3-25). This confirmed that the generated clones were true iPSCs.

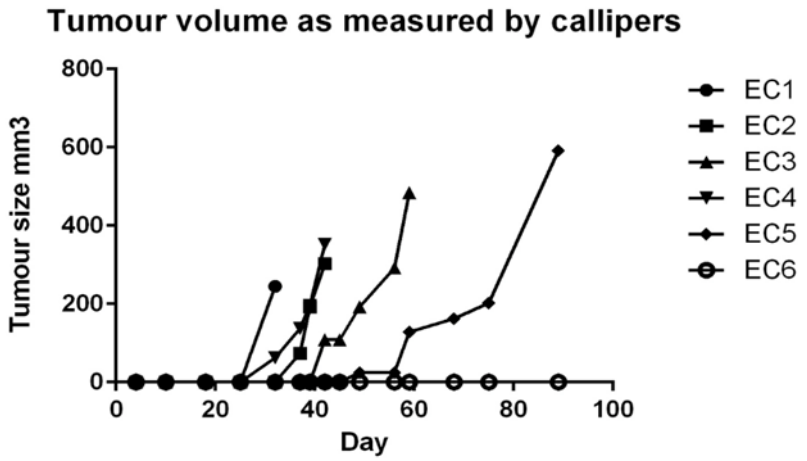

Figure 3-23. Tumour growth monitored by calliper measurements in 6 mice (EC1-EC6). Tumours formed from the iPSCs from day 32 and grew rapidly. Late growing tumour EC5 showed a range of more complex tissues including hair follicle formation.

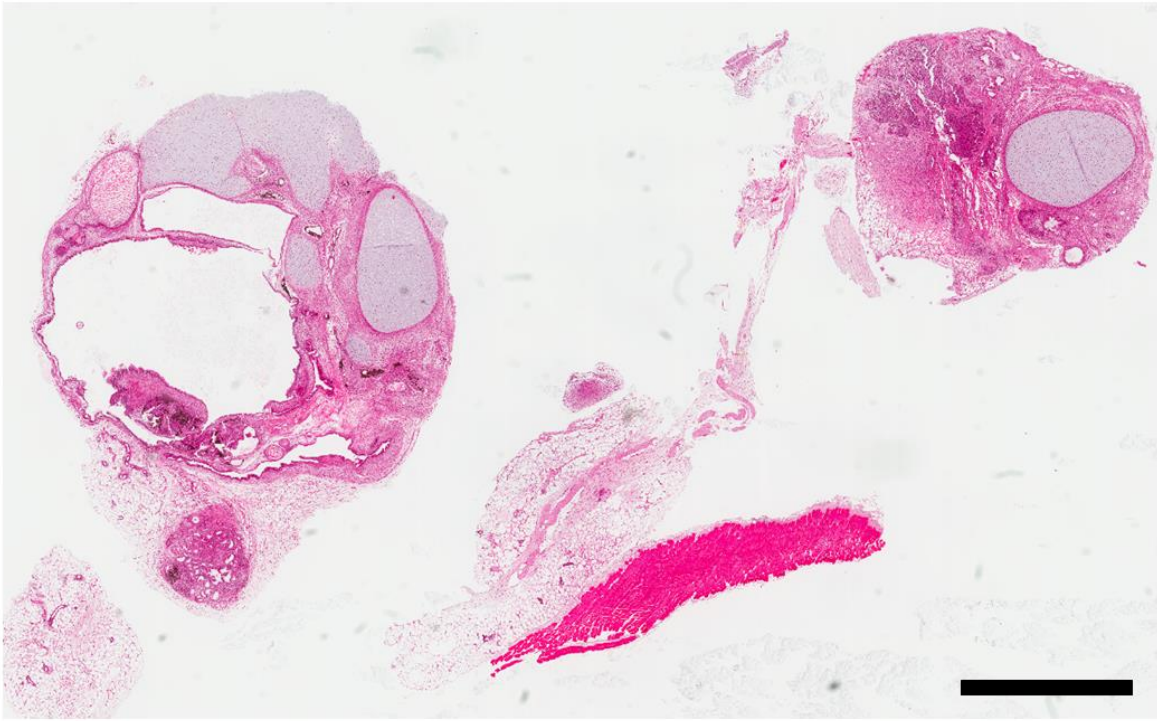

Figure 3-24. Low magnification image showing a representative H&E stained teratoma section. The teratoma contains tissues from all three embryonic germ layers. Scale bar 2mm.

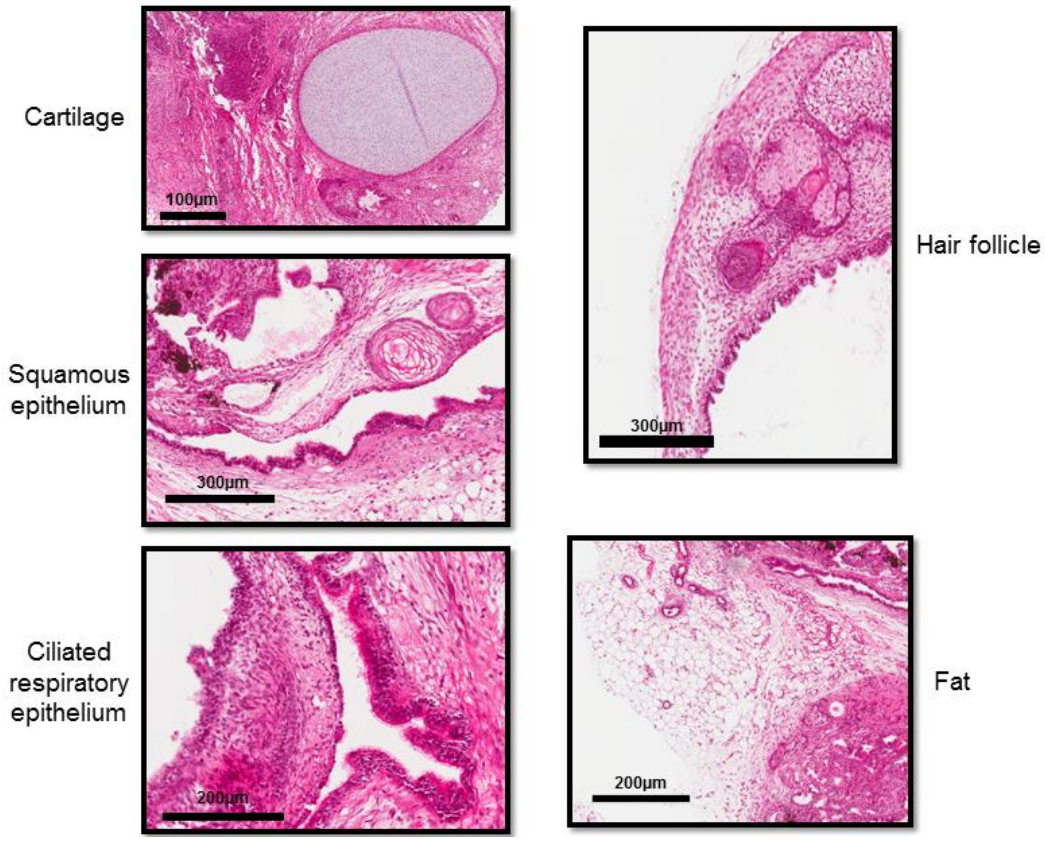

Figure 3-25. High magnification images from the above H&E stained teratoma section showing formation of cartilage, squamous epithelium, ciliated respiratory epithelium, hair follicle and fat.

3.3.8 Reprogramming prostate epithelial cells using Cytotune 2.0 Sendai viral vectors

As previously discussed, the parental cell of origin can impact on the differentiation potential of iPSCs due to an epigenetic memory which remains present after reprogramming (Kim *et al.*, 2007). Whilst prostate fibroblasts are generated from mesoderm, prostate epithelium is endodermal in origin. Therefore, generation of iPSCs from both prostate fibroblasts and epithelial cells would allow comparison of their differentiation capacity and determine if their differential germ layer origin would impact upon this.

Due to their sensitivity to passaging, for the initial epithelial cell transduction, cell number was estimated by counts performed in the flask rather than harvesting, counting and replating the cells. The Cytotune 2.0 vectors were added to the culture at the same MOI of 5-5-3 (KOS, Myc, Klf4) used for reprogramming the prostate fibroblasts, and were left for 24 hours at which point the media was removed and fresh media added. Visible cell death was evident by 24 hours. Media was changed every 48 hours and cultures were monitored for any morphological changes. On day 7, cells were transferred to a hESC environment consisting of a MEF feeder layers and hESC medium. This was chosen rather than the feeder-free based E8 and vitronectin method used during fibroblast reprogramming to provide support to the epithelial cells following passage. After transfer to feeder-dependent ESC culture however, the cells continued to die and no colony formation occurred.

Due to the high levels of cell death experienced, MOI for subsequent epithelial transductions was reduced. 3 patient samples were transduced using 2 different methods. The first sample was reprogrammed in the original flask whilst the remaining 2 samples were seeded onto gelatin coated 12 well plates (3 wells per patient sample) to give a more accurate calculation of MOI. Again, the cells were transduced with virus for 24 hours. Following this, fresh media was added and changed every 48 hours. For the sample transduced in its original flask, cell death was visible by 48 hours post transduction. By day 13, potential colonies could be identified which showed a typical ESC morphology of small cells with large nuclei,

similar to those identified during reprogramming of prostate fibroblasts. These areas were transferred to either MEFs or vitronectin on day 15 for further culture however, regardless of the surface the cells were transferred to, no growth occurred and the cells were lost (Figure 3-26).

For the 2 samples transduced on gelatin-coated plates, media was changed on day 7 to E8 medium and by day 8 colonies were visible in both samples. As before, these colonies consisted of small cells with large nuclei similar to ESCs. These were either kept on gelatin, transferred to vitronectin on day 8, or transferred to vitronectin on day 11. The cells kept on gelatin showed increased proliferation and cell death, but no growth of colonies was identified. The cells transferred to vitronectin on day 8 showed an initial increase in proliferation but from day 15 onwards significant cell death occurred and again no colonies were identified. Finally, the cells transferred to vitronectin on day 11 showed no proliferation but high levels of cell death occurred as with the other samples (Figure 3-26). At day 26, remaining cells were harvested for RNA extraction to analyse transcript expression of the Sendai virus backbone and reprogramming vectors. Unfortunately, the quality and yield of RNA generated from these samples was very poor and primer dimers were present in several samples and genes. Overall, transduction of primary prostate epithelial cells with the Cytotune 2.0 reprogramming vectors resulted in initial proliferation and appearance of colonies followed by cell death, regardless of whether the cells were transferred to vitronectin or kept in their original wells. This suggested that the epithelial cells were stalled during the initiation phase of reprogramming, whereby they lose somatic cell characteristics and show enhanced proliferation and morphologic changes, but failed to enter the maturation phase, a well-known phenomenon during cellular reprogramming (David and Polo, 2014).

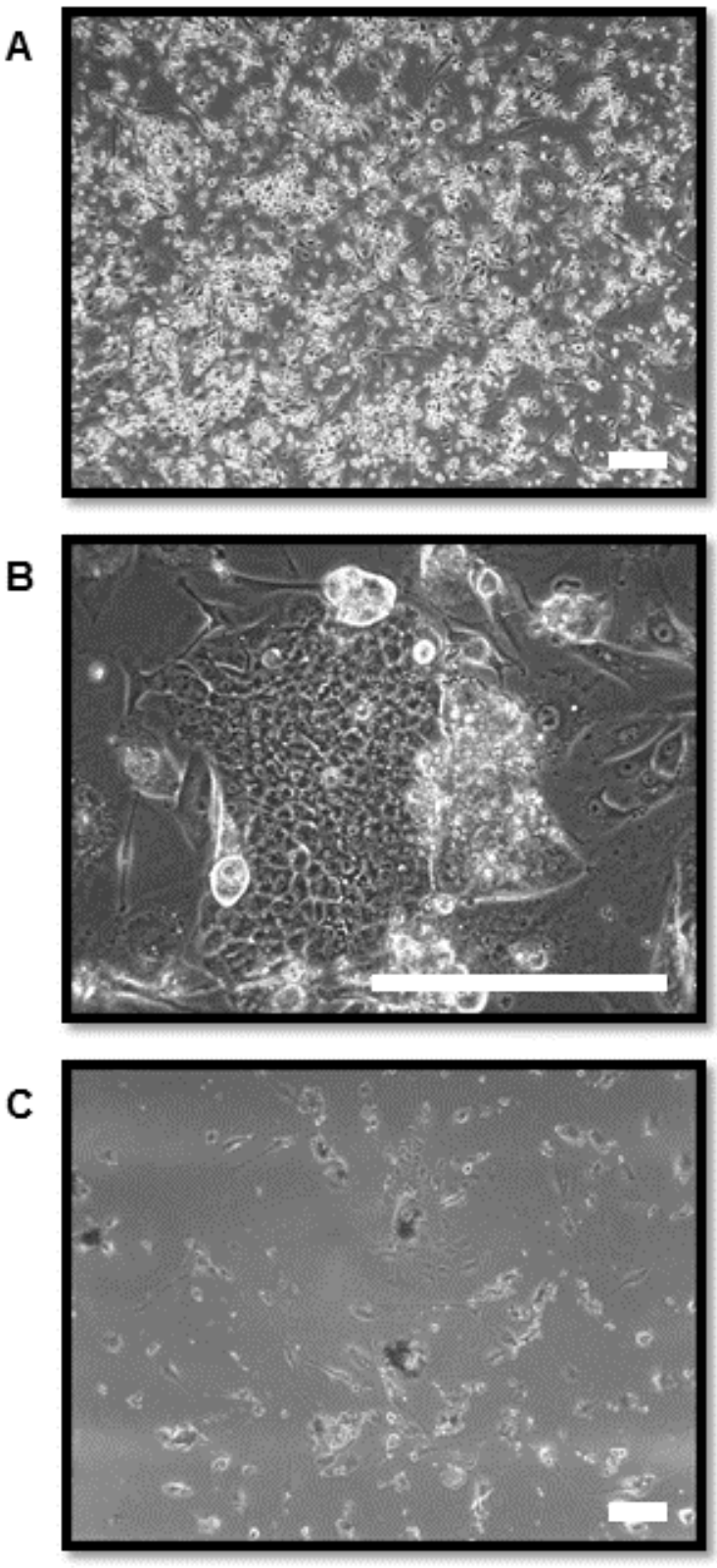

Figure 3-26. Phase contrast micrographs of epithelial cultures following transduction. High levels of cell death were evident following viral transduction (A) before the appearance of colonies (B). Following transfer to vitronectin or MEFS, high levels of cell death occurred and colonies were lost (C). Scale bars 25μm.

The failure of the Cytotune vectors to generate iPSCs from prostate epithelia also suggested that the efficiency of the viral vectors may vary between prostate stromal and epithelial cells. To investigate this hypothesis, the ability of Sendai viral vectors to enter the cells was determined using an EmGFP Sendai vector for matched patient stromal and epithelial cells. As previously, cells were seeded out and allowed to settle for 24 hours before addition of the EmGFP vector at MOI 0, 1, 10, 20 or 40. After 48 hours, cells were imaged and harvested for FACS sorting. It was clear there was a visual difference in efficiency of Sendai virus entry between prostate epithelial and stromal cell (Figure 3-27). This was confirmed by FACS data which showed an MOI of 10 giving 100% GFP positivity in the stromal cells but less than 50% positivity in the epithelial cells (Figure 3-28). To reprogram epithelial cells using the Cytotune 2.0 vectors, a much higher MOI would be required which would be toxic to the cells. This was not further investigated.

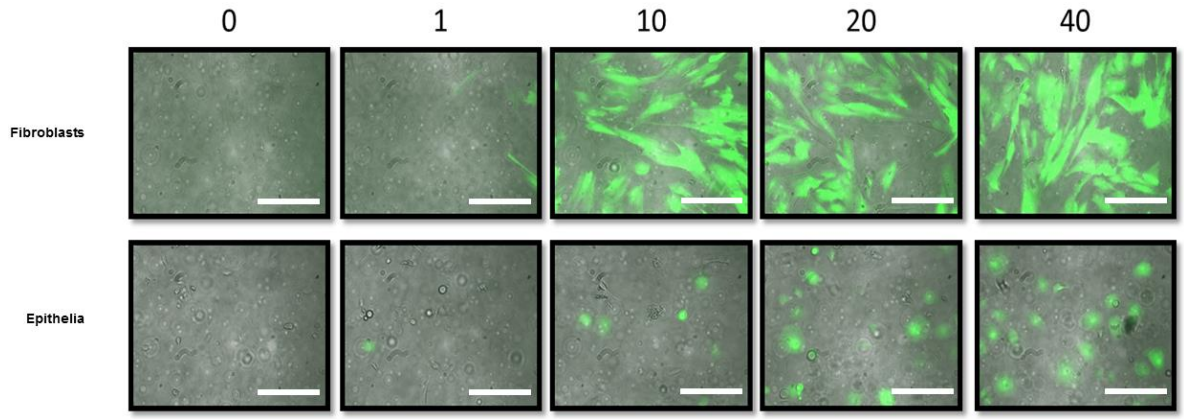

Figure 3-27. Fluorescent images showing expression of GFP in prostate fibroblasts and epithelial cells at MOI 0, 1, 10, 20 and 40 after 48 hours of incubation with the EmGFP Sendai control virus. A clear difference in GFP positivity can be seen with much lower expression in epithelia versus fibroblasts for all MOI tested. Scale bar 25µm.

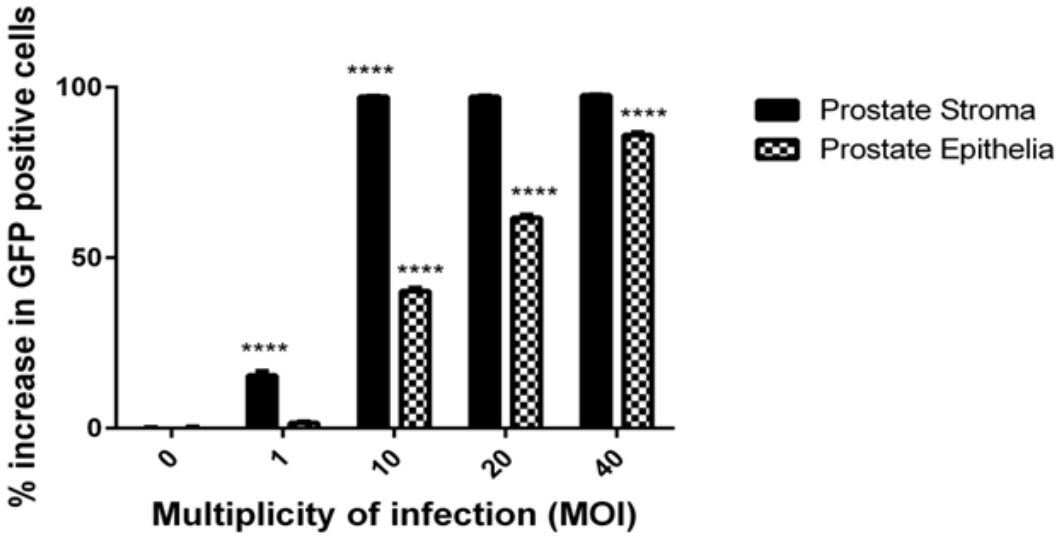

Figure 3-28. Percentage of GFP positive cells at MOI 0, 1, 10, 20 and 40 in matched prostate stroma and epithelial cells after 48 hours of incubation with the EmGFP control Sendai virus. Prostate epithelial cells show significantly lower GFP positivity versus prostate stroma.

3.4 Discussion

iPSCs provide a limitless supply of patient-derived cells which can be used for drug testing, disease modelling and studying development. It has been shown that iPSCs retain an epigenetic memory from their parental cell of origin which results in a skewed differentiation potential, therefore generation of iPSCs from the tissue of interest is important for downstream differentiation capacity. In this study, primary prostate fibroblasts were reprogrammed to iPSCs, termed ProiPSCs, for the first time using non-integrating Cytotune Sendai viral vectors.

In this chapter, the successful generation of integration-free iPSCs from primary prostate fibroblasts has been shown. In total 49 colonies were generated giving a reprogramming efficiency of 0.33%, 10-fold higher than previously shown for iPSC generation from prostate fibroblasts using a lentiviral approach (Moad *et al.*, 2013). As well as the improved efficiency, the Sendai viral vectors are also advantageous due to their enhanced safety profile, non-integrating life cycle and gradual clearance from the transduced cells. The Cytotune vectors also allowed generation of iPSCs in a feeder- and xeno-free environment.

The generated iPSCs show characteristics of pluripotency including expression of stem cell markers such as OCT4, SOX2, NANOG, SSEA4 and alkaline phosphatase.

The cells are karyotypically normal and show 100% identity to the parental fibroblasts as measured by DNA fingerprinting. Furthermore, the iPSCs are able to differentiate into cells from the three embryonic germ layers both *in vitro*, by formation of EBs, and *in vivo* by teratoma formation after subcutaneous injection into NSG mice, therefore reaching the gold standard for iPSC characterisation and confirming their identity as true iPSCs.

Attempts to generate iPSCs from primary prostate epithelia were also made, however no colonies were generated as cells were lost due to toxicity of the virus. Transduction of prostate fibroblasts and epithelial cells with a EmGFP vector identified that a significantly higher MOI is required to obtain a sufficient level of viral entry into prostate epithelial cells in comparison to prostate fibroblasts. This contrasts with Ono et al.,(Ono *et al.*, 2012) who were able to generate iPSCs from human nasal epithelial cells. However, for human nasal epithelial cells transduction with the GFP control Sendai vector at an MOI of 3-4 was high enough to show a significant percentage of GFP positive cells, whilst in our hands prostate epithelial cells required an MOI 20 or above to achieve 50% GFP positive cells. Therefore, alternative methods of reprogramming may be required for use with prostate epithelial cells. Zhao et al., published attempts to generate iPSCs from prostate epithelial cells using lentiviral vectors, low oxygen environment and addition of chemical factors (Zhao *et al.*, 2013). However, the cells produced were only partially reprogrammed and were unable to form teratomas or to differentiate into prostatic epithelium either *in vitro* or *in vivo*. The lack of iPSC generation from prostate epithelial cells using either method suggests that these cells require optimised protocols to achieve full reprogramming to a truly pluripotent state.

Chapter 4: Generation of prostatic tissue from patient-derived prostate iPSCs *in vivo* using tissue recombination with rodent UGM

4.1 Introduction

This chapter will describe the generation of prostate tissue from ProiPSCs using a tissue recombination approach utilising inductive rat UGM. The UGM drives differentiation of the prostate epithelium during normal prostate morphogenesis. Tissue recombinants generated from rodent UGM and adult endodermally-derived epithelium can also generate prostatic tissue when engrafted into mice. Subsequently, it was shown that UGM and SVM can direct the differentiation of hESCs into prostate, generating a novel model for prostate development from pluripotent stem cells (Taylor *et al.*, 2006; Cai *et al.*, 2013). The prostatic tissue formed from the hESCs showed expression of prostate specific genes including Nkx3.1, AR and PSA, as well as correct localisation of basal and luminal cells as indicated by CK expression. However, the viability of this method for further study of prostate development is limited due to its use of hESCs and the ethical issues with which they are associated. As hESCs and iPSCs are functionally equivalent, we hypothesised that tissue recombinants of rat UGM and iPSCs should also form prostatic tissue when grafted under the renal capsule of mice.

As the generation of prostatic tissue has not been shown for iPSCs using this method, we decided to trial a range of ratios of UGM to iPSCs to determine the optimum cell concentrations for prostate differentiation. Taylor et al., used ~1000 hESCs with $5x10^4$ UGM (a ratio of 1:50) to successfully generate prostatic tissue *in vivo,* whilst a subsequent study used $4x10^4$ hESCs with $1x10^5$ UGM (a ratio of 1:2.5) (Taylor *et al.*, 2006; Cai *et al.*, 2013). We decided to use ratios of approximately 1:2.5, 1:25, 1:125 and 1:250 (iPSCs to UGM). As iPSCs engrafted alone *in vivo* form teratomas, we postulated that when the ratio of iPSCs to UGM was low, more nonspecific differentiation was likely to occur. In contrast, we expected tissue recombinants with low iPSC and high UGM number to form tissues consisting of less spontaneous differentiation and increased prostate specific differentiation.

4.2 Aims

- To trial a range of cell ratios to generate prostatic tissue from iPSCs under the influence of UGM
- To characterise the generated tissue in comparison to normal human primary prostate tissue

4.3 Results

4.3.1 Determining cell numbers in iPSC colonies

Generation of tissue recombinants can use either single cell suspensions, cell clumps or pieces of cells or tissue. In the original study using hESCs with UGM, pieces of hESC colonies were used to maintain viability of the cells which are vulnerable as a single cell suspension (Taylor *et al.*, 2006), whilst a subsequent study used single cell suspensions of hESCs and UGM (Cai *et al.*, 2013). To preserve the viability of the iPSCs, we used pieces of colonies rather than a single cell suspension approach. To generate tissue recombinants from the ProiPSCs, the number of cells per iPSC colony needed to be determined. To do this, individual colonies were marked and measured using ImageJ software to determine colony area. Colonies were then manually picked, digested to a single cell suspension and counted on a BioRad TC20™ automated cell counter with trypan blue to distinguish live cells. The total number of live cells for each colony was then plotted against the colony area in mm^2 to generate a standard curve as shown in (Figure 4-1). This was used to estimate cell numbers when picking colonies for generation of the tissue recombinants.

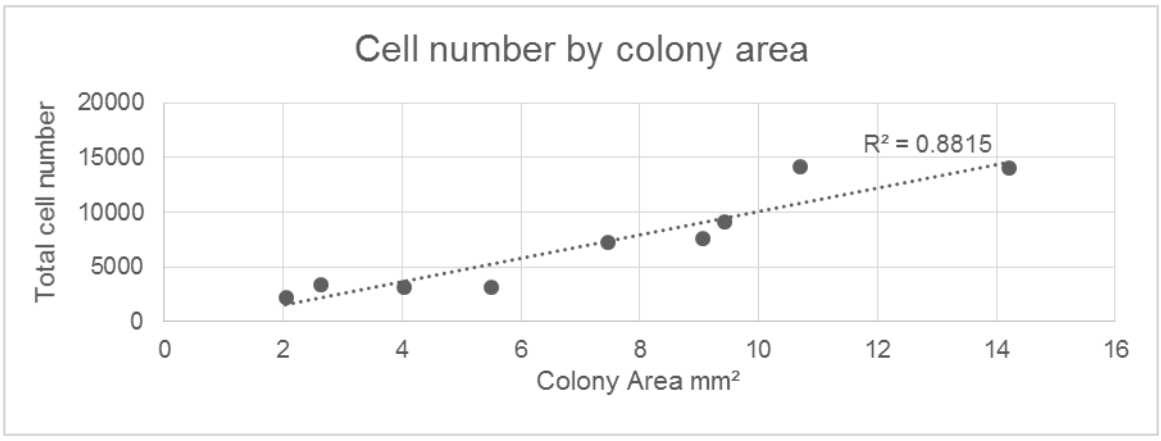

Figure 4-1. Standard curve showing total live cell number vs colony area in mm2 for ProiPSCs.

4.3.2 Morphology of tissue recombinants

iPSC colony pieces were combined in collagen with a complete urogenital mesenchyme containing approximately 250,000 cells. Recombinants were left overnight in RPMI media at 37°C before being grafted under the renal capsule of nude mice which had been castrated and then implanted with a testosterone pellet to control for any variances in testosterone secretion. Grafts were harvested from 6 weeks onwards, fixed in formalin and embedded into paraffin for sectioning and histological analysis. Grafts from each ratio tested were morphologically very different. The highest ratio of iPSC to UGM (1:250) generated a small graft whilst the smallest ratio (1:2.5) resulted in formation of a very large structure which appeared to be a teratoma and had completely taken over the kidney (Figure 4-2). Ratios in between these generated grafts similar in size to the BPH1 control grafts.

H&E staining was performed on the harvested grafts to see the overall morphology of the tissue generated. As suspected, the lowest ratio of iPSCs to UGM had generated a large teratoma (Figure 4-3). In contrast, the highest ratio which should provide more specific differentiation had formed a very small graft with no evidence of teratoma formation. The intermediate ratios formed grafts of a similar size and appearance to the BPH1 control. These grafts also contained cystic structures which are apparent in teratomas.

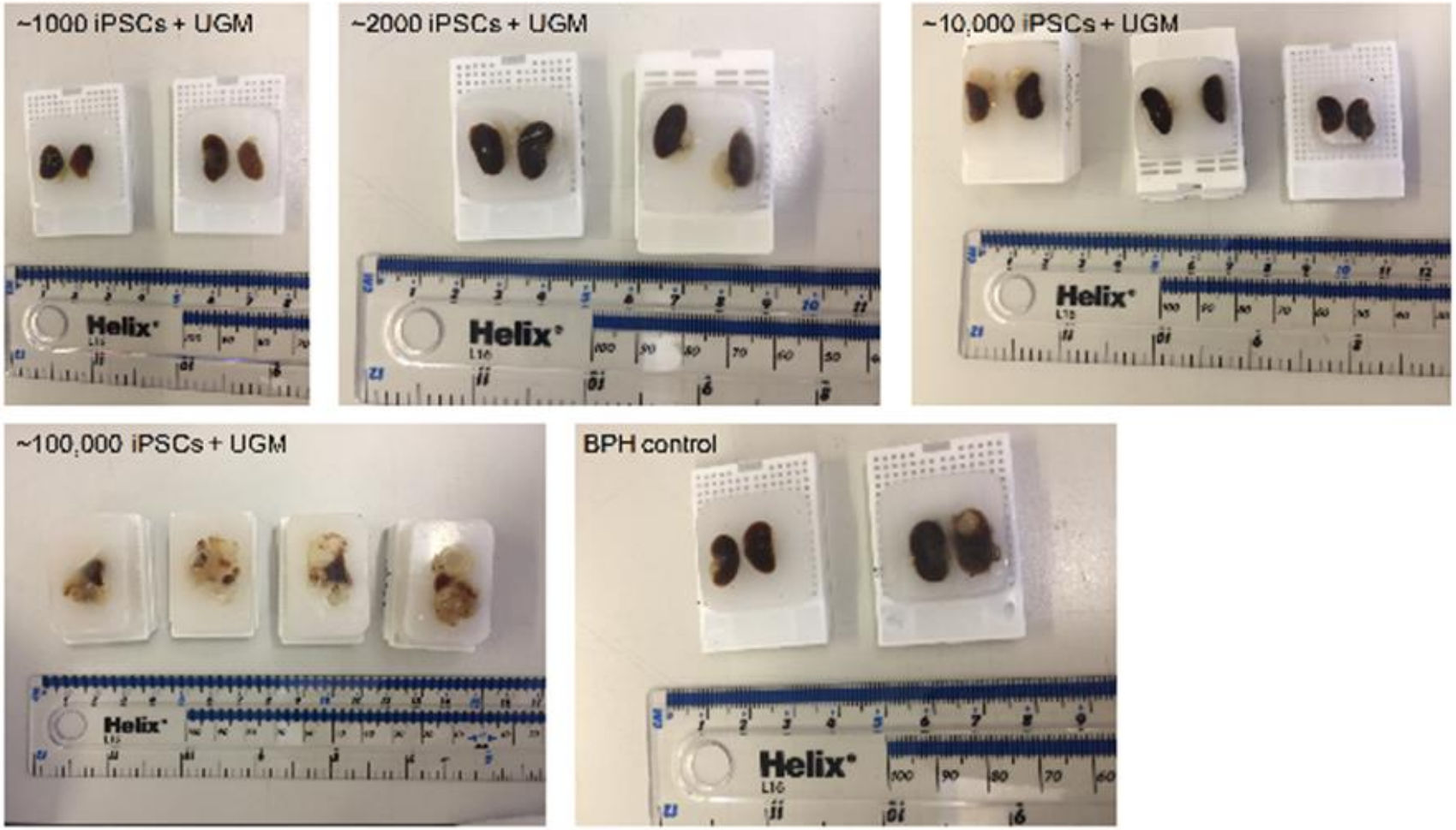

Figure 4-2. Gross appearance of tissue recombinants following renal capsule grafting in nude mice. The size and appearance of grafts varied significantly between the cell ratios tested. BPH1 cells with UGM were grafted as a positive control.

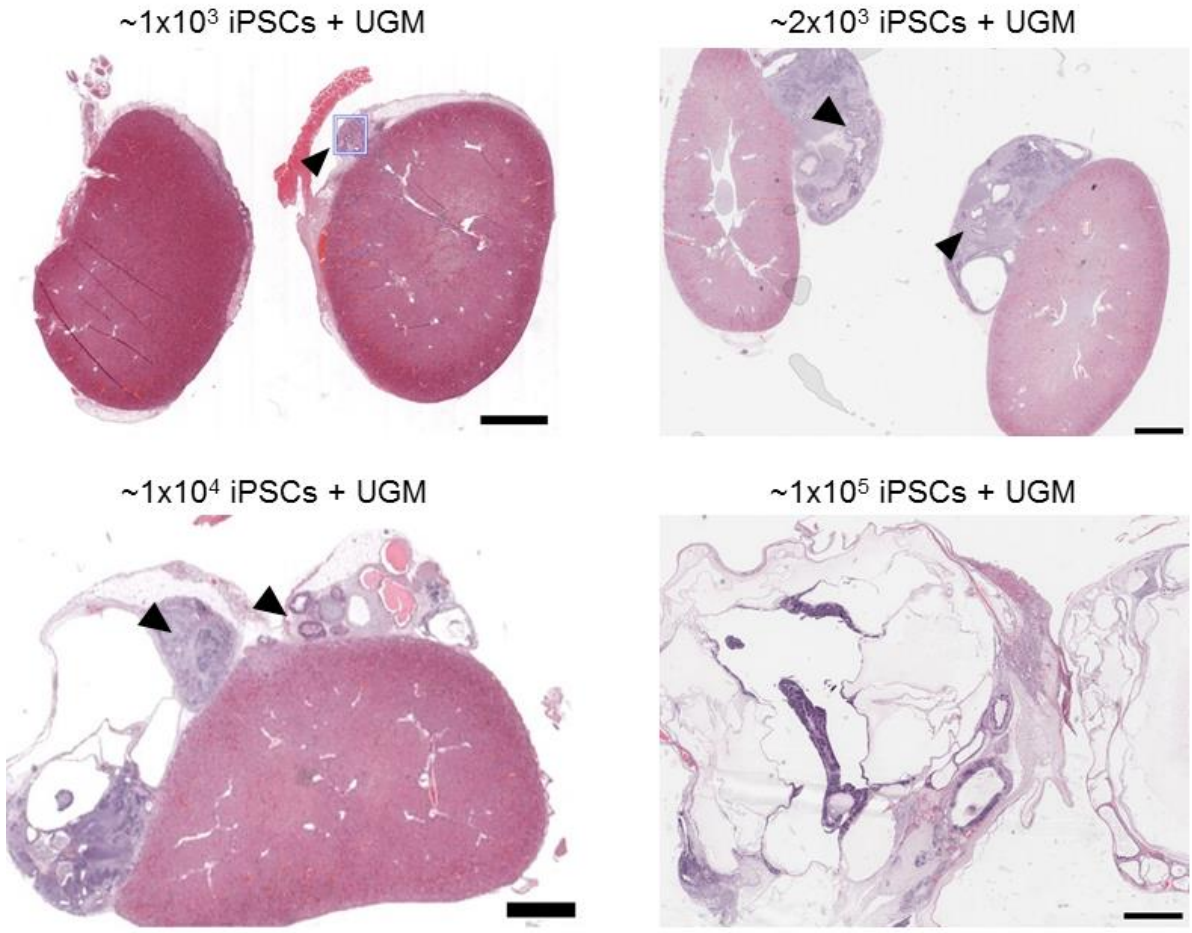

Figure 4-3. H&E staining showing entire grafts from the ratios tested. As the ratio of iPSCs to UGM becomes lower, grafts become larger in size and more reminiscent of teratomas. Arrow heads mark areas of epithelial like glands. Scale bar 2mm.

H&E staining showed that the 1:250 ratio graft consisted mostly of epithelial tissue surrounded by smooth muscle and fibroblasts. Several epithelial glands could be seen, some of which appeared to be secretory (Figure 4-4A). The presence of these glands and evidence of secretions were promising, but some of the nuclei had a speckled appearance due to the presence of small intranuclear bodies which are characteristic of mouse nuclei (Figure 4-4B)(Cunha and Vanderslice, 1984). Staining of tissue sections with Hoescht 33258 allowed identification of mouse and human nuclei. Mouse-derived glands showed intense speckled staining whilst human cells lack the presence of intranuclear bodies and show a diffuse staining pattern (Figure 4-5).

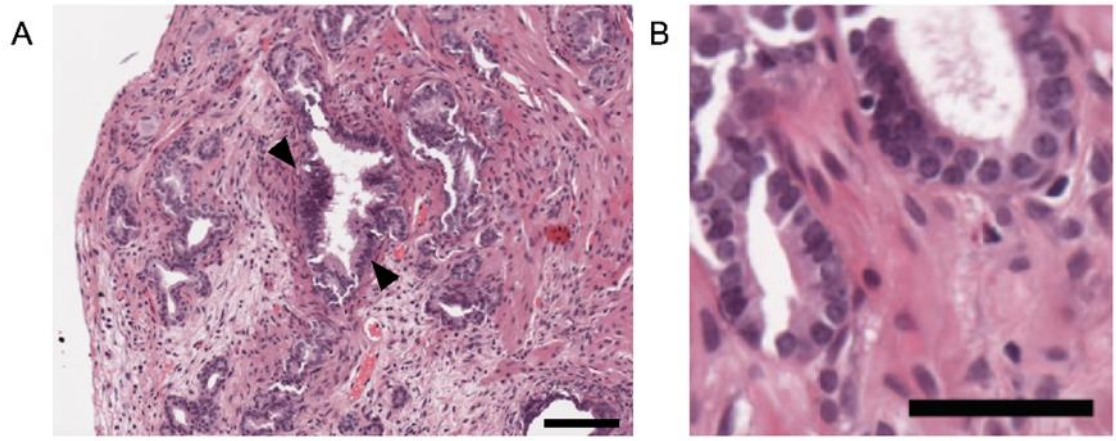

Figure 4-4. H&E staining of 1:250 ratio graft. A) The majority of tissue formed was glandular epithelium, some of which appeared secretory (arrowheads). This was surrounded by smooth muscle and fibroblasts. Scale bar 100μm. B) High magnification image of glands containing nuclei with a speckled appearance, scale bar 50μm.

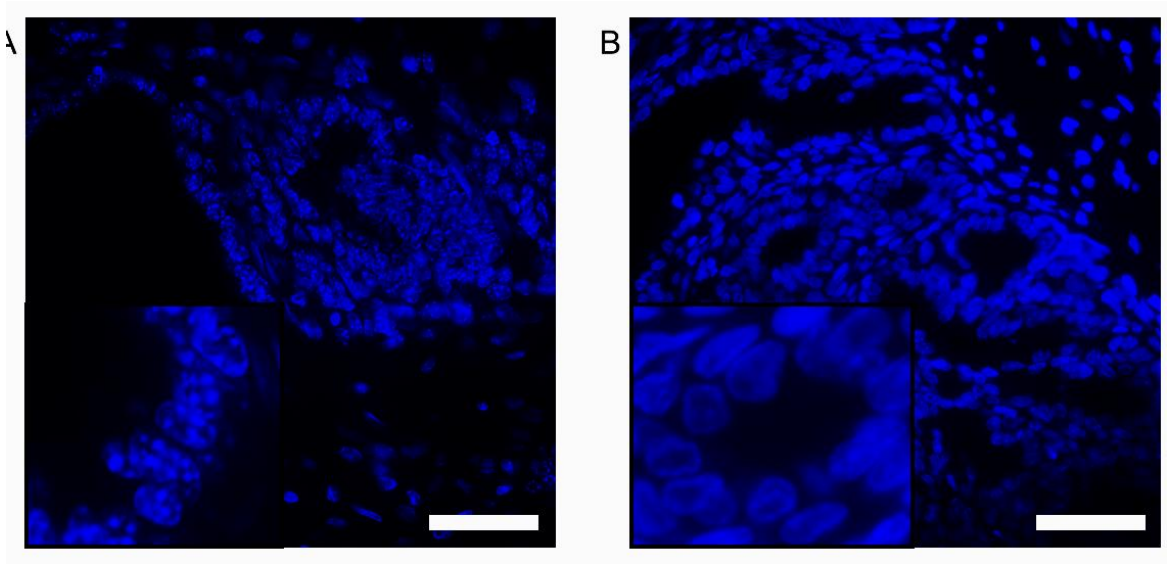

Figure 4-5. Sections of generated grafts stained with Hoescht 33258. A) Glands formed from mouse cells can be identified by presence of brightly stained speckles. B) In contrast, human-derived glandular structures showed a diffuse staining pattern with lack of intranuclear bodies. Insets show higher magnification images of nuclei. Scale bars 50μm.

The 1:125 ratio produced a graft with several tissue types, including epithelium, smooth muscle, cartilage and cystic structures (Figure 4-6). The presence of a variety of tissue types provides further evidence for the pluripotency of the ProiPSCs and suggests that the differentiation is becoming less specific as we expected with a decreasing influence of UGM. At this ratio, the major tissue present in the graft was still epithelium. Two types of epithelial tissue were identified; small clusters of epithelial cells with no lumen, and more glandular-like structures with dual layers of cells surrounding clear lumens (Figure 4-7).

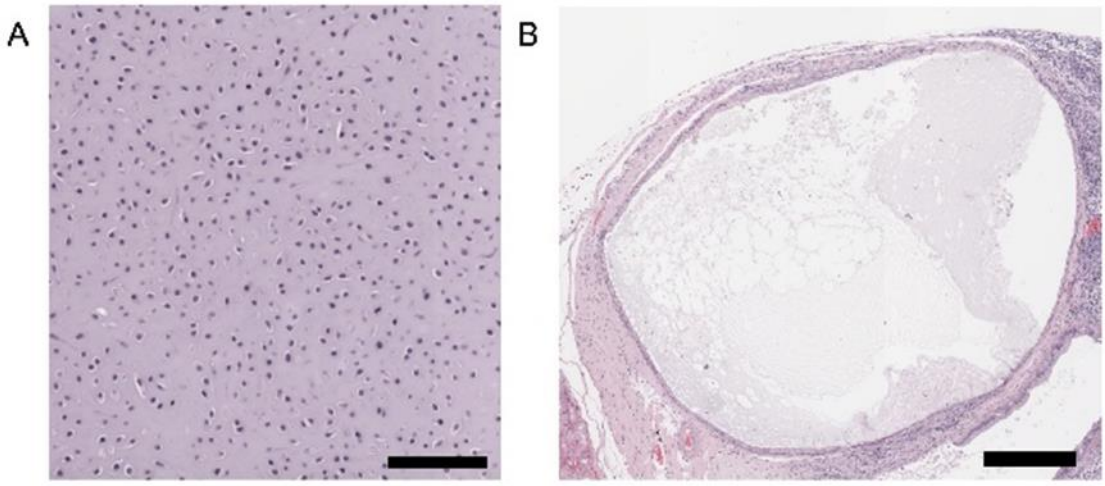

Figure 4-6. A) Cartilage (scale bar 100μm). B) Large cystic structure (scale bar 400μm).

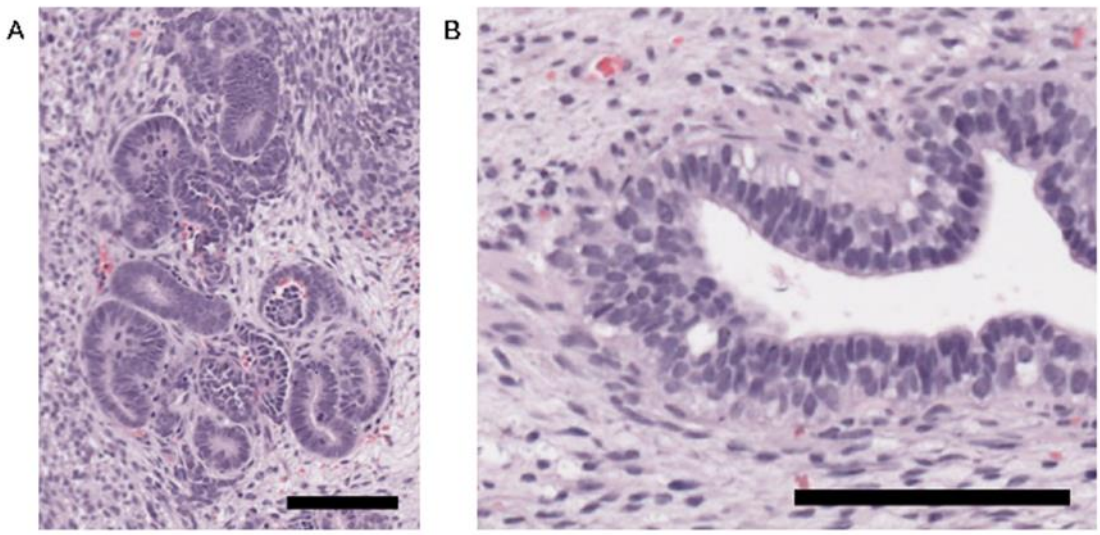

Figure 4-7. H&E staining showing epithelial cells within the graft. A) Small epithelial cell clusters with no lumen. B) A more glandular-like structure with multi-layered epithelium and a clear lumen. Scale bars 100μm.

A ratio of 1:25 formed a wider spectrum of tissues including the presence of ectodermal derivatives such as neuroepithelial rosettes and pigmented epithelium (Figure 4-8). Some areas of epithelium were present but these were usually located very near to the kidney and in some cases glandular tissue could be seen in the kidney itself, suggesting a potential mouse origin (Figure 4-9). The graft also contained cartilage, fat and smooth muscle. In general, this ratio appears to produce a more teratoma-like graft characterised by the presence of tissue from all three embryonic germ layers.

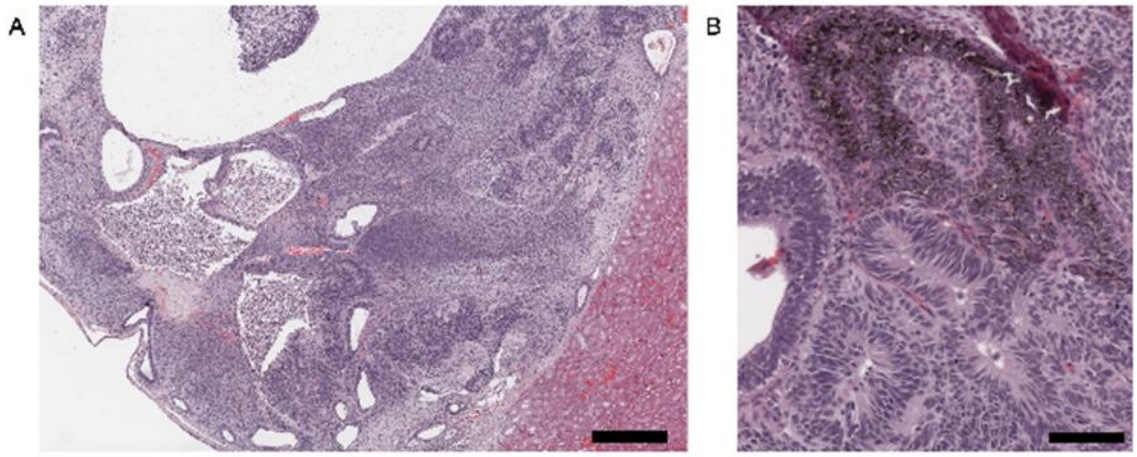

Figure 4-8. A ratio of 1:25 produced large amounts of neuroepithelium and large cysts as shown in (A), scale bar 500μm. B) Neuroepithelial rosettes and pigmented tissue at a higher magnification confirming ectodermal differentiation. Scale bar 100μm.

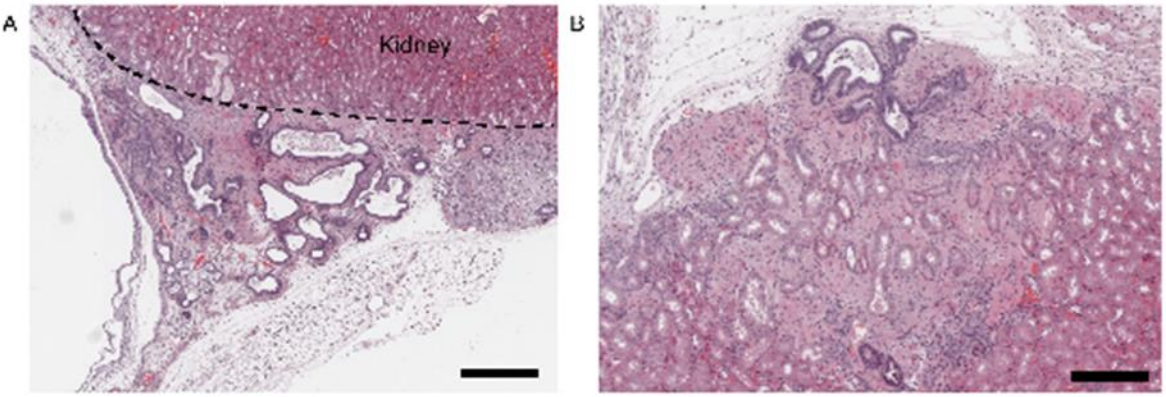

Figure 4-9. Epithelium in this graft was always found close to the kidney suggesting potential mouse origin (A, scale bar 500μm). In some areas, the kidney was clearly altered with changes in cell morphology and presence of glandular-like structures emerging (B, scale bar 250μm).

At the lowest ratio of 1:2.5, a teratoma-like structure was generated as expected. This mostly consisted of large cysts and ectodermal tissue including large volumes of neuroepithelial rosettes (Figure 4-10). At this ratio, the pluripotency of the iPSCs appears to completely take over and the resultant graft consumes the kidney. Some epithelial areas were still visible, generally around the outer edges of the graft (Figure 4-10C).

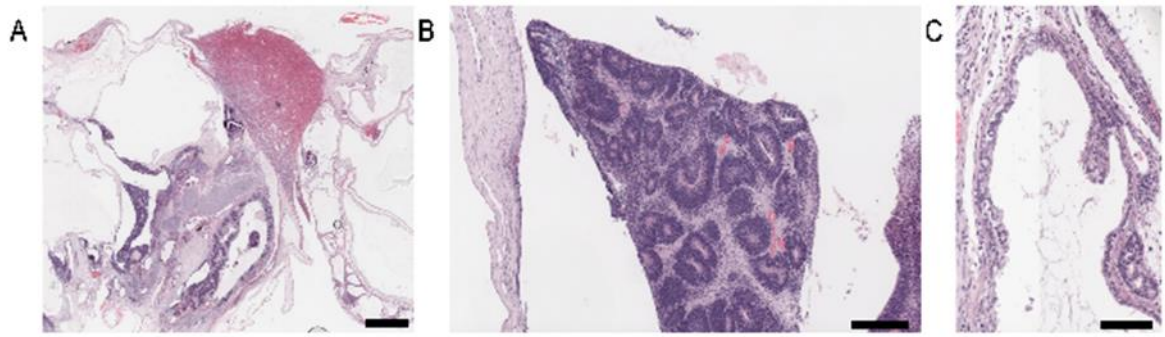

Figure 4-10. A) Teratoma formation taking over the kidney with presence of large cysts, scale bar 2mm. B) An area of neuroepithelium in the graft, scale bar 250μm. C) Some areas of glandular epithelium remained present, scale bar 100μm.

The ratio of iPSCs to UGM appears to greatly impact the overall morphology and tissues of the resultant graft (summarised in Table 4-1). As expected, a large ratio with significantly more UGM than iPSCs results in a very small graft containing mostly epithelial tissue, whilst a small ratio of iPSCs to UGM generates a teratoma consisting of multiple tissue types, as there is not enough inductive mesenchyme to control the iPSC differentiation. From H&E staining, it was clear that the grafts from a ratio of 1:250 and 1:125 iPSCs to UGM form the most epithelial tissue and thus initial staining concentrated on these grafts.

iPSC number	UGM number	Ratio	Result
1000	250,000	1:250	Small graft, mostly epithelial
2000	250,000	1:125	Medium graft with epithelial areas, some cysts
10,000	250,000	1:25	Large graft, epithelial areas, large cysts and ectodermal tissue
100,000	250,000	1:2.5	Very large teratoma, mostly ectodermal tissue and cysts

Table 4-1. Summary of findings from H&E staining of tissue recombinants

4.3.3 Confirmation of iPSC-derived tissue using human specific mitochondrial staining

Due to the nature of the tissue recombination method and subsequent xenografting, any potential epithelium could have formed from the iPSCs, mouse cells, rat UGM or contaminating UGE. As this study was interested only in formation of prostatic epithelium from the ProiPSCs which are human in origin, sections were stained with an anti-human mitochondrial antibody. Human specific mitochondrial antibodies are often used for detection of human tissue or cells in xenograft models (Hylander *et al.*, 2013; Thibaudeau *et al.*, 2014). In our experiment, use of the mitochondrial marker is advantageous as it recognises cells from all lineages. Any positive staining would indicate which glands were human in origin and therefore were generated from the ProiPSCs. An alternative method for distinguishing human, mouse and rat cells described by Vander Griend at al., could also have been utilised. This method takes advantage of the increased telomere length in rodents versus humans, and uses a pair of centromere-specific DNA probes which will recognise only human and mouse, but not rat centromeres. Performing dual centromere and telomere FISH allows determination of the origin of tissues present in tissue recombinants at single cell resolution (Vander Griend *et al.*, 2009).

The epithelial areas in the smallest graft (ratio ~1:250) did not stain positively for the human specific marker, so further investigation of their marker profile was not pursued (Figure 4-11A). The source of the non-human epithelial cells may be mouse, due to the UGM inducing the mouse kidney or circulating pluripotent cells to form epithelium or rat, due to transdifferentiation of the UGM or the presence of contaminating UGE which would form prostatic epithelium under the influence of the UGM (Vander Griend *et al.*, 2009). The lack of any human cells at this ratio suggests that 1000 ProiPSCs is too small a number to be viable and therefore an increased cell number may improve survival and growth. This observation was based on a single graft and therefore analysis of further grafts will be required to confirm this finding. However, the entirety of the 1:125 ratio graft stained positive for human mitochondria, confirming that all tissue within the graft originated from the ProiPSCs (Figure 4-11B,C). All epithelial glands showed strong expression of human mitochondria (Figure 4-12) whilst the mouse kidney was negative acting as an internal negative control. At a higher magnification, a clear pattern of mitochondrial staining was evident in the cytoplasm of cells in epithelial glands and also in some

but not all areas of surrounding mesenchyme (Figure 4-13). We could therefore be confident that these epithelial areas of interest were derived from the ProiPSCs, and were able to take them forward for further analysis.

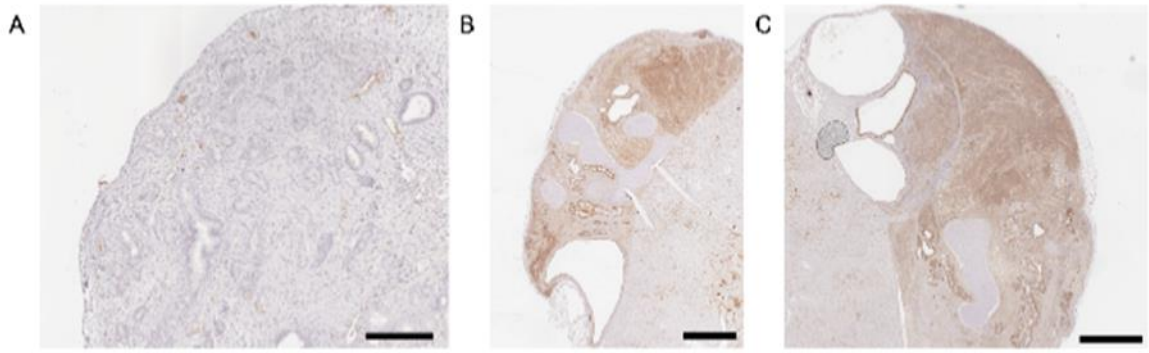

Figure 4-11. IHC for anti-human mitochondria. A) The entire 1:250 ratio graft was negative for the human specific mitochondrial marker suggesting the tissue originated from contaminating rat or mouse tissue (scale bar 200μm). B, C) In contrast the 1:125 ratio graft consisted of human tissue as confirmed by positive staining for human mitochondria (scale bar 1250μm).

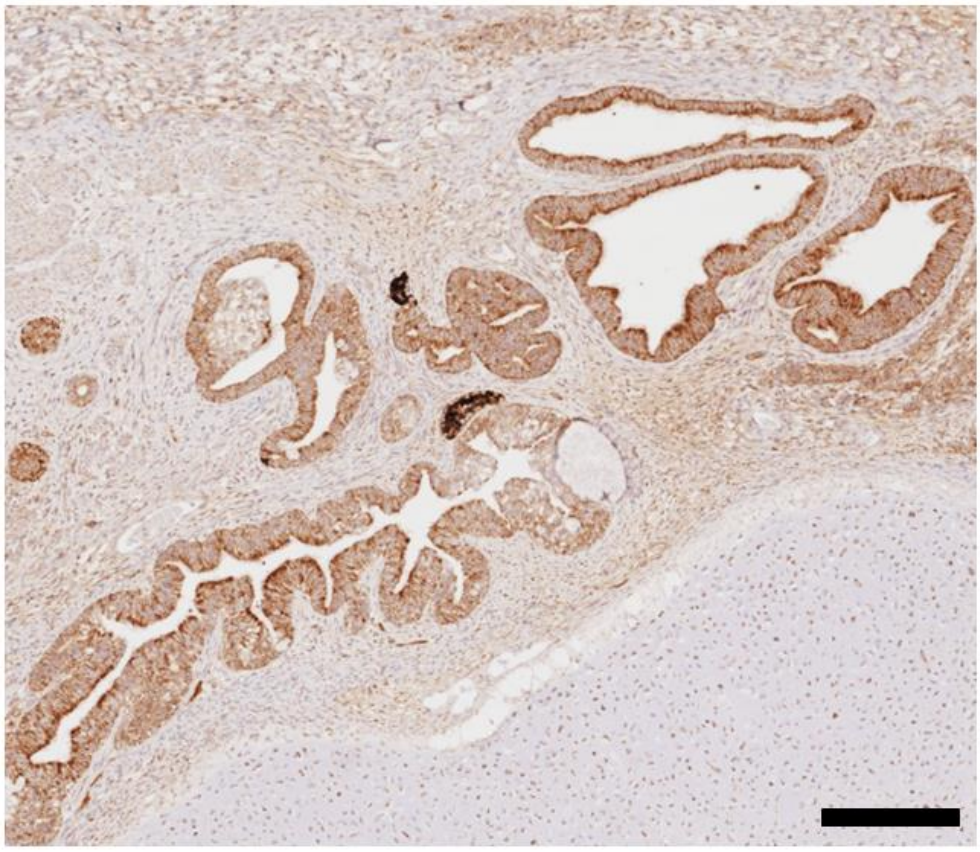

Figure 4-12. IHC for anti-human mitochondria in epithelial-like glands identified within the graft. Strong expression is seen in all areas confirming human origin. Scale bar 200μm.

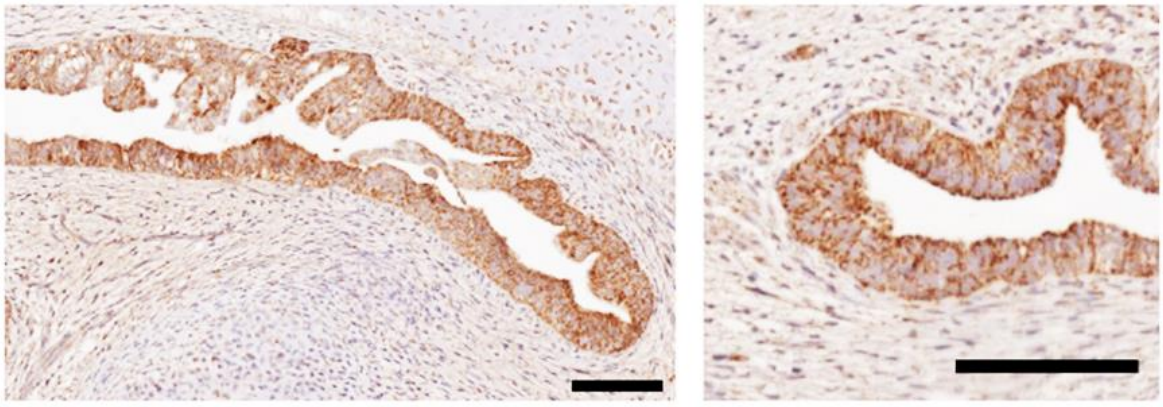

Figure 4-13. Higher magnification images of positive human mitochondrial staining in epithelial-like glands. Staining shows a speckled cytoplasmic distribution characteristic of mitochondria. Scale bar 100µm.

4.3.4 Marker expression in glandular tissue generated from iPSCs

Normal prostatic epithelial glands consist of a basal cell layer positive for p63 and a luminal cell layer positive for CK8/18. To confirm the epithelial identity of the areas of interest and determine their spatial organisation, IHC was performed for these markers. CK8/18 expression was widespread in the prospective epithelial glands with strong cell surface expression (Figure 4-14). In multi-layered glands, CK8/18 was restricted to the luminal cell layer confirming correct spatial organisation of the luminal compartment. The basal marker p63 was not as widely expressed, and was present in only a subset of epithelial glands. Expression of p63 was always nuclear and present purely in the basal cell layer (Figure 4-15A,B), confirming the presence of basal epithelial cells within the glands. Some areas of basal cell hyperplasia were also identified with expression of p63 in multiple basal cell layers (Figure 4-15C).

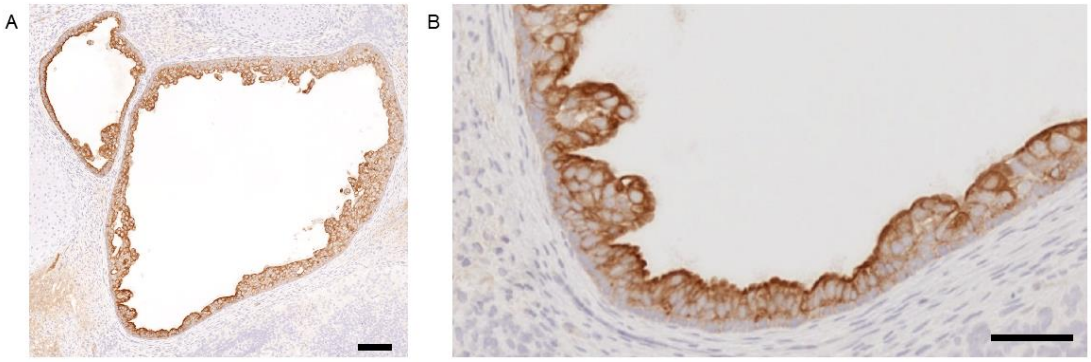

Figure 4-14. IHC for the luminal cell surface marker CK8/18. A) Clear CK8/18 expression in a glandular structure (scale bar 100µm). B) High magnification image showing CK8/18 expression localised at the cell surface of cells in the luminal layers whilst the basal layer remains negative (scale bar 50µm).

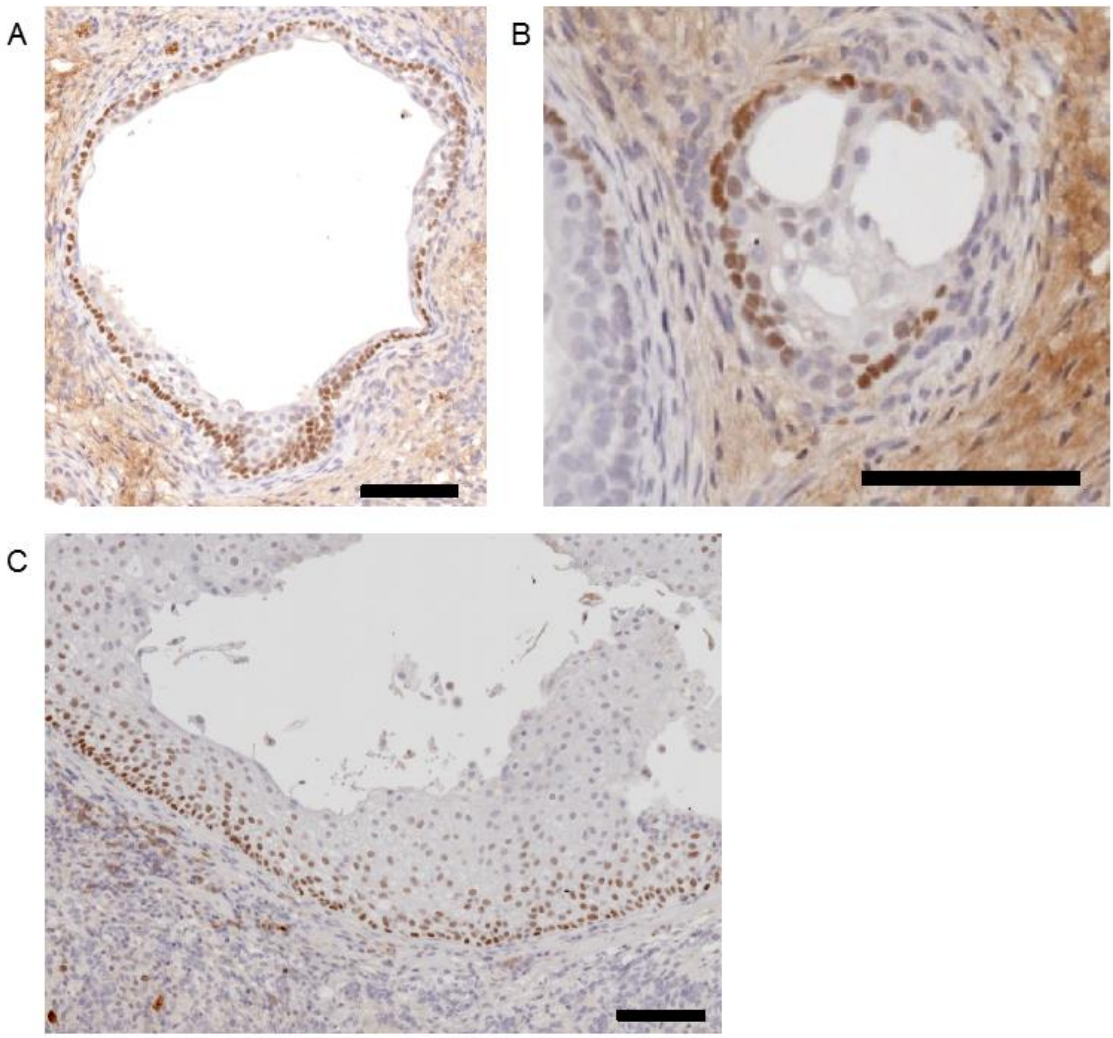

Figure 4-15. IHC for the basal cell marker p63. A,B) p63 is expressed in the basal cell layer of glandular structures alone. C) An area of basal cell hyperplasia. Scale bar 100μm.

The transcription factor FOXA1 has roles in the development of both the mammary and prostate glands (Bernardo and Keri, 2012). It is expressed throughout prostate organogenesis and this expression is maintained in the adult prostate gland due to the requirement of FOXA1 for AR-mediated activation of prostate genes (Mirosevich *et al.*, 2005; Bernardo and Keri, 2012). As FOXA1 is expressed at all stages of prostate development we decided to investigate its expression within the grafts. FOXA1 was strongly expressed in the majority of epithelial glands (Figure 4-16). As expected, expression was localised to the nucleus and no expression was identified in non-epithelial tissue. Some small cell clusters which appeared epithelial expressed no or very low FOXA1. These cell clusters also expressed low levels of CK8/18 and no p63, and did not have lumens (Figure 4-17). *Foxa1*$^{-/-}$ mouse prostates show formation of solid epithelial cords which lack a lumen (Gao *et al.*, 2005), suggesting

that the FOXA1 negative areas may have resulted from lack of FOXA1 induction in these epithelial cells, or alternatively could be very early epithelial structures which do not yet express FOXA1.

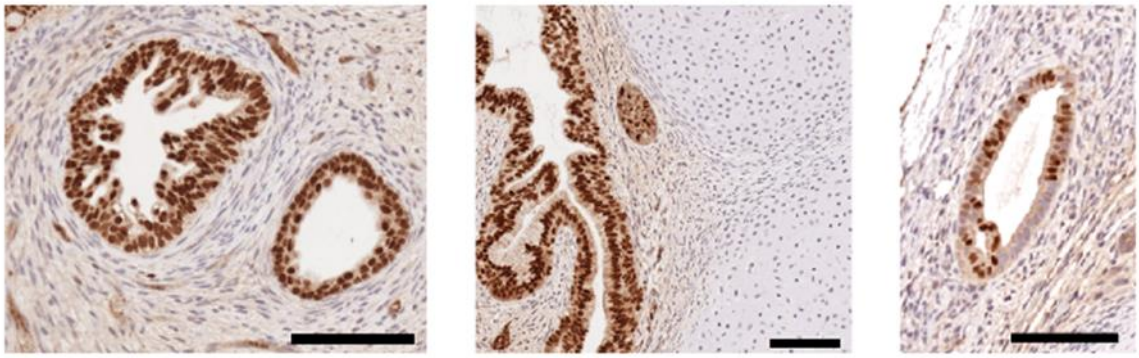

Figure 4-16. IHC for FOXA1. Epithelial glands showed strong positive staining. Expression was restricted to the nucleus as expected. Scale bar 100μm.

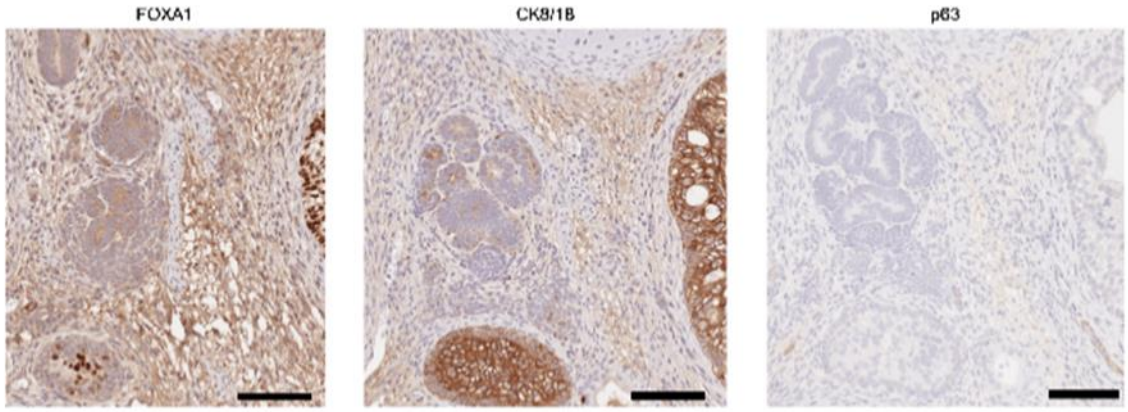

Figure 4-17 Area of epithelial cells which did not express FOXA1, CK8/18 or p63. Scale bar 100μm.

FOXA1, CK8/18 and p63 expression confirmed the epithelial origin of the glandular structures within the graft. Although FOXA1 is expressed in prostate organogenesis it is also expressed in several other endodermal derivatives including the liver and lung (Lee *et al.*, 2005; Wan *et al.*, 2005). To confirm prostate differentiation, the most critical markers are AR and PSA. AR is essential for prostate development, as *tfm* mice who lack functional AR do not develop prostates (Cunha and Lung, 1978). It is expressed in the nuclei of both prostate stroma and epithelium. Activation of AR leads to transcription of a multitude of AR-mediated genes including PSA. Secretion of PSA from luminal prostate epithelial cells confirms the functionality of these cells (Wang *et al.*, 2001). As PSA is both human and prostate specific, expression in the grafts would confirm full prostatic differentiation.

IHC confirmed the expression of AR in both the epithelial glands and surrounding stroma (Figure 4-18). Expression was strongly nuclear and was present predominantly in the luminal cell layer. In smaller glands, some cells were not AR positive, consistent with studies on foetal prostate tissue showing that solid epithelial buds do not express AR and throughout foetal development AR is only expressed focally (Letellier *et al.*, 2007).

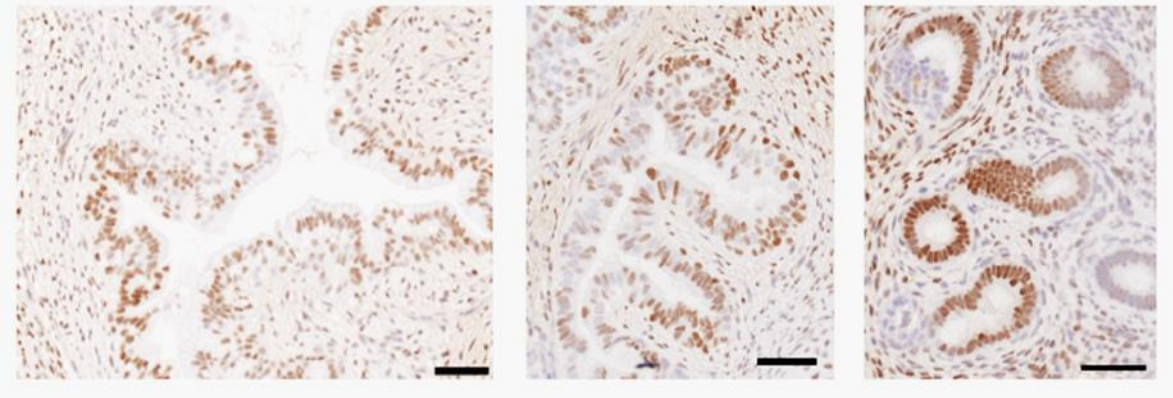

Figure 4-18. AR expression in tissue recombinants formed from ProiPSCs and UGM. AR is expressed in the nucleus of glandular epithelial cells and the surrounding stroma. Scale bar 50μm.

IHC for PSA confirmed PSA expression on the surface of the luminal epithelial cells within glands (Figure 4-19), although this was not present in all glands. As some glands appeared to still be developing, it may be that a longer timescale of *in vivo* growth is required for all glandular epithelium to express PSA. This is congruent with the focal AR expression, again suggesting that these areas may represent less mature prostatic tissue.

A ratio of 1:125 iPSCs to UGM generated grafts containing mostly epithelial glands which displayed normal basal and luminal layers and expressed AR, suggesting that of the ratios tested this was the optimum for generation of human prostatic tissue. Interestingly, a ratio of 1:25 did not generate any AR positive epithelium whilst the teratoma-like graft generated from a ratio of 1:2.5 iPSCs to UGM expressed AR in a subset of epithelial glands (Figure 4-20). This suggests that prostatic differentiation due to UGM influence still occurs at a much lower ratio but in much smaller volumes and is accompanied by non-specific differentiation. However, as only single grafts were analysed, investigation of multiple grafts per ratio will be required to determine if this is a consistent observation.

Prostatic glands also contain rare NE cells which express the neuroendocrine markers chromogranin A and synaptophysin but lack AR and PSA (Wang *et al.*, 2001; Shen and Abate-Shen, 2010). Immunofluorescence on the tissue recombinants showed presence of rare chromogranin A positive cells within the epithelial ducts (Figure 4-21), suggesting that neuroendocrine differentiation had occurred in the tissue recombinants, as chromogranin A is the major protein produced by prostatic neuroendocrine cells (Sciarra *et al.*, 2003). To confirm this, additional staining for synaptophysin as well as confirmation of lack of AR and PSA in these cells by triple IF will be required.

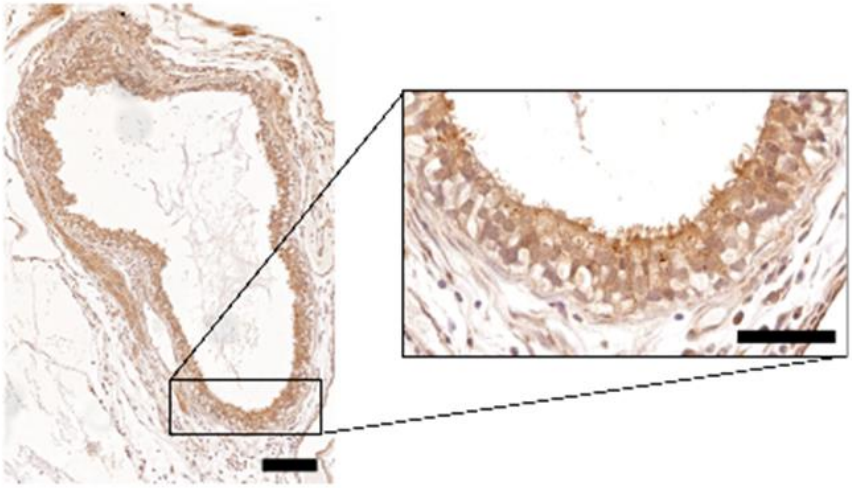

Figure 4-19. IHC showing expression of PSA in luminal cells and secreted into the lumen. Insert shows high magnification image. Scale bar 50μm.

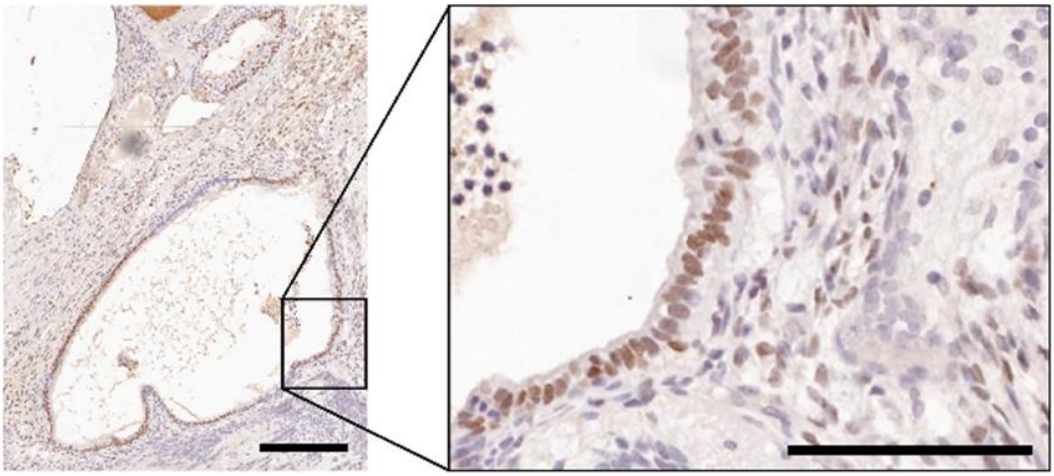

Figure 4-20. AR expressing epithelial cells within the 1:2.5 ratio graft. Some of the surrounding stromal cells are also AR positive. Scale bar 200μm, inset scale bar 100μm.

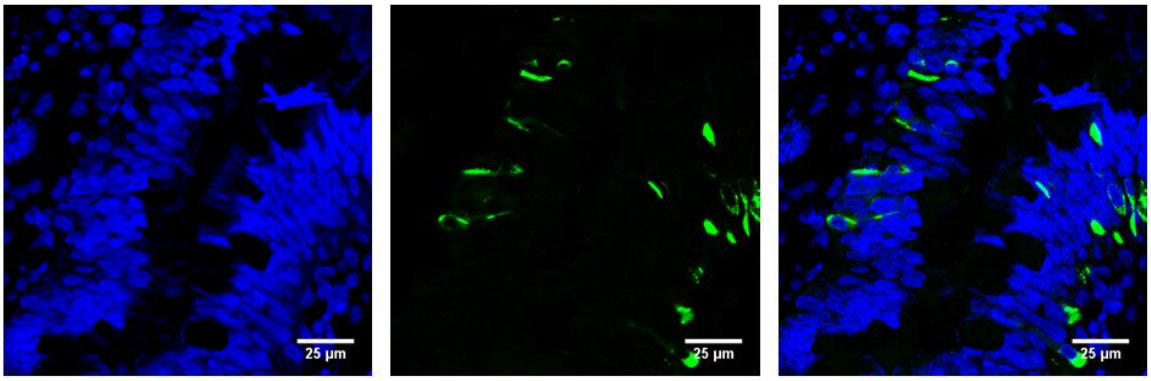

Figure 4-21. Chromogranin A expression (green) within epithelial glands of the tissue recombinants. Nuclei are counterstained with DAPI (blue). Scale bars 25µm.

4.3.5 Comparison to primary prostate tissue

To confirm that the tissue generated from iPSCs represented normal human tissue, sections from both the xenograft and primary prostate tissue were compared by IHC for the markers AR, PSA, CK8/18 and p63. As shown in Figure 4-22, the epithelial glands generated from ProiPSCs were representative of normal human prostate with expression of all markers present and correctly localised in both the iPSC-derived xenografts and primary prostate tissue. This confirms that tissue recombinants of ProiPSCs and rat UGM can generate fully differentiated human prostatic tissue.

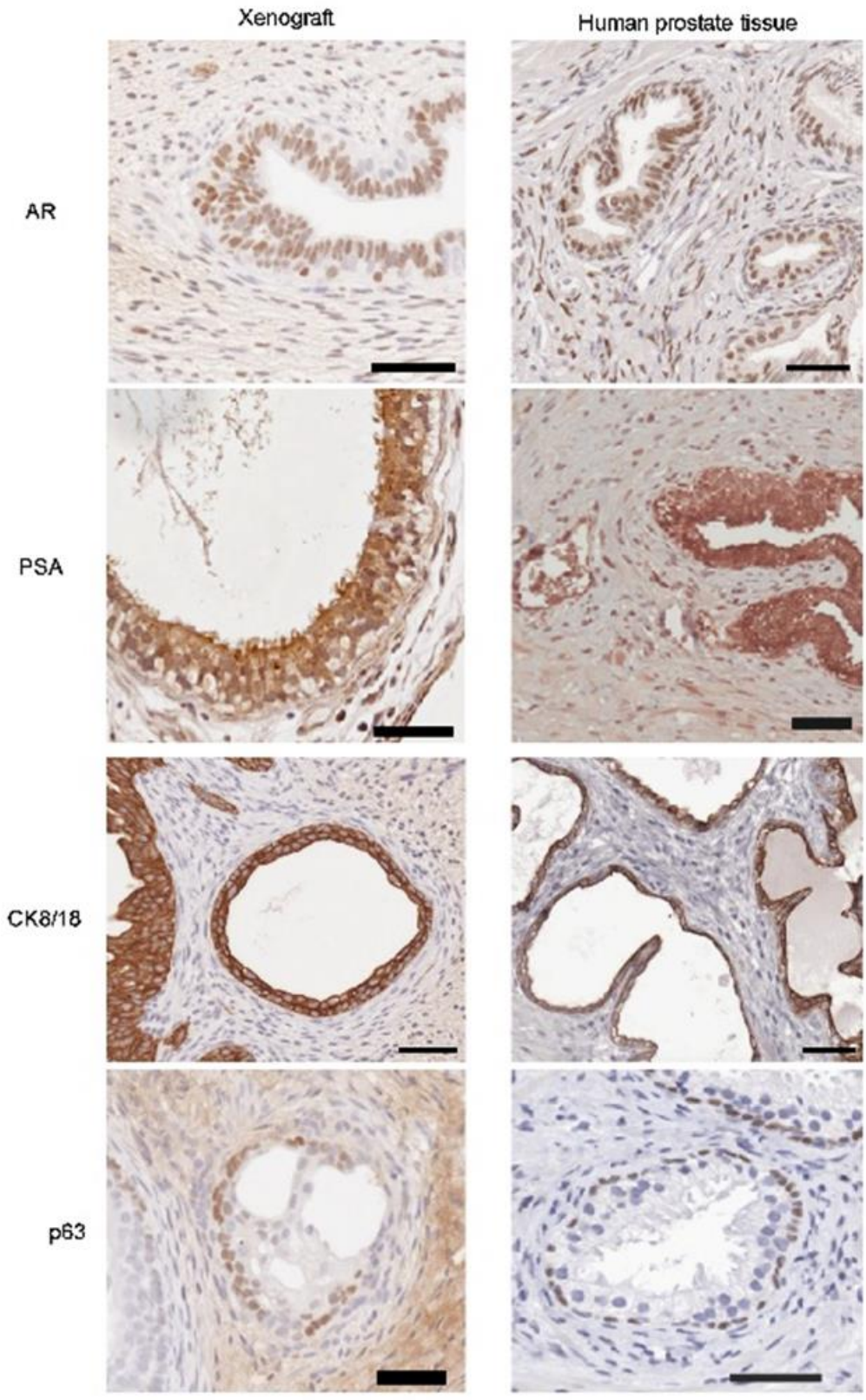

Figure 4-22. IHC for AR, PSA, CK8/18 and p63 in iPSC-derived xenografts and primary benign prostate tissue. iPSC-derived xenografts show full prostatic differentiation and expression of all markers expected in normal prostatic epithelium. Scale bar 50μm.

4.4 Conclusions

In this chapter, successful generation of terminally differentiated prostatic tissue from patient derived ProiPSCs has been shown. Using tissue recombination with inductive UGM, prostate epithelium has been generated *in vivo* which shows formation of basal and luminal cells, expresses the endodermal transcription factor FOXA1, AR and the prostate specific marker PSA as well as containing rare chromogranin A positive cells. By IHC, the expression of these markers recapitulates human benign prostate tissue samples. This confirms the suitability of this model to generate normal human prostate tissue for research. As iPSCs are an unlimited cell source which can rapidly proliferate, this method will allow a theoretically unlimited volume of prostate tissue to be generated without the ethical issues associated with prostatic tissue generated from hESCs.

Although it is beyond the scope of this current project, further staining of the generated tissue for other NE markers as well as for stromal markers including αSMA is essential to fully characterise the generated tissue. As the results presented in this chapter focused on a single graft for each ratio, analysis of further grafts will be needed to confirm the observations and differences seen between ratios. From data gathered so far, a ratio of 1:125 seems most appropriate for generation of predominantly prostatic tissue without presence of large volumes of non-specific tissue differentiation. Confirmation of this by analysing the repeats will give an optimised ratio for prostatic tissue formation from iPSCs using this method.

Chapter 5. Generation of an *in vitro* model of prostate development using human prostate derived iPSCs

5.1 Introduction

Current knowledge of prostate development and disease is hindered due to the lack of relevant human models of normal prostate development and their translation to study disease processes. iPSCs offer a limitless source of cells which could be used for developmental and disease modelling. To enable this, a reliable method for differentiation of iPSCs to prostate is required. In the previous chapter, generation of prostatic tissue from iPSCs using tissue recombination with UGM was discussed. This has built on previous studies showing the ability of UGM to direct prostate differentiation from hESCs (Taylor et al., 2006), and confirms the importance of epithelial-mesenchymal interactions during this process.

Ideally, *in vitro* differentiation of iPSCs is an attractive approach due to the reduced need and cost for host mice as well as the availability of *in vitro* cell cultures to subsequent manipulation and expansion. However, there is very limited literature on prostate differentiation *in vitro*. To date only one published study has shown the generation of prostate organoids *in vitro* from hESCs (Calderon-Gierszal and Prins, 2015). We therefore sought to replicate this using iPSCs. Due to the importance of the UGM in prostate development, as well as its proven ability to differentiate ProiPSCs to prostatic tissue *in vivo* as shown in the previous chapter, we hypothesised that UGM may also be able to direct differentiation of iPSCs to prostate *in vitro*. We therefore also used a UGM co-culture based method to drive prostate differentiation from iPSCs. This chapter will describe the methods trialled for directing human prostate and UT derived iPSCs to prostate epithelial cells *in vitro*.

5.2 Aims

- To prime iPSCs to form definitive endoderm
- To use a published growth factor based protocol to differentiate iPSCs to prostate organoids *in vitro*
- To use inductive UGM to drive iPSC differentiation to prostate in a novel 3D co-culture model

5.3 Results

5.3.1 Formation of definitive endoderm from prostate derived iPSCs

During embryogenesis, the prostate gland is formed from the urogenital sinus epithelium, an endodermal derivative. Recent literature regarding iPSC and hESC differentiation into a range of endodermal tissues has used generation of definitive endoderm from the pluripotent cells as the first step in the differentiation process (Spence *et al.*, 2011; Takebe *et al.*, 2013; Calderon-Gierszal and Prins, 2015). As iPSCs are pluripotent by nature, directing their differentiation down an endoderm lineage is likely to increase the purity of the differentiated cells by preventing ectodermal and mesodermal differentiation.

To generate definitive endoderm from the prostate derived iPSCs, an established method was used (D'Amour *et al.*, 2005). iPSCs were harvested, digested to a single cell suspension and seeded at a density of $2x10^6$ cells per well in a 6 well Matrigel-coated plate. After 24 hours, fresh DMEM/F12 medium containing 100ng/ml Activin A was added and over the next 2 days this was continued with the addition of FCS at increasing concentrations (Day 1 0%, Day 2 0.2%, Day 3 2%). After 24 hours of incubation with Activin A, cell death was clearly visible in the cells. Following this, a clear change in cell morphology was seen, with an increase in cell size and a reduction in nuclear size along with increased confluency of the cells (Figure 5-23).

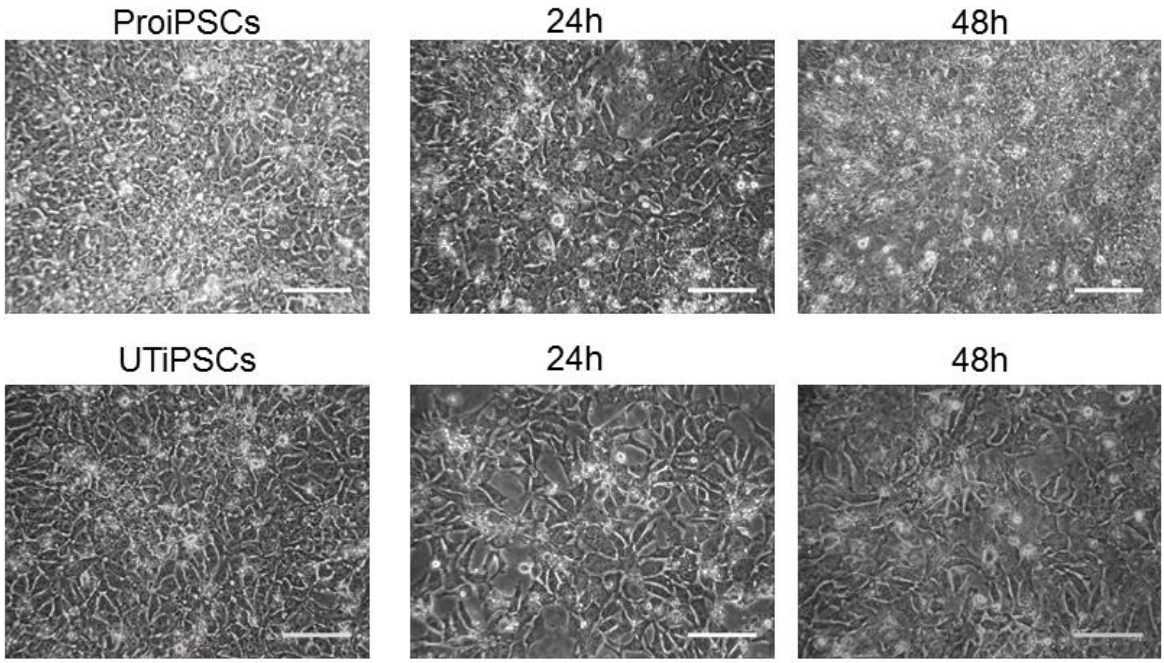

Figure 5-23. Alterations in cell morphology following addition of Activin A and increasing concentrations of FCS to ProiPSCs and UTiPSCs. Cells became larger and lost the high nuclear to cytoplasmic ratio which is typical of iPSCs. Scale bar 10μm.

Definitive endoderm formation was confirmed at transcript and protein level using RT-PCR and immunofluorescence respectively. RT-PCR analysis showed a strong upregulation in the definitive endoderm marker FOXA2 after 3 days of induction with Activin A in comparison to undifferentiated iPSCs (Figure 5-24). Immunofluorescence was initially carried out as a single stain, showing that the majority of cells express the DE markers FOXA2 and SOX17 in the nucleus (Figure 5-25). To confirm co-expression, dual immunofluorescence using both FOXA2 and SOX17 was performed. After DE induction, most cells expressed both markers, consistent with DE differentiation (Figure 5-26). Secondary antibody only controls imaged at the same gain and exposure confirmed the specificity of the staining.

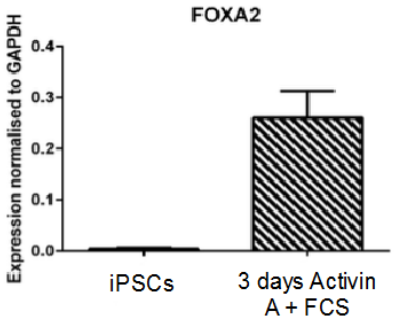

Figure 5-24. RT-PCR showed an increase in expression of the definitive endoderm marker FOXA2 in iPSCs treated with Activin A and increasing concentrations of FCS for 3 days.

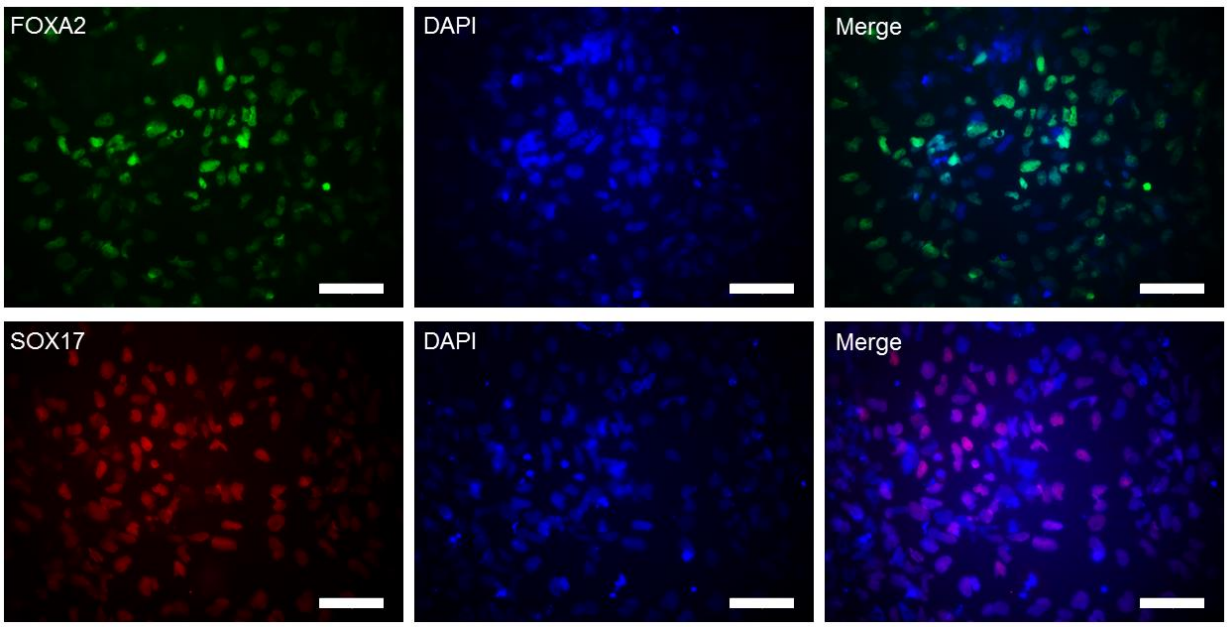

Figure 5-25. Immunofluorescence staining for the definitive endoderm markers FOXA2 (green) and SOX17 (red). Nuclei are stained with DAPI (blue). The majority of cells express FOXA2 and SOX17 confirming efficient induction of definitive endoderm. Scale bar 25μm.

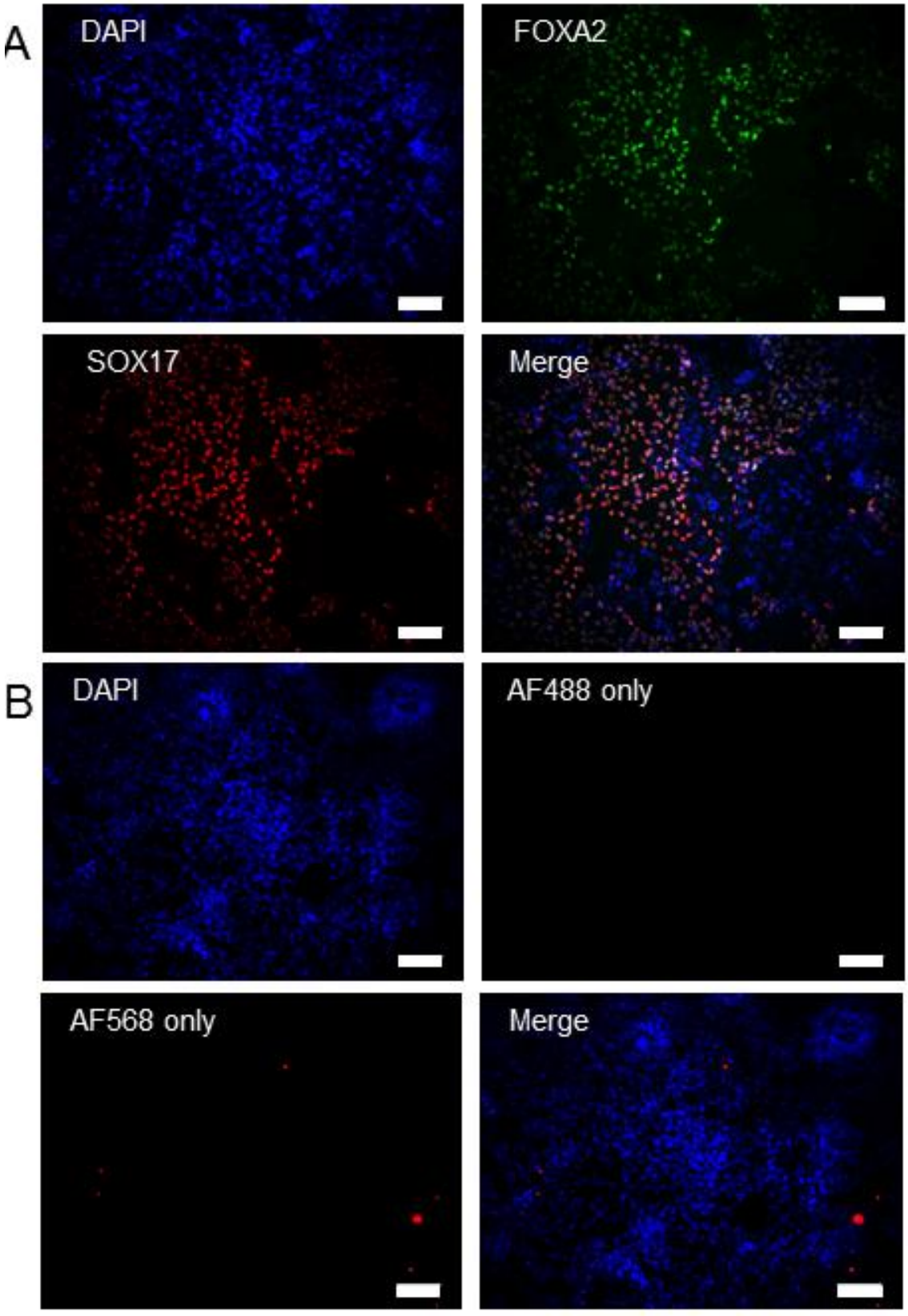

Figure 5-26. Dual immunofluorescence for the definitive endoderm markers FOXA2 (green) and SOX17 (red) in iPSCs treated for 3 days with 100ng/ml Activin A and increasing concentrations of FCS (A). Panel (B) shows secondary antibody only control taken for the same cells taken at the same gain and exposure. Nuclei are stained with DAPI (blue). Scale bar 10μm.

5.3.2 Growth factor driven prostate differentiation

Attempts to generate prostate specific differentiation are sparse in the current literature. However, a recent publication showed the ability to differentiate hESCs into prostate organoids using an *in vitro* growth factor driven method (Calderon-Gierszal and Prins, 2015). Briefly, iPSCs were specified to definitive endoderm using the protocol detailed above. Following this, endoderm cells were cultured in RPMI 1640 containing 500ng/ml FGF10 and 500ng/ml WNT10B for 4 days to specify a prostatic fate. 3D structures formed during this 'prostate specification' phase were subsequently transferred to Matrigel culture in prostate medium (prostate epithelial growth medium (PrEGM) and stromal cell medium (SCBM) supplemented with 2mM L-Glutamine, penicillin-streptomycin, 15mM HEPES, 500ng/ml R-Spondin1, 100ng/ml Noggin, 100ng/ml EGF, 1x B27 supplement, 10nM retinoic acid and 1.7μM testosterone).

Using this method, Calderon-Gierszal and Prins were able to generate epithelial organoids with lumens from hESCs which were surrounded by stromal cells. These epithelial organoids expressed CK8/18, AR, NKX3.1, PSA and TMPRSS2 whilst the surrounding stromal cells showed some expression of vimentin (Calderon-Gierszal and Prins, 2015). However, the basal-luminal organisation of the organoids was not complete, as CK8/18 expression was not restricted to the luminal layer and no basal cell markers were investigated with immunofluorescence. We aimed to use this same protocol to drive differentiation of our iPSCs to prostate organoids.

Following definitive endoderm generation, ProiPSC-derived endodermal cells were specified to prostate by culture in the presence of 500ng/ml FGF10 and 500ng/ml WNT10B for 4 days. After 72 hours, some 3D structures could be identified which varied in size and morphology as shown in Figure 5-27. However, the appearance of several structures was neuroepithelial-like with a rosette morphology (Figure 5-27C). These structures were morphologically different to the structures seen in the published paper, which showed a more spheroid-like or ductal appearance.

After 4 days, any 3D structures were transferred to a Matrigel "bead" for further culture in prostate medium (Calderon-Gierszal and Prins, 2015). The 3D structures grew slowly at first and from around day 3 small cellular growths from the structures could be seen. Between day 4 and 8, the organoids grew rapidly in size and cellular protrusions could be more clearly seen (Figure 5-28). A neuronal like morphology

was seen with thin outgrowths of what appeared to be dendrites from the organoids (Figure 5-29). This was not described in the published protocol, but does fit in with literature suggesting that the default differentiation path for pluripotent stem cells is neuronal differentiation (Schwartz *et al.*, 2008). The 3D structures continued to grow at a slower rate from this point although the neuronal-like outgrowths continued to expand. All organoids were harvested after 28 days of culture for RT-PCR and IHC.

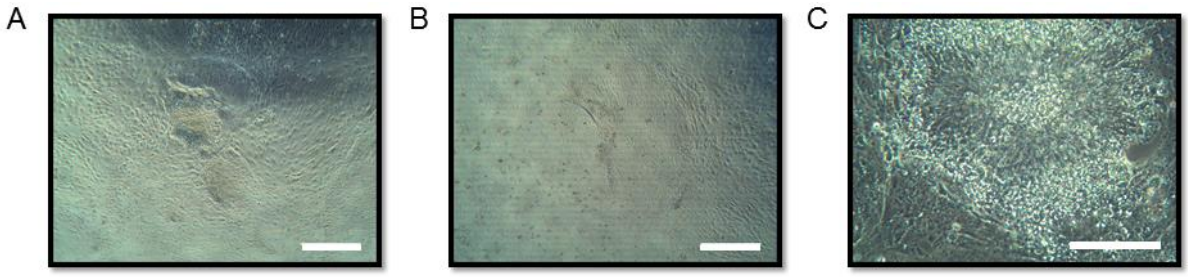

Figure 5-27. Phase contrast micrographs showing the variety of 3D structures visible after 96hr of culture with WNT10B and FGF10. A and C, scale bar 50μm. C) Neuronal rosette like structure, scale bar 15μm.

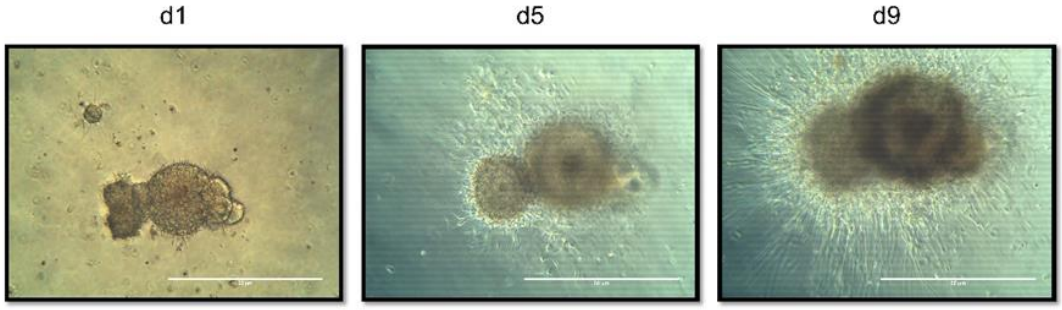

Figure 5-28. Phase contrast micrographs following growth of an organoid from day 1 to day 9 of culture. The organoids grew rapidly and by day 5 cellular protrusions could be clearly seen. These protrusions also show a rapid growth. Scale bar 50μm.

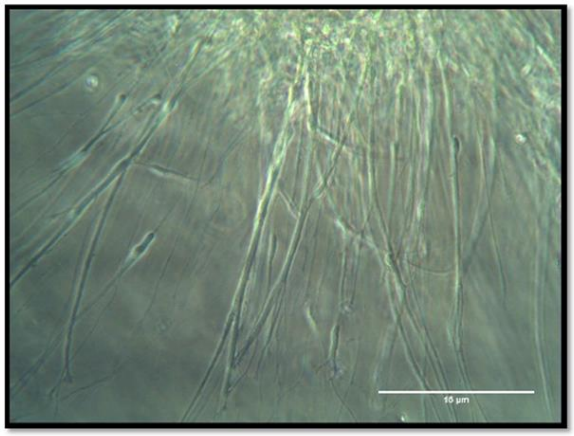

Figure 5-29. High magnification phase contrast micrograph showing the protrusions emerging from an organoid at day 9. The cells have a neuronal-like morphology. Scale bar 15μm.

Prostate specific differentiation was assessed using the prostate markers AR and Nkx3.1, the definitive endoderm marker FOXA2 and prostate mesenchymal marker αSMA. As expected, FOXA2 expression decreased following the prostate differentiation protocol and this was accompanied by a slight increase in AR expression (Figure 5-30). Unfortunately, the water control for Nkx3.1 was contaminated so this gene was discarded from the analysis. αSMA remained the same throughout.

Organoids were also sectioned for histological analysis; however, no visible structures were identified in the sections as most organoids were kept for PCR. Therefore, the growth factor differentiation protocol was repeated with an increased input of cells to increase the yield and allow histological analysis of the generated structures. Furthermore, we decided to include UTiPSCs in the repeated experiment in case of potential differences in differentiation capacity between the two iPSC lines.

For the second experiment, ProiPSCs and UTiPSCs were differentiated to definitive endoderm as detailed above. The cells were either cultured in 500ng/ml FGF10 and 500ng/ml WNT10B to specify prostatic fate, or in control medium (RPMI 1640 containing 2% FCS, 2mM L-Glutamine and penicillin-streptomycin alone without the presence of the morphogens). From as early as 24 hours, 3D structures could be seen in the ProiPSC-derived DE cells in both control and FGF10/WNT10B treated wells (Figure 5-31A). After 72 hours, 3D structures were also identified in the UTiPSC-derived DE cells under treatment and control conditions (Figure 5-31B). As in the previous experiment, these varied in size and morphology, and expanded over the 4-day period to form large, dense structures. In the published protocol, presence of such structures in the control well was not discussed. As these structures were also identified in the control arm for both iPSC lines, they were taken forward in the experiment to determine if the prostate specification phase influenced the differentiation and final phenotype of the resultant organoids.

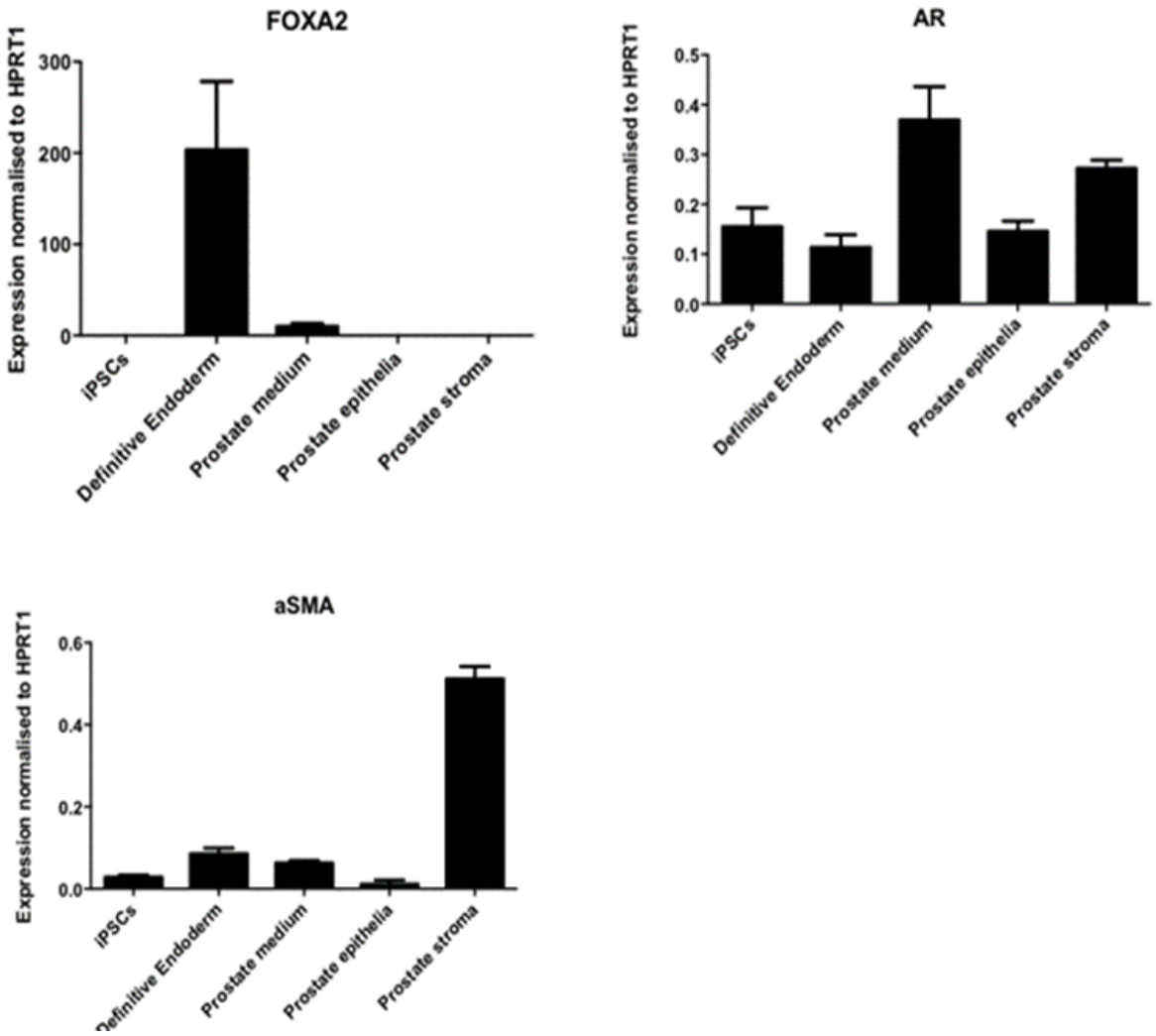

Figure 5-30. RT-PCR analysis of the endoderm marker FOXA2, prostate marker AR and stromal marker αSMA. Cells cultured in prostate medium show a downregulation of FOXA2 expression and an increase in AR expression. αSMA remains the same.

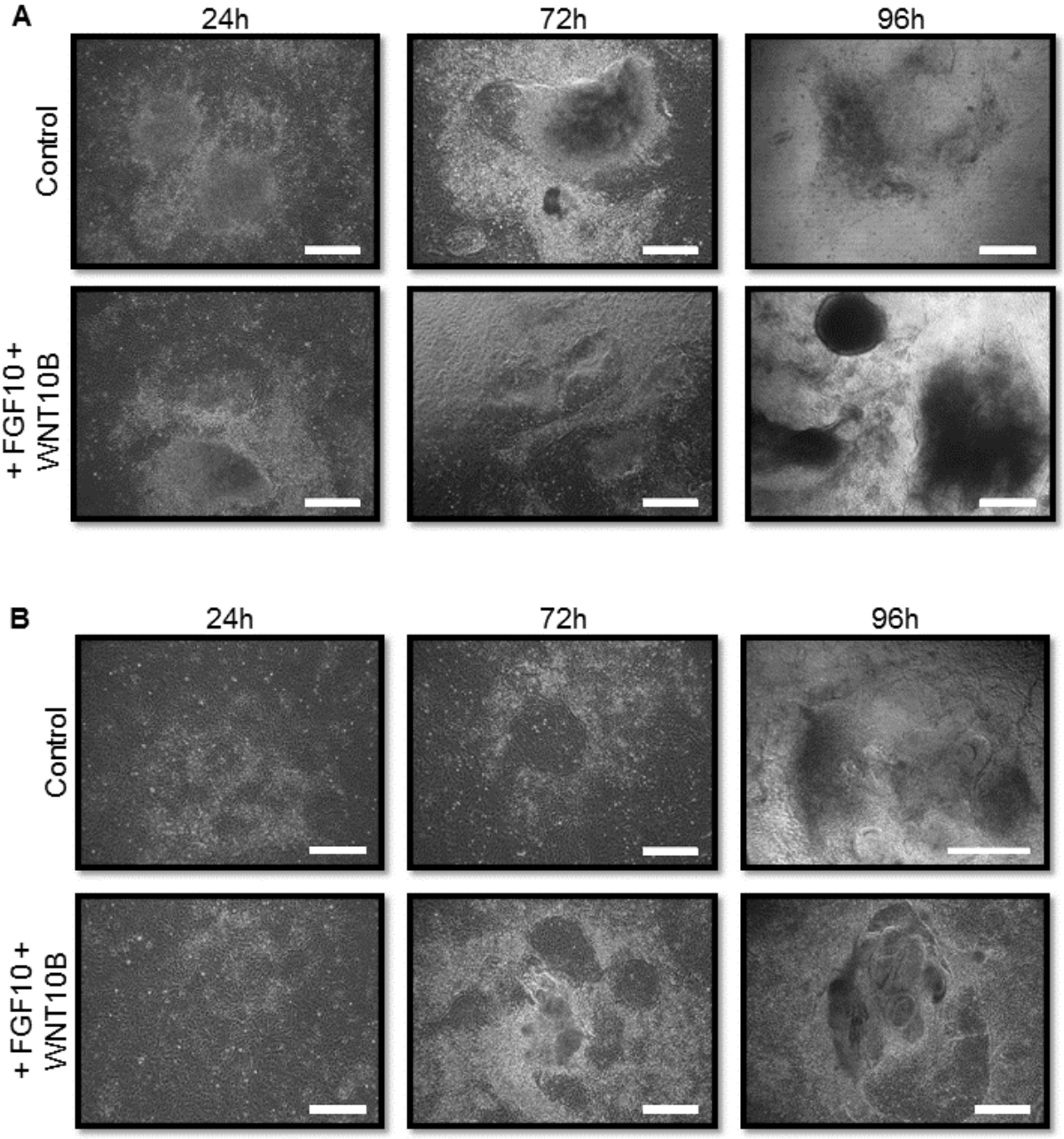

Figure 5-31. Phase contrast micrographs showing the emergence of 3D structures within both control and FGF10+WNT10B treated wells of ProiPSC (A) and UTiPSC (B) derived definitive endoderm. Scale bar 25μm.

All 3D structures which formed in either the prostate specification or control well were transferred to Matrigel culture in prostate medium (PrEGM 1:2 SCBM supplemented with R-Spondin 1, EGF, Noggin, B27, retinoic acid and DHT). Both the control (no specification) and “prostate specification” 3D structures continued to grow, generating mostly spheroid-like structures reminiscent of embryoid bodies (Figure 5-32). No visual differences could be identified between those structures which had been specified to prostatic differentiation and those which had not.

At around day 6, neuronal-like cellular outgrowths were identified once again in both the control and growth factor treated structures (

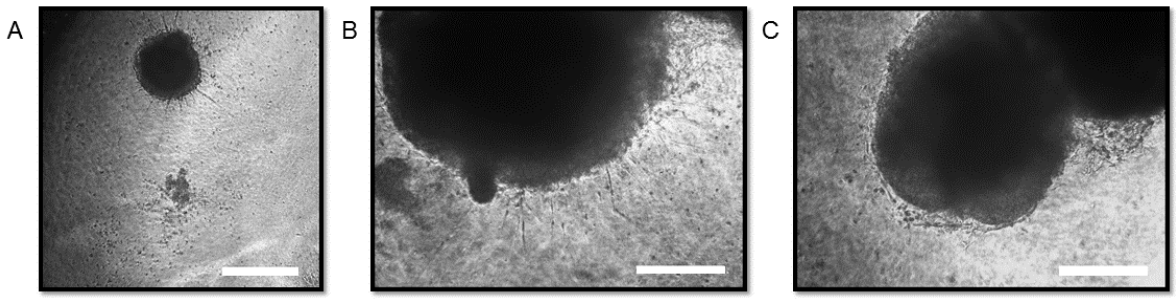

Figure 5-33). The protrusions were long and thin, and expanded rapidly to form apparent networks of cells.

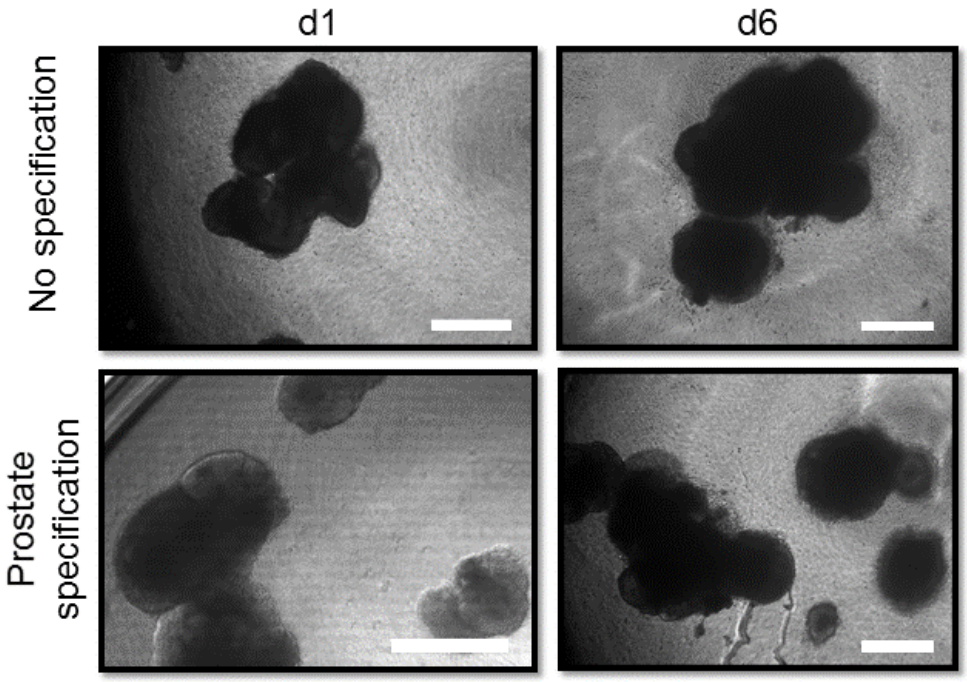

Figure 5-32. Phase contrast micrographs of 3D structures growing in Matrigel at d1 and d6. Structures from both “prostate specification” and control no specification wells grew at the same rate following transfer to floating Matrigel culture in prostate medium. Scale bar 50μm.

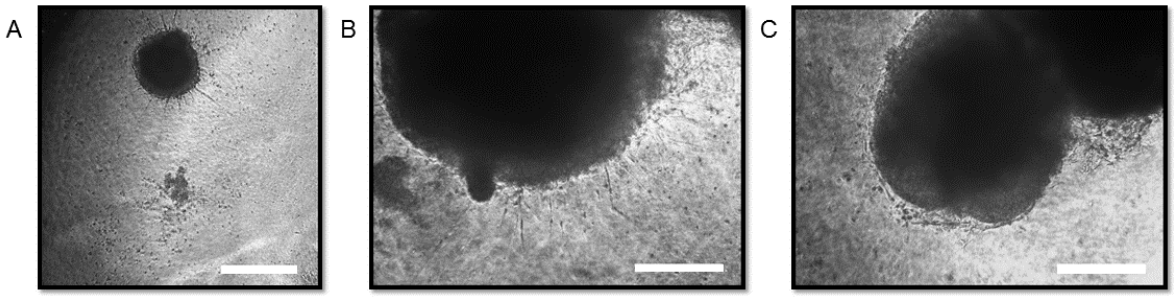

Figure 5-33. Phase contrast micrographs showing neuronal-like outgrowths in 3D structures emerging at day 6 (A) and 10 (B, C).

After 28 days of culture, all wells were harvested for either RT-PCR or histological analysis. H&E staining showed that both control and growth factor treated spheroids had a range of cell morphologies present within each organoid. The majority of cells appeared mesenchymal and neuronal-like with small potential epithelial areas as shown in Figure 5-34. This is consistent with the morphology of the structures which appeared similar to EBs.

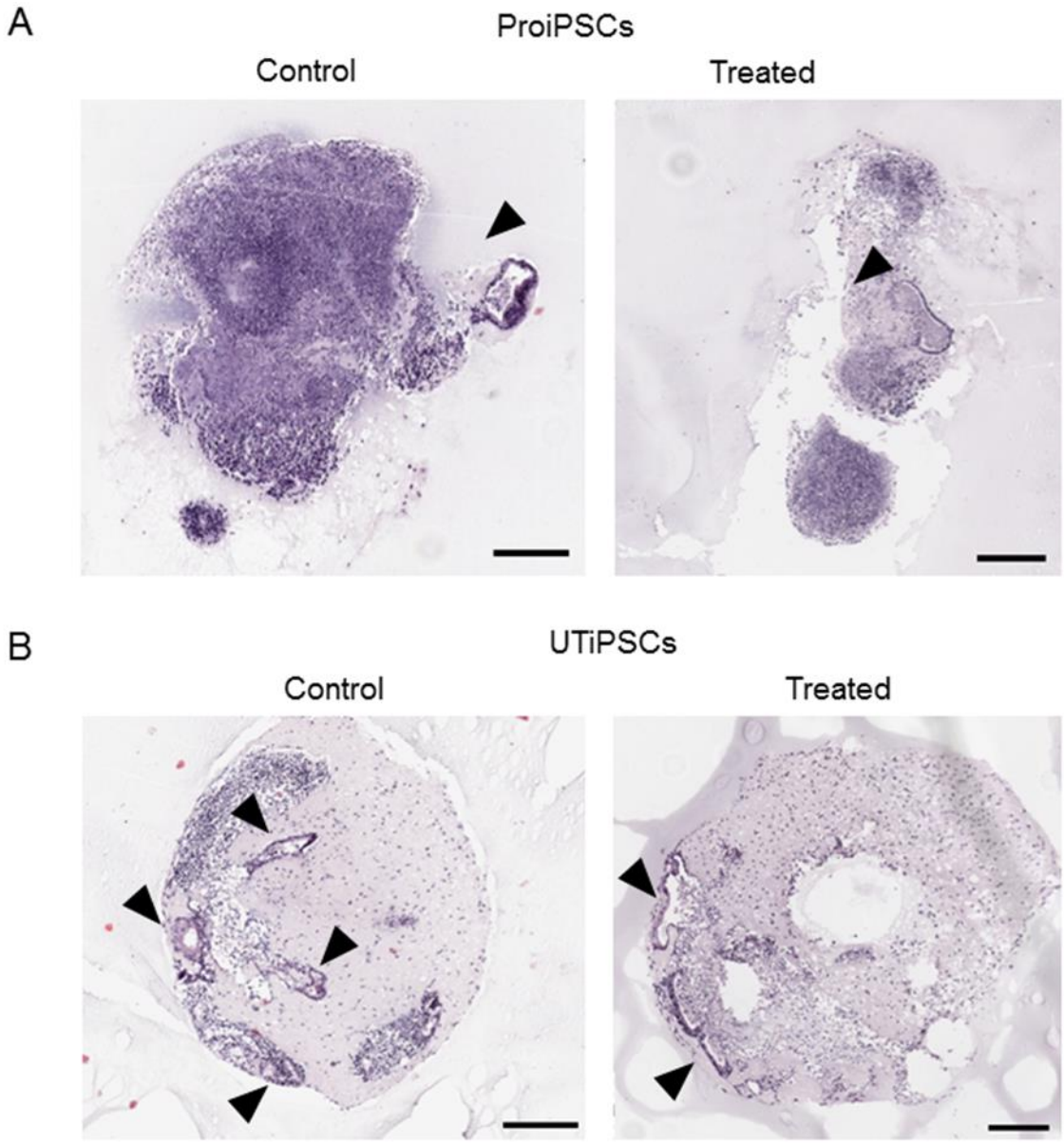

Figure 5-34. H&E staining for ProiPSC (A) and UTiPSC (B) derived spheroids. Arrowheads mark potential areas of epithelial differentiation. Scale bar = 250μm.

IHC staining for mesodermal (vimentin), neuronal (βIII Tubulin) and epithelial (CK8/18 and p63) markers was undertaken to confirm the suspected cell types. As expected, most of the spheroid consisted of cells which expressed vimentin and/ or βIII tubulin in both control and prostate medium slides and for both ProiPSCs (Figure 5-35) and UTiPSCs (Figure 5-36). Vimentin was always localised to the periphery of the organoid whilst βIII tubulin expression occurred in a more diffuse pattern across the organoid. The potential epithelial areas were all positive for the luminal epithelial marker CK8/18, but no expression of the basal marker p63 was identified.

To interrogate prostate specific differentiation, AR and PSA expression was analysed in the spheroids using IHC. Some weak AR expression was identified in a subset of cells in all spheroids regardless of whether prostate specification was used (Figure 5-37). No PSA could be identified in any of the structures (Figure 5-38). This suggests that some prostatic differentiation has occurred but the AR is not functional resulting in lack of PSA expression. The presence of AR, albeit at low levels, regardless of prostate specification suggests that at least in our hands, priming DE cells from UT and ProiPSCs with FGF10 and WNT10B did not affect their differentiation.

Calderon-Gierzsal and Prins demonstrated differentiation of hESCs to prostate organoids which expressed prostate specific genes and were functional as demonstrated by PSA secretion. In our hands, we were unable to fully recapitulate the results of their publication with either ProiPSCs or UTiPSCs. Some prostatic differentiation was achieved with weak expression of AR but absence of PSA expression showed that the AR was inactive. Furthermore, as well as expression of the epithelial marker CK8/18, the 3D structures generated with this method also contained cells from the other embryonic germ layers as confirmed by expression of βIII tubulin and vimentin. Therefore, this method generates EB-like spheroids from

the iPSC lines tested in this study, suggesting further refinement is required to generate purely prostatic differentiation.

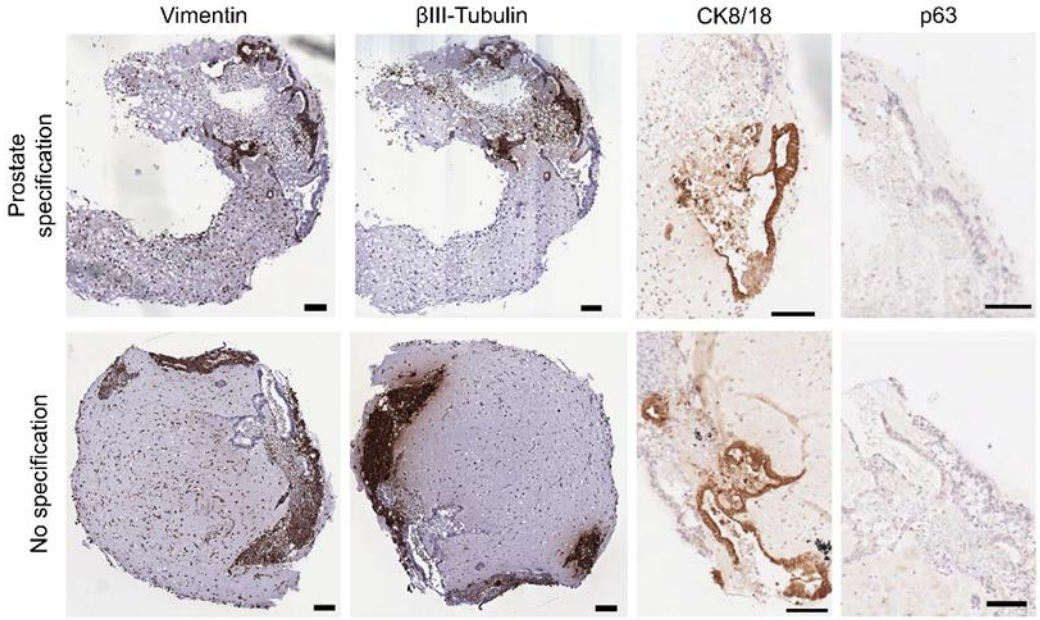

Figure 5-35. IHC analysis for the mesodermal marker vimentin, ectodermal marker βIII tubulin, luminal epithelial marker CK8/18 and basal marker p63 in spheroids derived from ProiPSCs. Scale bar 100μm.

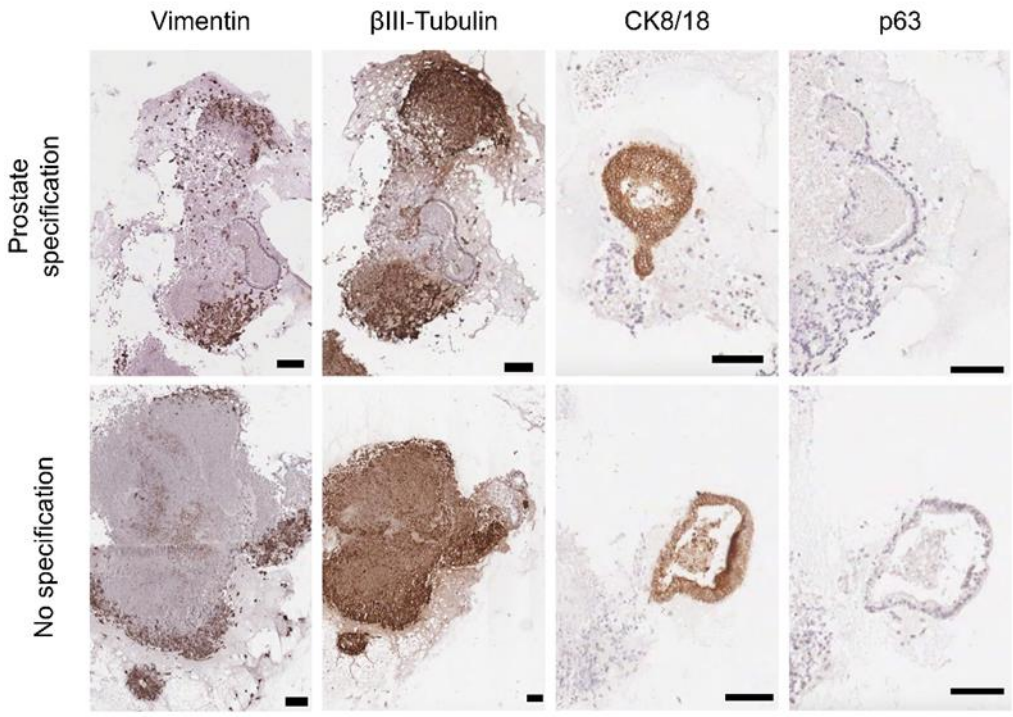

Figure 5-36. IHC analysis for the mesodermal marker vimentin, ectodermal marker βIII tubulin, luminal epithelial marker CK8/18 and basal marker p63 in spheroids derived from UTiPSCs. Scale bar 100μm.

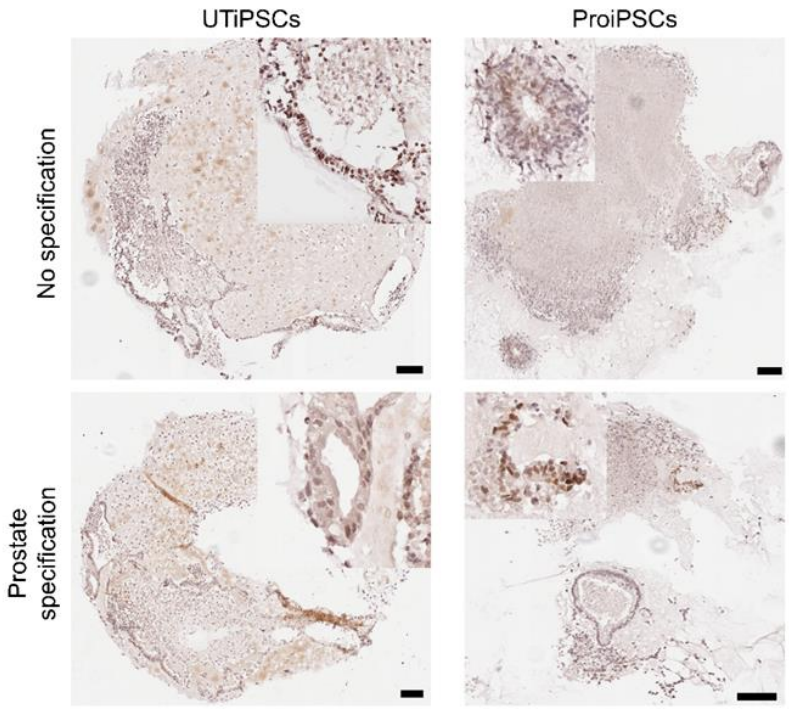

Figure 5-37. IHC for AR expression in UTiPSCs and ProiPSCs with and without prostate specification and cultured in 3D with prostate medium. Scale bar 100μm. Insets show high magnification image of areas with weak AR expression.

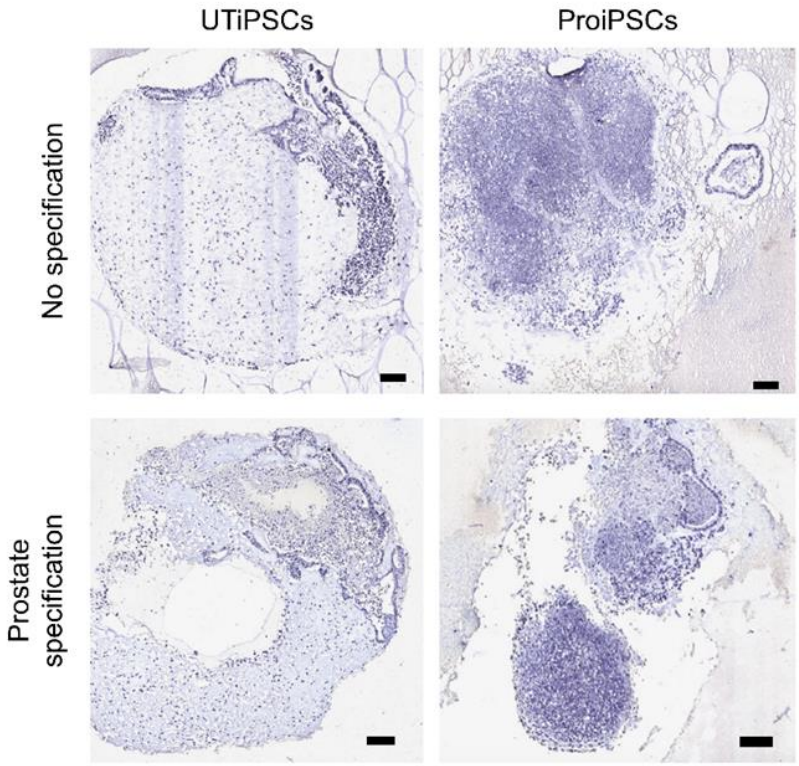

Figure 5-38.IHC for PSA expression in UTiPSCs and ProiPSCs with and without prostate specification. Scale bar 100μm.

5.3.3 3D co-culture of definitive endoderm and UGM cells to drive prostate differentiation

The results obtained from the growth factor differentiation method above suggested that the protocol did not contain the entire repertoire of factors at the correct concentrations to direct prostate specific differentiation of iPSCs. During normal embryonic development, prostate epithelial cell differentiation is driven by the UGM which secretes a range of paracrine factors which promote epithelial growth and differentiation. However, the precise factors are not yet fully determined. *In vivo* experiments using rodent UGM combined with adult epithelium and hESCs have shown that prostatic tissue can be generated in this manner. In chapter 4 of this thesis, successful generation of prostatic tissue from tissue recombinants of ProiPSCs and rat UGM is discussed. However, to date no studies have explored whether UGM cells can be used to drive differentiation of pluripotent cells to prostate *in vitro*. We therefore aimed to use rat UGM in a 3D co-culture system to determine if this inductive potential can be replicated and sustained *in vitro*.

To reduce non-specific differentiation, ProiPSCs and UTiPSCs were again differentiated to definitive endoderm using Activin A and increasing concentrations of FCS. Following this, endoderm cells were combined with rat UGM cells in Matrigel at

two ratios: 10,000 DE cells to 35:000 UGM cells (1:3.5) or 5,000 DE cells to 35,000 UGM cells (1:7). After the Matrigel had set, DMEM/F12 supplemented with 2% insulin-transferrin-selenium (ITS) and 10nM DHT was added. This was also supplemented with ROCK inhibitor to promote the survival of single cell suspension of DE. This medium was chosen as it is serum-free and has been previously used for successful *in vitro* culture of UGS (Lipinski *et al.*, 2005; Bryant *et al.*, 2014). Cultures were monitored daily by microscopy and media was changed every 48 hours. After 7 days of culture, the medium was changed to UGM conditioned medium (CM) to ensure the cells still received UGM secreted factors once the UGM lost its inductive ability. UGM CM was collected by culturing whole UGM pieces in DMEM/F12, 2% ITS and 10nM DHT. CM was collected at days 2, 4, 5, 6 and 7, filter sterilised and aliquoted to ensure each aliquot contained equal amounts of CM from each day of collection to mitigate the potential differences in factors secreted over time. Once the media was changed to UGM CM, media changes took place twice per week.

In both ProiPSCs and UTiPSCs, a ratio of 5000 DE cells to 35,000 UGM proved non-permissive for growth and the cultures were abortive. However, the 10,000 DE cells to 35,000 UGM appeared viable with apparent clusters of cells visible from day 6 (Figure 5-39). After 10 days of culture, small round structures could be seen in the UTiPSC arm of the experiment. These showed rapid growth and by day 13 large spheroids were present. Morphologically, the spheroids appeared to consist of a single cell layer with a large lumen (Figure 5-40). Typically, they were closely associated with clumps of cells, which were mesenchymal in appearance. We hypothesised that these cells were the UGM providing structural support as well as paracrine signalling to the differentiating iPSCs. The culture also contained smaller, dense clumps of cells which did not show further proliferation. In contrast, the ProiPSCs formed aggregates which grew poorly and no spheroid formation was observed. After 3 weeks of 3D culture, the organoids were harvested for histological analysis. H&E staining showed the presence of two types of organoid; a single cell organoid with large lumen and smaller dense organoids which appeared less well organised (Figure 5-41).

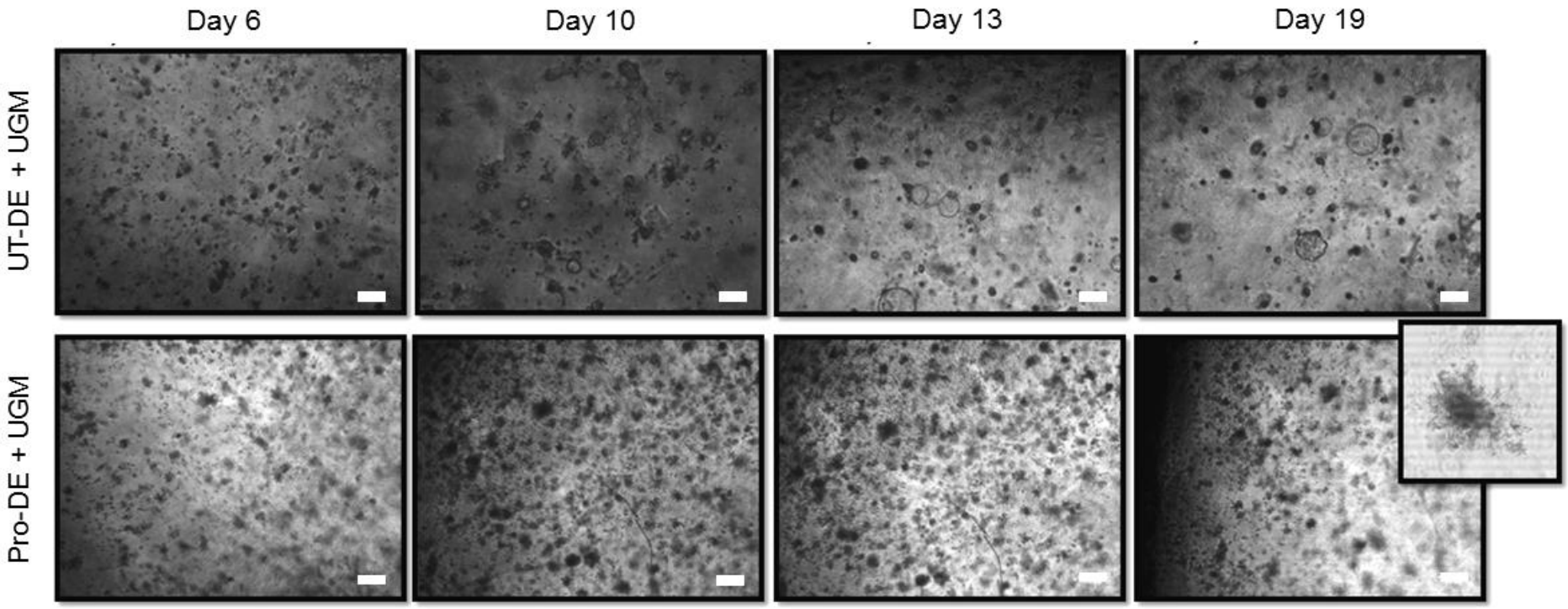

Figure 5-39. Phase contrast micrographs showing morphology of iPSC-derived DE cells co-cultured with UGM. DE cells from UT and ProiPSCs appear as clusters until day 10 when small spheroids were identified in the UT-DE arm. These spheroids grew rapidly whilst the small clusters of cells did not proliferate. In the Pro-DE arm, aggregates of cells formed but these did not grow well and no spheroid formation was seen. Scale bar 1000μm.

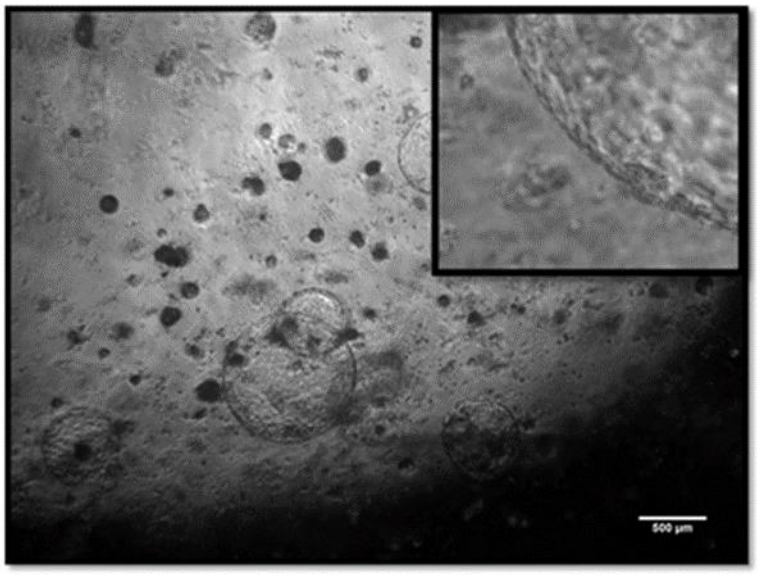

Figure 5-40. Phase contrast micrograph showing the two types of spheroids present in the UT-DE wells. Scale bar 500µm. Inset shows high magnification of a large spheroid showing presence of a thin outer layer of cells.

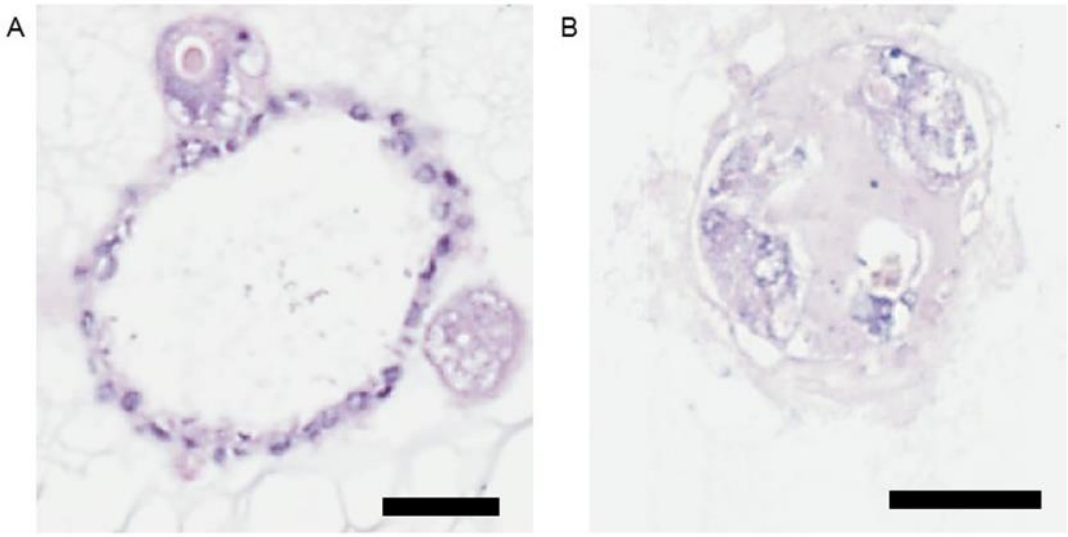

Figure 5-41. H&E staining showing the two types of structure identified in UTiPSC-derived DE cells co-cultured with UGM. (A) A large spheroid with a single layer of cells surrounding a large lumen, (B) A smaller, denser spheroid which lacks a lumen. These smaller spheroids appear quite disorganised. Scale bar 50µm.

The structures were first stained for a human specific mitochondrial marker, which confirmed the spheroids were generated from human cells rather than the rat UGM or any contaminating rat cells present after tissue dissection (Figure 5-42). IHC staining for pan CK, CK8/18, 34βe12 and vimentin confirmed that the structures were formed predominantly from epithelial cells with some areas of vimentin co-expression (Figure 5-43). In addition, the luminal marker CK8/18 and the basal marker 34βe12 were expressed in all cells suggesting that the structures were early epithelial organoids. During prostate development, early prostatic ducts are characterised by co-expression of these two markers (Wang *et al.*, 2001).

To interrogate prostate-specific differentiation, the spheroids were then stained for Nkx3.1, AR and PSA. Some low-level Nkx3.1 expression was seen but no AR or PSA expression was identified (Figure 5-44). We hypothesised that this was due to the short time of differentiation, and therefore decided to repeat the experiment with a larger number of cells to allow harvesting of the differentiated cells at multiple time-points and allow interrogation of protein expression by IHC and transcript level expression using RNA sequencing.

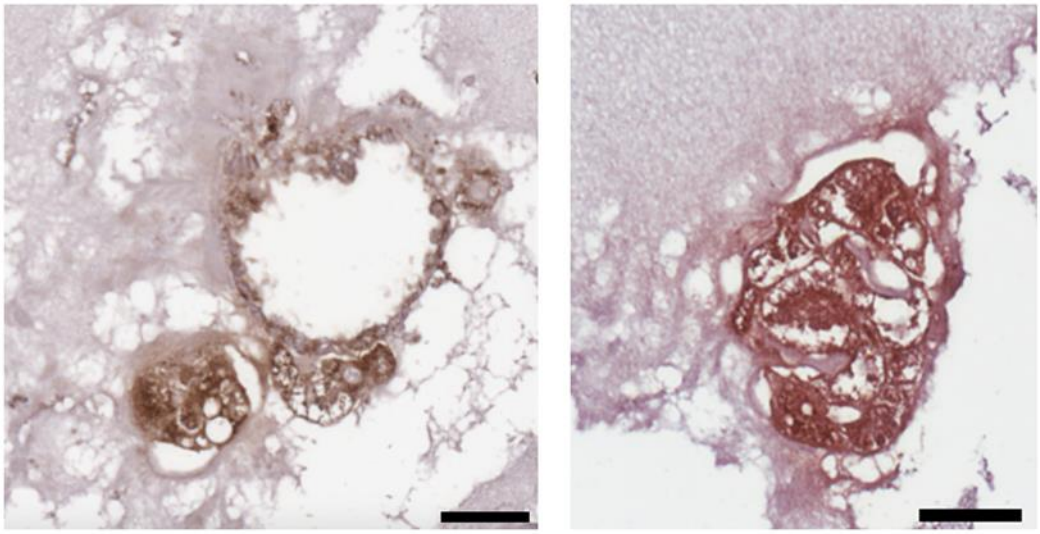

Figure 5-42. IHC for anti-human mitochondria confirms that both types of spheroid are human in origin. Scale bar 50μm.

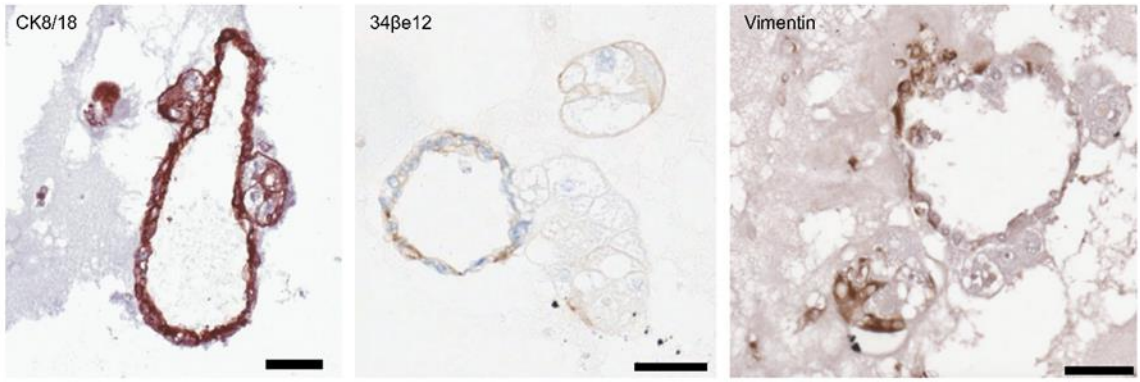

Figure 5-43. IHC for CK8/18, 34βe12 and vimentin. Scale bar 50μm.

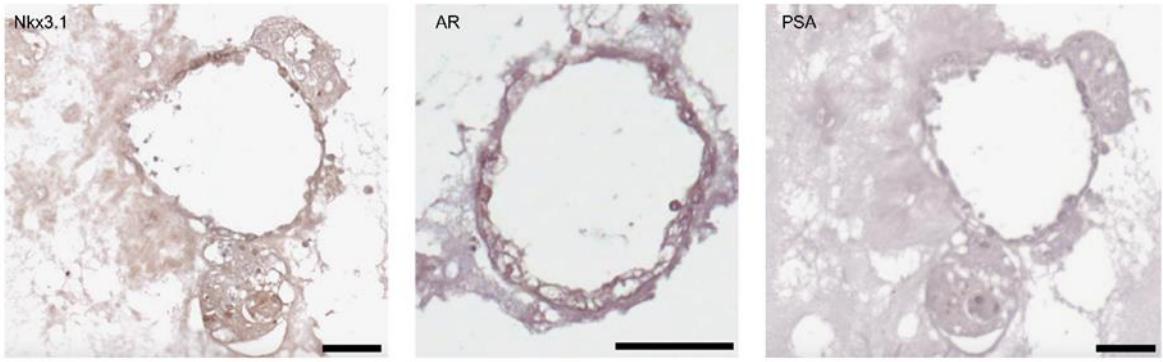

Figure 5-44. IHC for the prostate markers Nkx3.1, AR and PSA. Some weak Nkx3.1 expression is seen but no AR or PSA expression is present. Scale bar 50μm.

For the second experiment, a different ProiPSC clone was used to determine if the lack of growth in the first experiment was clone-specific, as differences in the ability of iPSC clones from the same initial culture to differentiate are known to exist. A single ratio of 10,000 DE cells to 35,000 UGM was used in this experiment. As with the previous experiment, media was changed to UGM CM at day 7. At week 6, media was changed to prostate organoid medium which has previously been used for successful culture of human prostate organoids (Karthaus *et al.*, 2014) as we hypothesised that this would support the maintenance of the organoids once they were established. Additionally, UGM alone and iPSC-derived DE alone control wells were also set up to confirm that the differentiation was a result of the UGM and not due to factors contained within the media.

After 24 hours, small clusters of cells could be identified in both the UT and ProiPSC cultures. There appeared to be two types of structures; small spheroids which appeared to have a single layer of cells surrounding a central lumen, and clusters of cells which appeared to be fibroblasts. Both structures grew well, with the spheres doubling in size over the first week of culture and the fibroblast-like cells forming cell aggregates (Figure 5-45 and Figure 5-46). Interestingly, as the cells continued to grow, the fibroblast-like clusters seemed to surround the spheroids, suggesting that the UGM grows around the developing spheres to direct their differentiation (Figure 5-47).

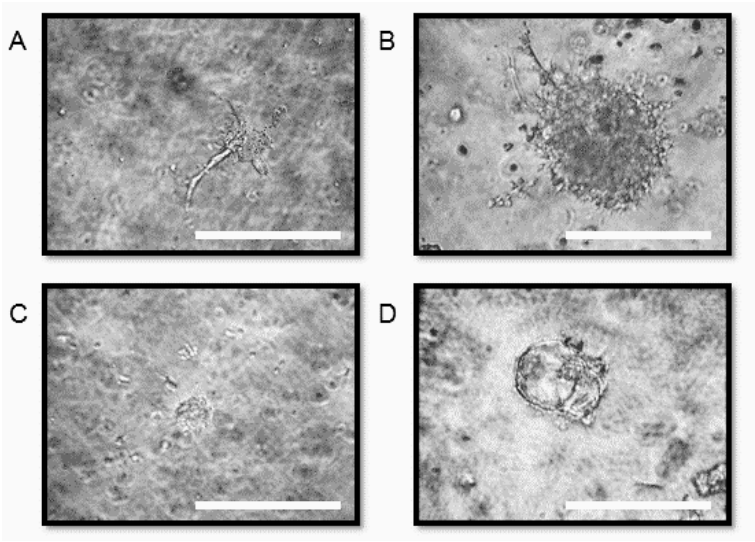

Figure 5-45. Phase contrast micrographs of UTiPSC-derived DE and UGM cells in 3D co-culture at 24 hours (A,C), 6 days (D) and 8 days (B) of culture. Two types of structure can be identified; fibroblast-like cells which form clusters (A,B), and small spheroids (C,D). Scale bar 25μm.

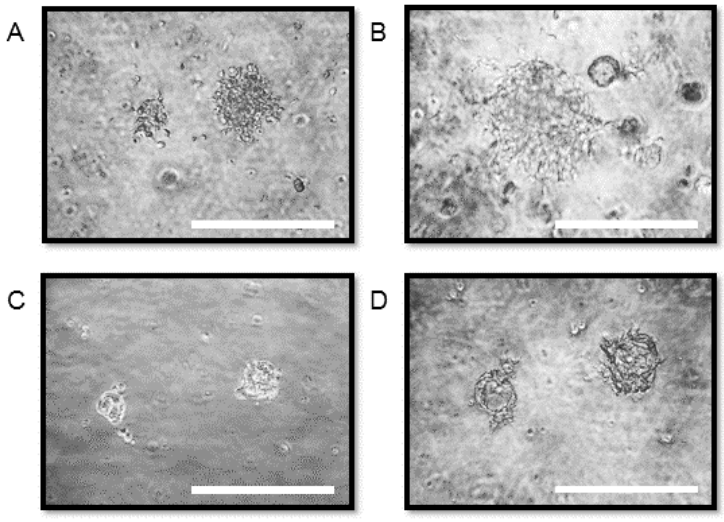

Figure 5-46. Phase contrast micrographs of ProiPSC-derived DE and UGM cells in 3D co-culture at 24 hours (A,C), 6 days (D) and 8 days (B) of culture. Two types of structure can be identified; fibroblast-like cells which form clusters (A,B), and small spheroids (C,D). Scale bar 25μm.

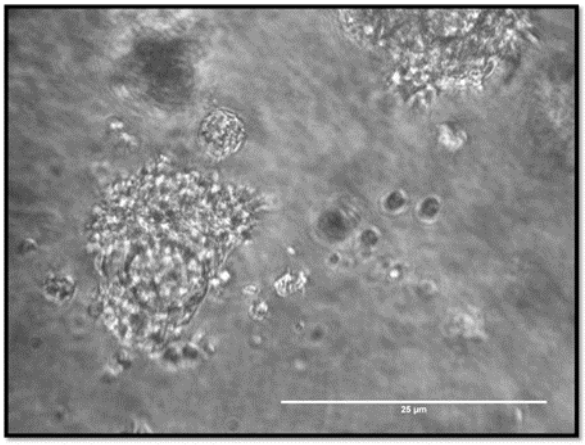

Figure 5-47. Phase contrast micrograph showing fibroblast-like cells surrounding a small spheroid. Scale bar 25μm.

After 6 days, two different types of spheroid could be identified. The first type consisted of large spheroids which grew rapidly (Figure 5-48), which we hypothesised were the epithelial organoids identified in the first experiment. The second type, small spheres, were slow growing. At day 10, small dense “budding” structures could be seen in both UT and ProiPSC arms which appeared to have formed from the small slow growing spheres (Figure 5-49A). These appeared to cluster around the larger spheroids as shown in Figure 5-50B, and we hypothesised that these could potentially be UGM cells. In published organ culture experiments, similar budding structures emerge from the UGS (Rowley and Tindall, 1987).

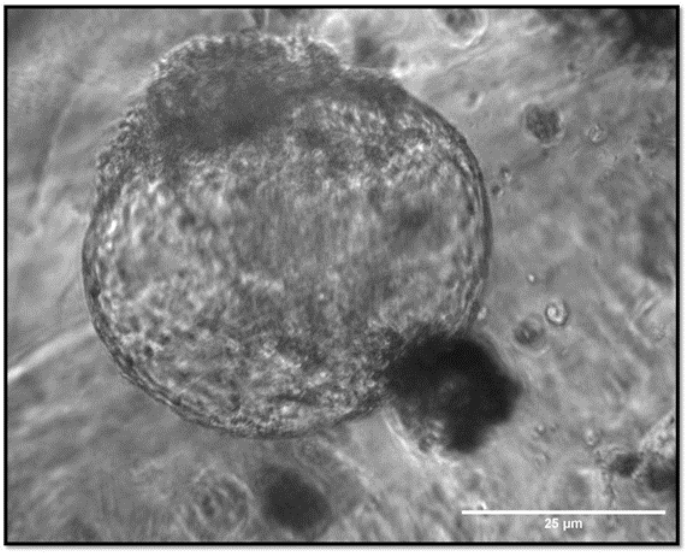

Figure 5-48. Phase contrast micrograph showing a typical spheroid with a single layer of cells surrounding a large lumen. Scale bar 25μm.

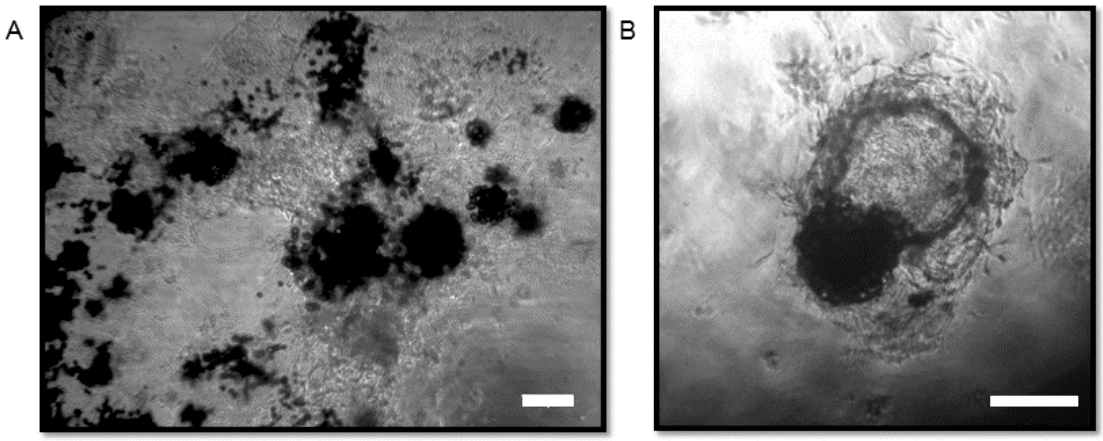

Figure 5-49. Phase contrast micrographs showing (A) the appearance of dense spheres and (B) an area of dense spheres and fibroblast-like cells clustering around a spheroid. Scale bar 25μm.

The large spheroids continued to grow well, in both UT and ProiPSC arms, and as in the previous experiment appeared to be formed from a single layer of cells (Figure 5-50B). Some spheroids expanded to form a dual layer of cells (Figure 5-50A). At high magnification, the spheroids had a clear defined outer border (Figure 5-51). The spheroids continued to grow rapidly until week 4 of culture, at which point their growth began to slow. Spheroid counts performed during the fourth week of culture confirm that the number of spheroids remained the same with no further spheroid formation (

Figure 5-52). Interestingly, the number of large spheroids formed was significantly higher in UTiPSCs versus ProiPSCs (p<0.0001). By week 6, spheroids had reached a diameter of up to 125μm and could be seen with the naked eye. Cultures continued to be monitored by microscopy. Control wells consisting of UGM or DE cells alone failed to grow.

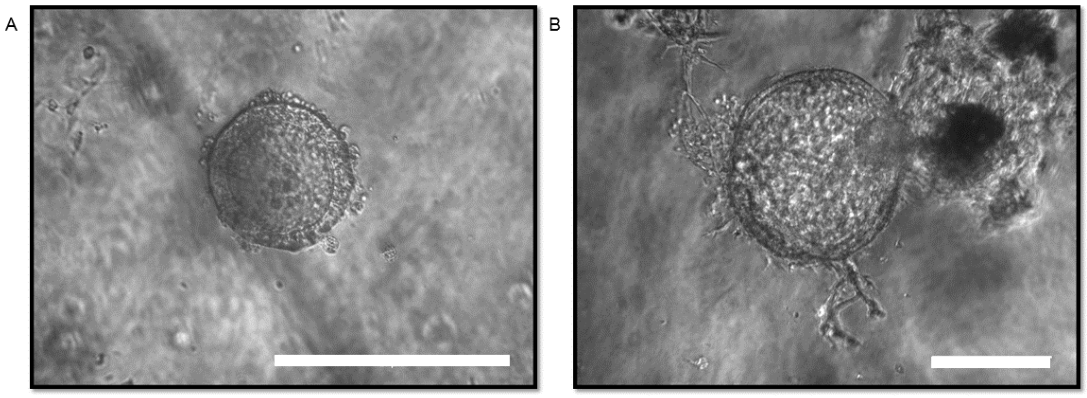

Figure 5-50. Phase contrast micrographs showing two different spheroids. A) A spheroid which has expanded to form what appears to be a dual layer of cells. B) A

typical spheroid showing a thin single layer of cells and large lumen surrounded by fibroblast-like cells and dense spheres. Scale bar 25μm.

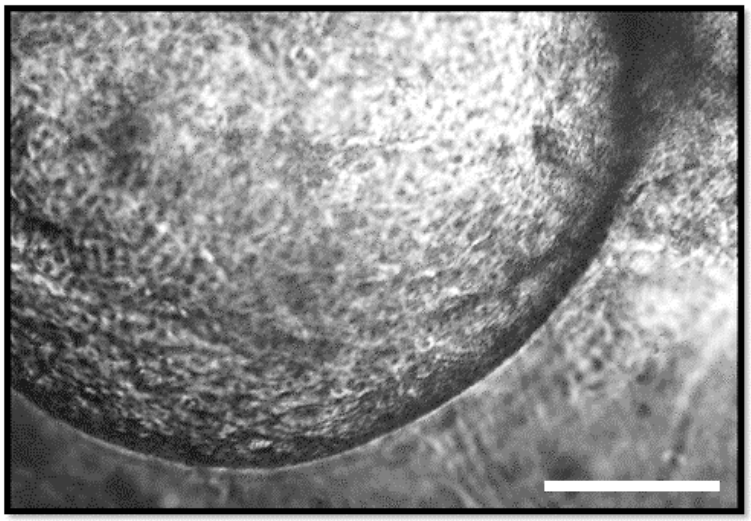

Figure 5-51. Phase contrast micrograph at high magnification showing the clear border of the spheroid. Scale bar 25μm.

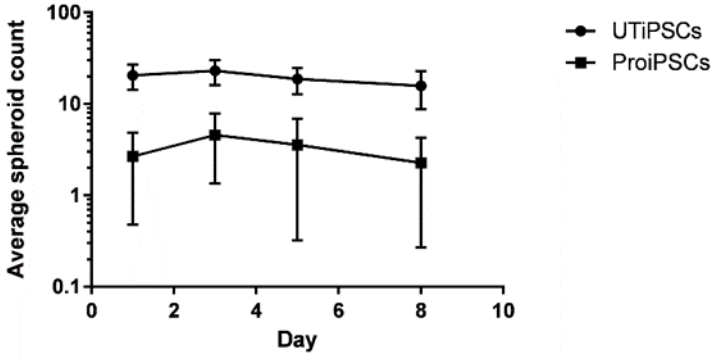

Figure 5-52. Graph showing the average number of spheroids per well for UTiPSCs and ProiPSCs. UTiPSCs formed significantly more spheroids ($p<0.0001$). Error bars represent standard deviation (SD), n=10.

Wells were harvested at 6 and 8 weeks of culture and cells extracted for RNA sequencing or whole wells fixed, embedded in paraffin and sectioned for histological analysis. H&E staining was performed to investigate the overall morphology of the 3D structures and identify differences between the two iPSC lines. The large spheroids identified in the UTiPSC wells were multi-layered with lumens, whilst the structures generated from ProiPSCs were generally denser, with lack of or very small lumens (Figure 5-53, Figure 5-54).

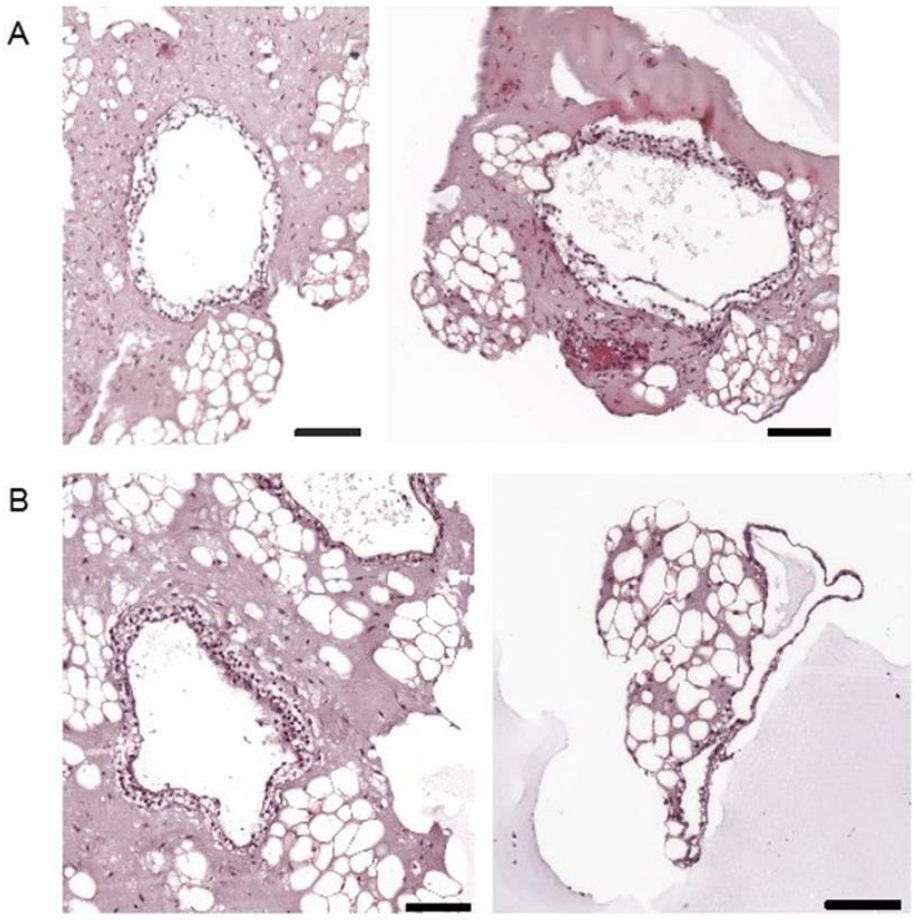

Figure 5-53. H&E staining of structures formed from UTiPSC-derived DE cells co-culture with UGM for 6 weeks (A) and 8 weeks (B). The structures generally have large lumens surrounded by multi-layered cells. Scale bar 100μm.

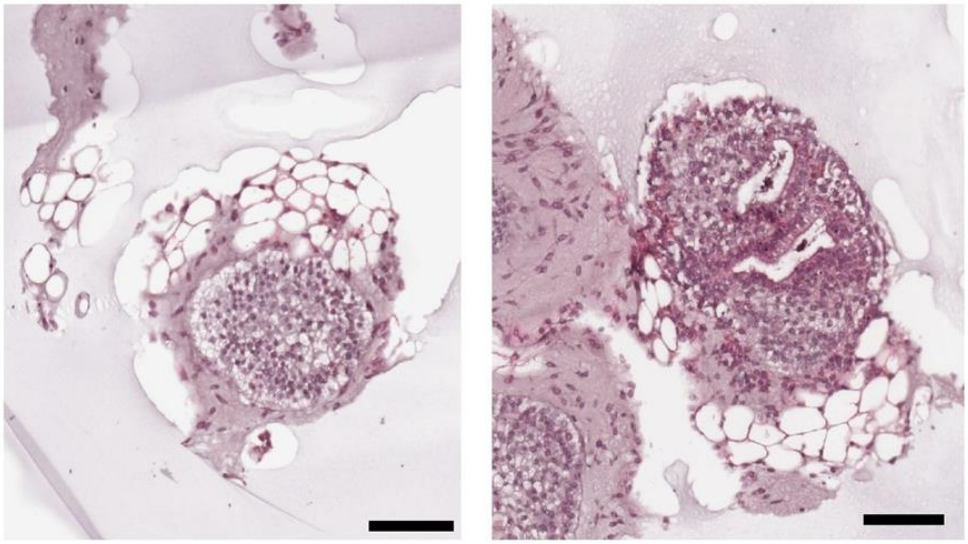

Figure 5-54. H&E staining of structures formed from ProiPSC-derived DE cells co-cultured with UGM for 8 weeks. In contrast to the UTiPSC derived structures, ProiPSC structures had no or very small lumens. Scale bar 100μm.

IHC was performed to determine the nature of the structures. Staining for the human specific mitochondrial marker was first performed to confirm the origin of the spheroids. All spheroids showed staining for human specific mitochondria, confirming their origin from the iPSCs rather than the rat UGM cells (Figure 5-55). Interestingly, the dense “budding” structures which were seen within the culture and were associated with the formation of spheroids were negative for human mitochondria (Figure 5-56). This confirmed our hypothesis that these were in fact UGM cells surrounding the developing iPSC-derived structures.

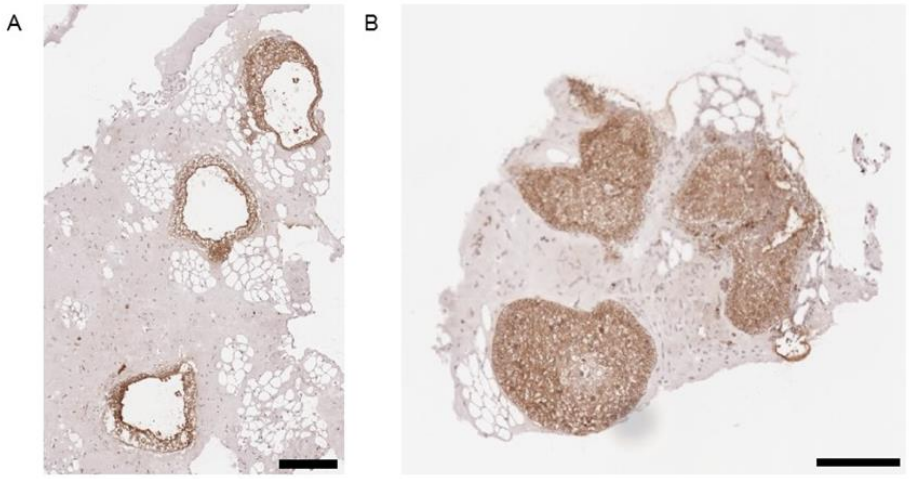

Figure 5-55. IHC for human specific mitochondrial marker to determine the origin of the spheroids. Brown staining confirms expression of human mitochondria and thus the human origin of the cells. A) UTiPSC derived spheroids, B) ProiPSC derived spheroids. Scale bar 200μm.

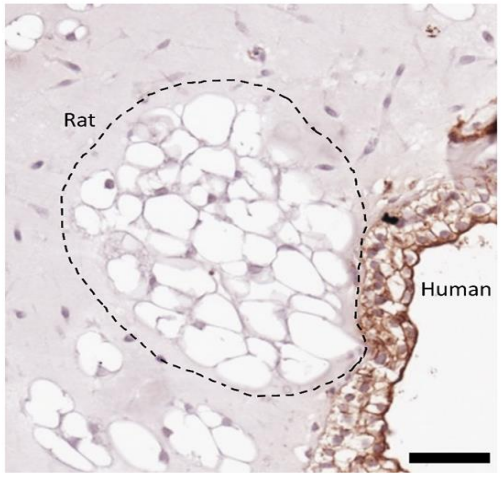

Figure 5-56. High magnification image of IHC staining for anti-human mitochondria. The cells stained brown are human in origin, whilst the blue-purple cells are not. As suspected, the cells and dense spheres clustering around the human spheroids appear to be UGM. Scale bar 50μm.

Expression of the luminal marker CK8/18 and basal markers 34βe12 and p63 was then investigated by IF to determine if the structures were epithelial. In UTiPSC-derived structures at week 6, 34βe12 was expressed in the basal and middle layers of the organoid but not the luminal side (Figure 5-57). p63 expression was restricted to the true basal layer, suggesting that the middle layers of the structure may be an intermediate cell population. 34βe12 recognises CK 1, 5, 10 and 14, which are present in normal squamous epithelium (Sturm *et al.*, 2003). Interestingly, squamous epithelium is known to be found in foetal and infant prostates (Goldman, 1940), and is thought to be a result of exposure to oestrogens during development (Sugimura *et al.*, 1988). This suggests that the middle cell layer in the organoids may represent squamous epithelial cells which are a normal developmental phenomenon. CK8/18 expression in contrast was restricted to the luminal layer only. The combination of expression of these markers confirms that the structures generated are epithelial organoids which show correct polarisation with formation of both basal and luminal cell layers, as well as a potential intermediate population of cells.

To determine prostate specific differentiation, AR and PSA expression were also investigated using IF. At week 6, nuclear AR and cytoplasmic PSA expression was present but very weak suggesting that these UTiPSC-derived organoids are at an early stage of prostatic differentiation (Figure 5-57). By week 8, clear cytoplasmic PSA expression with a classical speckled appearance was evident in the luminal cell layer of the organoids confirming functional prostatic differentiation (Figure 5-59). Week 8 organoids continued to express high CK8/18 on the cell surface of the luminal cell layer (Figure 5-58) as well as nuclear p63 in the basal cell layer (Figure 5-59).

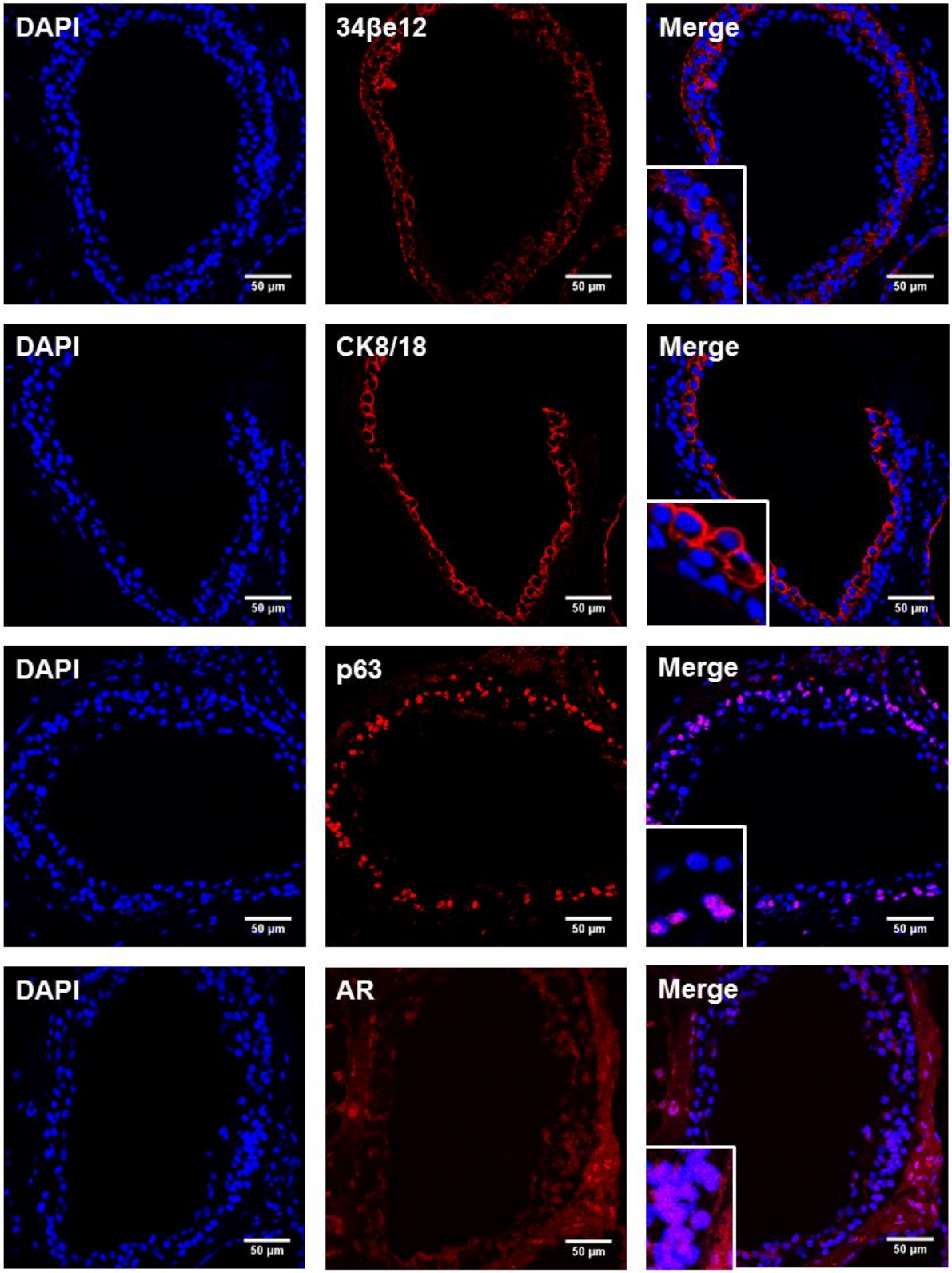

Figure 5-57. IF showing presence of 34βe12, CK8/18, p63 and AR expression in UT-DE derived organoids after 6 weeks of co-culture with rat UGM. Nuclei are stained with DAPI (blue). Scale bars 50µm.

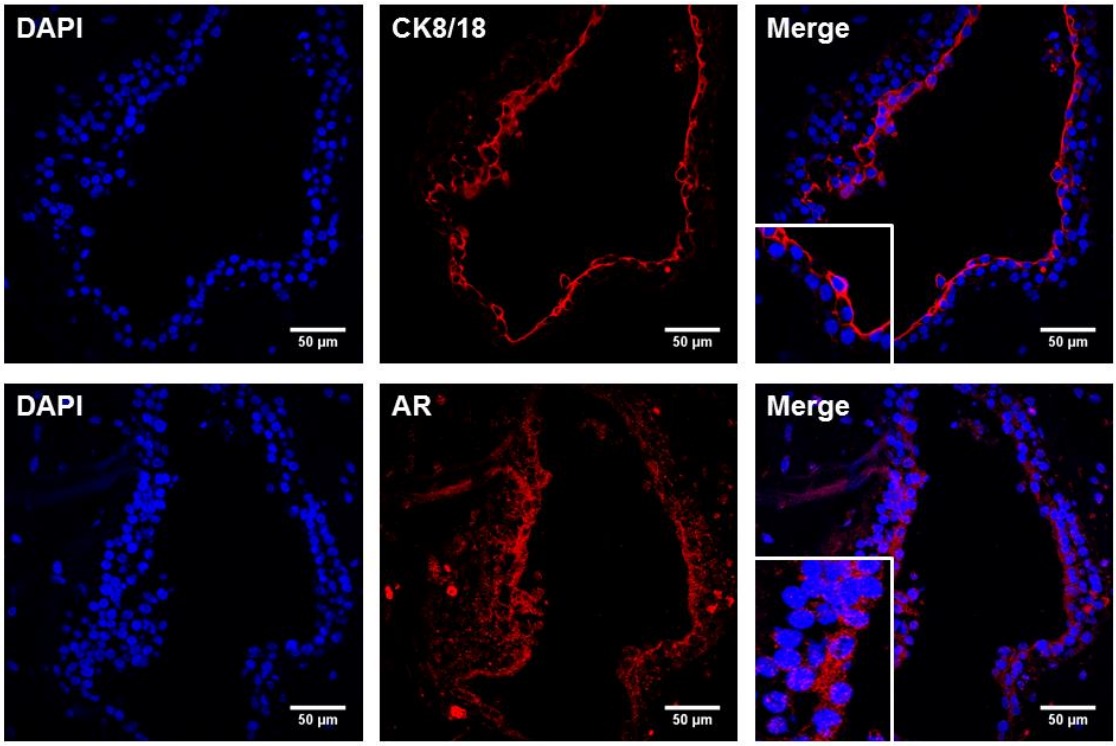

Figure 5-58. IF for the luminal cell marker Ck8/18 and AR in UTiPSC-derived organoids after 8 weeks of culture. CK8/18 is expressed on the surface of the luminal cells. AR is expressed in both the nuclei and cytoplasm. Nuclei are stained with DAPI (blue).

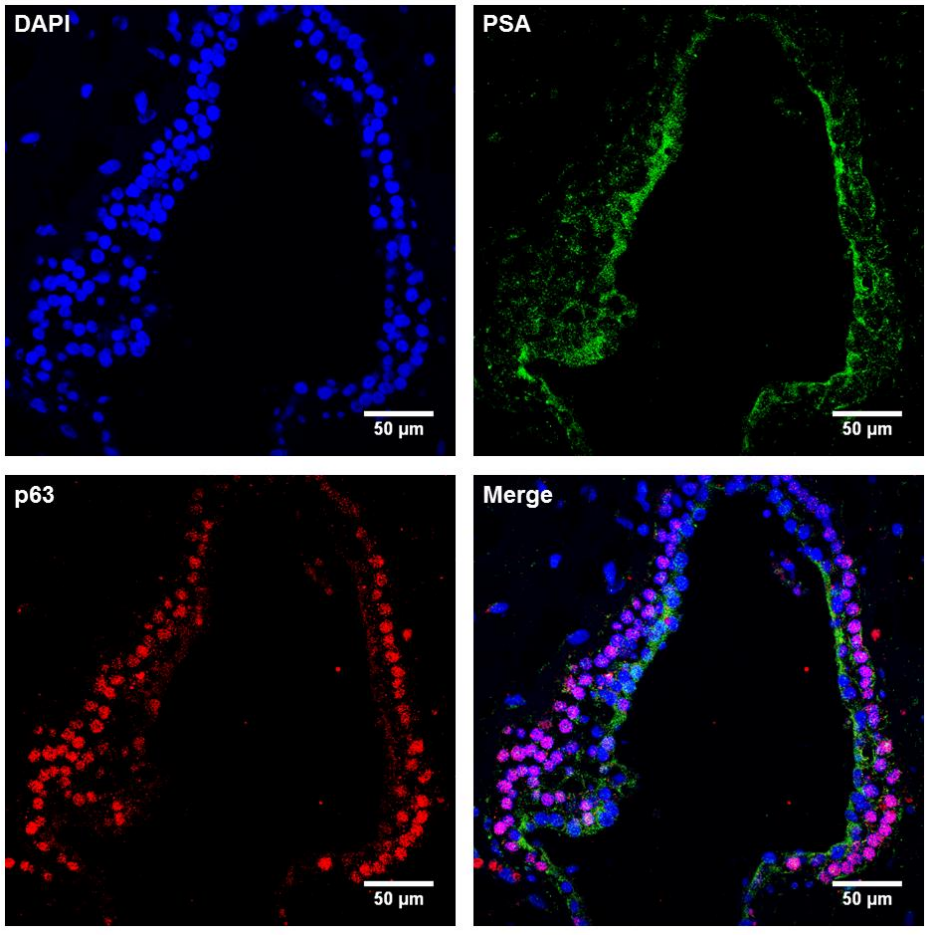

Figure 5-59. Dual IF for PSA (green) and p63 (red) showing luminal cytoplasmic and basal nuclear expression respectively. Nuclei are stained with DAPI (blue).

ProiPSC-derived structures, in agreement with their morphology based on H&E staining, were mostly 34βe12 positive at week 6 with CK8/18 expression restricted to the small luminal-like areas identified (Figure 5-60). No p63 expression was identified at this time-point. In contrast with UTiPSC-derived structures, nuclear AR was expressed earlier and at a higher level in the Pro-iPSCs derived cells, suggesting these cells are able to express prostate specific markers at an earlier stage of differentiation. This may be a result of an epigenetic memory from the parental cells which the iPSCs were derived from. This is a documented phenomenon in iPSCs and can affect the differentiation capacity of the cells (Kim *et al.*, 2010a). By week 8, the iPSC-derived organoids also expressed PSA in the luminal cell layer which was restricted to the very luminal edge of the cells (Figure 5-61), again confirming prostatic differentiation and the functional ability of the organoid.

Samples were also collected from iPSCs, DE cells and differentiated cells at weeks 6, 8 and 12 to harvest cells for RNA sequencing. Although the results from this are outside of the scope of this thesis due to time constraints, they will provide key information on gene expression patterns in developing human prostate organoids. In summary, we have demonstrated for the first time the ability of rat UGM to direct the differentiation of iPSCs to prostate organoids *in vitro* using a 3D co-culture approach combined with organoid specific medium. The organoids show basal and luminal differentiation by the correct localisation of CK8/18, p63 and 34βe12. In addition, the organoids express AR and PSA, confirming functional prostatic differentiation. The difference in marker expression between week 6 and 8 of culture shows that the cells progress and differentiate further with time.

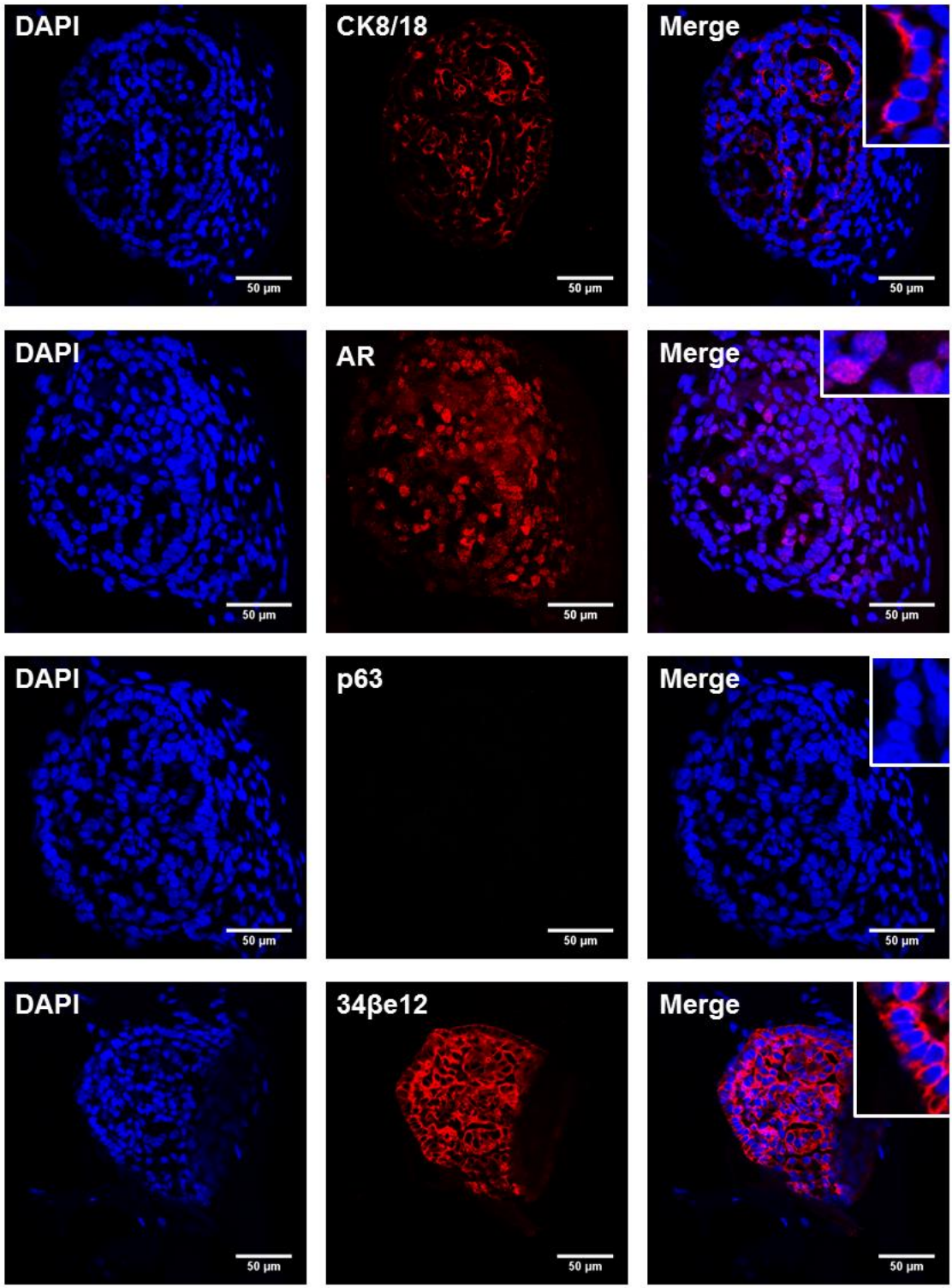

Figure 5-60. IF of ProiPSC-derived organoids after 6 weeks of co-culture with UGM. The organoids express the luminal cell marker CK8/18 in a subset of cells surrounding small lumen-like areas. Nuclear AR expression is also evident in the majority of cells. No p63 expression is seen but all cells are 34βe12 positive.

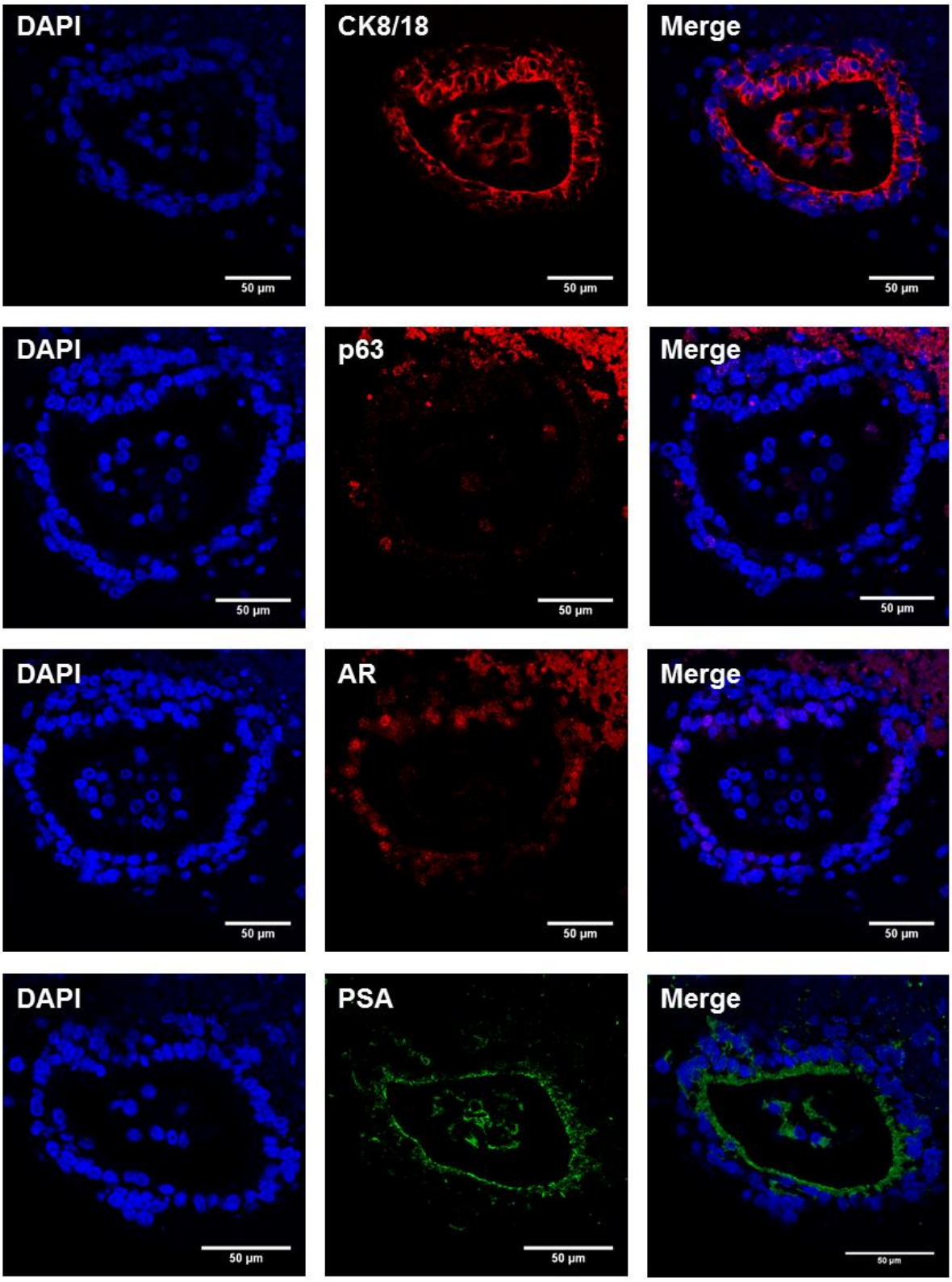

Figure 5-61. IF on ProiPSC-derived organoids after 8 weeks of co-culture with UGM. CK8/18 expression is restricted to the luminal layer of cells in the organoid whilst p63 is expressed only in the basal layer. Nuclear AR expression and cytoplasmic PSA in the luminal layer confirm prostatic differentiation.

5.4 Discussion

iPSCs offer huge opportunities for use in modelling human development and disease as well as drug testing. Generation of organoids from iPSCs provides a more physiologically relevant in vitro model which consists of all cell types present within the organ of interest, can be maintained over a long period and does not require the use of large amounts of primary tissue (Fatehullah *et al.*, 2016). However, to fulfil this, directed differentiation of the iPSCs to the cell types of interest is required. In this chapter, attempts have been made to differentiate patient derived ProiPSCs and UTiPSCs to prostate epithelial organoids using two approaches. The first approach, using a cocktail of growth factors to attempt to specify prostatic fate followed by organoid culture in prostate medium did not yield pure prostate organoids from either UTiPSCs or ProiPSCs, although this method has previously been used to generate prostate organoids from hESCs (Calderon-Gierszal and Prins, 2015). Using this method, iPSCs formed EB-like spheroids which consisted of cells from the 3 embryonic germ layers, rather than prostatic organoids as shown in the published paper. Furthermore, we also saw formation of spheroids from control cells which did not undergo prostate specification. When cultured in prostate medium in 3D cultures, these spheroids were identical to those which had undergone prostate specification with WNT10B and FGF10, suggesting that, at least in our hands, the combination of these factors does not specify a prostatic fate. Although some areas of AR expression were identified, non-specific differentiation, particularly of neuronal cells, limits this method of differentiation.

An alternative method for differentiation of iPSCs is the use of co-culture with other cell types. During prostate development, the UGM directs the formation and differentiation of prostate epithelium by release of a range of paracrine signals which are not fully known. In tissue recombination experiments, UGM can drive hESCs to form prostatic tissue in vivo, and in chapter 4 of this thesis we show ProiPSCs are also able to form prostate glands using this model. We hypothesised that under the correct culture conditions, UGM cells may also be able to direct differentiation of iPSCs to prostate. We used a 3D co-culture method to grow ProiPSCs and UGM cells in serum-free media permissive for UGM growth. Following growth of the cells and formation of organoids, medium was then changed to prostate organoid medium to support their growth and maintenance.

Using this method, we have generated epithelial organoids which show correct spatial organisation with basal and luminal cell layers. In addition, these organoids express nuclear AR and show functional ability by expression of PSA. This provides a novel in vitro model of human prostate development in 3D culture using patient derived iPSCs, a theoretically unlimited cell source which is not associated with the same ethical issues as hESCs. Although the time constraints of this PhD did not allow further investigation of the pathways underlying this differentiation model, RNA sequencing using the samples collected from each stage of differentiation will provide information on the differences in gene expression and will allow interrogation of pathways activated during human prostate development.

Chapter 6. Discussion and conclusions

Prostate diseases are highly prevalent, resulting in both morbidity and mortality. Despite the development of a range of therapies, diseases such as prostate cancer and BPH remain problematic. One potential reason for this is the lack of a normal human prostate model. Unlike many other organs, a relevant model for the normal development of the human prostate does not currently exist. Whilst the importance of the UGM in driving prostate epithelial cell differentiation is well established, only some of the many factors involved in this complex developmental process have been identified. In addition, much of the research in this area has been carried out in mice. Whilst these experiments have contributed greatly to our understanding of specific factors important in prostate development, they do not translate fully to the human setting due to fundamental differences in prostate size, architecture and disease susceptibility. Therefore, the generation of a model which can be used to research both prostate development and disease is critical to further our understanding in this area.

6.1 iPSC generation from primary human prostate fibroblasts

One attractive method to generate developmental and disease models is the use of stem cells. Due to their capacity for both self-renewal and differentiation, stem cells represent a virtually infinite supply of cells for use in research. Although several putative markers have been identified for prostate stem cells, a complete marker profile has not been described, therefore isolation of true prostate stem cells remains challenging (Takao and Tsujimura, 2008).

Pluripotent stem cells such as ESCs and iPSCs represent an alternative to adult stem cells. In the current literature, hESCs have been used to generate prostate epithelial cells and tissue both *in vitro* and *in vivo*. Whilst these methods have shown that stem cells are able to successfully differentiate along a prostatic lineage, they are limited in their use as a widespread model due to the ethical issues associated with hESCs and subsequent stringent legislation surrounding their use. iPSCs represent a source of unlimited cells which possess the defining properties of hESCs including self-renewal and the ability to generate multiple cell types. As iPSCs can be generated from somatic cells, they also circumvent the requirement for embryos and therefore are not limited by ethical concerns. In recent years, the process of iPSC generation and culture has been greatly improved. The development of non-

integrative reprogramming methods including RNA, protein and Sendai virus methods have allowed iPSCs to be generated without concerns of viral integration and disruption of the host cell genome. iPSC culture has also developed from initial feeder-dependent culture to more defined environments using ECMs and development of xeno-free media.

In this project, fibroblasts isolated from human prostate specimens were successfully reprogrammed to generate integration-free iPSCs. The resulting cells were karyotypically normal and possessed typical hESC properties including rapid proliferation and expression of pluripotency markers. Their identity as iPSCs was confirmed by their ability to generate cells from the three embryonic germ layers by EB formation *in vitro* and teratoma formation *in vivo*. The iPSCs were generated at a higher efficiency than found with previous lentiviral-based approaches used in our lab, and are stable in culture after multiple passage and freeze-thawing. These cells therefore can be used as a renewable cell source for further research. Using this reprogramming method in prostate fibroblasts from a range of different patients would allow generation of a bank of ProiPSCs which should encompass the heterogeneity of prostate tissue.

6.2 Generating iPSCs from primary human prostate epithelial cells

As epigenetic memory can affect the differentiation capacity of iPSCs, we hypothesised that iPSCs derived from prostate epithelium may be more easily driven to prostatic epithelial differentiation in comparison to prostate fibroblast derived iPSCs. Therefore, we used the same Sendai vectors in an attempt to reprogram patient prostate epithelial cells. To support the epithelial cells, which are very sensitive to passaging, the Cytotune 2.0 vectors were added directly to the flask of cells and feeder dependent iPSC culture with MEFs was used. However, despite these modifications, significant cell death occurred and no colonies were formed. Cell death during reprogramming can occur by several mechanisms including apoptosis, which is well documented during the reprogramming process, with upregulation of the apoptotic proteases caspase 3 and 8 following transduction of reprogramming factors (Li *et al.*, 2010a). However, cell death may also have occurred due to autophagy, which is induced by Sox2 mediated downregulation of mTOR (Wang *et al.*, 2013), or interferon response to viral infection which can result in sensitisation of cultured cells to apoptosis (Barber, 2001).

To prevent the high levels of cell death, the MOI was reduced and different methods were employed including plating the cells on collagen prior to reprogramming, transferring the cells at different time points following viral infection, and use of both feeder-dependent and feeder-free culture. Unfortunately, despite initial increases in proliferation and colony formation, no iPSC colonies were identified in any of the conditions used. The presence of colonies early in the reprogramming process which failed to grow suggests that the cells became stalled. This is consistent with the literature which shows that in fibroblasts infected with the OSKM transgenes, approximately 20% of cells show early reprogramming with expression of Tra-1-60, however only ~1% of these partially reprogrammed cells progress to complete reprogramming (Tanabe *et al.*, 2013).

This common phenomenon of stalling at the maturation phase of reprogramming is the limiting step in iPSC generation (Tanabe *et al.*, 2013) and as such has prompted research into improving this process. Nanog has been identified as a critical factor in the maturation phase of reprogramming. Whilst *Nanog*$^{-/-}$ cells can undergo early reprogramming, they are unable to reach a completely reprogrammed state (Wei *et al.*, 2015). Furthermore, inhibition of MAP kinase (MEK) and glycogen synthase kinase (GSK3) with the addition of leukaemia inhibitory factor (LIF) to the reprogramming process has been shown to activate Nanog and promote complete reprogramming of the cells (Theunissen *et al.*, 2011). Methylation has also been implicated in reprogramming, with DNA hypermethylation identified in pluripotency genes in partially reprogrammed cells. Inhibition of DNA methyltransferase with 5-aza-cytidine induced cells to become fully reprogrammed, and this finding was replicated using small interfering RNAs or lentiviral short hairpin RNAs (shRNAs) against DNA (cytosine-5)-methyltransferase 1 (*Dnmt1*) (Mikkelsen *et al.*, 2008). Inclusion of histone deacetylase (HDAC) inhibitors has also been shown to enhance reprogramming, with valproic acid in particular resulting in a 100-fold increase in reprogramming efficiency and allowing efficient generation of iPSCs using only 3 factors (Oct4, Sox2, and Klf4) (Huangfu *et al.*, 2008). Critically, knockdown of HDAC2 with shRNA also improves the reprogramming efficiency by specifically promoting the maturation phase with enhanced expression of genes including *Nanog, Sall4, Esrrb, Rex, Tcl1* and *Cripto* (Wei *et al.*, 2015). These methods may be useful in generating iPSCs from prostate epithelial cells by overcoming the block to maturation which appeared to occur during our attempts at reprogramming.

We also hypothesised that Sendai virus vectors may be less efficient at infecting prostate epithelial cells. Investigation of this using a control GFP Sendai virus confirmed that the efficiency of viral infection was significantly lower in prostate epithelial cells in comparison to prostate fibroblasts. As generation of iPSCs requires infection of the target cell with 3 separate vectors (KOS, Klf4 and c-Myc), this low efficiency is very problematic. Interestingly, human nasal epithelial cells have been successfully reprogrammed with Sendai virus vectors with a reprogramming efficiency of 0.07% for MOI 3 and 0.1% with MOI 4 (Ono *et al.*, 2012). When a GFP control vector was used, high GFP expression was seen in nasal epithelial cells, which contrasts with very low expression in the prostate epithelial cells used in this project. As Sendai virus binds to cells through α2,3-linked sialic acids (Markwell and Paulson, 1980; Markwell *et al.*, 1981; Suzuki *et al.*, 1985), which are known to be expressed in the human airway (Kumlin *et al.*, 2008), the ability for Sendai virus vectors to infect nasal epithelial cells with a much higher efficiency than for prostate epithelial cells may be explained at least in part by expression of α2,3-linked sialic acids in these cell types.

In general, we found that prostate epithelial cells were more difficult to culture than prostate fibroblasts, and did not respond well to passaging. During iPSC generation with Sendai virus vectors, the cells must be passaged and transferred to an ESC environment before formation of iPSC colonies. Therefore, our methods of prostate epithelial cell culture and passaging require further refinement to allow a more stable starting population of cells for reprogramming. Due to the inefficiency of Sendai virus entry into the prostate epithelial cells, other reprogramming methods should be trialled. This may allow generation of iPSCs from human prostate epithelial cells in the future which could then be compared to prostate fibroblast-derived iPSCs to determine if the cellular and germ layer origin of the iPSCs impacts their ability to differentiate.

For example, oriP/EBNA-1 episomal vectors have been used to generate iPSCs from urine-derived renal epithelial cells with a high efficiency of 1.5%. Using this method, efficiency of iPSC generation was 10 to 100-fold higher in epithelial cells versus fibroblasts. Addition of a microRNA302/367 cassette whose expression has been previously shown to facilitate iPSC generation resulted in a fourfold increased efficiency for iPSC generation from urinary epithelial cells. This enhanced reprogramming was attributed to the fact that the epithelial cells do not undergo MET

and therefore the reprogramming process is accelerated in these cells. However, subsequent characterisation of the urinary renal epithelial cells showed that they possessed endogenous Tra-1-60 and Tra-1-81 expression which is a hallmark of undifferentiated pluripotent stem cells. Although these methods may improve the reprogramming of prostate epithelial cells, it is possible that their success in reprogramming urine derived cells was due to the high endogenous pluripotency factor expression, which correlated with enhanced reprogramming efficiency in these cells (Drozd *et al.*, 2015).

6.3 Generation of prostatic tissue *in vivo* using tissue recombination with rat UGM

This project also demonstrated for the first time the successful generation of prostate tissue from iPSCs, using a tissue recombination approach with inductive rat UGM to drive prostatic differentiation. Previously, this method has been used to generate prostatic tissue from both adult stem cells and hESCs. In human prostate cells from patient samples, $Cd49^{hi}$ $Trop2^{hi}$ basal cells can generate prostatic tissue when engrafted along with rat UGM under the renal capsule of host mice. This tissue contains basal, luminal and NE cells, although the NE cells were positive for synaptophysin but not chromogranin A, suggesting incomplete NE differentiation (Goldstein *et al.*, 2008). Using hESCs, this method can generate the full breadth of prostatic differentiation (Taylor *et al.*, 2006; Cai *et al.*, 2013). As this approach had not been previously used with iPSCs, several ratios of iPSCs to UGM were trialled. From the initial analysis of grafts, a ratio of 1:125 appeared to give the most epithelial tissue formation with minimal non-specific differentiation. However, this observation was based upon only 1 sample per ratio and therefore analysis of the repeats is necessary to confirm the finding. Following such analysis, the ratio could be optimised further to reduce or possibly abrogate non-specific differentiation.

The prostatic tissue formed from iPSCs using this method contained both basal and luminal epithelial cells and showed expression of the prostatic markers AR and PSA confirming functional prostatic differentiation. Rare cells expressing the NE marker chromogranin A were also identified, although further staining for synaptophysin as well as confirmation that these cells lack AR and PSA expression will be required to confirm their identity as NE cells. To complete the analysis, dual IF should be performed to confirm the same cells express both AR and PSA, and to confirm with increased clarity the division into basal and luminal cell layers as well as the

differences in marker expression between the two cell populations. Investigation into cell polarisation, through expression of integrins such as α2β1 and cell adhesion molecules such as E-cadherin will also be important to confirm that the cells are both fully differentiated and correctly polarised. Furthermore, analysis of markers expressed by the stromal tissue surrounding the epithelial glands should be undertaken to determine if these associated cells express normal prostatic stromal markers such as αSMA.

The ability of iPSCs generated from human prostate fibroblasts to generate prostatic epithelial glands *in vivo* using this method circumvents the need for hESCs and their associated ethical issues and limited tissue availability. This model could be used in the future to study human prostate development at different stages throughout growth of the grafts to determine differential gene expression and identify key pathways which regulate human prostatic differentiation. This method could also be used to generate normal prostatic tissue for research by using a bank of patient-derived iPSCs rather than requiring large volumes of primary patient tissue.

6.4 Growth factor based differentiation of iPSCs to prostate organoids *in vitro*

Ideally, an *in vitro* method for prostate differentiation would be most useful. Animal experiments are strictly regulated and require significant hands-on time and specialist skills for surgical engraftment of cells. Furthermore, laboratory animals are expensive and experiments are limited in number by the practicality of caring for these animals. In addition, real-time monitoring and manipulation of cells grown *in vivo* is extremely difficult. To date, there is very limited literature on the differentiation of stem cells to prostate *in vitro*. The sole publication showing generation of prostatic cells from hESCs *in vitro* used a growth factor based differentiation method. This method is based largely upon a protocol for iPSC-derived intestinal organoids which used FGF4 and WNT3A to pattern posterior endoderm and hindgut differentiation (Spence *et al.*, 2011). To specify prostate differentiation, FGF10 and WNT10B were used, based on the importance of FGF and WNT signalling in prostate development. FGF10 is a UGM-secreted factor (Thomson and Cunha, 1999), whilst WNT10B is secreted by the UGE prior to bud formation (Keil *et al.*, 2012).

In our hands, ProiPSCs and UTiPSCs which had been differentiated to endoderm went on to form 3D structures in both WNT10B and FGF10 treated and control wells which were cultured in the basal medium without addition of any growth factors.

Interestingly, in the original publication, substitution of WNT10B for WNT3A also resulted in formation of spheroids but these were small and did not grow (Calderon-Gierszal and Prins, 2015). In addition, culture of both control and treated 3D structures in the prostate medium used by Calderon-Gierzsal and Prins resulted in formation of EB-like structures with areas of weak AR positivity. This suggests that, at least in our hands, this method can generate areas of early prostatic differentiation but this is accompanied by significant non-specific differentiation. As AR expression has not been identified in our pluripotency tests by embryoid bodies or teratoma formation, this protocol seems to provide some specific cues but is not sufficient to drive purely prostatic differentiation from ProiPSCs or UTiPSCs in our hands. Interestingly, AR has also been identified in other tissues including the brain, which shows strong AR expression (Dart *et al.*, 2013). Therefore it is possible that the AR positive cells identified in our differentiated cells could be AR expressing neuronal cells.

The difference in results obtained using this method with our iPSCs in comparison with the hESCs used by Calderon-Gierszal and Prins could be a result of differences in the iPSC clones which were used in our experiment. Both genetic and functional heterogeneity have been observed in iPSC clones from the same cell type from the same patient. Genetic heterogeneity between clones from the same patient and even the same clone at different passages are a known phenomenon in iPSCs (Winkler *et al.*, 2013). Functional differences between iPSC clones have also been well documented in the literature. Using 24 iPSC clones derived from skin fibroblasts of a single mouse, differences in differentiation potential could be identified. Of the 24 clones, 1 clone was completely unable to generate haematopoietic progenitor cells, despite passing tests to confirm an iPSC identity including teratoma formation (Li *et al.*, 2015). Differences in osteogenic and chrondrogenic differentiation between iPSC clones from the same cell source have also been reported, providing further evidence for clonal variation (Nasu *et al.*, 2013).

In our hands, significant neuronal differentiation occurred in both UTiPSCs and ProiPSCs differentiated using this method. During development, the neural tube is one of the earliest tissues to form (Schwartz *et al.*, 2008). A “default” neuronal differentiation program is known to occur in ESCs and iPSCs, with the presence of doublecortin-positive cells identified at the periphery of PSC colonies as well as within the surrounding MEFs, consistent with neuronal differentiation as doublecortin

is a neuronal marker associated with migrating neuroblasts (Schwartz *et al.*, 2008). The default model is based upon the idea that neural induction is a result of BMP inhibition in the embryonic ectoderm, and that the ectodermal cells will differentiate into neural tissue in the absence of any specific signalling (Munoz-Sanjuan and Brivanlou, 2002). Evidence for this default model has been collected using ESCs. mESCs which were cultured without feeders, serum, growth factors or cell-cell contact showed predominantly neuronal differentiation, with 82% of viable cells expressing the neuroepithelial marker Nestin (Tropepe *et al.*, 2001). Similarly, culture of hESCs in a defined system free from known neurogenic inducers resulted in an almost uniform culture of neuroepithelial cells which displayed a neuronal rosette morphology and expressed the early neural marker Pax6 (LaVaute *et al.*, 2009). The results of our growth factor based experiments indicate that in our iPSCs, a neural fate does predominate, even in the presence of external signals which have induced a prostatic fate in hESCs. We hypothesise that the growth factors used in this protocol are not enough to drive a purely prostatic differentiation, and therefore neuronal differentiation persists in our cells.

6.5 A novel 3D co-culture method for generation of prostate organoids from iPSCs *in vitro*

In recent years, prostate organoids have been generated using patient derived prostatic tissue. Whilst Chua et al., generated prostate organoids consisting of an outer layer of intermediate cells and an inner luminal layer, Karthaus et al., were able to generate organoids with a more mature phenotype where cells in each layer expressed either basal or luminal markers alone (Chua *et al.*, 2014; Karthaus *et al.*, 2014). Whilst these methods allow for generation of prostatic organoids from human cells, they require the use of cells from primary culture, which can be difficult. Furthermore, these organoids do not contain NE cells and therefore do not fully represent the organisation of the prostate gland *in vivo* (Karthaus *et al.*, 2014). Finally, although these patient derived organoids may be used for modelling disease and therapeutic testing, they cannot be used to study the development of the human prostate as they are formed from bi-potent cells which already possess a prostatic identity.

In chapter 4 of this thesis, the ability of rat UGM to direct the differentiation of ProiPSCs to prostatic tissue *in vivo* was shown. By this method, ProiPSCs could form glandular epithelium which expressed the prostate markers AR and PSA, and

showed correct basal and luminal differentiation by expression of p63 and CK8/18. By IHC, the expression of these markers was comparable to benign adult prostate tissue, confirming full prostatic differentiation. This provides a model of normal prostate development and circumvents the requirement for hESCs, whose use is limited due to ethical concerns and stringent regulations. However, this method still has limitations including the need for host animals, the length of the experiment and the lack of information gained during the formation of the tissue. Ideally, an *in vitro* model of prostate development is required to allow gain of real-time information and easy visual monitoring of differentiation. Using a previously published protocol for generation of prostatic organoids from hESCs (Calderon-Gierszal and Prins, 2015), we were unable to form purely prostatic cells from UT and ProiPSCs, suggesting that the growth factors used in this method were not enough to drive pure prostatic differentiation from our iPSCs. As the UGM drives prostatic differentiation during normal development, and we have shown the ability of the UGM to generate prostatic tissue from ProiPSCs *in vivo*, we hypothesised that harnessing the inductive ability of UGM may allow us to differentiate iPSCs to prostatic organoids *in vitro*.

Using Pro- and UTiPSCs with rat UGM in a 3D co-culture system, we generated epithelial organoids which have a p63 positive basal layer and CK8/18 positive luminal layer surrounding a clear lumen. The organoids express AR and PSA confirming terminal prostatic differentiation. This shows that iPSCs derived from urological tissues can form organoids *in vitro* which recapitulate the structure and expression markers which are typical of normal human prostate. As both Pro- and UT-derived iPSCs were capable of forming prostatic organoids, this suggests that the differentiation of these cells was truly induced by the method of 3D co-culture with inductive mesenchyme, rather than a consequence of residual epigenetic memory within the iPSCs. Furthermore, the iPSCs were used for differentiation at late passage, at which point epigenetic memory is unlikely to persist. To complete the analysis of the organoids, and to determine if NE cells are also formed during this process, investigation of chromogranin A and other NE markers is required. Quantification of AR and PSA expressing cells would confirm the purity of the cell population formed using this method. Investigation of cell polarisation by looking at expression of integrins and cadherins will also be important. In the organoids harvested at week 6, where expression of PSA is weak, analysis of PAP would also be useful to see if alternative prostatic proteins are produced at this early stage of

differentiation. Finally, Ki67 staining or use of a BrdU assay would be useful to investigate proliferation of the organoids.

Interestingly, the differences seen between the UTiPSC and ProiPSC derived organoids are reminiscent of differences between organoids formed from prostate basal and luminal cells. Karthaus et al., demonstrated that whilst luminal cell-derived organoids possessed large lumens, similar to our UTiPSC derived organoids, basal cell-derived organoids consisted of multiple lumens within each organoid which were surrounded by CK8 positive cells (Karthaus *et al.*, 2014). This phenomenon of multiple lumens surrounded by CK8 positive cells was also seen in ProiPSC derived organoids after 6 weeks of culture, although by 8 weeks more “luminal-like” structures with a single larger lumen were identified, suggesting that cells may progress from an initially basal-like organoid to a more luminal-like organoid over time.

During differentiation of iPSCs using this model, samples were collected at a range of time points for RNA sequencing. Although at this time, samples of whole organoids were taken, the cells could have been sorted into their individual compartments to allow analysis of each cell type. By comparing samples from iPSCs, DE cells and the prostate organoids at different stages of differentiation, we hope to generate an expression signature associated with each stage of prostate development. Currently, such signatures have only been determined for mouse prostate organogenesis. By analysing gene expression in samples taken from a range of stages throughout murine prostate development, three phases of development were identified; prostate induction, branching morphogenesis and secretory differentiation, as well as several genes which had not previously been implicated in prostate development (Pritchard *et al.*, 2009). Human specific prostate development is yet to be interrogated in this manner, primarily due to lack of a human model system. The culture technique developed in chapter 5 of this thesis provides a novel *in vitro* model of normal human prostate development which can be used to study prostate differentiation and the factors which play a role in this process. Determination of the factors secreted by the UGM in this system which act upon the iPSC derived DE cells to drive prostatic epithelial differentiation might allow a more defined approach in the future. This could be analysed using mass spectrometry of conditioned medium secreted by UGM cells in culture.

Determining the length of culture and the passage number which these organoids can reach will be important to their feasibility as an *in vitro* model, with adult prostate organoids able to grow in culture for over 12 months without phenotypic changes or altered karyotype (Karthaus *et al.*, 2014). Generation of prostate organoids from a bank of patient-derived iPSCs would be useful to encompass the clinical heterogeneity of prostate tissue. Comparison of patient matched urological tissue derived iPSCs with iPSCs generated from more accessible tissue sources such as skin or urine would allow us to determine if the cellular origin of the iPSCs limits their differentiation. If cells from skin or urine-derived epithelial cells are also able to form prostatic organoids using our 3D co-culture system, this would enhance the ease of generating patient specific models using less invasive methods of tissue collection.

6.6 Conclusions and future directions

In summary, iPSCs represent a promising source of cells for research into human development and disease. We have shown successful generation of iPSCs from primary prostate fibroblasts using an integration-free method. These cells express typical pluripotent stem cell markers and are able to form cells from the three embryonic germ layers *in vitro* and *in vivo*. Attempts to reprogram primary prostate epithelial cells were significantly more challenging, and disappointingly no iPSC colonies were generated. Optimisation of prostate epithelial cell culture, passaging and the reprogramming method may enhance the viability of these cells following addition of the pluripotency factors.

We have used a tissue recombination approach with inductive rat UGM to drive differentiation from our ProiPSCs *in vivo* resulting in formation of prostatic tissue. This has provided us with a simple method for iPSC differentiation along a prostatic lineage, although further analysis of repeats is required to draw complete conclusions on the optimum ratio for prostate specific differentiation. By harnessing this inductive potential of UGM, we subsequently generated a novel 3D co-culture model which allows formation of prostatic organoids from both ProiPSCs and UTiPSCs *in vitro*. These organoids are phenotypically similar to both normal prostate tissue and human prostatic organoids generated from adult prostate epithelial cells. Further interrogation of these organoids including quantification of AR expressing cells and expression of NE and stromal cell markers will be useful to determine the purity of the cells generated by this method and would also determine if the UGM is able to

drive complete NE differentiation. This would be particularly advantageous as current human prostate organoids described in the literature do not include NE cells.

RNA sequencing from samples collected during this experiment will also provide further information on differential gene expression and the pathways which are involved in prostatic differentiation. This model can be used for interrogation of the breadth of factors secreted by the UGM which drive human prostate development, which to date are not fully understood. This could allow for a refinement of differentiation protocols and the ability to generate prostate organoids from our iPSCs without the requirement for UGM. This model may also be used for identification of stem cells within the developing prostate and the markers which define them, as current research is limited by lack of a definitive marker profile for these cells.

Finally, the ProiPSC model also holds great potential for high-throughput organoid culture to interrogate prostate carcinogenesis. Organoids are amenable to epigenetic manipulation using a range of strategies including lentiviral expression of mutant genes and CRISPR/Cas9 gene editing which would allow introduction of common prostate cancer phenotypes such as deletion of PTENT, RB1, TP53 and TMPRSS2-ERG (Taylor *et al.*, 2010) and subsequent analysis of the impact this has (Dutta *et al.*, 2016). This may be advantageous in addressing some of the limitations of current prostate cancer organoids including low efficiency of organoid establishment and overgrowth of normal epithelial cells or tumour-associated cells (Gao *et al.*, 2014). In addition, investigating the effects of AR inhibitors such as bicalutamide and enzalutamide on the prostate organoids could provide a model of castration on a molecular level.

References

Aasen, T. and Izpisua Belmonte, J.C. (2010) 'Isolation and cultivation of human keratinocytes from skin or plucked hair for the generation of induced pluripotent stem cells', *Nat Protoc*, 5(2), pp. 371-82.

Allgeier, S.H., Lin, T.M., Vezina, C.M., Moore, R.W., Fritz, W.A., Chiu, S.Y., Zhang, C. and Peterson, R.E. (2008) 'WNT5A selectively inhibits mouse ventral prostate development', *Dev Biol*, 324(1), pp. 10-7.

Amit, M., Carpenter, M.K., Inokuma, M.S., Chiu, C.P., Harris, C.P., Waknitz, M.A., Itskovitz-Eldor, J. and Thomson, J.A. (2000) 'Clonally derived human embryonic stem cell lines maintain pluripotency and proliferative potential for prolonged periods of culture', *Dev Biol*, 227(2), pp. 271-8.

Amit, M., Margulets, V., Segev, H., Shariki, K., Laevsky, I., Coleman, R. and Itskovitz-Eldor, J. (2003) 'Human feeder layers for human embryonic stem cells', *Biol Reprod*, 68(6), pp. 2150-6.

Amit, M.I.-E., J. (2012) 'Atlas of human pluripotent stem cells: derivation and culturing.', in *Stem Cell Biology and Regenerative Medicine*. Humana Press.

Ban, H., Nishishita, N., Fusaki, N., Tabata, T., Saeki, K., Shikamura, M., Takada, N., Inoue, M., Hasegawa, M., Kawamata, S. and Nishikawa, S. (2011) 'Efficient generation of transgene-free human induced pluripotent stem cells (iPSCs) by temperature-sensitive Sendai virus vectors', *Proc Natl Acad Sci U S A*, 108(34), pp. 14234-9.

Banerjee, I., Sharma, N. and Yarmush, M. (2011) 'Impact of co-culture on pancreatic differentiation of embryonic stem cells', *J Tissue Eng Regen Med*, 5(4), pp. 313-23.

Barber, G.N. (2001) 'Host defense, viruses and apoptosis', *Cell Death Differ*, 8(2), pp. 113-26.

Bello, D., Webber, M.M., Kleinman, H.K., Wartinger, D.D. and Rhim, J.S. (1997) 'Androgen responsive adult human prostatic epithelial cell lines immortalized by human papillomavirus 18', *Carcinogenesis*, 18(6), pp. 1215-23.

Ben-Porath, I., Thomson, M.W., Carey, V.J., Ge, R., Bell, G.W., Regev, A. and Weinberg, R.A. (2008) 'An embryonic stem cell-like gene expression signature in poorly differentiated aggressive human tumors', *Nat Genet*, 40(5), pp. 499-507.

Berman, D.M., Desai, N., Wang, X., Karhadkar, S.S., Reynon, M., Abate-Shen, C., Beachy, P.A. and Shen, M.M. (2004) 'Roles for Hedgehog signaling in androgen production and prostate ductal morphogenesis', *Dev Biol*, 267(2), pp. 387-98.

Bernal, J.A. (2013) 'RNA-based tools for nuclear reprogramming and lineage-conversion: towards clinical applications', *J Cardiovasc Transl Res*, 6(6), pp. 956-68.

Bernardo, G.M. and Keri, R.A. (2012) 'FOXA1: a transcription factor with parallel functions in development and cancer', *Biosci Rep*, 32(2), pp. 113-30.

Berruti, A., Tucci, M., Mosca, A., Tarabuzzi, R., Gorzegno, G., Terrone, C., Vana, F., Lamanna, G., Tampellini, M., Porpiglia, F., Angeli, A., Scarpa, R.M. and Dogliotti, L. (2005) 'Predictive factors for skeletal complications in hormone-refractory prostate cancer patients with metastatic bone disease', *Br J Cancer*, 93(6), pp. 633-8.

Berthon, P., Cussenot, O., Hopwood, L., Leduc, A. and Maitland, N. (1995) 'Functional expression of sv40 in normal human prostatic epithelial and fibroblastic cells - differentiation pattern of nontumorigenic cell-lines', *Int J Oncol*, 6(2), pp. 333-43.

Bhatia-Gaur, R., Donjacour, A.A., Sciavolino, P.J., Kim, M., Desai, N., Young, P., Norton, C.R., Gridley, T., Cardiff, R.D., Cunha, G.R., Abate-Shen, C. and Shen, M.M. (1999) 'Roles for Nkx3.1 in prostate development and cancer', *Genes Dev*, 13(8), pp. 966-77.

Bhavsar, A. and Verma, S. (2014) 'Anatomic imaging of the prostate', *Biomed Res Int*, 2014, p. 728539.
Boj, S.F., Hwang, C.I., Baker, L.A., Chio, II, Engle, D.D., Corbo, V., Jager, M., Ponz-Sarvise, M., Tiriac, H., Spector, M.S., Gracanin, A., Oni, T., Yu, K.H., van Boxtel, R., Huch, M., Rivera, K.D., Wilson, J.P., Feigin, M.E., Ohlund, D., Handly-Santana, A., Ardito-Abraham, C.M., Ludwig, M., Elyada, E., Alagesan, B., Biffi, G., Yordanov, G.N., Delcuze, B., Creighton, B., Wright, K., Park, Y., Morsink, F.H., Molenaar, I.Q., Borel Rinkes, I.H., Cuppen, E., Hao, Y., Jin, Y., Nijman, I.J., Iacobuzio-Donahue, C., Leach, S.D., Pappin, D.J., Hammell, M., Klimstra, D.S., Basturk, O., Hruban, R.H., Offerhaus, G.J., Vries, R.G., Clevers, H. and Tuveson, D.A. (2015) 'Organoid models of human and mouse ductal pancreatic cancer', *Cell*, 160(1-2), pp. 324-38.
Bonkhoff, H. and Remberger, K. (1996) 'Differentiation pathways and histogenetic aspects of normal and abnormal prostatic growth: a stem cell model', *Prostate*, 28(2), pp. 98-106.
Bonkhoff, H., Stein, U. and Remberger, K. (1994) 'The proliferative function of basal cells in the normal and hyperplastic human prostate', *Prostate*, 24(3), pp. 114-8.
Braam, S.R., Zeinstra, L., Litjens, S., Ward-van Oostwaard, D., van den Brink, S., van Laake, L., Lebrin, F., Kats, P., Hochstenbach, R., Passier, R., Sonnenberg, A. and Mummery, C.L. (2008) 'Recombinant vitronectin is a functionally defined substrate that supports human embryonic stem cell self-renewal via alphavbeta5 integrin', *Stem Cells*, 26(9), pp. 2257-65.
Brambrink, T., Foreman, R., Welstead, G.G., Lengner, C.J., Wernig, M., Suh, H. and Jaenisch, R. (2008) 'Sequential expression of pluripotency markers during direct reprogramming of mouse somatic cells', *Cell Stem Cell*, 2(2), pp. 151-9.
Brinkmann, A.O., Blok, L.J., de Ruiter, P.E., Doesburg, P., Steketee, K., Berrevoets, C.A. and Trapman, J. (1999) 'Mechanisms of androgen receptor activation and function', *J Steroid Biochem Mol Biol*, 69(1-6), pp. 307-13.
Bryant, S.L., Francis, J.C., Lokody, I.B., Wang, H., Risbridger, G.P., Loveland, K.L. and Swain, A. (2014) 'Sex specific retinoic acid signaling is required for the initiation of urogenital sinus bud development', *Dev Biol*, 395(2), pp. 209-17.
Buganim, Y., Faddah, D.A., Cheng, A.W., Itskovich, E., Markoulaki, S., Ganz, K., Klemm, S.L., van Oudenaarden, A. and Jaenisch, R. (2012) 'Single-cell expression analyses during cellular reprogramming reveal an early stochastic and a late hierarchic phase', *Cell*, 150(6), pp. 1209-22.
Buganim, Y., Faddah, D.A. and Jaenisch, R. (2013) 'Mechanisms and models of somatic cell reprogramming', *Nat Rev Genet*, 14(6), pp. 427-39.
Cai, Y., Kregel, S. and Vander Griend, D.J. (2013) 'Formation of human prostate epithelium using tissue recombination of rodent urogenital sinus mesenchyme and human stem cells', *J Vis Exp*, (76).
Calderon-Gierszal, E.L. and Prins, G.S. (2015) 'Directed Differentiation of Human Embryonic Stem Cells into Prostate Organoids In Vitro and its Perturbation by Low-Dose Bisphenol A Exposure', *PLoS One*, 10(7), p. e0133238.
Cancer Research UK. Available at: http://www.cancerresearchuk.org/health-professional/cancer-statistics/statistics-by-cancer-type/prostate-cancer#heading-Five (Accessed: 6.7.17).
Carey, B.W., Markoulaki, S., Hanna, J., Saha, K., Gao, Q., Mitalipova, M. and Jaenisch, R. (2009) 'Reprogramming of murine and human somatic cells using a single polycistronic vector', *Proc Natl Acad Sci U S A*, 106(1), pp. 157-62.
Carlson, B.M. (2009) *Human Embryology and Developmental Biology E-Book*. Philadelphia, PA: Mosby.
Cary, L.C., Goebel, M., Corsaro, B.G., Wang, H.G., Rosen, E. and Fraser, M.J. (1989) 'Transposon mutagenesis of baculoviruses: analysis of Trichoplusia ni

transposon IFP2 insertions within the FP-locus of nuclear polyhedrosis viruses', *Virology*, 172(1), pp. 156-69.
Ceder, J.A., Jansson, L., Helczynski, L. and Abrahamsson, P.A. (2008) 'Delta-like 1 (Dlk-1), a novel marker of prostate basal and candidate epithelial stem cells, is downregulated by notch signalling in intermediate/transit amplifying cells of the human prostate', *Eur Urol*, 54(6), pp. 1344-53.
Celiz, A.D., Smith, J.G., Langer, R., Anderson, D.G., Winkler, D.A., Barrett, D.A., Davies, M.C., Young, L.E., Denning, C. and Alexander, M.R. (2014) 'Materials for stem cell factories of the future', *Nat Mater*, 13(6), pp. 570-9.
Chang, C.W., Lai, Y.S., Pawlik, K.M., Liu, K., Sun, C.W., Li, C., Schoeb, T.R. and Townes, T.M. (2009) 'Polycistronic lentiviral vector for "hit and run" reprogramming of adult skin fibroblasts to induced pluripotent stem cells', *Stem Cells*, 27(5), pp. 1042-9.
Chen, G., Gulbranson, D.R., Hou, Z., Bolin, J.M., Ruotti, V., Probasco, M.D., Smuga-Otto, K., Howden, S.E., Diol, N.R., Propson, N.E., Wagner, R., Lee, G.O., Antosiewicz-Bourget, J., Teng, J.M. and Thomson, J.A. (2011) 'Chemically defined conditions for human iPSC derivation and culture', *Nat Methods*, 8(5), pp. 424-9.
Chen, H., Mutton, L.N., Prins, G.S. and Bieberich, C.J. (2005) 'Distinct regulatory elements mediate the dynamic expression pattern of Nkx3.1', *Dev Dyn*, 234(4), pp. 961-73.
Chen, Y.W., Huang, S.X., de Carvalho, A., Ho, S.H., Islam, M.N., Volpi, S., Notarangelo, L.D., Ciancanelli, M., Casanova, J.L., Bhattacharya, J., Liang, A.F., Palermo, L.M., Porotto, M., Moscona, A. and Snoeck, H.W. (2017) 'A three-dimensional model of human lung development and disease from pluripotent stem cells', *Nat Cell Biol*, 19(5), pp. 542-549.
Cheon, D.J. and Orsulic, S. (2011) 'Mouse models of cancer', *Annu Rev Pathol*, 6, pp. 95-119.
Chin, M.H., Mason, M.J., Xie, W., Volinia, S., Singer, M., Peterson, C., Ambartsumyan, G., Aimiuwu, O., Richter, L., Zhang, J., Khvorostov, I., Ott, V., Grunstein, M., Lavon, N., Benvenisty, N., Croce, C.M., Clark, A.T., Baxter, T., Pyle, A.D., Teitell, M.A., Pelegrini, M., Plath, K. and Lowry, W.E. (2009) 'Induced pluripotent stem cells and embryonic stem cells are distinguished by gene expression signatures', *Cell Stem Cell*, 5(1), pp. 111-23.
Choi, J., Lee, S., Mallard, W., Clement, K., Tagliazucchi, G.M., Lim, H., Choi, I.Y., Ferrari, F., Tsankov, A.M., Pop, R., Lee, G., Rinn, J.L., Meissner, A., Park, P.J. and Hochedlinger, K. (2015) 'A comparison of genetically matched cell lines reveals the equivalence of human iPSCs and ESCs', *Nat Biotechnol*, 33(11), pp. 1173-81.
Chou, B.K., Mali, P., Huang, X., Ye, Z., Dowey, S.N., Resar, L.M., Zou, C., Zhang, Y.A., Tong, J. and Cheng, L. (2011) 'Efficient human iPS cell derivation by a non-integrating plasmid from blood cells with unique epigenetic and gene expression signatures', *Cell Res*, 21(3), pp. 518-29.
Chua, C.W., Shibata, M., Lei, M., Toivanen, R., Barlow, L.J., Bergren, S.K., Badani, K.K., McKiernan, J.M., Benson, M.C., Hibshoosh, H. and Shen, M.M. (2014) 'Single luminal epithelial progenitors can generate prostate organoids in culture', *Nat Cell Biol*, 16(10), pp. 951-61, 1-4.
Collins, A.T., Habib, F.K., Maitland, N.J. and Neal, D.E. (2001) 'Identification and isolation of human prostate epithelial stem cells based on alpha(2)beta(1)-integrin expression', *J Cell Sci*, 114(Pt 21), pp. 3865-72.
Cook, C., Vezina, C.M., Allgeier, S.H., Shaw, A., Yu, M., Peterson, R.E. and Bushman, W. (2007) 'Noggin is required for normal lobe patterning and ductal budding in the mouse prostate', *Dev Biol*, 312(1), pp. 217-30.

Cowan, C.A., Atienza, J., Melton, D.A. and Eggan, K. (2005) 'Nuclear reprogramming of somatic cells after fusion with human embryonic stem cells', *Science*, 309(5739), pp. 1369-73.
Cunha, G.R., Fujii, H., Neubauer, B.L., Shannon, J.M., Sawyer, L. and Reese, B.A. (1983) 'Epithelial-mesenchymal interactions in prostatic development. I. morphological observations of prostatic induction by urogenital sinus mesenchyme in epithelium of the adult rodent urinary bladder', *J Cell Biol*, 96(6), pp. 1662-70.
Cunha, G.R., Hayward, S.W. and Wang, Y.Z. (2002) 'Role of stroma in carcinogenesis of the prostate', *Differentiation*, 70(9-10), pp. 473-85.
Cunha, G.R. and Lung, B. (1978) 'The possible influence of temporal factors in androgenic responsiveness of urogenital tissue recombinants from wild-type and androgen-insensitive (Tfm) mice', *J Exp Zool*, 205(2), pp. 181-93.
Cunha, G.R. and Vanderslice, K.D. (1984) 'Identification in histological sections of species origin of cells from mouse, rat and human', *Stain Technol*, 59(1), pp. 7-12.
Cussenot, O., Berthon, P., Berger, R., Mowszowicz, I., Faille, A., Hojman, F., Teillac, P., Le Duc, A. and Calvo, F. (1991) 'Immortalization of human adult normal prostatic epithelial cells by liposomes containing large T-SV40 gene', *J Urol*, 146(3), pp. 881-6.
D'Amour, K.A., Agulnick, A.D., Eliazer, S., Kelly, O.G., Kroon, E. and Baetge, E.E. (2005) 'Efficient differentiation of human embryonic stem cells to definitive endoderm', *Nat Biotechnol*, 23(12), pp. 1534-41.
Dart, D.A., Waxman, J., Aboagye, E.O. and Bevan, C.L. (2013) 'Visualising androgen receptor activity in male and female mice', *PLoS One*, 8(8), p. e71694.
David, L. and Polo, J.M. (2014) 'Phases of reprogramming', *Stem Cell Res*, 12(3), pp. 754-61.
De Marzo, A.M., Platz, E.A., Sutcliffe, S., Xu, J., Gronberg, H., Drake, C.G., Nakai, Y., Isaacs, W.B. and Nelson, W.G. (2007) 'Inflammation in prostate carcinogenesis', *Nat Rev Cancer*, 7(4), pp. 256-69.
DeCherney, I.H., Nathan, L., Laufer, N., Roman, A.S. (2013) 'Embryology of the urogenital system and congenital abnormalities.', in *Current Diagnosis and Treatment. Obstetrics and Gynecology.* 11 edn., pp. 38-66.
Ding, S., Wu, X., Li, G., Han, M., Zhuang, Y. and Xu, T. (2005) 'Efficient transposition of the piggyBac (PB) transposon in mammalian cells and mice', *Cell*, 122(3), pp. 473-83.
Donjacour, A.A., Thomson, A.A. and Cunha, G.R. (2003) 'FGF-10 plays an essential role in the growth of the fetal prostate', *Dev Biol*, 261(1), pp. 39-54.
Drab, M., Haller, H., Bychkov, R., Erdmann, B., Lindschau, C., Haase, H., Morano, I., Luft, F.C. and Wobus, A.M. (1997) 'From totipotent embryonic stem cells to spontaneously contracting smooth muscle cells: a retinoic acid and db-cAMP in vitro differentiation model', *FASEB J*, 11(11), pp. 905-15.
Drozd, A.M., Walczak, M.P., Piaskowski, S., Stoczynska-Fidelus, E., Rieske, P. and Grzela, D.P. (2015) 'Generation of human iPSCs from cells of fibroblastic and epithelial origin by means of the oriP/EBNA-1 episomal reprogramming system', *Stem Cell Res Ther*, 6, p. 122.
Dutta, A., Le Magnen, C., Mitrofanova, A., Ouyang, X., Califano, A. and Abate-Shen, C. (2016) 'Identification of an NKX3.1-G9a-UTY transcriptional regulatory network that controls prostate differentiation', *Science*, 352(6293), pp. 1576-80.
Fatehullah, A., Tan, S.H. and Barker, N. (2016) 'Organoids as an in vitro model of human development and disease', *Nat Cell Biol*, 18(3), pp. 246-54.
Fujie, Y., Fusaki, N., Katayama, T., Hamasaki, M., Soejima, Y., Soga, M., Ban, H., Hasegawa, M., Yamashita, S., Kimura, S., Suzuki, S., Matsuzawa, T., Akari, H. and Era, T. (2014) 'New type of Sendai virus vector provides transgene-free iPS cells derived from chimpanzee blood', *PLoS One*, 9(12), p. e113052.

Fusaki, N., Ban, H., Nishiyama, A., Saeki, K. and Hasegawa, M. (2009) 'Efficient induction of transgene-free human pluripotent stem cells using a vector based on Sendai virus, an RNA virus that does not integrate into the host genome', *Proc Jpn Acad Ser B Phys Biol Sci*, 85(8), pp. 348-62.
Gao, D., Vela, I., Sboner, A., Iaquinta, P.J., Karthaus, W.R., Gopalan, A., Dowling, C., Wanjala, J.N., Undvall, E.A., Arora, V.K., Wongvipat, J., Kossai, M., Ramazanoglu, S., Barboza, L.P., Di, W., Cao, Z., Zhang, Q.F., Sirota, I., Ran, L., MacDonald, T.Y., Beltran, H., Mosquera, J.M., Touijer, K.A., Scardino, P.T., Laudone, V.P., Curtis, K.R., Rathkopf, D.E., Morris, M.J., Danila, D.C., Slovin, S.F., Solomon, S.B., Eastham, J.A., Chi, P., Carver, B., Rubin, M.A., Scher, H.I., Clevers, H., Sawyers, C.L. and Chen, Y. (2014) 'Organoid cultures derived from patients with advanced prostate cancer', *Cell*, 159(1), pp. 176-87.
Gao, N., Ishii, K., Mirosevich, J., Kuwajima, S., Oppenheimer, S.R., Roberts, R.L., Jiang, M., Yu, X., Shappell, S.B., Caprioli, R.M., Stoffel, M., Hayward, S.W. and Matusik, R.J. (2005) 'Forkhead box A1 regulates prostate ductal morphogenesis and promotes epithelial cell maturation', *Development*, 132(15), pp. 3431-43.
Gao, N., Zhang, J., Rao, M.A., Case, T.C., Mirosevich, J., Wang, Y., Jin, R., Gupta, A., Rennie, P.S. and Matusik, R.J. (2003) 'The role of hepatocyte nuclear factor-3 alpha (Forkhead Box A1) and androgen receptor in transcriptional regulation of prostatic genes', *Mol Endocrinol*, 17(8), pp. 1484-507.
Ghosh, Z., Wilson, K.D., Wu, Y., Hu, S., Quertermous, T. and Wu, J.C. (2010) 'Persistent donor cell gene expression among human induced pluripotent stem cells contributes to differences with human embryonic stem cells', *PLoS One*, 5(2), p. e8975.
Giorgetti, A., Montserrat, N., Aasen, T., Gonzalez, F., Rodriguez-Piza, I., Vassena, R., Raya, A., Boue, S., Barrero, M.J., Corbella, B.A., Torrabadella, M., Veiga, A. and Izpisua Belmonte, J.C. (2009) 'Generation of induced pluripotent stem cells from human cord blood using OCT4 and SOX2', *Cell Stem Cell*, 5(4), pp. 353-7.
Goldman, H.B.a.S. (1940) 'Metaplasia of the epithelium of the prostatic glands, utriole and urethra of the fetus and newborn infant', *Archives of Pathology*, 29.
Goldstein, A.S., Lawson, D.A., Cheng, D., Sun, W., Garraway, I.P. and Witte, O.N. (2008) 'Trop2 identifies a subpopulation of murine and human prostate basal cells with stem cell characteristics', *Proc Natl Acad Sci U S A*, 105(52), pp. 20882-7.
Golipour, A., David, L., Liu, Y., Jayakumaran, G., Hirsch, C.L., Trcka, D. and Wrana, J.L. (2012) 'A late transition in somatic cell reprogramming requires regulators distinct from the pluripotency network', *Cell Stem Cell*, 11(6), pp. 769-82.
Greber, B., Coulon, P., Zhang, M., Moritz, S., Frank, S., Muller-Molina, A.J., Arauzo-Bravo, M.J., Han, D.W., Pape, H.C. and Scholer, H.R. (2011) 'FGF signalling inhibits neural induction in human embryonic stem cells', *EMBO J*, 30(24), pp. 4874-84.
Grishina, I.B., Kim, S.Y., Ferrara, C., Makarenkova, H.P. and Walden, P.D. (2005) 'BMP7 inhibits branching morphogenesis in the prostate gland and interferes with Notch signaling', *Dev Biol*, 288(2), pp. 334-47.
Gurdon, J.B. (1962) 'The developmental capacity of nuclei taken from intestinal epithelium cells of feeding tadpoles', *J Embryol Exp Morphol*, 10, pp. 622-40.
Gurdon, J.B. and Uehlinger, V. (1966) '"Fertile" intestine nuclei', *Nature*, 210(5042), pp. 1240-1.
Hamazaki, T., Iiboshi, Y., Oka, M., Papst, P.J., Meacham, A.M., Zon, L.I. and Terada, N. (2001) 'Hepatic maturation in differentiating embryonic stem cells in vitro', *FEBS Lett*, 497(1), pp. 15-9.
Hamilton, W., Boyd, J., Mossman, H. (1959) *Human Embryology*. Baltimore: Williams and Wilkins Co.

Harris, W.P., Mostaghel, E.A., Nelson, P.S. and Montgomery, B. (2009) 'Androgen deprivation therapy: progress in understanding mechanisms of resistance and optimizing androgen depletion', *Nat Clin Pract Urol*, 6(2), pp. 76-85.
Hayward, S.W. and Cunha, G.R. (2000) 'The prostate: development and physiology', *Radiol Clin North Am*, 38(1), pp. 1-14.
Hayward, S.W., Dahiya, R., Cunha, G.R., Bartek, J., Deshpande, N. and Narayan, P. (1995) 'Establishment and characterization of an immortalized but non-transformed human prostate epithelial cell line: BPH-1', *In Vitro Cell Dev Biol Anim*, 31(1), pp. 14-24.
Hu, K., Yu, J., Suknuntha, K., Tian, S., Montgomery, K., Choi, K.D., Stewart, R., Thomson, J.A. and Slukvin, II (2011) 'Efficient generation of transgene-free induced pluripotent stem cells from normal and neoplastic bone marrow and cord blood mononuclear cells', *Blood*, 117(14), pp. e109-19.
Huang, L., Pu, Y., Hepps, D., Danielpour, D. and Prins, G.S. (2007) 'Posterior Hox gene expression and differential androgen regulation in the developing and adult rat prostate lobes', *Endocrinology*, 148(3), pp. 1235-45.
Huangfu, D., Maehr, R., Guo, W., Eijkelenboom, A., Snitow, M., Chen, A.E. and Melton, D.A. (2008) 'Induction of pluripotent stem cells by defined factors is greatly improved by small-molecule compounds', *Nat Biotechnol*, 26(7), pp. 795-7.
Huch, M., Gehart, H., van Boxtel, R., Hamer, K., Blokzijl, F., Verstegen, M.M., Ellis, E., van Wenum, M., Fuchs, S.A., de Ligt, J., van de Wetering, M., Sasaki, N., Boers, S.J., Kemperman, H., de Jonge, J., Ijzermans, J.N., Nieuwenhuis, E.E., Hoekstra, R., Strom, S., Vries, R.R., van der Laan, L.J., Cuppen, E. and Clevers, H. (2015) 'Long-term culture of genome-stable bipotent stem cells from adult human liver', *Cell*, 160(1-2), pp. 299-312.
Hylander, B.L., Punt, N., Tang, H., Hillman, J., Vaughan, M., Bshara, W., Pitoniak, R. and Repasky, E.A. (2013) 'Origin of the vasculature supporting growth of primary patient tumor xenografts', *J Transl Med*, 11, p. 110.
Imamoto, T., Suzuki, H., Yano, M., Kawamura, K., Kamiya, N., Araki, K., Komiya, A., Nihei, N., Naya, Y. and Ichikawa, T. (2008) 'The role of testosterone in the pathogenesis of prostate cancer', *Int J Urol*, 15(6), pp. 472-80.
Inoue, M., Tokusumi, Y., Ban, H., Kanaya, T., Tokusumi, T., Nagai, Y., Iida, A. and Hasegawa, M. (2003) 'Nontransmissible virus-like particle formation by F-deficient sendai virus is temperature sensitive and reduced by mutations in M and HN proteins', *J Virol*, 77(5), pp. 3238-46.
International Stem Cell Banking Initiative 5 (2009) 'Consensus Guidance for Banking and Supply of Human Embryonic Stem Cell Lines for Research Purposes' [journal article]. Stem Cell Reviews and Reports, pp. 301-314 4. Available at: http://dx.doi.org/10.1007/s12015-009-9085-x.
International Stem Cell Initiative, Adewumi, O., Aflatoonian, B., Ahrlund-Richter, L., Amit, M., Andrews, P.W., Beighton, G., Bello, P.A., Benvenisty, N., Berry, L.S., Bevan, S., Blum, B., Brooking, J., Chen, K.G., Choo, A.B., Churchill, G.A., Corbel, M., Damjanov, I., Draper, J.S., Dvorak, P., Emanuelsson, K., Fleck, R.A., Ford, A., Gertow, K., Gertsenstein, M., Gokhale, P.J., Hamilton, R.S., Hampl, A., Healy, L.E., Hovatta, O., Hyllner, J., Imreh, M.P., Itskovitz-Eldor, J., Jackson, J., Johnson, J.L., Jones, M., Kee, K., King, B.L., Knowles, B.B., Lako, M., Lebrin, F., Mallon, B.S., Manning, D., Mayshar, Y., McKay, R.D., Michalska, A.E., Mikkola, M., Mileikovsky, M., Minger, S.L., Moore, H.D., Mummery, C.L., Nagy, A., Nakatsuji, N., O'Brien, C.M., Oh, S.K., Olsson, C., Otonkoski, T., Park, K.Y., Passier, R., Patel, H., Patel, M., Pedersen, R., Pera, M.F., Piekarczyk, M.S., Pera, R.A., Reubinoff, B.E., Robins, A.J., Rossant, J., Rugg-Gunn, P., Schulz, T.C., Semb, H., Sherrer, E.S., Siemen, H., Stacey, G.N., Stojkovic, M., Suemori, H., Szatkiewicz, J., Turetsky, T., Tuuri, T., van

den Brink, S., Vintersten, K., Vuoristo, S., Ward, D., Weaver, T.A., Young, L.A. and Zhang, W. (2007) 'Characterization of human embryonic stem cell lines by the International Stem Cell Initiative', *Nat Biotechnol*, 25(7), pp. 803-16.
Isaacs, J.T. (1985) 'Control of cell proliferation and cell death in the normal and neoplastic prostate: a stem cell model', in C.H. Rodgers at al. (ed.) *Benign Prostatic Hyperplasia*. Washington: NIH, pp. 85-94.
Ito, R., Takahashi, T., Katano, I. and Ito, M. (2012) 'Current advances in humanized mouse models', *Cell Mol Immunol*, 9(3), pp. 208-14.
Itskovitz-Eldor, J., Schuldiner, M., Karsenti, D., Eden, A., Yanuka, O., Amit, M., Soreq, H. and Benvenisty, N. (2000) 'Differentiation of human embryonic stem cells into embryoid bodies compromising the three embryonic germ layers', *Mol Med*, 6(2), pp. 88-95.
Jaenisch, R. and Young, R. (2008) 'Stem cells, the molecular circuitry of pluripotency and nuclear reprogramming', *Cell*, 132(4), pp. 567-82.
Jahner, D., Stuhlmann, H., Stewart, C.L., Harbers, K., Lohler, J., Simon, I. and Jaenisch, R. (1982) 'De novo methylation and expression of retroviral genomes during mouse embryogenesis', *Nature*, 298(5875), pp. 623-8.
Jeter, C.R., Liu, B., Liu, X., Chen, X., Liu, C., Calhoun-Davis, T., Repass, J., Zaehres, H., Shen, J.J. and Tang, D.G. (2011) 'NANOG promotes cancer stem cell characteristics and prostate cancer resistance to androgen deprivation', *Oncogene*, 30(36), pp. 3833-45.
Jones, P.H., Harper, S. and Watt, F.M. (1995) 'Stem cell patterning and fate in human epidermis', *Cell*, 80(1), pp. 83-93.
Kamb, A. (2005) 'What's wrong with our cancer models?', *Nat Rev Drug Discov*, 4(2), pp. 161-165.
Karthaus, W.R., Iaquinta, P.J., Drost, J., Gracanin, A., van Boxtel, R., Wongvipat, J., Dowling, C.M., Gao, D., Begthel, H., Sachs, N., Vries, R.G., Cuppen, E., Chen, Y., Sawyers, C.L. and Clevers, H.C. (2014) 'Identification of multipotent luminal progenitor cells in human prostate organoid cultures', *Cell*, 159(1), pp. 163-75.
Keil, K.P., Mehta, V., Abler, L.L., Joshi, P.S., Schmitz, C.T. and Vezina, C.M. (2012) 'Visualization and quantification of mouse prostate development by in situ hybridization', *Differentiation*, 84(3), pp. 232-9.
Keller, G.M. (1995) 'In vitro differentiation of embryonic stem cells', *Curr Opin Cell Biol*, 7(6), pp. 862-9.
Khan, M., Narayanan, K., Lu, H., Choo, Y., Du, C., Wiradharma, N., Yang, Y.Y. and Wan, A.C. (2013) 'Delivery of reprogramming factors into fibroblasts for generation of non-genetic induced pluripotent stem cells using a cationic bolaamphiphile as a non-viral vector', *Biomaterials*, 34(21), pp. 5336-43.
Kim, D., Kim, C.H., Moon, J.I., Chung, Y.G., Chang, M.Y., Han, B.S., Ko, S., Yang, E., Cha, K.Y., Lanza, R. and Kim, K.S. (2009) 'Generation of human induced pluripotent stem cells by direct delivery of reprogramming proteins', *Cell Stem Cell*, 4(6), pp. 472-6.
Kim, J.S., Choi, H.W., Choi, S. and Do, J.T. (2011) 'Reprogrammed pluripotent stem cells from somatic cells', *Int J Stem Cells*, 4(1), pp. 1-8.
Kim, K., Doi, A., Wen, B., Ng, K., Zhao, R., Cahan, P., Kim, J., Aryee, M.J., Ji, H., Ehrlich, L.I., Yabuuchi, A., Takeuchi, A., Cunniff, K.C., Hongguang, H., McKinney-Freeman, S., Naveiras, O., Yoon, T.J., Irizarry, R.A., Jung, N., Seita, J., Hanna, J., Murakami, P., Jaenisch, R., Weissleder, R., Orkin, S.H., Weissman, I.L., Feinberg, A.P. and Daley, G.Q. (2010a) 'Epigenetic memory in induced pluripotent stem cells', *Nature*, 467(7313), pp. 285-90.
Kim, P.T., Hoffman, B.G., Plesner, A., Helgason, C.D., Verchere, C.B., Chung, S.W., Warnock, G.L., Mui, A.L. and Ong, C.J. (2010b) 'Differentiation of mouse embryonic

stem cells into endoderm without embryoid body formation', *PLoS One*, 5(11), p. e14146.
Kim, S., Kim, G.J., Miyoshi, H., Moon, S.H., Ahn, S.E., Lee, J.H., Lee, H.J., Cha, K.Y. and Chung, H.M. (2007) 'Efficiency of the elongation factor-1alpha promoter in mammalian embryonic stem cells using lentiviral gene delivery systems', *Stem Cells Dev*, 16(4), pp. 537-45.
Kirby, M., Hirst, C. and Crawford, E.D. (2011) 'Characterising the castration-resistant prostate cancer population: a systematic review', *Int J Clin Pract*, 65(11), pp. 1180-92.
Kleinman, H.K., McGarvey, M.L., Hassell, J.R., Star, V.L., Cannon, F.B., Laurie, G.W. and Martin, G.R. (1986) 'Basement membrane complexes with biological activity', *Biochemistry*, 25(2), pp. 312-8.
Kondo, M., Wagers, A.J., Manz, M.G., Prohaska, S.S., Scherer, D.C., Beilhack, G.F., Shizuru, J.A. and Weissman, I.L. (2003) 'Biology of hematopoietic stem cells and progenitors: implications for clinical application', *Annu Rev Immunol*, 21, pp. 759-806.
Krause, D.S., Theise, N.D., Collector, M.I., Henegariu, O., Hwang, S., Gardner, R., Neutzel, S. and Sharkis, S.J. (2001) 'Multi-organ, multi-lineage engraftment by a single bone marrow-derived stem cell', *Cell*, 105(3), pp. 369-77.
Kumlin, U., Olofsson, S., Dimock, K. and Arnberg, N. (2008) 'Sialic acid tissue distribution and influenza virus tropism', *Influenza and Other Respiratory Viruses*, 2(5), pp. 147-154.
Kurita, T., Medina, R.T., Mills, A.A. and Cunha, G.R. (2004) 'Role of p63 and basal cells in the prostate', *Development*, 131(20), pp. 4955-64.
Lamb, R.A., Kolakofsky, D (1996) 'Paramyxoviridae: the viruses and their replication', in Philadelphia: Lippincott-Raven, pp. 1177-1204.
Lamm, M.L., Catbagan, W.S., Laciak, R.J., Barnett, D.H., Hebner, C.M., Gaffield, W., Walterhouse, D., Iannaccone, P. and Bushman, W. (2002) 'Sonic hedgehog activates mesenchymal Gli1 expression during prostate ductal bud formation', *Dev Biol*, 249(2), pp. 349-66.
Lamm, M.L., Podlasek, C.A., Barnett, D.H., Lee, J., Clemens, J.Q., Hebner, C.M. and Bushman, W. (2001) 'Mesenchymal factor bone morphogenetic protein 4 restricts ductal budding and branching morphogenesis in the developing prostate', *Dev Biol*, 232(2), pp. 301-14.
Lang, S.H., Frame, F.M. and Collins, A.T. (2009) 'Prostate cancer stem cells', *J Pathol*, 217(2), pp. 299-306.
Lang, S.H., Sharrard, R.M., Stark, M., Villette, J.M. and Maitland, N.J. (2001a) 'Prostate epithelial cell lines form spheroids with evidence of glandular differentiation in three-dimensional Matrigel cultures', *Br J Cancer*, 85(4), pp. 590-9.
Lang, S.H., Stark, M., Collins, A., Paul, A.B., Stower, M.J. and Maitland, N.J. (2001b) 'Experimental prostate epithelial morphogenesis in response to stroma and three-dimensional matrigel culture', *Cell Growth Differ*, 12(12), pp. 631-40.
LaVaute, T.M., Yoo, Y.D., Pankratz, M.T., Weick, J.P., Gerstner, J.R. and Zhang, S.C. (2009) 'Regulation of neural specification from human embryonic stem cells by BMP and FGF', *Stem Cells*, 27(8), pp. 1741-9.
Lee, C.S., Friedman, J.R., Fulmer, J.T. and Kaestner, K.H. (2005) 'The initiation of liver development is dependent on Foxa transcription factors', *Nature*, 435(7044), pp. 944-7.
Lee, K.L. and Peehl, D.M. (2004) 'Molecular and cellular pathogenesis of benign prostatic hyperplasia', *J Urol*, 172(5 Pt 1), pp. 1784-91.
Letellier, G., Perez, M.J., Yacoub, M., Levillain, P., Cussenot, O. and Fromont, G. (2007) 'Epithelial phenotypes in the developing human prostate', *J Histochem Cytochem*, 55(9), pp. 885-90.

Levenberg, S., Golub, J.S., Amit, M., Itskovitz-Eldor, J. and Langer, R. (2002) 'Endothelial cells derived from human embryonic stem cells', *Proc Natl Acad Sci U S A*, 99(7), pp. 4391-6.
Li, A., Simmons, P.J. and Kaur, P. (1998) 'Identification and isolation of candidate human keratinocyte stem cells based on cell surface phenotype', *Proc Natl Acad Sci U S A*, 95(7), pp. 3902-7.
Li, C., Klco, J.M., Helton, N.M., George, D.R., Mudd, J.L., Miller, C.A., Lu, C., Fulton, R., O'Laughlin, M., Fronick, C., Wilson, R.K. and Ley, T.J. (2015) 'Genetic heterogeneity of induced pluripotent stem cells: results from 24 clones derived from a single C57BL/6 mouse', *PLoS One*, 10(3), p. e0120585.
Li, F., He, Z., Shen, J., Huang, Q., Li, W., Liu, X., He, Y., Wolf, F. and Li, C.-Y. (2010a) 'Apoptotic Caspases Regulate Induction of iPSCs from Human Fibroblasts', *Cell Stem Cell*, 7(4), pp. 508-520.
Li, H.O., Zhu, Y.F., Asakawa, M., Kuma, H., Hirata, T., Ueda, Y., Lee, Y.S., Fukumura, M., Iida, A., Kato, A., Nagai, Y. and Hasegawa, M. (2000) 'A cytoplasmic RNA vector derived from nontransmissible Sendai virus with efficient gene transfer and expression', *J Virol*, 74(14), pp. 6564-9.
Li, R., Liang, J., Ni, S., Zhou, T., Qing, X., Li, H., He, W., Chen, J., Li, F., Zhuang, Q., Qin, B., Xu, J., Li, W., Yang, J., Gan, Y., Qin, D., Feng, S., Song, H., Yang, D., Zhang, B., Zeng, L., Lai, L., Esteban, M.A. and Pei, D. (2010b) 'A mesenchymal-to-epithelial transition initiates and is required for the nuclear reprogramming of mouse fibroblasts', *Cell Stem Cell*, 7(1), pp. 51-63.
Lilja, H. (1985) 'A kallikrein-like serine protease in prostatic fluid cleaves the predominant seminal vesicle protein', *J Clin Invest*, 76(5), pp. 1899-903.
Lilja, H. and Abrahamsson, P.A. (1988) 'Three predominant proteins secreted by the human prostate gland', *Prostate*, 12(1), pp. 29-38.
Lin, V.K., Wang, S.Y., Vazquez, D.V., C, C.X., Zhang, S. and Tang, L. (2007) 'Prostatic stromal cells derived from benign prostatic hyperplasia specimens possess stem cell like property', *Prostate*, 67(12), pp. 1265-76.
Lipinski, R.J., Cook, C.H., Barnett, D.H., Gipp, J.J., Peterson, R.E. and Bushman, W. (2005) 'Sonic hedgehog signaling regulates the expression of insulin-like growth factor binding protein-6 during fetal prostate development', *Dev Dyn*, 233(3), pp. 829-36.
Liu, Y., Cheng, D., Li, Z., Gao, X. and Wang, H. (2012) 'The gene expression profiles of induced pluripotent stem cells (iPSCs) generated by a non-integrating method are more similar to embryonic stem cells than those of iPSCs generated by an integrating method', *Genet Mol Biol*, 35(3), pp. 693-700.
Loh, Y.H., Agarwal, S., Park, I.H., Urbach, A., Huo, H., Heffner, G.C., Kim, K., Miller, J.D., Ng, K. and Daley, G.Q. (2009) 'Generation of induced pluripotent stem cells from human blood', *Blood*, 113(22), pp. 5476-9.
Ludwig, T.E., Levenstein, M.E., Jones, J.M., Berggren, W.T., Mitchen, E.R., Frane, J.L., Crandall, L.J., Daigh, C.A., Conard, K.R., Piekarczyk, M.S., Llanas, R.A. and Thomson, J.A. (2006) 'Derivation of human embryonic stem cells in defined conditions', *Nat Biotechnol*, 24(2), pp. 185-7.
Lund, R.J., Narva, E. and Lahesmaa, R. (2012) 'Genetic and epigenetic stability of human pluripotent stem cells', *Nat Rev Genet*, 13(10), pp. 732-744.
Mali, P., Chou, B.K., Yen, J., Ye, Z., Zou, J., Dowey, S., Brodsky, R.A., Ohm, J.E., Yu, W., Baylin, S.B., Yusa, K., Bradley, A., Meyers, D.J., Mukherjee, C., Cole, P.A. and Cheng, L. (2010) 'Butyrate greatly enhances derivation of human induced pluripotent stem cells by promoting epigenetic remodeling and the expression of pluripotency-associated genes', *Stem Cells*, 28(4), pp. 713-20.

Malik, N. and Rao, M.S. (2013) 'A review of the methods for human iPSC derivation', *Methods Mol Biol*, 997, pp. 23-33.
Mallon, B.S., Park, K.Y., Chen, K.G., Hamilton, R.S. and McKay, R.D. (2006) 'Toward xeno-free culture of human embryonic stem cells', *Int J Biochem Cell Biol*, 38(7), pp. 1063-75.
Marchetto, M.C., Yeo, G.W., Kainohana, O., Marsala, M., Gage, F.H. and Muotri, A.R. (2009) 'Transcriptional signature and memory retention of human-induced pluripotent stem cells', *PLoS One*, 4(9), p. e7076.
Marker, P.C., Donjacour, A.A., Dahiya, R. and Cunha, G.R. (2003) 'Hormonal, cellular, and molecular control of prostatic development', *Dev Biol*, 253(2), pp. 165-74.
Markwell, M.A. and Paulson, J.C. (1980) 'Sendai virus utilizes specific sialyloligosaccharides as host cell receptor determinants', *Proceedings of the National Academy of Sciences of the United States of America*, 77(10), pp. 5693-5697.
Markwell, M.A., Svennerholm, L. and Paulson, J.C. (1981) 'Specific gangliosides function as host cell receptors for Sendai virus', *Proc Natl Acad Sci U S A*, 78(9), pp. 5406-10.
Marques, R.B., Dits, N.F., Erkens-Schulze, S., van Weerden, W.M. and Jenster, G. (2010) 'Bypass mechanisms of the androgen receptor pathway in therapy-resistant prostate cancer cell models', *PLoS One*, 5(10), p. e13500.
Marti, M., Mulero, L., Pardo, C., Morera, C., Carrio, M., Laricchia-Robbio, L., Esteban, C.R. and Izpisua Belmonte, J.C. (2013) 'Characterization of pluripotent stem cells', *Nat Protoc*, 8(2), pp. 223-53.
May, T., Hauser, H. and Wirth, D. (2004) 'Transcriptional control of SV40 T-antigen expression allows a complete reversion of immortalization', *Nucleic Acids Res*, 32(18), pp. 5529-38.
McLaren, A. (1976) *Mammalian Chimaeras*. Cambridge University Press

McNeal, J.E. (1978) 'Origin and evolution of benign prostatic enlargement', *Invest Urol*, 15(4), pp. 340-5.
Meeks, J.J. and Schaeffer, E.M. (2011) 'Genetic regulation of prostate development', *J Androl*, 32(3), pp. 210-7.
Mikkelsen, T.S., Hanna, J., Zhang, X., Ku, M., Wernig, M., Schorderet, P., Bernstein, B.E., Jaenisch, R., Lander, E.S. and Meissner, A. (2008) 'Dissecting direct reprogramming through integrative genomic analysis', *Nature*, 454(7200), pp. 49-55.
Min, H., Danilenko, D.M., Scully, S.A., Bolon, B., Ring, B.D., Tarpley, J.E., DeRose, M. and Simonet, W.S. (1998) 'Fgf-10 is required for both limb and lung development and exhibits striking functional similarity to Drosophila branchless', *Genes Dev*, 12(20), pp. 3156-61.
Mirosevich, J., Gao, N. and Matusik, R.J. (2005) 'Expression of Foxa transcription factors in the developing and adult murine prostate', *Prostate*, 62(4), pp. 339-52.
Missol-Kolka, E., Karbanová, J., Janich, P., Haase, M., Fargeas, C. A., Huttner, W. B. and Corbeil, D. (2011) 'Prominin-1 (CD133) is not restricted to stem cells located in the basal compartment of murine and human prostate', *Prostate*, 71, pp. 254-267.
Mitchell, D.J., Kim, D.T., Steinman, L., Fathman, C.G. and Rothbard, J.B. (2000) 'Polyarginine enters cells more efficiently than other polycationic homopolymers', *J Pept Res*, 56(5), pp. 318-25.
Moad, M., Hannezo, E., Buczacki, S.J., Wilson, L., El-Sherif, A., Sims, D., Pickard, R., Wright, N.A., Williamson, S.C., Turnbull, D.M., Taylor, R.W., Greaves, L., Robson, C.N., Simons, B.D. and Heer, R. (2017) 'Multipotent Basal Stem Cells,

Maintained in Localized Proximal Niches, Support Directed Long-Ranging Epithelial Flows in Human Prostates', *Cell Rep*, 20(7), pp. 1609-1622.
Moad, M., Pal, D., Hepburn, A.C., Williamson, S.C., Wilson, L., Lako, M., Armstrong, L., Hayward, S.W., Franco, O.E., Cates, J.M., Fordham, S.E., Przyborski, S., Carr-Wilkinson, J., Robson, C.N. and Heer, R. (2013) 'A novel model of urinary tract differentiation, tissue regeneration, and disease: reprogramming human prostate and bladder cells into induced pluripotent stem cells', *Eur Urol*, 64(5), pp. 753-61.
Mukherjee, S. and Thrasher, A.J. (2011) 'iPSCs: Unstable origins?', *Mol Ther*, 19(7), pp. 1188-90.
Mummery, C., Ward-van Oostwaard, D., Doevendans, P., Spijker, R., van den Brink, S., Hassink, R., van der Heyden, M., Opthof, T., Pera, M., de la Riviere, A.B., Passier, R. and Tertoolen, L. (2003) 'Differentiation of human embryonic stem cells to cardiomyocytes: role of coculture with visceral endoderm-like cells', *Circulation*, 107(21), pp. 2733-40.
Munoz-Sanjuan, I. and Brivanlou, A.H. (2002) 'Neural induction, the default model and embryonic stem cells', *Nat Rev Neurosci*, 3(4), pp. 271-80.
Murakami, T., Saitoh, I., Inada, E., Kurosawa, M., Iwase, Y., Noguchi, H., Terao, Y., Yamasaki, Y., Hayasaki, H. and Sato, M. (2013) 'STO Feeder Cells Are Useful for Propagation of Primarily Cultured Human Deciduous Dental Pulp Cells by Eliminating Contaminating Bacteria and Promoting Cellular Outgrowth', *Cell Medicine*, 6(1-2), pp. 75-81.
Nagy, A., Rossant, J., Nagy, R., Abramow-Newerly, W. and Roder, J.C. (1993) 'Derivation of completely cell culture-derived mice from early-passage embryonic stem cells', *Proc Natl Acad Sci U S A*, 90(18), pp. 8424-8.
Nakagawa, M., Koyanagi, M., Tanabe, K., Takahashi, K., Ichisaka, T., Aoi, T., Okita, K., Mochiduki, Y., Takizawa, N. and Yamanaka, S. (2008) 'Generation of induced pluripotent stem cells without Myc from mouse and human fibroblasts', *Nat Biotechnol*, 26(1), pp. 101-6.
Nakanishi, M. and Otsu, M. (2012) 'Development of Sendai virus vectors and their potential applications in gene therapy and regenerative medicine', *Curr Gene Ther*, 12(5), pp. 410-6.
Nasu, A., Ikeya, M., Yamamoto, T., Watanabe, A., Jin, Y., Matsumoto, Y., Hayakawa, K., Amano, N., Sato, S., Osafune, K., Aoyama, T., Nakamura, T., Kato, T. and Toguchida, J. (2013) 'Genetically matched human iPS cells reveal that propensity for cartilage and bone differentiation differs with clones, not cell type of origin', *PLoS One*, 8(1), p. e53771.
Newman, A.M. and Cooper, J.B. (2010) 'Lab-specific gene expression signatures in pluripotent stem cells', *Cell Stem Cell*, 7(2), pp. 258-62.
Niranjan, B., Lawrence, M.G., Papargiris, M.M., Richards, M.G., Hussain, S., Frydenberg, M., Pedersen, J., Taylor, R.A. and Risbridger, G.P. (2013) 'Primary culture and propagation of human prostate epithelial cells', *Methods Mol Biol*, 945, pp. 365-82.
Nori, S., Okada, Y., Nishimura, S., Sasaki, T., Itakura, G., Kobayashi, Y., Renault-Mihara, F., Shimizu, A., Koya, I., Yoshida, R., Kudoh, J., Koike, M., Uchiyama, Y., Ikeda, E., Toyama, Y., Nakamura, M. and Okano, H. (2015) 'Long-term safety issues of iPSC-based cell therapy in a spinal cord injury model: oncogenic transformation with epithelial-mesenchymal transition', *Stem Cell Reports*, 4(3), pp. 360-73.
O'Connor, M.D., Kardel, M.D., Iosfina, I., Youssef, D., Lu, M., Li, M.M., Vercauteren, S., Nagy, A. and Eaves, C.J. (2008) 'Alkaline phosphatase-positive colony formation is a sensitive, specific, and quantitative indicator of undifferentiated human embryonic stem cells', *Stem Cells*, 26(5), pp. 1109-16.

Okita, K., Ichisaka, T. and Yamanaka, S. (2007) 'Generation of germline-competent induced pluripotent stem cells', *Nature*, 448(7151), pp. 313-7.
Ono, M., Hamada, Y., Horiuchi, Y., Matsuo-Takasaki, M., Imoto, Y., Satomi, K., Arinami, T., Hasegawa, M., Fujioka, T., Nakamura, Y. and Noguchi, E. (2012) 'Generation of induced pluripotent stem cells from human nasal epithelial cells using a Sendai virus vector', *PLoS One*, 7(8), p. e42855.
Packer, J.R. and Maitland, N.J. (2016) 'The molecular and cellular origin of human prostate cancer', *Biochim Biophys Acta*, 1863(6 Pt A), pp. 1238-60.
Pal, D. (2014) *Induced Pluripotent Stem-cell re-programming in the elderly prostate*. Newcastle University.
Peehl, D.M. (2005) 'Primary cell cultures as models of prostate cancer development', *Endocr Relat Cancer*, 12(1), pp. 19-47.
Peehl, D.M., Leung, G.K. and Wong, S.T. (1994) 'Keratin expression: a measure of phenotypic modulation of human prostatic epithelial cells by growth inhibitory factors', *Cell Tissue Res*, 277(1), pp. 11-8.
Peng, Z., Skoog, L., Hellborg, H., Jonstam, G., Wingmo, I.L., Hjalm-Eriksson, M., Harmenberg, U., Cedermark, G.C., Andersson, K., Ahrlund-Richter, L., Pramana, S., Pawitan, Y., Nister, M., Nilsson, S. and Li, C. (2014) 'An expression signature at diagnosis to estimate prostate cancer patients' overall survival', *Prostate Cancer Prostatic Dis*, 17(1), pp. 81-90.
Pignon, J.-C., Grisanzio, C., Geng, Y., Song, J., Shivdasani, R.A. and Signoretti, S. (2013) 'p63-expressing cells are the stem cells of developing prostate, bladder, and colorectal epithelia', *Proceedings of the National Academy of Sciences of the United States of America*, 110(20), pp. 8105-8110.
Podlasek, C.A., Clemens, J.Q. and Bushman, W. (1999a) 'Hoxa-13 gene mutation results in abnormal seminal vesicle and prostate development', *J Urol*, 161(5), pp. 1655-61.
Podlasek, C.A., Duboule, D. and Bushman, W. (1997) 'Male accessory sex organ morphogenesis is altered by loss of function of Hoxd-13', *Dev Dyn*, 208(4), pp. 454-65.
Podlasek, C.A., Seo, R.M., Clemens, J.Q., Ma, L., Maas, R.L. and Bushman, W. (1999b) 'Hoxa-10 deficient male mice exhibit abnormal development of the accessory sex organs', *Dev Dyn*, 214(1), pp. 1-12.
Prajapati, A., Gupta, S., Mistry, B. and Gupta, S. (2013) 'Prostate stem cells in the development of benign prostate hyperplasia and prostate cancer: emerging role and concepts', *Biomed Res Int*, 2013, p. 107954.
Pritchard, C., Mecham, B., Dumpit, R., Coleman, I., Bhattacharjee, M., Chen, Q., Sikes, R.A. and Nelson, P.S. (2009) 'Conserved gene expression programs integrate mammalian prostate development and tumorigenesis', *Cancer Res*, 69(5), pp. 1739-47.
Reich, O., Gratzke, C., Bachmann, A., Seitz, M., Schlenker, B., Hermanek, P., Lack, N., Stief, C.G. and Urology Section of the Bavarian Working Group for Quality, A. (2008) 'Morbidity, mortality and early outcome of transurethral resection of the prostate: a prospective multicenter evaluation of 10,654 patients', *J Urol*, 180(1), pp. 246-9.
Reubinoff, B.E., Pera, M.F., Fong, C.Y., Trounson, A. and Bongso, A. (2000) 'Embryonic stem cell lines from human blastocysts: somatic differentiation in vitro', *Nat Biotechnol*, 18(4), pp. 399-404.
Rhim, J.S., Li, H. and Furusato, B. (2011) 'Novel human prostate epithelial cell culture models for the study of carcinogenesis and of normal stem cells and cancer stem cells', *Adv Exp Med Biol*, 720, pp. 71-80.

Richardson, G.D., Robson, C.N., Lang, S.H., Neal, D.E., Maitland, N.J. and Collins, A.T. (2004) 'CD133, a novel marker for human prostatic epithelial stem cells', *J Cell Sci*, 117(Pt 16), pp. 3539-45.
Roehrborn, C., McConnell, J. (2002) 'Etiology, pathophysiology, epidemiology and natural history of benign prostatic hyperplasia.', in Walsh P, R.A., Vaughan E, Wein A. (ed.) *Campbell's Urology*. 8th edn. Philadelphia: Saunders, pp. 1297–1336.
Roehrborn, C.G. (2005) 'Benign prostatic hyperplasia: an overview', *Rev Urol*, 7 Suppl 9, pp. S3-S14.
Rogers, M.B., Hosler, B.A. and Gudas, L.J. (1991) 'Specific expression of a retinoic acid-regulated, zinc-finger gene, Rex-1, in preimplantation embryos, trophoblast and spermatocytes', *Development*, 113(3), pp. 815-24.
Rouhani, F., Kumasaka, N., de Brito, M.C., Bradley, A., Vallier, L. and Gaffney, D. (2014) 'Genetic background drives transcriptional variation in human induced pluripotent stem cells', *PLoS Genet*, 10(6), p. e1004432.
Rowley, D.R. and Tindall, D.J. (1987) 'Responses of NBT-II bladder carcinoma cells to conditioned medium from normal fetal urogenital sinus', *Cancer Res*, 47(11), pp. 2955-60.
Saffarini, C.M., McDonnell, E.V., Amin, A., Spade, D.J., Huse, S.M., Kostadinov, S., Hall, S.J. and Boekelheide, K. (2013) 'Maturation of the developing human fetal prostate in a rodent xenograft model', *Prostate*, 73(16), pp. 1761-75.
Samavarchi-Tehrani, P., Golipour, A., David, L., Sung, H.K., Beyer, T.A., Datti, A., Woltjen, K., Nagy, A. and Wrana, J.L. (2010) 'Functional genomics reveals a BMP-driven mesenchymal-to-epithelial transition in the initiation of somatic cell reprogramming', *Cell Stem Cell*, 7(1), pp. 64-77.
Sar, M., Lubahn, D.B., French, F.S. and Wilson, E.M. (1990) 'Immunohistochemical localization of the androgen receptor in rat and human tissues', *Endocrinology*, 127(6), pp. 3180-6.
Sathananthan, A.H. and Trounson, A. (2005) 'Human embryonic stem cells and their spontaneous differentiation', *Ital J Anat Embryol*, 110(2 Suppl 1), pp. 151-7.
Sato, T., Stange, D.E., Ferrante, M., Vries, R.G., Van Es, J.H., Van den Brink, S., Van Houdt, W.J., Pronk, A., Van Gorp, J., Siersema, P.D. and Clevers, H. (2011) 'Long-term expansion of epithelial organoids from human colon, adenoma, adenocarcinoma, and Barrett's epithelium', *Gastroenterology*, 141(5), pp. 1762-72.
Sato, T., Vries, R.G., Snippert, H.J., van de Wetering, M., Barker, N., Stange, D.E., van Es, J.H., Abo, A., Kujala, P., Peters, P.J. and Clevers, H. (2009) 'Single Lgr5 stem cells build crypt-villus structures in vitro without a mesenchymal niche', *Nature*, 459(7244), pp. 262-5.
Schaeffer, E.M., Marchionni, L., Huang, Z., Simons, B., Blackman, A., Yu, W., Parmigiani, G. and Berman, D.M. (2008) 'Androgen-induced programs for prostate epithelial growth and invasion arise in embryogenesis and are reactivated in cancer', *Oncogene*, 27(57), pp. 7180-91.
Schwartz, P.H., Brick, D.J., Stover, A.E., Loring, J.F. and Muller, F.J. (2008) 'Differentiation of neural lineage cells from human pluripotent stem cells', *Methods*, 45(2), pp. 142-58.
Sciarra, A., Mariotti, G., Gentile, V., Voria, G., Pastore, A., Monti, S. and Di Silverio, F. (2003) 'Neuroendocrine differentiation in human prostate tissue: is it detectable and treatable?', *BJU Int*, 91(5), pp. 438-45.
Seki, T. and Fukuda, K. (2015) 'Methods of induced pluripotent stem cells for clinical application', *World J Stem Cells*, 7(1), pp. 116-25.
Shannon, J.M. and Cunha, G.R. (1983) 'Autoradiographic localization of androgen binding in the developing mouse prostate', *Prostate*, 4(4), pp. 367-73.

Shappell, S.B., Thomas, G.V., Roberts, R.L., Herbert, R., Ittmann, M.M., Rubin, M.A., Humphrey, P.A., Sundberg, J.P., Rozengurt, N., Barrios, R., Ward, J.M. and Cardiff, R.D. (2004) 'Prostate pathology of genetically engineered mice: definitions and classification. The consensus report from the Bar Harbor meeting of the Mouse Models of Human Cancer Consortium Prostate Pathology Committee', *Cancer Res*, 64(6), pp. 2270-305.
Sharma, Naomi L., Massie, Charlie E., Ramos-Montoya, A., Zecchini, V., Scott, Helen E., Lamb, Alastair D., MacArthur, S., Stark, R., Warren, Anne Y., Mills, Ian G. and Neal, David E. (2013) 'The Androgen Receptor Induces a Distinct Transcriptional Program in Castration-Resistant Prostate Cancer in Man', *Cancer Cell*, 23(1), pp. 35-47.
Shay, J.W. and Wright, W.E. (2000) 'Hayflick, his limit, and cellular ageing', *Nat Rev Mol Cell Biol*, 1(1), pp. 72-76.
Shen, M.M. and Abate-Shen, C. (2010) 'Molecular genetics of prostate cancer: new prospects for old challenges', *Genes Dev*, 24(18), pp. 1967-2000.
Shinohara, T., Avarbock, M.R. and Brinster, R.L. (1999) 'beta1- and alpha6-integrin are surface markers on mouse spermatogonial stem cells', *Proc Natl Acad Sci U S A*, 96(10), pp. 5504-9.
Signoretti, S., Waltregny, D., Dilks, J., Isaac, B., Lin, D., Garraway, L., Yang, A., Montironi, R., McKeon, F. and Loda, M. (2000) 'p63 is a prostate basal cell marker and is required for prostate development', *Am J Pathol*, 157(6), pp. 1769-75.
Singh, U., Quintanilla, R.H., Grecian, S., Gee, K.R., Rao, M.S. and Lakshmipathy, U. (2012) 'Novel live alkaline phosphatase substrate for identification of pluripotent stem cells', *Stem Cell Rev*, 8(3), pp. 1021-9.
Smith, K.P., Luong, M.X. and Stein, G.S. (2009) 'Pluripotency: toward a gold standard for human ES and iPS cells', *J Cell Physiol*, 220(1), pp. 21-9.
Sommer, C.A., Sommer, A.G., Longmire, T.A., Christodoulou, C., Thomas, D.D., Gostissa, M., Alt, F.W., Murphy, G.J., Kotton, D.N. and Mostoslavsky, G. (2010) 'Excision of reprogramming transgenes improves the differentiation potential of iPS cells generated with a single excisable vector', *Stem Cells*, 28(1), pp. 64-74.
Sommer, C.A., Stadtfeld, M., Murphy, G.J., Hochedlinger, K., Kotton, D.N. and Mostoslavsky, G. (2009) 'Induced pluripotent stem cell generation using a single lentiviral stem cell cassette', *Stem Cells*, 27(3), pp. 543-9.
Spence, J.R., Mayhew, C.N., Rankin, S.A., Kuhar, M.F., Vallance, J.E., Tolle, K., Hoskins, E.E., Kalinichenko, V.V., Wells, S.I., Zorn, A.M., Shroyer, N.F. and Wells, J.M. (2011) 'Directed differentiation of human pluripotent stem cells into intestinal tissue in vitro', *Nature*, 470(7332), pp. 105-9.
Stewart, C.L., Stuhlmann, H., Jahner, D. and Jaenisch, R. (1982) 'De novo methylation, expression, and infectivity of retroviral genomes introduced into embryonal carcinoma cells', *Proc Natl Acad Sci U S A*, 79(13), pp. 4098-102.
Sturm, N., Rossi, G., Lantuejoul, S., Laverriere, M.H., Papotti, M., Brichon, P.Y., Brambilla, C. and Brambilla, E. (2003) '34BetaE12 expression along the whole spectrum of neuroendocrine proliferations of the lung, from neuroendocrine cell hyperplasia to small cell carcinoma', *Histopathology*, 42(2), pp. 156-66.
Sugimura, Y., Cunha, G.R., Yonemura, C.U. and Kawamura, J. (1988) 'Temporal and spatial factors in diethylstilbestrol-induced squamous metaplasia of the developing human prostate', *Hum Pathol*, 19(2), pp. 133-9.
Sugimura, Y., Foster, B.A., Hom, Y.K., Lipschutz, J.H., Rubin, J.S., Finch, P.W., Aaronson, S.A., Hayashi, N., Kawamura, J. and Cunha, G.R. (1996) 'Keratinocyte growth factor (KGF) can replace testosterone in the ductal branching morphogenesis of the rat ventral prostate', *Int J Dev Biol*, 40(5), pp. 941-51.

Suzuki, Y., Suzuki, T., Matsunaga, M. and Matsumoto, M. (1985) 'Gangliosides as paramyxovirus receptor. Structural requirement of sialo-oligosaccharides in receptors for hemagglutinating virus of Japan (Sendai virus) and Newcastle disease virus', *J Biochem*, 97(4), pp. 1189-99.
Szczyrba, J., Niesen, A., Wagner, M., Wandernoth, P.M., Aumuller, G. and Wennemuth, G. (2017) 'Neuroendocrine Cells of the Prostate Derive from the Neural Crest', *J Biol Chem*, 292(5), pp. 2021-2031.
Tada, M., Takahama, Y., Abe, K., Nakatsuji, N. and Tada, T. (2001) 'Nuclear reprogramming of somatic cells by in vitro hybridization with ES cells', *Curr Biol*, 11(19), pp. 1553-8.
Takahashi, K., Tanabe, K., Ohnuki, M., Narita, M., Ichisaka, T., Tomoda, K. and Yamanaka, S. (2007) 'Induction of pluripotent stem cells from adult human fibroblasts by defined factors', *Cell*, 131(5), pp. 861-72.
Takahashi, K. and Yamanaka, S. (2006) 'Induction of pluripotent stem cells from mouse embryonic and adult fibroblast cultures by defined factors', *Cell*, 126(4), pp. 663-76.
Takao, T. and Tsujimura, A. (2008) 'Prostate stem cells: the niche and cell markers', *Int J Urol*, 15(4), pp. 289-94.
Takasato, M., Er, P.X., Chiu, H.S., Maier, B., Baillie, G.J., Ferguson, C., Parton, R.G., Wolvetang, E.J., Roost, M.S., Chuva de Sousa Lopes, S.M. and Little, M.H. (2015) 'Kidney organoids from human iPS cells contain multiple lineages and model human nephrogenesis', *Nature*, 526(7574), pp. 564-8.
Takebe, T., Sekine, K., Enomura, M., Koike, H., Kimura, M., Ogaeri, T., Zhang, R.R., Ueno, Y., Zheng, Y.W., Koike, N., Aoyama, S., Adachi, Y. and Taniguchi, H. (2013) 'Vascularized and functional human liver from an iPSC-derived organ bud transplant', *Nature*, 499(7459), pp. 481-4.
Takeda, H., Mizuno, T. and Lasnitzki, I. (1985) 'Autoradiographic studies of androgen-binding sites in the rat urogenital sinus and postnatal prostate', *J Endocrinol*, 104(1), pp. 87-92.
Talos, F., Mitrofanova, A., Bergren, S.K., Califano, A. and Shen, M.M. (2017) 'A computational systems approach identifies synergistic specification genes that facilitate lineage conversion to prostate tissue', *Nat Commun*, 8, p. 14662.
Tammam, S., Malak, P., Correa, D., Rothfuss, O., Azzazy, H.M., Lamprecht, A. and Schulze-Osthoff, K. (2016) 'Nuclear delivery of recombinant OCT4 by chitosan nanoparticles for transgene-free generation of protein-induced pluripotent stem cells', *Oncotarget*, 7(25), pp. 37728-37739.
Tanabe, K., Nakamura, M., Narita, M., Takahashi, K. and Yamanaka, S. (2013) 'Maturation, not initiation, is the major roadblock during reprogramming toward pluripotency from human fibroblasts', *Proc Natl Acad Sci U S A*, 110(30), pp. 12172-9.
Taylor, B.S., Schultz, N., Hieronymus, H., Gopalan, A., Xiao, Y., Carver, B.S., Arora, V.K., Kaushik, P., Cerami, E., Reva, B., Antipin, Y., Mitsiades, N., Landers, T., Dolgalev, I., Major, J.E., Wilson, M., Socci, N.D., Lash, A.E., Heguy, A., Eastham, J.A., Scher, H.I., Reuter, V.E., Scardino, P.T., Sander, C., Sawyers, C.L., Gerald, W.L. and for the, M.P.C.O.G. (2010) 'Integrative genomic profiling of human prostate cancer', *Cancer cell*, 18(1), pp. 11-22.
Taylor, R.A., Cowin, P.A., Cunha, G.R., Pera, M., Trounson, A.O., Pedersen, J. and Risbridger, G.P. (2006) 'Formation of human prostate tissue from embryonic stem cells', *Nat Methods*, 3(3), pp. 179-81.
Theunissen, T.W., van Oosten, A.L., Castelo-Branco, G., Hall, J., Smith, A. and Silva, J.C. (2011) 'Nanog overcomes reprogramming barriers and induces pluripotency in minimal conditions', *Curr Biol*, 21(1), pp. 65-71.

Thibaudeau, L., Taubenberger, A.V., Holzapfel, B.M., Quent, V.M., Fuehrmann, T., Hesami, P., Brown, T.D., Dalton, P.D., Power, C.A., Hollier, B.G. and Hutmacher, D.W. (2014) 'A tissue-engineered humanized xenograft model of human breast cancer metastasis to bone', *Dis Model Mech*, 7(2), pp. 299-309.
Thomson, A.A. and Cunha, G.R. (1999) 'Prostatic growth and development are regulated by FGF10', *Development*, 126(16), pp. 3693-701.
Thomson, J.A., Itskovitz-Eldor, J., Shapiro, S.S., Waknitz, M.A., Swiergiel, J.J., Marshall, V.S. and Jones, J.M. (1998) 'Embryonic stem cell lines derived from human blastocysts', *Science*, 282(5391), pp. 1145-7.
Thorpe, A. and Neal, D. (2003) 'Benign prostatic hyperplasia', *The Lancet*, 361(9366), pp. 1359-1367.
Tian, X.C., Kubota, C., Enright, B. and Yang, X. (2003) 'Cloning animals by somatic cell nuclear transfer--biological factors', *Reprod Biol Endocrinol*, 1, p. 98.
Timms, B.G. (2008) 'Prostate development: a historical perspective', *Differentiation*, 76(6), pp. 565-77.
Tropepe, V., Hitoshi, S., Sirard, C., Mak, T.W., Rossant, J. and van der Kooy, D. (2001) 'Direct neural fate specification from embryonic stem cells: a primitive mammalian neural stem cell stage acquired through a default mechanism', *Neuron*, 30(1), pp. 65-78.
Tsujimura, A., Koikawa, Y., Salm, S., Takao, T., Coetzee, S., Moscatelli, D., Shapiro, E., Lepor, H., Sun, T.T. and Wilson, E.L. (2002) 'Proximal location of mouse prostate epithelial stem cells: a model of prostatic homeostasis', *J Cell Biol*, 157(7), pp. 1257-65.
Untergasser, G., Madersbacher, S. and Berger, P. (2005) 'Benign prostatic hyperplasia: age-related tissue-remodeling', *Exp Gerontol*, 40(3), pp. 121-8.
van Bokhoven, A., Varella-Garcia, M., Korch, C., Johannes, W.U., Smith, E.E., Miller, H.L., Nordeen, S.K., Miller, G.J. and Lucia, M.S. (2003) 'Molecular characterization of human prostate carcinoma cell lines', *Prostate*, 57(3), pp. 205-25.
Vander Griend, D.J., Konishi, Y., De Marzo, A.M., Isaacs, J.T. and Meeker, A.K. (2009) 'Dual-label centromere and telomere FISH identifies human, rat, and mouse cell contribution to Multispecies recombinant urogenital sinus xenografts', *Prostate*, 69(14), pp. 1557-64.
Vanpoucke, G., Orr, B., Grace, O.C., Chan, R., Ashley, G.R., Williams, K., Franco, O.E., Hayward, S.W. and Thomson, A.A. (2007) 'Transcriptional profiling of inductive mesenchyme to identify molecules involved in prostate development and disease', *Genome Biol*, 8(10), p. R213.
Verze, P., Cai, T. and Lorenzetti, S. (2016) 'The role of the prostate in male fertility, health and disease', *Nat Rev Urol*, 13(7), pp. 379-86.
Wagers, A.J. and Weissman, I.L. (2004) 'Plasticity of adult stem cells', *Cell*, 116(5), pp. 639-48.
Wakayama, T., Tabar, V., Rodriguez, I., Perry, A.C., Studer, L. and Mombaerts, P. (2001) 'Differentiation of embryonic stem cell lines generated from adult somatic cells by nuclear transfer', *Science*, 292(5517), pp. 740-3.
Wan, H., Dingle, S., Xu, Y., Besnard, V., Kaestner, K.H., Ang, S.L., Wert, S., Stahlman, M.T. and Whitsett, J.A. (2005) 'Compensatory roles of Foxa1 and Foxa2 during lung morphogenesis', *J Biol Chem*, 280(14), pp. 13809-16.
Wang, S., Gao, D. and Chen, Y. (2017) 'The potential of organoids in urological cancer research', *Nat Rev Urol*, 14(7), pp. 401-414.
Wang, S., Xia, P., Ye, B., Huang, G., Liu, J. and Fan, Z. (2013) 'Transient activation of autophagy via Sox2-mediated suppression of mTOR is an important early step in reprogramming to pluripotency', *Cell Stem Cell*, 13(5), pp. 617-25.

Wang, X., Kruithof-de Julio, M., Economides, K.D., Walker, D., Yu, H., Halili, M.V., Hu, Y.P., Price, S.M., Abate-Shen, C. and Shen, M.M. (2009) 'A luminal epithelial stem cell that is a cell of origin for prostate cancer', *Nature*, 461(7263), pp. 495-500.
Wang, X.D., Shou, J., Wong, P., French, D.M. and Gao, W.Q. (2004) 'Notch1-expressing cells are indispensable for prostatic branching morphogenesis during development and re-growth following castration and androgen replacement', *J Biol Chem*, 279(23), pp. 24733-44.
Wang, Y., Hayward, S., Cao, M., Thayer, K. and Cunha, G. (2001) 'Cell differentiation lineage in the prostate', *Differentiation*, 68(4-5), pp. 270-9.
Warren, L., Manos, P.D., Ahfeldt, T., Loh, Y.H., Li, H., Lau, F., Ebina, W., Mandal, P.K., Smith, Z.D., Meissner, A., Daley, G.Q., Brack, A.S., Collins, J.J., Cowan, C., Schlaeger, T.M. and Rossi, D.J. (2010) 'Highly efficient reprogramming to pluripotency and directed differentiation of human cells with synthetic modified mRNA', *Cell Stem Cell*, 7(5), pp. 618-30.
Watanabe, K., Ueno, M., Kamiya, D., Nishiyama, A., Matsumura, M., Wataya, T., Takahashi, J.B., Nishikawa, S., Nishikawa, S., Muguruma, K. and Sasai, Y. (2007) 'A ROCK inhibitor permits survival of dissociated human embryonic stem cells', *Nat Biotechnol*, 25(6), pp. 681-6.
Webber, M.M., Bello, D., Kleinman, H.K., Wartinger, D.D., Williams, D.E. and Rhim, J.S. (1996) 'Prostate specific antigen and androgen receptor induction and characterization of an immortalized adult human prostatic epithelial cell line', *Carcinogenesis*, 17(8), pp. 1641-6.
Wei, T., Chen, W., Wang, X., Zhang, M., Chen, J., Zhu, S., Chen, L., Yang, D., Wang, G., Jia, W., Yu, Y., Duan, T., Wu, M., Liu, H., Gao, S. and Kang, J. (2015) 'An HDAC2-TET1 switch at distinct chromatin regions significantly promotes the maturation of pre-iPS to iPS cells', *Nucleic Acids Res*, 43(11), pp. 5409-22.
Wilmut, I., Schnieke, A.E., McWhir, J., Kind, A.J. and Campbell, K.H. (1997) 'Viable offspring derived from fetal and adult mammalian cells', *Nature*, 385(6619), pp. 810-3.
Wilson, M.H., Coates, C.J. and George, A.L., Jr. (2007) 'PiggyBac transposon-mediated gene transfer in human cells', *Mol Ther*, 15(1), pp. 139-45.
Wilt, T.J. and N'Dow, J. (2008) 'Benign prostatic hyperplasia. Part 2--management', *BMJ*, 336(7637), pp. 206-10.
Winkler, T., Hong, S.G., Decker, J.E., Morgan, M.J., Wu, C., Hughes, W.M.t., Yang, Y., Wangsa, D., Padilla-Nash, H.M., Ried, T., Young, N.S., Dunbar, C.E. and Calado, R.T. (2013) 'Defective telomere elongation and hematopoiesis from telomerase-mutant aplastic anemia iPSCs', *J Clin Invest*, 123(5), pp. 1952-63.
Woltjen, K., Michael, I.P., Mohseni, P., Desai, R., Mileikovsky, M., Hamalainen, R., Cowling, R., Wang, W., Liu, P., Gertsenstein, M., Kaji, K., Sung, H.K. and Nagy, A. (2009) 'piggyBac transposition reprograms fibroblasts to induced pluripotent stem cells', *Nature*, 458(7239), pp. 766-70.
Xu, C., Inokuma, M.S., Denham, J., Golds, K., Kundu, P., Gold, J.D. and Carpenter, M.K. (2001) 'Feeder-free growth of undifferentiated human embryonic stem cells', *Nat Biotechnol*, 19(10), pp. 971-4.
Xue, Y., Smedts, F., Ruijter, E.T., Debruyne, F.M., de la Rosette, J.J. and Schalken, J.A. (2001) 'Branching activity in the human prostate: a closer look at the structure of small glandular buds', *Eur Urol*, 39(2), pp. 222-31.
Yamanaka, S. (2009) 'A fresh look at iPS cells', *Cell*, 137(1), pp. 13-7.
Yamanaka, S. and Blau, H.M. (2010) 'Nuclear reprogramming to a pluripotent state by three approaches', *Nature*, 465(7299), pp. 704-12.

Yin, A.H., Miraglia, S., Zanjani, E.D., Almeida-Porada, G., Ogawa, M., Leary, A.G., Olweus, J., Kearney, J. and Buck, D.W. (1997) 'AC133, a novel marker for human hematopoietic stem and progenitor cells', *Blood*, 90(12), pp. 5002-12.
Yu, J., Hu, K., Smuga-Otto, K., Tian, S., Stewart, R., Slukvin, II and Thomson, J.A. (2009a) 'Human induced pluripotent stem cells free of vector and transgene sequences', *Science*, 324(5928), pp. 797-801.
Yu, S.-Q., Lai, K.-P., Xia, S.-J., Chang, H.-C., Chang, C. and Yeh, S. (2009b) 'The diverse and contrasting effects of using human prostate cancer cell lines to study androgen receptor roles in prostate cancer', *Asian Journal of Andrology*, 11(1), pp. 39-48.
Yusa, K., Rad, R., Takeda, J. and Bradley, A. (2009) 'Generation of transgene-free induced pluripotent mouse stem cells by the piggyBac transposon', *Nat Methods*, 6(5), pp. 363-9.
Zhang, M., Scholer, H.R. and Greber, B. (2013) 'Rapid and efficient generation of neurons from human pluripotent stem cells in a multititre plate format', *J Vis Exp*, (73), p. e4335.
Zhang, W.Y., de Almeida, P.E. and Wu, J.C. (2008) 'Teratoma formation: A tool for monitoring pluripotency in stem cell research', in *StemBook*. Cambridge (MA).
Zhao, H., Sun, N., Young, S.R., Nolley, R., Santos, J., Wu, J.C. and Peehl, D.M. (2013) 'Induced pluripotency of human prostatic epithelial cells', *PLoS One*, 8(5), p. e64503.
Zhou, H., Wu, S., Joo, J.Y., Zhu, S., Han, D.W., Lin, T., Trauger, S., Bien, G., Yao, S., Zhu, Y., Siuzdak, G., Scholer, H.R., Duan, L. and Ding, S. (2009) 'Generation of induced pluripotent stem cells using recombinant proteins', *Cell Stem Cell*, 4(5), pp. 381-4.
Zhou, T., Benda, C., Duzinger, S., Huang, Y., Li, X., Li, Y., Guo, X., Cao, G., Chen, S., Hao, L., Chan, Y.C., Ng, K.M., Ho, J.C., Wieser, M., Wu, J., Redl, H., Tse, H.F., Grillari, J., Grillari-Voglauer, R., Pei, D. and Esteban, M.A. (2011) 'Generation of induced pluripotent stem cells from urine', *J Am Soc Nephrol*, 22(7), pp. 1221-8.